Role of the relaxin-3/RXFP3 system in the mouse: Focus on septohippocampal function and memory

Mouna Haidar

BA, Grad Dip (Psych) (Deakin)

Submitted in total fulfilment of the requirements of the degree of Doctor of Philosophy

The Florey Institute of Neuroscience and Mental Health
and Florey Department of Neuroscience and Mental Health
Faculty of Medicine, Dentistry and Health Sciences
The University of Melbourne
Parkville, Victoria, Australia

July 2017

Abstract

Anatomical and functional studies have suggested that the highly conserved neuropeptide relaxin-3 plays an important role in a diverse range of functions, including behavioural arousal, stress responses and cognitive processes. Within rodent brain, relaxin-3 is primarily expressed by γ-aminobutyric acid (GABA) neurons in the pontine *nucleus incertus* (NI) that project to a number of forebrain areas containing its cognate G-protein-coupled receptor, relaxin-family peptide 3 receptor, RXFP3. Importantly, the relaxin-3/RXFP3 system performs synergistic and complementary roles to monoamine signalling (i.e. noradrenaline (NA)/locus coeruleus (LC) and serotonin (5-HT)/dorsal raphe (DR) systems) within shared downstream target regions. It has previously been established that relaxin-3-containing nerve fibres and RXFP3 mRNA and binding sites are strongly expressed in the main nodes of the septohippocampal system (SHS), including the medial septum/diagonal band of Broca (MS/DB) and hippocampal formation. Indeed, anatomical studies in the rat have demonstrated that relaxin-3-positive nerve fibres terminate on MS/DB GABAergic and cholinergic neurons that project to hippocampus, and functional studies have demonstrated that the relaxin-3/ RXFP3 system within the MS/DB modulates hippocampal theta rhythm and spatial working memory. However, the precise neurochemical and physiological mechanism(s) by which the relaxin-3/RXFP3 system modulates hippocampal activity are largely unknown and there are no studies of this system in mice. Therefore, to address this gap in knowledge, the studies described in this thesis investigated the role of the relaxin-3/RXFP3 system in the mouse in three key areas: (1) hippocampal function and memory; (2) progression of neurodegenerative disease; and (3) affective states and stress responses.

Initial anatomical studies revealed that relaxin-3-positive nerve fibres/boutons make close contacts with multiple GABA neuron populations in the hippocampus, including a large population of somatostatin (SST)-positive neurons in the dentate gyrus hilus (DG hilus), and a smaller population of neurons expressing the calcium-binding proteins, parvalbumin (PV) and calretinin (CR). In subsequent functional studies, a 'floxed' RXFP3 mouse strain was validated and Cre-recombinase-mediated depletion of RXFP3 from the DG hilus in adult mice produced impairments in spatial reference and working memory. Together, these findings suggest endogenous relaxin-3/RXFP3 signalling is important for normal cognitive function via

modulation of inhibitory GABA networks, including effects on the SST neurons that regulate the activity of principal cells and hippocampal oscillatory activity.

Determining the role that relaxin-3/RXFP3 signalling plays in hippocampal function and cognition, and any synergistic actions with ascending monoamine systems, is important in relation to potential causative and/or therapeutic roles that relaxin-3/RXFP3 signalling play in disease. Dysfunction of ascending monoamine systems is a feature of several neurological diseases, including tauopathies and related neurodegenerative dementias, but it is not known if damage to the NI relaxin-3 system might contribute to cognitive decline in a similar way to the disruption of brainstem monoamine transmission in the hippocampus and frontal cortex. Therefore, using quantitative histochemical methods, the number and viability of relaxin-3 neurons in the NI was assessed in a cohort of transgenic tau-P301L mice and age- and strain-matched controls. The tau-P301L mouse is a model of human tauopathy and carries the P301L mutation (tau-4R/2N-P301L) in the tau protein, which is critical for binding to microtubules to aid their stabilization, essential for axonal transport, whereas under pathological conditions, phosphorylated tau results in aggregates that are toxic to neurons. A reduced number of relaxin-3-immunoreactive neurons was detected in the NI of 7 – 8 month old tau-P301L mice, relative to age matched controls, suggesting that reduced activity of the relaxin-3/RXFP3 system may contribute to cognitive decline in tauopathies and related disorders. This initial study of relaxin-3 neurons in a preclinical model of neurodegenerative disease indicates that further research in this and other models is warranted, including correlative studies of relaxin-3 mRNA levels and measures of relaxin-3 fibre and RXFP3 densities in key nodes of the septohippocampal system.

In a series of functional studies, the relationship between the relaxin-3/RXFP3 system and monoamine signalling in controlling stress responses and affective states was explored by examining the impact of monoamine deficiency on the behavioural profile of normal C57BL/6J mice and mice with a constitutive whole-of-life deletion of the relaxin-3 or RXFP3 genes. Monoamine deficiency was achieved by withdrawal from chronic methamphetamine treatment. It was hypothesized that endogenous relaxin-3/RXFP3 signalling may compensate for the temporary reduction in monoamine signalling and reduce the depressive- and anxiety-like behaviours associated with methamphetamine withdrawal. Depressive- and anxiety-like behaviours were assessed in relaxin-3 and RXFP3 knockout (KO) mice and their wildtype (WT)

littermates following withdrawal from escalating doses of methamphetamine. All groups of mice (relaxin-3 and RXFP3 KO, and WT) displayed similar sensitivity to chronic methamphetamine withdrawal in measures of body weight change, behavioural despair and anxiety-like behaviours. These data indicate that a global deficiency in endogenous brain relaxin-3/RXFP3 signalling does not exacerbate depressive- and affective-like behaviours observed during chronic methamphetamine withdrawal.

In summary, these studies have demonstrated that relaxin-3/RXFP3 signalling can modulate hippocampal-dependent spatial reference and working memory most likely via modulation of key GABAergic neuron populations in the hippocampus. Furthermore, evidence was obtained that relaxin-3 neurons are dysregulated in a mouse model of tauopathy, further highlighting the importance of this system for healthy cognition. The identification of the contribution of the relaxin-3/RXFP3 system to hippocampal function and cognition encourages further research to identify the potential therapeutic value of RXFP3 targeted drugs to enhance cognitive functioning and improved mental health in a range of neurodegenerative and psychiatric diseases.

Declaration

I hereby certify that:

i. this thesis comprises only my original work towards the degree of Doctor of Philosophy, except those studies indicated in the preface,

ii. due acknowledgement has been made in the text to all other material used,

iii. the thesis is less than 100,000 words in length, exclusive of tables, figures, bibliography and appendices.

Mouna Haidar

Preface

This thesis contains no material which has been accepted for the award of another degree or qualification, and no research conducted prior to PhD candidature enrolment. To the best of my knowledge, this thesis contains no previously published material or material written by another person, except where reference is made in the text of the thesis.

Chapters 2 and 4 of this thesis comprise manuscripts, which have been accepted for publication in the peer-reviewed journals *Hippocampus* and *Neurochemical Research*, respectively. I, Mouna Haidar, am the first and primary author of both manuscripts, and contributed more than 50% of the experimental planning, execution, and preparation of the research data for publication.

My primary supervisor, Andrew Gundlach, and co-supervisor, Craig Smith, provided supervision, intellectual input, assistance with study design, technical guidance, and editing of the manuscripts and this thesis.

Acknowledgements

Firstly, I would like to thank my primary supervisor, Andrew Gundlach, for your endless support and encouragement throughout every step of my PhD candidature. I sincerely appreciate your major time commitment throughout my studies and your passion and enthusiasm for everything science related has had a significant impact on me as a junior researcher. You gave me the opportunity to grow and to develop multifaceted skill sets which has shaped the researcher I am today, and has given me the opportunity to use these valuable and fundamental skills in the next part of my career journey. It has been a privilege working in your laboratory, and invaluable working with you.

I would like to thank my co-supervisor, Craig Smith. I could not have gotten through the first year of my PhD without your patience, support and encouragement. As a psychology graduate, I started my PhD with no laboratory experience, and a scant understanding of neuroscience. You took me 'under your wing' and taught me all the practical fundamentals, so I wouldn't know what I do today or be the more confident researcher I am without your guidance. I sincerely appreciate your outstanding time and effort over the last four years.

I would like to thank past and present members of the Gundlach Laboratory, for providing a fun, caring, supportive and positive environment. Firstly, many thanks to Sherie Ma for your insightful guidance in immunohistochemistry and microscopy. It has been a privilege to work with such a talented neuroscientist. Special thanks to Berenice Chua, who was with me every step of the way in the first year of my candidature, and with whom I spent endless hours in the secluded (dark) behaviour and procedure rooms in the animal facility - you made these long days enjoyable.

My project would not have been successful without the talented staff at The Florey. In particular, I would like to thank Danny Drieberg, Brett Purcell and Travis Featherby for having a solution to my (many) technical problems at all times. A big thanks to our talented animal breeding facility team, including Ana Hudson and Krista Brown. Of course, I would like to thank our talented microscopy team, including Verena Wimmer and Carolina Chavez. Thank you for your support in 'everything microscopy' and for providing invaluable input into the planning and execution of imaging analysis for my projects. A big thanks to my PhD committee

members, Tony Hannan and Mathew Hale. Your input and advice into my project over the last four years has been highly appreciated and very valuable.

On a more personal note, thanks to my friends at The Florey with whom I have shared fun times, and for keeping me sane throughout the last few years. I couldn't have gotten through the last few years without you, and in your own way, you have all been an inspiration to me throughout my PhD. A special thanks goes to Cary (especially for the unlimited supply of chocolate), Val, my desk buddy Leigh, travel buddy Katie, Sarah, Dean, Andrew, Ihaia and others who made their mark. It has been a privilege working with you all, and I am immensely grateful to all of you. I look forward to keeping in contact, no matter where our next life and career moves take us.

Special thanks also to all my friends outside the Florey, thank you for keeping me sane at all times and helping me keep a healthy work/life balance. Your input on a personal level was invaluable, and I will always be grateful. Our friendships are strong, and we will forever grow together. I look forward to sharing new chapters of our lives in the years to come.

To Elliot, thank you for all your support and encouragement, your positive influence, understanding and friendship. I wouldn't have stayed sane without you. I am very grateful to have you in my life, and am looking forward to what the future holds. To my beautiful family, especially my big brother, Mo, and 'not-so-baby' sister Leanne, thank you for always being there for me and shaping the person I am today. It is incredible how much positive influence we have on each other, each in our own way. I am forever grateful to have the both of you in my life, along with my canine family members, Cuba and Archie of course.

Finally, to my mum, Maha, words would not be able to adequately describe the influence you have had on me, in every aspect of my life. Thank you for giving me the opportunity to do the things I have wanted to do and for always believing in me. You have taught me the importance of diligence and hard work, and challenge me every single day of my life. I will forever be grateful and am truly blessed to have you as my mum and best friend.

Table of Contents

Chapter 2
Role of relaxin-3/RXFP3 signalling within the hippocampus

Chapter 3
Neurochemical characterisation of the nucleus incertus in a transgenic mouse model of tauopathy

List of Abbreviations

5-HIAA	5-hydroxyindoleacetic acid (serotonin metabolite)
5-HT	5-hydroxytryptamine (serotonin)
5-HT1A	5-hydroxytryptamine receptor 1A
5-HT2A	5-hydroxytryptamine receptor 2A
AAV	adeno-associated virus
AChE	acetylcholinesterase
ACTH	adrenocorticotropin hormone
AD	Alzheimer's disease
ANOVA	analysis of variance
apoE4	apolipoprotein E4
AT1	angiotensin receptor 1
Aβ	amyloid beta
BDA	dextran biotin amine
BMA	basomedial amygdala
CA1	cornu ammonis region 1
CA3	cornu ammonis region 3
cAMP	cyclic adenosine monophosphate
CB	calbindin
CCK	cholecystokinin
CeA	central amygdala
ChAT	choline acetyltransferase
CNO	clozapine-N-oxide
CRF	corticotropin-releasing factor
CRF1	corticotropin-releasing factor receptor 1
CSF	cerebrospinal fluid
CTB	cholera toxin B
DA	dopamine
DG	dentate gyrus
DIO	double-floxed inverse orientation

DNA	deoxyribonucleic acid
DOR	delta opioid receptor
DR	dorsal raphe
DREADD	designer receptor exclusively activated by designer drugs
DSM-IV	diagnostic and statistical manual of mental disorders IV
dSN	dorsal to the substantia nigra
eGFP	enhanced green fluorescent protein
eNFT	extra-neuronal neurofibrillary tangle
eYFP	enhanced yellow fluorescent protein
FG	fluorogold
FTDP-17	frontotemporal dementia with parkinsonism-17
GABA	γ-aminobutyric acid
GAD	glutamate decarboxylase
GAD65	glutamate decarboxylase 65
GluR-A	glutamate receptor A
GPCR	G-protein-coupled receptor
GPCR135	G-protein-coupled receptor 135 (RXFP3)
GWAS	genome-wide association study
hM3Dq	human M3 muscarinic receptor Gq-coupled DREADD
hM4Di	human M4 muscarinic receptor Gi-coupled DREADD
HPA axis	hypothalamic pituitary adrenal axis
icv	intracerebroventricular
IGL	intergeniculate nucleus
iNFT	intra-neuronal neurofibrillary tangle
IR	immunoreactivity
IRES	internal ribosome entry site
ITI	inter-trial-interview
KO	knockout
LC	locus coeruleus
LTP	long-term potentiation
MDD	major depressive disorder

MeA	medial amygdala
METH	methamphetamine
mRNA	messenger ribonucleic acid
MS	medial septum
MS/DB	medial septum/diagonal band of Broca
MWM	Morris water maze
NA	noradrenaline
NFT	neurofibrillary tangle
NGF	nerve-growth factor
NHS	normal horse serum
NI	nucleus incertus
NIc	nucleus incertus *pars compacta*
NId	nucleus incertus *pars dissipata*
NMB	neuromedin-B
NPY	neuropeptide Y
OD	optical density
PAG	periaqueductal grey
PAL	passive avoidance learning
PAS	percentage alternation score
PB	phosphate buffer
PCPA	para-chlorophenylalanine
PFA	paraformaldehyde
PHA-L	Phaseolus vulgaris-leucoagglutinin
pNFT	pre-neuronal neurofibrillary tangle
PnR	pontine raphe nucleus
ptau	phosphorylated tau
PV	parvalbumin
PVN	paraventricular hypothalamic nucleus
R3(B1-22)R	relaxin-3 B-chain analogue (RXFP3 antagonist)
R3(BΔ23-27)R/I5	relaxin-3 B-chain, INSL5 A-chain (RXFP3 antagonist)
R3/I5	relaxin-3 B-chain, INSL5 A chain (RXFP3 agonist)

RLN3	relaxin-3
RM	repeated measures
RPO	reticular pontis oralis
RT	room temperature
RXFP1	relaxin family peptide 1 receptor
RXFP3	relaxin family peptide 3 receptor
SAL	saline
SALPR	somatostatin- and angiotensin-like peptide receptor
SAT	spontaneous alternation test
sCAG	short chicken beta-actin gene
SHS	septohippocampal system
SON	supraoptic nucleus
SST	somatostatin
SSTR2	somatostatin receptor 2
SUM	supramammillary nucleus
TrkA	tropomyosin receptor kinase A
VGLUT2	vesicular glutamate transporter 2
VIP	vasoactive intestinal polypeptide
VPAC1	VIP receptor 1
VTg	ventral tegmental nucleus of Gudden
WT	wildtype

Publications and Communications

The following publications include data from studies described in this thesis, and/or intellectual input and manuscript editing provided during my PhD candidature.

Publications in peer-reviewed journals

Haidar M, Guèvremont G, Zhang C, Bathgate RAD, Timofeeva E, Smith CM, Gundlach AL (2017). Relaxin-3 inputs target hippocampal interneurons and hilar deletion of relaxin-3 receptors in adult 'floxed RXFP3' mice impairs spatial reference memory. *Hippocampus* **27**, 529-546.

Haidar M, Guèvremont G, Zhang C, Bathgate RAD, Timofeeva E, Smith CM, Gundlach AL (2017). Deletion of hilar relaxin-3 receptor impairs spatial memory. *Hippocampus* **27**, Cover Image.

Haidar M, Lam M, Chua BE, Smith CM, Gundlach AL (2015). Sensitivity to chronic methamphetamine administration and withdrawal in mice with relaxin-3/RXFP3 deficiency. *Neurochemical Research* **41**, 481-491.

Lepeta K, Lourenco MV, Schweitzer BC, Adami PVM, Banerjee P, Catuara-Solarz S, de La Fuente Revenga M, Guillem AM, **Haidar M** et al. (2016). Synaptopathies: synaptic dysfunction in neurological disorders. *Journal of Neurochemistry* **138**, 785-805.

Smith CM, Chua BE, Zhang C, Walker AW, **Haidar M**, Hawkes D, Hossain MA, Shabanpoor F, Wade JD, Gundlach AL (2014). Central injection of relaxin-3 receptor antagonists reduces motivated food seeking and consumption in mice. *Behavioural Brain Research* **268**, 117-126.

Smith CM, Walker AW, Hosken IT, Chua BE, Zhang C, **Haidar M**, Gundlach AL (2014). Relaxin-3/RXFP3 networks: an emerging target for the treatment of depression and other neuropsychiatric diseases? *Frontiers in Pharmacology* **5**, 127.

Communications at national and international scientific meetings

Haidar M, Stanic D, Dutschmann M, Smith CM, Gundlach AL. Ascending peptidergic neurons in aging P301L tau mutant mice. **Oral Presentation**, *Alzheimer's Disease Workshop, with Prof Susan Greenfield (Oxford, UK)*, Melbourne, 2016.

Haidar M, Hawkes D, Guèvremont G, Ma S, Bathgate RAD, Timofeeva E, Smith CM, Gundlach AL. Control of the septohippocampal pathway and learning and memory by relaxin-3/RXFP3 signalling networks. **Oral Presentation**, *Institut du Cerveau et de la Moelle epiniere (ICM)/Florey Institute Joint Symposium*, Paris, France, 2016.

Haidar M, Hawkes D, Guèvremont G, Ma S, Bathgate RAD, Timofeeva E, Smith CM, Gundlach AL. Relaxin-3 inputs target hippocampal interneurons and hippocampal hilar-specific deletion of RXFP3 in adult mice impairs spatial reference memory. **Poster Presentation**, *Forum of Neuroscience Societies (FENS),* Copenhagen, Denmark, 2016.

Haidar M, Hawkes D, Guèvremont G, Olucha-Bordonau FE, Ma S, Bathgate RAD, Timofeeva E, Smith CM, Gundlach AL. Relaxin-3/RXFP3 networks and the septohippocampal pathway: Viral-based studies in transgenic mice. **Poster Presentation**, *7th International Conference on Relaxin and Related Peptides*, Kuching, Malaysia, 2015.

Haidar M, Hawkes D, Guèvremont G, Olucha-Bordonau F, Ma S, Bathgate RAD, Timofeeva E, Smith CM, Gundlach AL. Relaxin-3/RXFP3 neural networks and the septohippocampal pathway: Effects on learning and memory of viral-based changes in RXFP3 in transgenic mice. **Oral Presentation**, *International Society of Neurochemistry (ISN) Advanced School,* Cairns, 2015.

Haidar M, Hawkes D, Guèvremont G, Olucha-Bordonau F, Ma S, Bathgate RAD, Timofeeva E, Smith CM, Gundlach AL. Relaxin-3/RXFP3 neural networks and the septohippocampal pathway: Effects on learning and memory of viral-based changes in RXFP3 in transgenic mice. **Poster Presentation,** *International Society of Neurochemistry (ISN),* Cairns, 2015.

Haidar M, Hawkes D, Guèvremont G, Olucha-Bordonau F, Ma S, Bathgate RAD, Timofeeva E, Smith CM, Gundlach AL. Control of the septohippocampal pathway and learning and memory by relaxin-3/RXFP3 neural networks: Viral-based studies in transgenic mice. **Oral Presentation**

Student Data Blitz, *International Behavioural Neuroscience Society,* British Columbia, Canada, 2015.

Haidar M, Hawkes D, Guèvremont G, Olucha-Bordonau F, Ma S, Bathgate RAD, Timofeeva E, Smith CM, Gundlach AL. Control of the septohippocampal pathway and learning and memory by relaxin-3/RXFP3 neural networks: Viral-based studies in transgenic mice. **Poster Presentation**, *International Behavioural Neuroscience Society,* British Columbia, Canada, 2015.

Haidar M, Zhang C, Olucha-Bordonau F, Stanic D, Dutschmann M, Smith CM, Gundlach AL. Stress- and arousal- associated relaxin-3/RXFP3 networks and control of affect and cognition: Studies in transgenic mice. **Poster Presentation**, *International Congress of Neuroendocrinology,* Sydney, 2014.

Haidar M, Lam M, Chua BE, Smith CM, Gundlach AL. Behavioural profile of relaxin-3 deficient mice in the methamphetamine withdrawal model of monoamine depletion and depression. **Poster Presentation**, *Australasian Neuroscience Society (ANS) Meeting,* Adelaide, 2014.

Haidar M, Chua BE, Smith CM, Gundlach AL. Behavioural profile of relaxin-3 deficient mice in the methamphetamine withdrawal model of monoamine depletion and depression. **Poster Presentation**, *Australian Society for Medical Research (ASMR) Symposium,* Melbourne, 2013.

Scholarships and Awards

Alzheimer's Australia Dementia Research Foundation (AADRF) Postgraduate Scholarship (2014-2016)

International Behavioural Neuroscience Society (IBNS) Graduate Student Travel Award to attend IBNS Annual Meeting, Victoria, British Columbia, Canada (2015)

International Society of Neurochemistry (ISN) Advanced School Travel Award (in conjunction with Australasian Neuroscience Society (ANS), Fitzroy Island, Queensland, Australia (2015)

Geoff Tregear Travel Award to attend International Conference on Relaxin and Related Peptides, Kuching, Malaysia (2015)

Miller Postgraduate Travel Award to attend 10th Forum of Federation of European Neuroscience, Copenhagen, Denmark (2016)

CHAPTER 1

General Introduction

1.1 Neuropeptides: Important modulators of the hippocampus and other brain structures

Henry Gustov Molaison, known as 'Patient H.M.', suffered from severe amnesia as a result of a bilateral 'hippocampectomy' (a medial temporal lobe resection including the hippocampus, amygdala and adjacent parahippocampal gyrus) performed to treat his epilepsy. Studies of Patient H.M. lead to the first comprehensive insight into the role of the medial temporal lobe in cognition (Scoville and Milner, 1957; Squire, 2009). Up until these studies in 1953, it was believed that memory was a distributed property of the whole brain. The early descriptions of H.M. launched the modern era of memory research, influencing the direction of subsequent work which focused on the hippocampus and associated areas in several species including non-human primates (Mishkin, 1978; Squire and Zola-Morgan, 1991; Murray, 1992). Since these early studies, decades of research by many laboratories have helped establish the role played by the hippocampus, including the adjacent entorhinal and parahippocampal cortices, in memory and other cognitive functions and the associated neural mechanisms (see e.g. Bannerman et al., 2014; Moser et al., 2015 for review).

In more recent times, behavioural/cognitive neuroscientists have begun to understand how hippocampal function is modulated by upstream brain regions such as the basal forebrain (i.e. septal region, forming the septohippocampal system, SHS ;Brown and McKenna, 2015) and brainstem (i.e. dorsal raphe and the nucleus incertus, NI). In addition to classical neurotransmitters such as glutamate, γ-aminobutyric acid (GABA) and the monoamines, the role that neuropeptide transmitters play within the hippocampus to influence learning and memory has been recently highlighted (Hokfelt et al., 2000; Borbely et al., 2013). More broadly, based on their distribution in the brain and data from functional studies, neuropeptides are increasingly being recognised as regulators of several cognitive pathways (Ogren et al., 2010), including anxiety and depression circuits (Heilig et al., 1994; Holmes et al., 2002; Holmes et al., 2003). Prominent examples of such peptides include corticotropin-releasing factor (CRF), somatostatin (SST), vasoactive intestinal polypeptide (VIP), neuropeptide Y (NPY), the opioid peptides, and galanin (Ogren et al., 2010).

Targeting neuropeptide systems therapeutically has several potential advantages over 'classical' neurotransmitter systems (see Holmes et al., 2003 for review). Several

neuropeptides appear to be preferentially released under specific 'challenging' physiological conditions, such as stressful life events and disease states (Holmes et al., 2003). Therefore, drugs that target these neuropeptide systems might only affect disease-related behaviours (rather than 'basal' fundamental behaviours and neurological processes), hence reducing the likelihood of adverse side effects. For example, relatively specific protective/therapeutic roles of several neuropeptide receptor agonists and antagonists have been demonstrated in rodent models of Alzheimer's and Parkinson's disease (for review see, Borbély et al., 2013), including an SST_4 agonist (Sandoval et al., 2013), a VIP receptor agonist (VPAC1) (White et al., 2010), and a delta opioid receptor (DOR) antagonist (Cai and Ratka, 2012).

Neuropeptides range between 3-100 amino acids (i.e. up to 50 times larger than classical neurotransmitters) in size (Hokfelt et al., 2003), and neuropeptide/receptor systems are often highly conserved between species. Neuropeptides differ from classical neurotransmitters that are produced by enzymatic cascades and are recycled via reuptake at the synapse. Instead, neuropeptide-encoding mRNA transcripts are translated in the rough endoplasmic reticulum of neuronal cell bodies to form pre/pro-peptide precursors, that are packaged into large dense core vesicles and transported to nerve terminals by fast axonal transport (Gainer, 1981; Hokfelt et al., 2003). During this passage they are converted into their mature form via proteolytic cleavage, and neuropeptide signalling is mediated via both pre- and post-synaptic receptors - usually G-protein-coupled receptors (Branchek et al., 2000; Holmgren and Jensen, 2001; Hokfelt et al., 2003).

Importantly, neuropeptides usually coexist with other neurotransmitters acting as modulators at post-synaptic sites (Holmgren and Jensen, 2001). Several neuropeptides that modulate hippocampal activity via direct or indirect modulation of excitatory/inhibitory systems have been identified (Ogren et al., 2010; van den Pol, 2012; Gotzsche and Woldbye, 2016; Li et al., 2017). For example, many neuropeptides are present in hippocampal glutamatergic neurons including the opioid peptides, dynorphin, enkephalin, and nociception (Ogren et al., 2010). Activation of k-opioid receptors exerts an inhibitory effect on hippocampus glutamatergic pyramidal neurons, reducing hippocampal excitability (Simmons and Chavkin, 1996) and therefore inhibiting hippocampal transmission and induction of long-term potentiation (LTP) (Huge et al., 2009). Whereas populations of hippocampal GABAergic neurons co-express other neuropeptides, including VIP, cholecystokinin, dynorphin,

neurokinin B, substance P, NPY, and SST (Dun et al., 1994; Acsady et al., 1996; Freund and Buzsaki, 1996; Bering et al., 1997; Acsady et al., 2000; Billova et al., 2007; Antonucci et al., 2012), acting as intrinsic modulators of GABAergic signalling in the hippocampus. Additionally, extrinsic modulation of GABAergic hippocampal neurons has also been identified. For example, galanin coexists with NA in the LC, 5-HT in the DR nucleus, and with acetylcholine in the MS (Melander et al., 1986), and all these neurons project to the hippocampus. Thus, galanin is positioned to influence hippocampal function by modifying the inputs of NA, 5-HT and acetylcholine.

A quite recently discovered neuropeptide/receptor system that also modulates hippocampal activity and demonstrates therapeutic potential via modulation of the hippocampus and related brain regions is the 'relaxin-3/RXFP3' system, and this system is the focus of the research described in this thesis. Therefore, this introduction will briefly review the relaxin-3/RXFP3 system, including its anatomy, and its proposed neurochemical and functional relevance in modulating hippocampal activity and learning and memory, as well as the potential response of this system in neurodegenerative disease. Finally, as described above (Abstract), due to the synergistic relationship between the relaxin-3/RXFP3 system and monoamine signalling, the role of this system in controlling stress responses and affective states will be reviewed.

1.2 Relaxin-3

Relaxin-3 is a 5.5 kDa neuropeptide that consists of an A- and B-chain with two inter-chain disulphide bonds and one intra-chain disulphide bond (Bathgate et al., 2002). Relaxin-3 consists of 51 amino acids (in both humans and mice/rats), and was discovered by searching the Celera Genomics database in 2001 (Bathgate et al., 2002) for homologs of the peptide hormone relaxin. It is a member of the insulin/relaxin superfamily, which includes relaxin (relaxin-2 in humans) that plays a role in female reproductive physiology, promoting growth and softening of the cervix, and 'relaxing' the pelvic ligament during birth (for which relaxin owes its name) (Hisaw, 1926; Sherwood, 2004).

In contrast to the peripheral production and primary actions of relaxin (Sherwood, 2004), relaxin-3 is abundantly expressed within the mammalian brain (Bathgate et al., 2002; Burazin

et al., 2002). Its gene and peptide sequence and expression within the brain is highly conserved across species including zebrafish and fugu fish (Wilkinson et al., 2005), rodents (Ma et al., 2007; Smith et al., 2010), higher-order primates (Ma et al., 2009b), and humans (Liu et al., 2003). The neuroanatomical distribution of relaxin-3-containing neurons has been comprehensively studied in the rat (Tanaka et al., 2005; Ma et al., 2007; Banerjee et al., 2010), mouse (Smith et al., 2010) and macaque (*Macaca fascicularis*) brain (Ma et al., 2009b), revealing abundant expression of relaxin-3 within neurons of the pontine brainstem NI (**Figure 1.1A**). Smaller populations of neurons expressing relaxin-3 are also present in the pontine raphe nucleus (PnR), the anterior and posterior periaqueductal grey (PAG), and in an area dorsal to the substantia nigra (dSN) (Tanaka et al., 2005; Ma et al., 2007; Smith et al., 2010). In zebrafish, relaxin-3-like genes are expressed in two regions of the brainstem; one that is comparable to the PAG, and another that appears similar to the rodent NI (Donizetti et al., 2008). In the rhesus macaque (*Macaca mulatta*) and human brain, relaxin-3 is expressed in neurons in the dorsal and ventral tegmentum of the brainstem (Ma et al., 2009a), which is an area that corresponds to the location of the NI in mice and rats. Relaxin-3 has been detected within presynaptic vesicles (Tanaka et al., 2005), in line with its role as a 'releasable' neurotransmitter.

The NI contains the largest population of relaxin-3 expressing neurons in the rodent brain, with ~2000 relaxin-3 positive neurons in the rat NI, while the PnR contains ~350 neurons, the PAG ~550 neurons and the dSN ~350 neurons (Tanaka et al., 2005). In mice, there are ~440 relaxin-3-immunoreactive neurons in the NI, while the PAG contains ~110 cells, the PnR ~70 cells, and the dSN ~200 cells (Zhang C, personal communication).

1.3 Nucleus Incertus

In 1903, George L. Streeter described the NI or 'uncertain nucleus' as a midline region in the floor of the 4th ventricle in the human brain with unknown function (**Figure, 1.1B, C**; Streeter, 1903). The NI has also been describes as the *dorsal tegmental nucleus pars ventromedialis* (Morest, 1961; Cowan et al., 1964; Riley and Moore, 1981), *nucleus recessus pontis medialis* (Jennes et al., 1982), and *nucleus 'O'* (Meessen and Olszewski, 1949; Paxinos and Butcher, 1985). In the mouse and rat, the NI is located in the midline periventricular central grey in the pontine tegmentum, just ventral to the 4th ventricle (Goto et al., 2001; Bathgate et al., 2002;

Burazin et al., 2002). In the rat, the NI consist of two parts: the '*pars compacta*' (NIc, compact part) and the '*pars dissipata*' (NId, diffuse part) (Goto et al., 2001). The mouse NI is comprised of a bilateral medial pars compacta (NIc), which borders the sagittal midline, and more diffuse and lateral pars dissipata (NId) (Smith et al., 2010), similar to that described in the rat (Franklin and Paxinos, 1997; Goto et al., 2001; Olucha-Bordonau et al., 2003).

To date, two comprehensive anatomical studies in the rat have mapped the afferent and efferent connections of the NI (Goto et al., 2001; Olucha-Bordonau et al., 2003) using retrograde (cholera-toxin B, CTB and fluorogold, FG) and anterograde (Phaseolus vulgaris-leucoagglutinin, PHA-L and biotinylated dextran amine, BDA) tracers, respectively. The NI receives inputs from the prefrontal cortex, medial septum/diagonal band of Broca (MS/DB), intralaminar thalamic nuclei and regions of the hypothalamus, including the supramammillary nucleus. These inputs illustrate that the NI is highly integrated with circuits regulating higher cognitive processes and emotion. The NI sends strong efferent projections to distinct hypothalamic, amygdalar and thalamic nuclei, in addition to septal nuclei and the hippocampal formation, in a pattern that strongly overlaps the observed distribution of relaxin-3-immunoreactive (IR) fibres (Ma et al., 2007; Smith et al., 2010). Notably, following injection of an anterograde tracer (miniruby) into the rat NI, it was revealed that choline acetyltransferase (ChAT)-, parvalbumin (PV)- and calbindin (CB)-positive neurons in the MS/DB receive a direct NI innervation (Olucha-Bordonau et al., 2012). In contrast, retrograde and anterograde tracing studies have not been reported for the mouse NI. Nonetheless, the presence of relaxin-3-IR throughout the mouse brain suggests the distribution of relaxin-3-positive neuronal soma and axonal projections are similar to the rat (Smith et al., 2010).

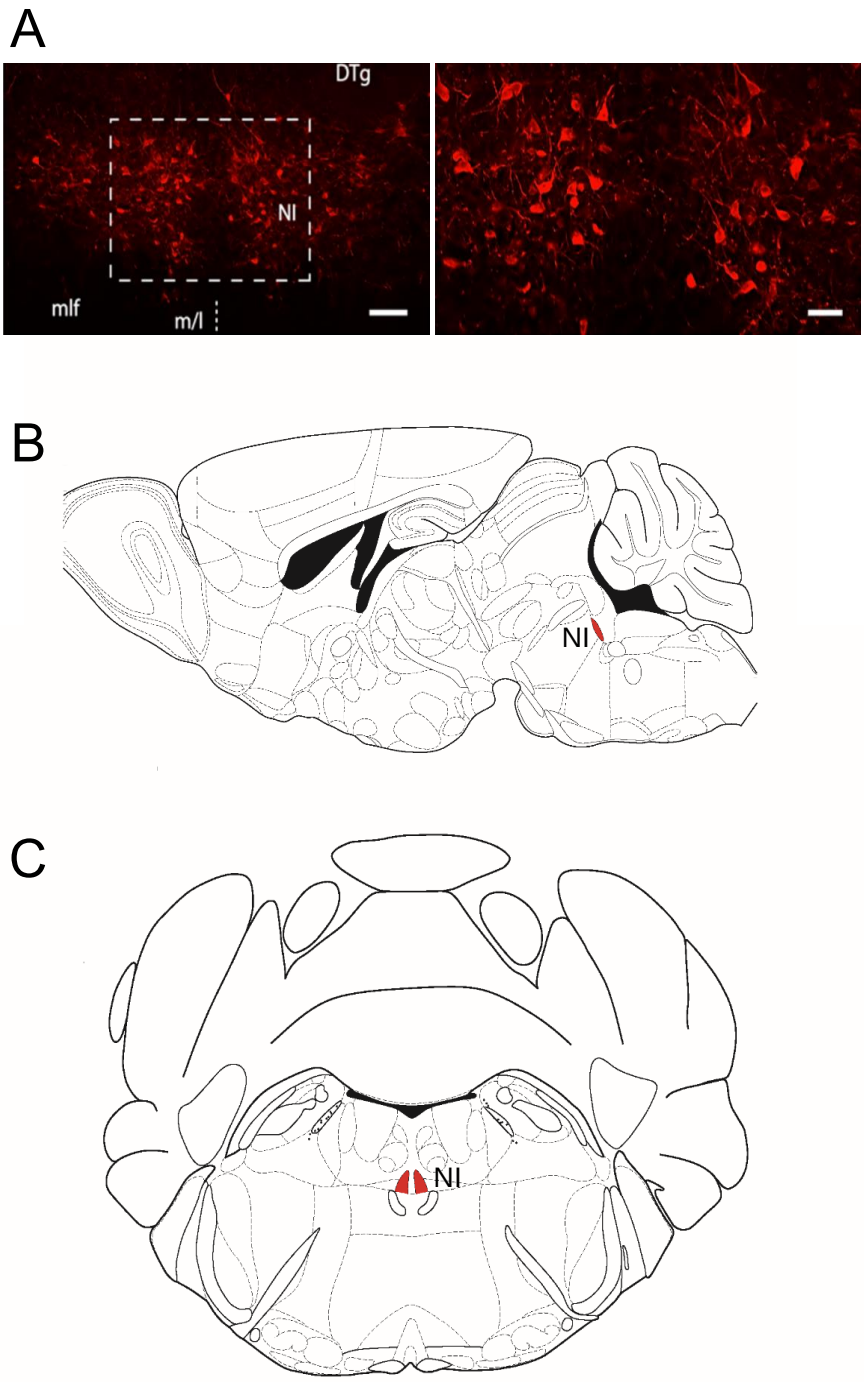

Figure 1.1. Relaxin-3 neurons in the mouse *nucleus incertus*

(A) Low (left) and high (right) magnification micrographs of a coronal section through the mouse nucleus incertus (NI), illustrating neurons positive for relaxin-3 immunoreactivity. The midline (m/l) is indicated with a dotted line. Anterior/posterior coordinates from bregma, -5.38 mm. Scale bar, 100 µm. (Adapted from Smith et al., 2014a). The location of the mouse nucleus incertus in (B) a sagittal section (bregma -5.4 to -5.52 mm) and (C) coronal view (bregma -5.4 mm) (shaded in red). Images in B and C adapted from Paxinos and Watson (2007). Abbreviations: DTg, dorsal tegmental nucleus; NI, nucleus incertus; MLF, medial longitudinal fasciculus.

1.3.1 Neurochemical characterisation of relaxin-3-positive neurons in the nucleus incertus

Neurons in the rat NI express the GABA-synthesising enzyme, glutamate decarboxylase (GAD) (Ford et al., 1995; Olucha-Bordonau et al., 2003). Subsequent immunohistochemical experiments found that the majority of relaxin-3 NI neurons express GAD65, and therefore likely produce and release the inhibitory amino acid neurotransmitter GABA (Ma et al., 2007). Notably, the vesicular glutamate transporter-2 (VGLUT2) has been reported to be expressed in rat NI neurons that project to the MS (Cervera-Ferri et al., 2012), but VGLUT2 was not expressed in relaxin-3-positive neurons (Ma et al., 2007). Rat NI neurons also express high levels of the calcium-binding proteins, CB and CR, but not PV (Ma et al., 2007). More recently, relaxin-3 was found to be co-expressed to varying degrees with GABA, CB *and* CR in rat NI (Singleton CE et al., 2017, ms in preparation). Although some differences have been observed in the neurochemical profile of mouse and rat relaxin-3 NI neurons (Zhang C, Ma S, personal communication), the available data suggest that relaxin-3 can be co-released with GABA from NI neurons, and that relaxin-3 can perform complementary inhibitory roles to GABA in target areas such as the septum and hippocampus (see below).

In addition to relaxin-3, a number of other neuropeptides have also been identified within rat NI neurons, including cholecystokinin (CCK) (Kubota et al., 1985; Olucha-Bordonau et al., 2003), substance P, galanin, dynorphin (Sutin & Jacobowitz 1988), neurotensin (Jennes et al., 1982) and a 'ranatensin-like peptide', neuromedin-B (NMB) (Chronwall et al., 1985). The enzyme AChE has been detected within rat NI neurons (Sutin and Jacobowitz, 1988; Olucha-Bordonau et al., 2003), suggesting the NI may be functionally influenced by acetylcholine (see Ryan et al., 2011 for review; Ma and Gundlach, 2015).

Immunohistochemical studies have revealed that CRF receptor 1 (CRF_1) is expressed by the majority of relaxin-3 NI neurons in the rat (Tanaka et al., 2005). In line with these findings, increased c-*fos* expression was observed within the NI following intracerebroventricular (icv) administration of CRF, and following a water immersion-restraint stress protocol (Tanaka et al., 2005). Interestingly, acute swim stress provokes rapid CRF-dependent increases in relaxin-3 mRNA expression in rat NI neurons (Banerjee et al., 2010), while CRF-induced depolarisation of relaxin-3 NI neurons was prevented by the CRF_1 antagonist, NBI35965 (Ma et al., 2013).

The sources of this afferent CRF are likely to be numerous, and include the lateral preoptic hypothalamus (Ma et al., 2013). An intrinsic CRF innervation is also possible, as a recent study identified CRF mRNA within the rat NI (Walker et al., 2016). A small population of CRF-IR neurons were also observed in the NI of the rat, and mouse (using a CRF-reporter mouse strain, Crh-IRES-CrexAi14), and in both cases a small number of neurons appeared to co-express relaxin-3 (Walker et al., 2016). Relaxin-3-positive neurons in the rat NI express 5-HT_{1A} receptors (Miyamoto et al., 2008), and 5-HT depletion (chemically induced by intraperitoneal (i.p) injection of p-chlorophenylalanine (PCPA) significantly increased relaxin-3 mRNA in the NI, suggesting 5-HT neurons from the DR directly innervate NI relaxin-3 neurons and act to inhibit relaxin-3 expression. In a more recent study, administration of an anxiogenic drug, FG-7142, followed by exposure to an elevated plus maze resulted in an increase in c-*fos* expression in 5-HT neurons in the DR (dorsal and ventrolateral regions) and relaxin-3 neurons in the NI of adult rats (Lawther et al., 2015). These data support the hypothesis that the relaxin-3 system in the NI and 5-HT system in the DR interact to form part of a network involved in the control of anxiety-related behaviour. Furthermore, immunohistochemical and electrophysiological studies in rat have shown that NI relaxin-3 neurons co express and orexin-2 receptors (OX_2), and are depolarised in response to bath application of orexin-A (Blasiak et al., 2015), providing additional support the NI may be involved in arousal and motivated behaviours.

Importantly, recent studies in our laboratory have identified the selective expression of tropomyosin receptor kinase A (TrkA) by relaxin-3 positive neurons in the rat NI (Singleton CE et al., ms in preparation), consistent with the detection of TrkA-IR in the rat NI in an earlier study in which the NI was incorrectly identified (Sobreviela et al., 1994). TrkA is a high affinity nerve-growth factor (NGF) receptor, which regulates synaptic strength and plasticity and is required for normal cognitive functioning (Woolf et al., 2001; Rispoli et al., 2008; Liu et al., 2014). Notably however, TrkA-IR was not co-localized with relaxin-3-IR in the mouse NI (Zhang C et al, unpublished observation), indicating a major difference in the nature of trophic support utilised by these neurons in these two main experimental species.

1.3.2 Ascending projections of relaxin-3 nucleus incertus neurons

Neuronal fibres and terminals containing relaxin-3-IR are broadly distributed throughout the rodent brain (**Figure 1.2**; Ma et al., 2007; Smith et al., 2010), including a dense innervation of the septal nuclei, amygdala, hippocampal formation, and hypothalamic nuclei. This distribution closely matches the distribution of NI efferent projections (Tanaka et al., 2005; Ma et al., 2007; Smith et al., 2010), providing strong evidence that may contribute to relaxin-3 may contribute to some or all of the functional roles of the NI (see section 1.5.1.2).

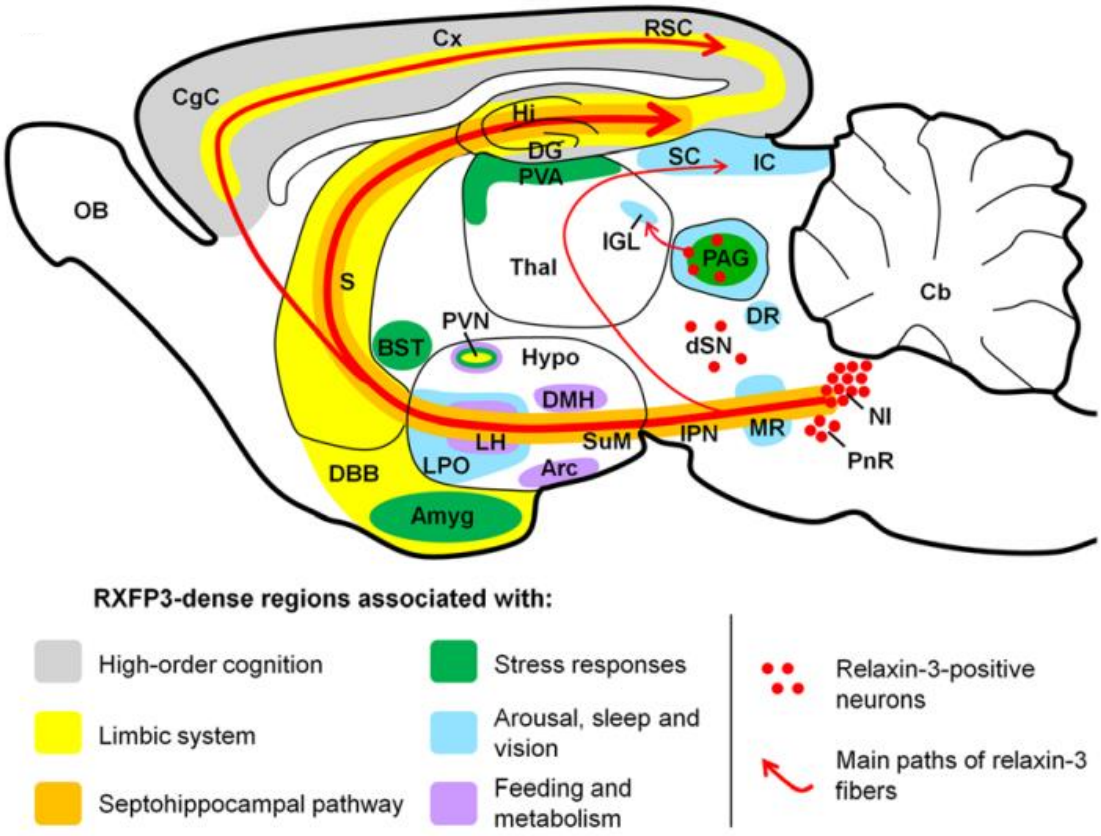

Figure 1.2. Distribution of the relaxin-3/RXFP3 system in rodent brain

Schematic parasagittal representation of the rodent brain, illustrating the ascending relaxin-3 system and the distribution of RXFP3 in regions grouped by functions (Smith et al. 2014). Relaxin-3 expressing neurons (red dots) broadly project (red arrows) throughout the brain from distinct populations in the nucleus incertus, periaqueductal grey, pontine raphe and an area dorsal to the substantia nigra. RXFP3-dense regions strongly overlap with the presence of dense relaxin-3 immunoreactive fibres. Relevant publications: relaxin mRNA and IR (Osheroff and Ho, 1993; Burazin et al., 2005); relaxin binding sites (Osheroff and Ho, 1993; Burazin et al., 2005; Ma et al., 2007); relaxin-3 IR fibres (Tanaka et al., 2005; Ma et al., 2007; Smith et al., 2010); RXFP3 mRNA and binding sites (Sutton et al., 2004; Smith et al., 2010). Abbreviations (alphabetical order): Amyg, amygdala; Arc, arcuate nucleus, BST, bed nucleus of stria terminalis; Cb, cerebellum; CgC, cingulate cortex; Cx, cerebral cortex; DBB,

diagonal band of Broca; DG, dentate gyrus; DMH, dorsomedial nucleus of hypothalamus; DR, dorsal raphe nucleus; dSN, region dorsal to the substantia nigra; Hi, hippocampus; Hypo, hypothalamus; IC inferior colliculus; IGL, intergeniculate leaflet; IPN, interpeduncular nucleus; LH, lateral hypothalamus; LPO, lateral preoptic area; MR, median raphe; NI, nucleus incertus; OB, olfactory bulb; PAG, periaqueductal grey; PnR, pontine raphe; PVA, paraventricular thalamic area; PVN, paraventricular hypothalamic area; RSC, retrosplenial cortex; S, septum; SC, superior colliculus; SuM, supramammillary nucleus; Thal, thalamus.

Relaxin-3-positive axonal projections are prominent within the SHS, with the highest density of relaxin-3-IR in the rodent forebrain in the MS (Ma et al., 2007; Smith et al., 2010), whereas lower levels are observed in the adjacent lateral septum (LS). Within the hippocampus, relaxin-3-IR is present at a high density in the oriens layer, and a moderate density in the bordering alveus, and a much low density in the pyramidal cell layer (**Figure 1.3**). Within the dentate gyrus (DG), a moderate density of relaxin-3-IR is detected throughout the hilus layer.

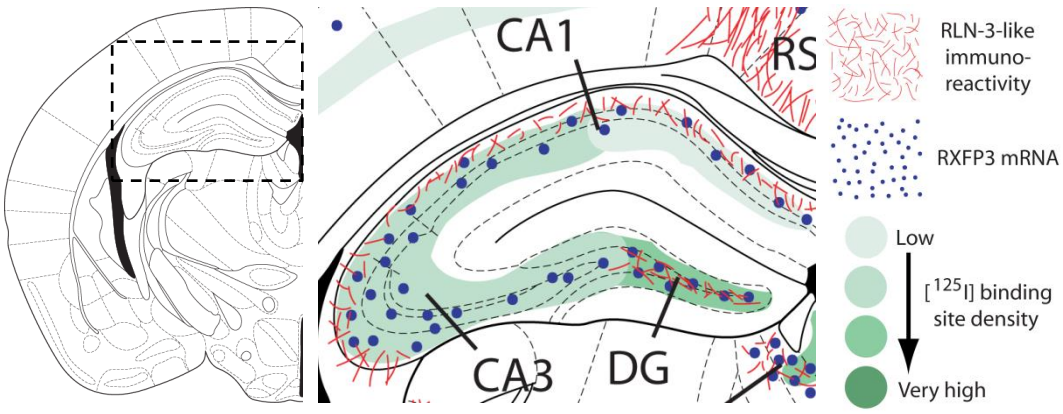

Figure 1.3. Distribution of relaxin-3 and RXFP3 in mouse dorsal hippocampus

Left: Coronal drawing of mouse brain at -1.94 mm relative to bregma, adapted from the stereotaxic atlas of Paxinos and Watson (2007). *Middle:* Schematic representation of the distribution and densities of relaxin-3 (RLN-3)-like immunoreactivity (red lines), RXFP3 mRNA (blue dotes) and RXFP3 binding sites labelled by [^{125}I]-R3/I5 (green areas), in a coronal section of all subfields of mouse dorsal hippocampus. *Right:* Legend.

Other brain regions which display prominent relaxin-3-positive neuronal projections include the hypothalamus, where high densities of relaxin-3-IR fibres are observed adjacent to the supraoptic nucleus (SON), and a low density is observed within the paraventricular hypothalamic nucleus (PVN). The amygdala also contains relaxin-3-IR fibres with low to moderate densities in the central (CeA), medial (MeA) and basomedial (BMA) nuclei. A detailed summary of the distribution of relaxin-3-IR fibres in the rat and mouse brain can be found in Ma et al. (2007) and Smith et al. (2010), respectively.

1.4 Relaxin family peptide 3 receptor (RXFP3) and its distribution in brain

The cognate receptor for relaxin-3 is RXFP3, a seven-transmembrane domain G-protein-coupled receptor known as GPCR135 (G-protein-coupled receptor 135; Liu et al., 2003; Sutton et al., 2004). It was initially discovered in 2000 using low stringency hybridization screening of a human cerebral cortex cDNA library (Matsumoto et al., 2000), and was given the name somatostatin- and angiotensin-like peptide receptor (SALPR) due to its high amino acid sequence similarity with the SST (SSTR5) and angiotensin (AT1) receptors. Considerable evidence suggests that RXFP3 is the preferred endogenous receptor for relaxin-3 (Bathgate et al., 2013). Cell-based assays have revealed that following relaxin-3 binding; RXFP3 couples to $G_{i/o}$-proteins resulting in inhibition of adenylate cyclase, and a reduction of cytoplasmic cyclic adenosine monophosphate (cAMP) accumulation (Liu et al., 2003). Reduced cAMP levels in neurons is often associated with hyperpolarisation, which further supports the notion that relaxin-3 performs a synergistic inhibitory function to GABA upon release.

However, bath application of a specific RXFP3 agonist, R3/I5, resulted in an activation of RXFP3-positive neurons in the rat IGL, which co-express NPY. Conversely, RXFP3-positive and NPY-negative neurons *were* hyperpolarised (Blasiak et al., 2013). In a more recent study, RXFP3 activation by the selective agonist, RXFP3-A2 (Shabanpoor et al., 2012), resulted in a reduction in firing frequency of the majority of recorded (responsive) neurons in the magnocellular and parvocellular regions of the PVN, whereas a small number of PVN neurons displayed an increase in firing frequency (Kania et al., 2017). Taken together, these data suggest heterogeneous effects following RXFP3 activation. In addition to RXFP3's inhibitory effect via the cAMP pathway, these differential results suggest RXFP3 may also activate the MAPK pathway (Kocan et al 2016), in specific target neuron populations. In cell based studies,

RXFP3 activation stimulates the extracellular signal-regulated kinase (ERK) 1/2 pathway through a protein kinase C-dependent mechanism, resulting in downstream changes in gene expression (van der Westhuizen et al., 2007).

Furthermore, both human and rat RXFP3 proteins consist of 469 amino acids, whereas the mouse RXFP3 contains 472 amino acids. Rat and mouse RXFP3 share high sequence homology with human RXFP3 (86% and 85%, respectively) and with each other (94%) (van der Westhuizen et al., 2007).

The neuroanatomical distribution of RXFP3 mRNA and binding sites has been assessed in mouse and rat brain using *in situ* hybridization and radioligand binding studies, respectively (**Figure 1.4**; Sutton et al., 2004; Ma et al., 2007; Smith et al., 2010), revealing a strong overlap with relaxin-3-IR fibres (Ma et al., 2007; Smith et al., 2010) in regions such as the septum, hippocampus, amygdala, lateral and paraventricular hypothalamus, interpeduncular and supramammillary nuclei, periaqueductal grey, and raphe nuclei. The RXFP3 distribution in non-human primate or human has not yet been described in detail, but there is evidence of similarities in *Macaca fascicularis* (Ma et al., 2009b) with the distribution seen in rodents.

1.4.1 Neurochemical characterisation of RXFP3-positive neurons

Although mapping the regional distribution of RXFP3 mRNA/binding sites has been informative in predicting the putative function of relaxin-3/RXFP3 signalling, it is still largely unknown which specific populations of neurons express RXFP3 within the different brain regions. Such information is crucial for determining the precise neural substrates through which relaxin-3/RXFP3 signalling modulates behaviour. Due to the unavailability of a specific RXFP3 antibody, conventional double-label immunohistochemical studies to neurochemically 'phenotype' RXFP3-positive neurons are not possible. In light of this limitation, a recent series of double-and triple-label immunohistochemical experiments using characterised relaxin-3 antisera and antisera for protein markers expressed by MS neurons in the rat (Olucha-Bordonau et al., 2012) observed relaxin-3 positive nerve fibres/terminals in close contact with MS ChAT-, PV-, and GAD67-positive neurons that project to the hippocampus, as well as contacts with local CB- and CR-positive neurons (Olucha-Bordonau et al., 2012). Consistent with this observation, in similar studies in the mouse relaxin-3-positive nerve fibres were observed in close apposition with MS/DB PV and ChAT-positive neurons and some contacts with MS CR-positive neurons (Haidar M, Tin K, Gundlach AL, unpublished data). Taken together, these data suggest RXFP3 within the MS/DB is expressed by neuronal populations important for the modulation of hippocampal function.

In order to visualize RXFP3-expressing neurons, our laboratory is also investigating a 'knock-in' transgenic mouse strain in which the Cre recombinase enzyme is expressed under the control of the RXFP3 promoter. These mice have been crossed with a second strain of mouse that expresses eYFP under the control of the strong Rosa26 promoter downstream of a floxed stop codon. In these resultant mice, Cre recombinase can potentially excise the stop codon exclusively within RXFP3-expressing neurons, allowing visualisation of these neurons by fluorescent microscopy in combination with immuno-labelling of other candidate markers. Although the validation of this mouse line is still ongoing, it should eventually allow RXFP3 neurons within at least some key brain regions to be neurochemically characterised.

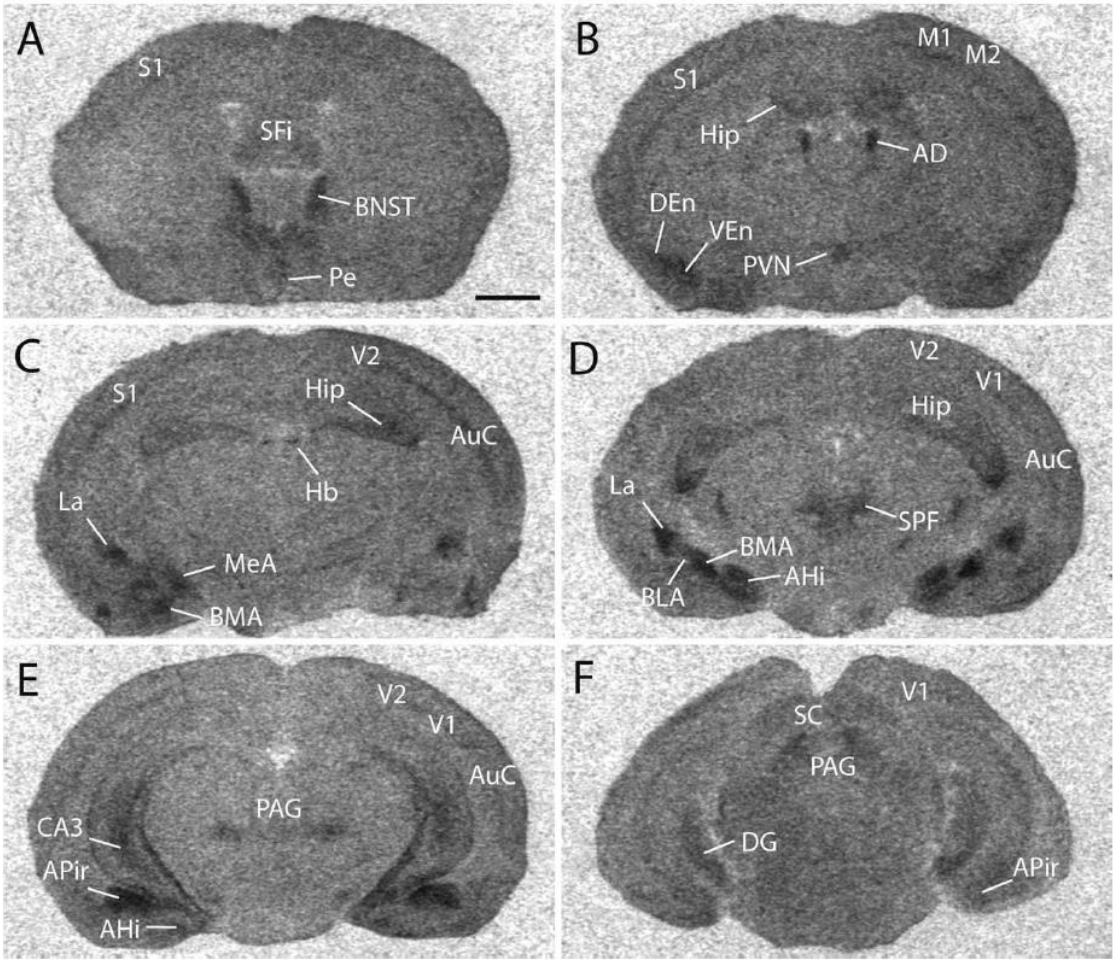

Figure 1.4. Distribution of RXFP3 mRNA in mouse brain

Distribution of RXFP3 mRNA in mouse forebrain detected by *in situ* hybridization (Smith et al. 2010). X-ray film autoradiograms of [^{125}I]-R3/I5 binding sites in selected coronal sections of the forebrain at the level of (A) bed nucleus stria terminalis; (B) hypothalamic paraventricular nucleus; (C) anterior amygdala and dorsal hippocampus; (D) posterior amygdala and anterior periaqueductal grey; (E) ventral hippocampus; (F) superior colliculus. Scale bar, 1.25 mm. Abbreviations (alphabetical order): AD, anterodorsal thalamic nucleus; AHi, amygdalohippocampal area; APir, amygdalopiriform transition area; AuC, auditory cortex; BLA, basolateral amygdala; BMA, basomedial amygdala; BNST, bed nucleus of stria terminalis; CA3, cornu ammonis 3 hippocampus; DEn, dorsal endopiriform nucleus; DG, dentate gyrus hippocampus; Hb, habenula; Hip, Hippocampus; La, lateral amygdala; M1, primary motor cortex; M2, secondary motor cortex; MeA, medial amygdala; Pe, periventricular hypothalamic nucleus; S1, primary somatosensory cortex; SC, superior colliculus; V1, primary visual cortex; V2, secondary visual corte

1.5 Studies to investigate three key features of the relaxin-3/RXFP3 system

This thesis describes studies that investigated three aspects of the relaxin-3/RXFP3 system:

i) The role of relaxin-3/RXFP3 signalling within the hippocampus (Chapter 2)
ii) The potential loss of relaxin-3 neurons in a mouse line with tauopathy-related neurodegeneration (Chapter 3)
iii) The ability of relaxin-3/RXFP3 signalling to interact with monoamine signalling (Chapter 4).

In addition to the introductory descriptions provided below, further introductory background information is provided in each separate experimental chapter.

1.5.1 Role of relaxin-3/RXFP3 signalling within the hippocampus?

As mentioned, relaxin-3-positive nerve fibres/terminals and RXPF3 mRNA-expressing neurons are enriched in the hippocampus, but two key features of relaxin-3/RXFP3 biology within the hippocampus that remain unknown are:

i) the neurochemical identity of RXFP3-positive neurons within the different regions of the hippocampus, and
ii) the physiological and behavioural effects of modulation of relaxin-3/RXFP3 signalling within the hippocampus.

1.5.1.1 Identity of RXFP3-expressing neurons within the hippocampus?

The hippocampus is a bilateral structure located in the medial temporal lobe, spanning across a dorsal-to-ventral axis in rodents, and a posterior-to-anterior axis in humans (Strange et al., 2014). The dorsal and ventral portions have different connectivity with cortical and subcortical structures, leading to differing functional roles (for reveiw see, Bannerman et al., 2014). Spatial memory and anxiety-related functions of the hippocampus are predominantly mediated by the dorsal (Morris et al., 2006) and ventral sub-regions respectively (Bannerman et al., 2003; Morris et al., 2006; Fanselow and Dong, 2010; Bannerman et al., 2014). Importantly, the connectivity and functionality of the dorsal and ventral regions of the hippocampus are highly conserved across species (Manns and Eichenbaum, 2006).

The hippocampal formation consists of three cytoarchitectonically distinct regions, namely the dentate gyrus, the subiculum and the hippocampus proper consisting of Cornu Ammonis (CA)-1, -2 and -3 (**Figure 1.5**, van Strien et al., 2009). The hippocampal formation comprises quite distinct layers including the hilus (polymorph layer) of the DG; the stratum oriens (SO) in the CA regions, comprising afferent and efferent fibres and interneurons; the granule cell layer in the DG; the pyramidal cell layer in the CA regions and subiculum, which are composed of principal cells and interneurons; and the molecular layer (the stratum molecular) in the DG and subiculum. Furthermore, the CA regions are further subdivided into multiple layers, with the stratum radiatum and the stratum lacunosum-molecular in all CA regions, and a third layer (stratum lucidum) exclusively in the CA1 and CA3 regions. In turn, the parahippocampal region consists of the medial and lateral entorhinal and perirhinal cortices, and the post-rhinal (in rodents) or parahippocampal (in humans) cortex.

The hippocampus is populated by a large diversity of GABAergic interneurons, representing approximately 10% of the total hippocampal neuronal population (for review see, Freund and Buzsaki, 1996; Somogyi and Klausberger, 2005; Katona et al., 2016; Schmid et al., 2016; Stefanelli et al., 2016). While glutamatergic cells in the hippocampus predominantly modulate neuronal excitability of local circuits, GABAergic interneurons provide inhibitory control of both local circuits and projection regions. For example, in the DG hilus, GABAergic interneurons inhibit granule cell excitability mainly via feedback circuits from mossy fibre collaterals, and via feed forward circuits from entorhinal cortex and contralateral hippocampal inputs (Freund and Buzsaki, 1996; Katona et al., 2016). Additionally, in the CA1, cells in the oriens layer are a major subclass of hippocampal interneurons involved in controlling synaptic plasticity (Leao et al., 2012; Mikulovic et al., 2015) and SST has been frequently used as a molecular marker for identification of CA1 oriens layer cells (Forro et al., 2015). Recent studies have suggested different subtypes of SST-positive neurons differ in their activity and function (see Muller and Remy, 2014 for review).

Ramon y Cajal provided the first description of several different morphological subtypes of interneurons in the cerebral cortex and hippocampus (Ramon y Cajal, 1893). In the hippocampus, interneurons are now divided into 21 different subtypes which can be distinguished based on axonal distribution, synaptic targets, neuropeptide or calcium-binding protein content and physiological characteristics (Freund and Buzsaki, 1996; Maccaferri and

Lacaille, 2003; Somogyi and Klausberger, 2005). For example, interneurons of the DG can be visualized with antibodies to neuropeptides including SST, CCK, NPY and VIP, or calcium-binding proteins PV, CB or calretinin (CR) (Jinno and Kosaka, 2002; Molgaard et al., 2014).

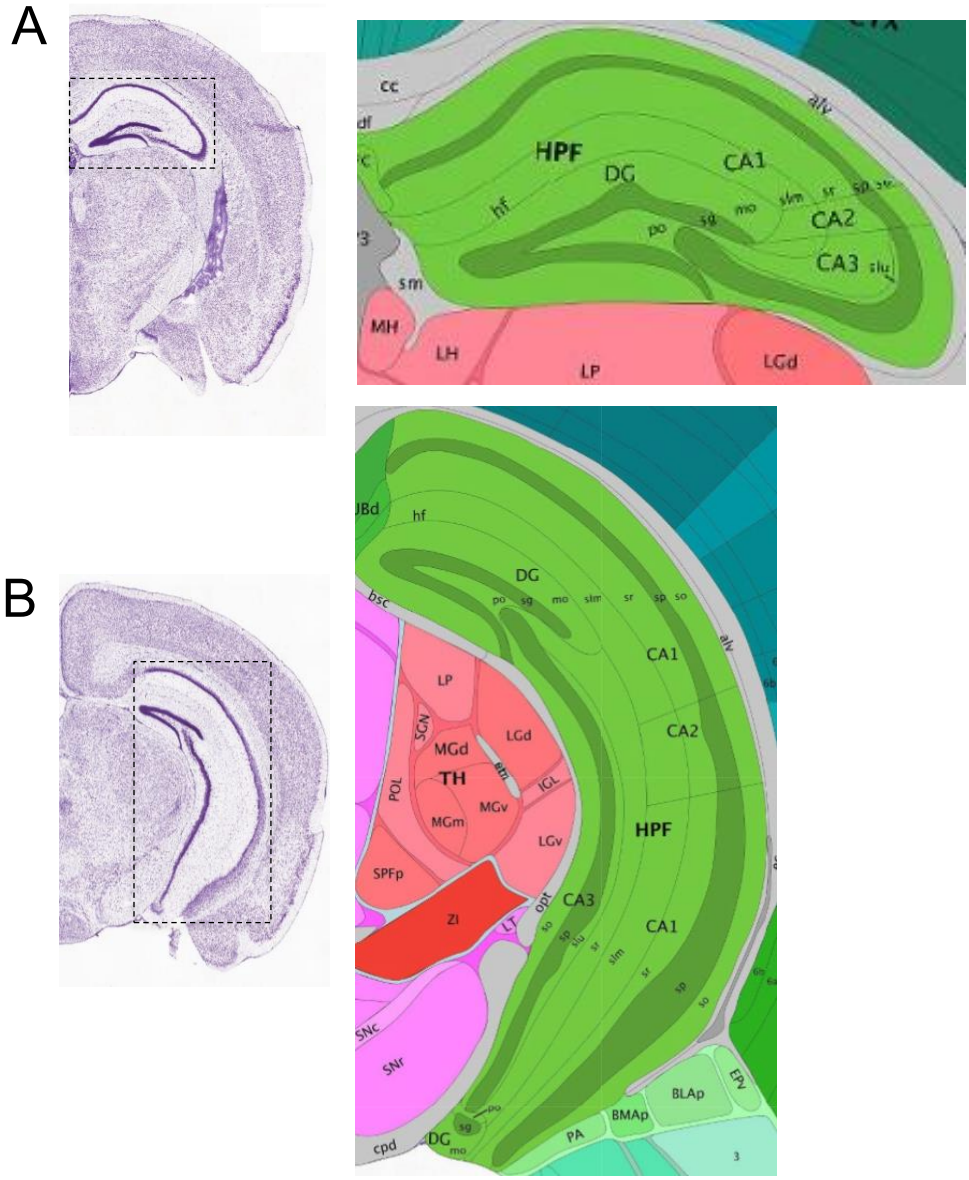

Figure 1.5. Coronal schematic of the mouse hippocampal region

Representative coronal Nissl (*left panel*) and brain map (*right panel*) of mouse dorsal (A) and ventral (B) hippocampus (and neighbouring regions) adapted from Allen Brain Institute Interactive Atlas <www.brain-map.org>. Abbreviations (alphabetical order): CA1, cornu ammonis-1; CA2, cornu ammonis-2; CA3, cornu ammonis-3; DG, dentate gyrus; FC, fasciola cinerea; hf, hippocampal fissure; HPF, hippocampal formation; po, polymorph layer; mo, molecular layer; sg, granule cell layer; slm, stratum lacunosum-moleculare; slu, stratum lucidem; so, stratum oriens; sp, pyramidal layer; sr, stratum radiatum.

Importantly, the distribution of relaxin-3 fibres and RXFP3 mRNA/binding sites in the hippocampal formation (Ma et al., 2007; Smith et al., 2010) is topographically similar to GABA expression in the hippocampus, particularly with the distributions of GABAergic subpopulations containing the neuropeptide SST, and the calcium-binding proteins PV, and CR (**Figure 1.6**, Freund and Buzsaki, 1996; Jinno and Kosaka, 2002; Baraban and Tallent, 2004). It is therefore very likely that GABAergic neurons within the hippocampus co-express RXFP3, supporting the proposal that relaxin-3/RXFP3 may confer some of its functional effects by directly inhibiting GABAergic neurons, and thereby indirectly disinhibiting principal neurons that are normally hyperpolarized by these GABAergic interneurons.

1.5.1.2 Role of relaxin-3/RXFP3 signalling within the hippocampus

The activity of GABAergic interneurons in the DG hilus is modulated by inputs from the septal nuclei. The MS/DB has been termed the hippocampal theta rhythm 'pacemaker' and consists of GABAergic and cholinergic neurons which provide alternating synchronous excitatory/inhibitory input to hippocampal neurons (Vertes and Kocsis, 1997; Wang, 2002) in all subfields, particularly the DG hilus (Wainer et al., 1984; Amaral and Kurz, 1985; Wainer et al., 1985; Lübke et al., 1997). More recently, glutamatergic projections from the MS/DB to the hippocampus have also been identified (Manns et al., 2001; Danik et al., 2003; Sotty et al., 2003; Danik et al., 2005). MS/DB cholinergic neurons innervate dendrites of pyramidal cells as well as cell bodies and dendrites of GABA- and SST containing interneurons (Frotscher and Léránth, 1985; Yamano and Luiten, 1989; Cobb and Davies, 2005), whereas GABAergic neurons specifically target hippocampal interneurons, providing inputs that in turn disinhibit pyramidal cells (Freund and Antal, 1988; Tóth et al., 1997). Interestingly, many of the hippocampal GABAergic cells that receive GABAergic septal projections are also immunoreactive for CCK, SST, or VIP, or contain one of the three major calcium-binding proteins CR, CB, or PV (Freund and Antal, 1988; Gulyas et al., 1990; Acsady et al., 1998).

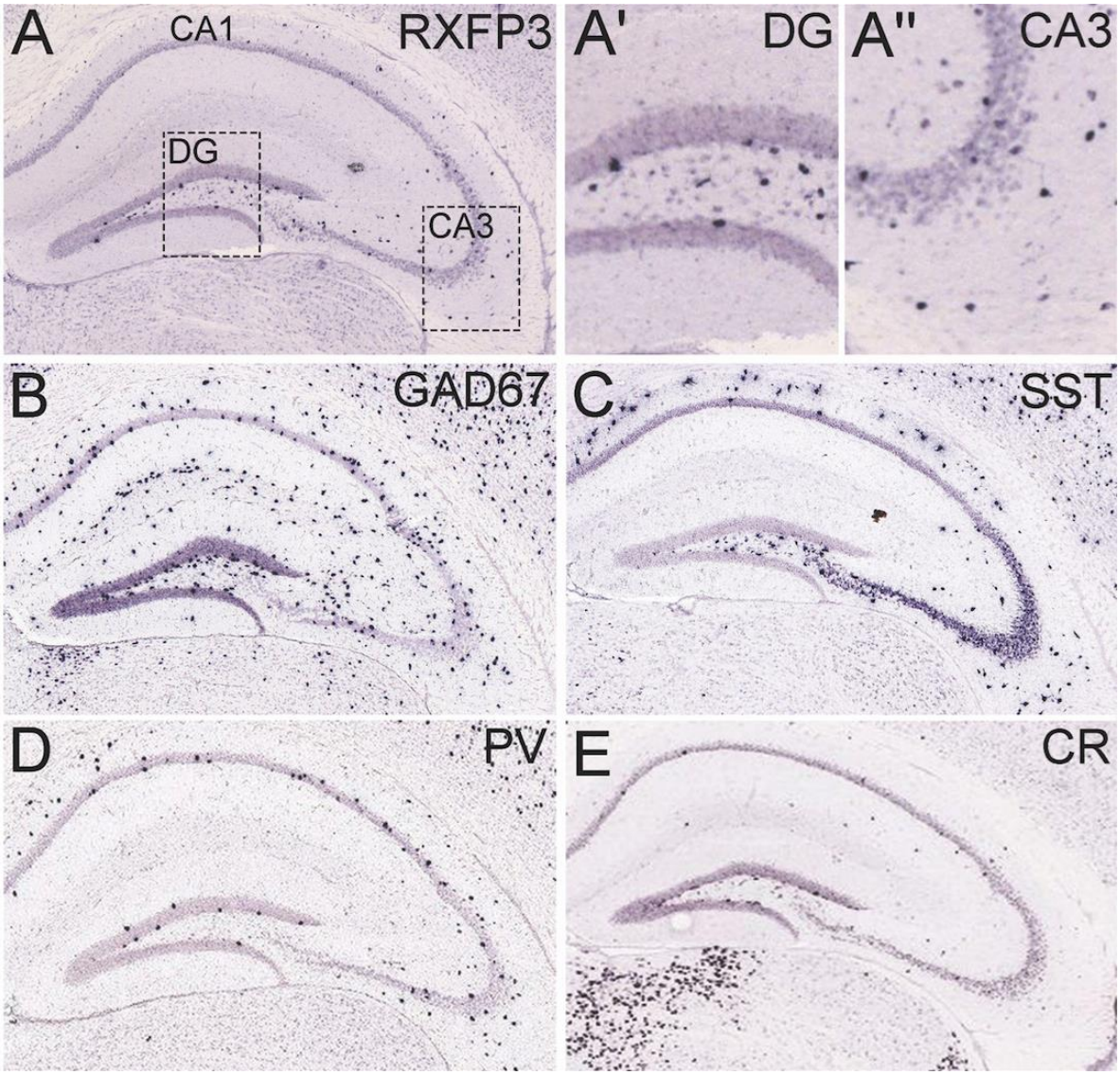

Figure 1.6. Comparative distribution in mouse dorsal hippocampus of RXFP3 mRNA and mRNAs encoding peptide and protein markers of hippocampal interneurons.

(A) Distribution of RXFP3 mRNA in adult mouse hippocampus with abundant expression detected in neurons located in CA1 stratum oriens, across the CA3 region and within the hilus of the dentate gyrus (DG) with higher magnification views of CA3 and DG (boxed areas) provided (A', A''). The comparative distribution of GAD67 (B), SST (C), PV (D), and CR (E) mRNAs illustrate the strong similarity between the distribution of RXFP3 mRNA positive neurons and *some* of the GAD67, SST, PV and CR mRNA positive neurons in the CA1 stratum oriens, CA3 region and hilus, suggesting that RXFP3 is expressed by a population of GABA interneurons (or projection neurons) in these areas. Images adapted from the Allen Brain Institute Gene Expression Atlas <www.brain-map.org>.

Hippocampal activity is also modulated by direct inputs (or via indirect projections to the MS/DB) from other subcortical regions including the SUM in the posterior hypothalamus, as well as serotonergic and noradrenergic projections from the DR and locus coeruleus (LC), respectively (Freund et al., 1990) (Milner et al., 1995; Bergado et al., 2007). Similarly, the bilateral reticular pontis oralis (RPO) nucleus in the brainstem relays through the MS to the hippocampus, and when activated/stimulated is highly effective at evoking hippocampal theta rhythm (Vertes and Martin, 1988; Vertes, 2005). Importantly, the adjacent NI receives strong input from the RPO (Teruel-Martí et al., 2008) and is involved in the modulation of hippocampal theta rhythm. Thus, the MS and the various other brain regions providing ascending inputs to hippocampus represent the main nodes of the SHS, and their combined activity strongly modulate hippocampal theta rhythm (**Figure 1.5**, see Brown and McKenna, 2015 for review).

Hippocampal theta rhythm is a state of hippocampal activity whereby a large proportion of principal neurons synchronously fire at a rate of ~4-10 Hz (in humans), which can be recorded by electroencephalography (Vertes and Kocsis, 1997). This pattern of activity is crucial for the hippocampus to execute its core functions in learning and memory (McNaughton and Gray, 2000).

Since the anatomical mapping of the NI (Goto et al., 2001; Olucha-Bordonau et al., 2003), experimental studies have tested the hypothesised physiological and behavioural involvement of this structure in the modulation of hippocampal theta rhythm and spatial memory (Teruel-Martí et al., 2008). In an early study by Nunez and colleagues (2006), electrical stimulation of the NI evoked hippocampal theta rhythm in urethane-anaesthetised rats, while theta rhythm evoked by RPO stimulation was abolished following electrolytic lesions of NI or by pharmacological inhibition with the $GABA_A$ agonist, muscimol. This suggests the NI may be a critical relay station in the pathway connecting the RPO with the MS/DB to initiate hippocampal theta rhythm. In support of this hypothesis, anterograde tracer (fluorescein-labeled dextran biotin amine (BDA), or dextran tetra-methyl rhodamine and biotin, (miniruby)) injections into the RPO revealed an abundant projection from the RPO to the NI (Teruel-Martí et al., 2008). This projection was confirmed by injections of retrograde tracer (hydroxystilbamidine methane sulfonate, Fluorogold) into the rat NI. Interestingly, injections of a retrograde tracer into the MS/DB further confirmed the strong NI-MS/DB

projection. More recently, descending projections from the MS/DB to the rat NI were observed (Sanchez-Perez et al., 2015) suggesting a bidirectional 'feedback loop' to modulate hippocampal theta rhythm via inputs to major nodes of the SHS.

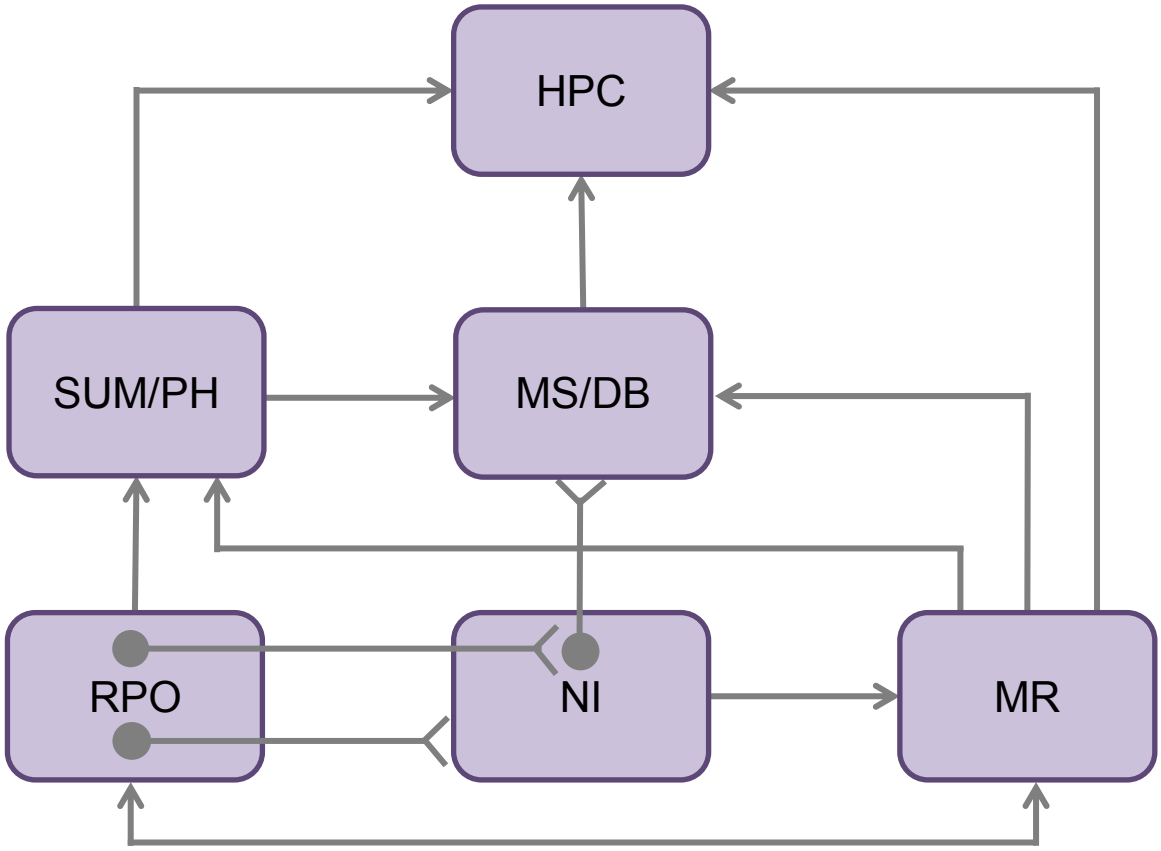

Figure 1.7. Schematic diagram illustrating the 'ponto-septal-hippocampal circuitry'

Schematic diagram illustrating the proposed position of the NI within the classic 'ponto-septal circuitry' involved in the control of hippocampal theta rhythm. NI GABA/relaxin-3 positive neurons receive input from neighbouring reticular pontis oralis (RPO) neurons, representing a putative pathway complementary to the well-established RPO-SUM-MS/DB circuit. The main efferent targets of the NI include the MR, SUM and MS/DB, as well as direct projections from the NI to the hippocampus. A direct connection between the RPO and neurons in the NI which project to the MS has been identified (adapted from Teruel-Marti et al. 2008). Abbreviations: HPC, hippocampus; MRn, median raphe nucleus; MS/DB, medial septum/diagonal band of Broca; NI, nucleus incertus; RPO, reticular pontis oralis; SUM/PH, supramammillary nucleus/posterior hypothalamus.

In further support of the capacity of the NI to modulate hippocampal theta rhythm and spatial memory, pharmacological blockade of the NI by lidocaine impaired the long-term spatial memory of adult rats in a Morris water maze (MWM) (Nategh et al., 2015). Similarly, inhibition of rat NI neurons using the hM4Di DREADD resulted in a deficiency in spatial working memory in a discrete reward alternation Y-maze task and a disruption of long-term

spatial memory in a MWM (Ong-Pålsson EKE et al., personal communication). Interestingly, electrolytic lesions of the rat NI resulted in a delayed extinction of conditioned freezing responses (Pereira et al., 2013), indicating a modulatory role of the NI in fear conditioning, possibly mediated via direct and/or indirect projections to the extended amygdala.

Although the ability of the NI to modulate SHS function may involve GABA and other neurotransmitters that are released by these neurons, importantly, relaxin-3/RXFP3 signalling appears to significantly contribute to this role. Functional studies have confirmed the regulation of hippocampal theta rhythm and memory by RXFP3 modulation in the MS. Direct administration of an RXFP3 agonist into the rat MS significantly enhanced hippocampal theta power in both anaesthetized rats and conscious rats moving freely in a home-cage environment (Ma et al., 2009c). In contrast, infusions of an RXFP3 antagonist significantly reduced hippocampal theta power in conscious rats, and attenuated hippocampal theta activity driven by electrical stimulation of the RPO in anaesthetized rats (Ma et al., 2009c). These pharmacological manipulations and resulting changes in hippocampal theta rhythm also translated into observable changes in behaviour. For example, infusions of an RXFP3 antagonist into the MS dose-dependently impaired the performance of rats in a spontaneous alternation plus maze task (Ma et al., 2009c), which is used to assess spatial working memory, and is hippocampal theta activity dependent (Iwahara et al., 1972; Fujisawa and Buzsáki, 2011). Interestingly, co-treatment with an RXFP3 agonist was able to significantly rescue the impairment observed in spatial working memory (Ma et al., 2009c). In a more recent study, icv infusion of RXFP3-A2 (Shabanpoor et al., 2012), a selective relaxin-3 receptor agonist, increased ERK phosphorylation in cholinergic neurons in the rat MS/DB, and resulted in an impairment in spatial working memory in a delayed spontaneous T-maze task (Albert-Gasco et al., 2017). In agreement with earlier anatomical studies (Olucha-Bordonau et al., 2012), these results suggest the relaxin-3/RXFP3 system may directly or indirectly modulate the activity and function of MS/DB cholinergic neuron activity.

1.5.2 The loss of relaxin-3 neurons in a mouse model of tauopathy

Alzheimer's disease (AD) is currently the most common age-dependent neurodegenerative disorder. A major neuropathological hallmark of AD is the formation of neurofibrillary tangles (NFTs, first described and depicted by Alois Alzheimer, Alzheimer, 1907), which are clumps of intra-neuronal filaments composed of abnormally hyperphosphorylated tau and aggregated microtubule-associated tau protein (Goedert and Spillantini, 2006; Wang and Mandelkow, 2016). NFTs are not unique to AD, but are also observed in other neurodegenerative diseases that are collectively designated as 'tauopathies'; including progressive supranuclear palsy, Pick's disease, Huntington's disease, frontotemporal dementia with parkinsonism (FTDP-17) (Hutton et al., 1998) and other tauopathies (Irwin, 2016).

Loss of memory is among the first symptoms reported by patients suffering from tauopathies, including AD. Memory dysfunctions are in part due to NFT accumulation in limbic regions, particularily the hippocampus which is known for its role in modulating memory functions, as well as neocortical regions (Braak and Braak, 1991). Importantly, dysfunction of the hippocampus, as well as other limbic cortical regions, occurs via two ways (described in Chapter 3, Section 3.2); (i) loss/damage of hippocampal neurons themselves, and/or (ii) loss/damage of afferent inputs (e.g. NA/LC and 5-HT/DR) that normally control hippocampal function (Clavaguera et al., 2009; Braak et al., 2011; de Calignon et al., 2012; Liu et al., 2012; Ahmed et al., 2014; Iba et al., 2015).

As summarised above (Section 1.5.1.1 and 1.5.1.2), relaxin-3-IR axonal fibres from the NI which project to the hippocampus are likely to play an important role in normal hippocampal function and cognition. Importantly, the NI and relaxin-3/RXFP3 systems are proposed to perform synergistic and complementary roles to monoamine signalling (i.e. NA/LC and 5HT/DR ascending brainstem systems which are damaged in tauopathies and related disease, Trillo et al., 2013) within shared efferent target brain regions (for review see, Smith et al., 2014a). Therefore, it is likely that any loss of NI/relaxin-3 neurons may contribute to memory dysfunction observed in tauopathies; however, whether relaxin-3 neurons in the NI are damaged or spared in neurodegenerative conditions such as tauopathy is unknown.

1.5.3 Relaxin-3/RXFP3 system interactions with monoamine signalling

Wakefulness and activated behavioural states are mediated by signalling of a range of ascending arousal neurotransmitter systems (Saper et al., 2005), including the monoamines 5-HT, NA, acetylcholine and dopamine (Nestler, 1998; Saper et al., 2005; Berridge et al., 2012), as well as a range of peptide systems (Hokfelt et al., 2003). Considerable anatomical evidence suggests the NI/relaxin-3 system contributes to a brainstem ascending arousal system (Ma et al., 2007; Smith et al., 2010). For example, as mentioned, relaxin-3 neurons project to many forebrain regions that regulate arousal, such as the midbrain, cortex, thalamus, and limbic and septohippocampal regions, in a similar way to ascending monoaminergic systems, in close agreement with LC/NA and DR/5-HT pathways. Indeed, NI/relaxin-3, LC/NA and DR/5-HT neural systems display highly overlapping efferent projection patterns.

Furthermore, functional studies have suggested relaxin-3/RXFP3 signalling involvement in a range of arousal-related functions which are also strongly modulated by LC/NA and DR/5-HT systems (Smith et al., 2014a). For example, arousal encompasses many behavioural processes including wakefulness and motivated goal-directed behaviour, responses to stress and anxiety, and hippocampal-dependent behavioural activation. These behaviours are strongly controlled by LC/NA and DR/5-HT systems, among other transmitter and peptide systems (Nestler, 1998; Saper et al., 2005; Berridge et al., 2012). Similarly, functional studies in mouse and rat have demonstrated that the relaxin-3/RXFP3 system performs similar functional roles to monoamine systems, suggesting that relaxin-3/RXFP3 signalling may work in a synergistic and complimentary manner. For example, relaxin-3/RXFP3 is functionally associated with sleep/wake states and circadian rhythm (Smith et al., 2012), feeding (McGowan et al., 2006; Ganella et al., 2013; Smith et al., 2014b) and motivation (Hosken et al., 2015), responses to stress (Tanaka et al., 2005; Banerjee et al., 2010; Watanabe et al., 2011; Walker et al., 2015) and anxiety (Ma et al., 2010; Ryan et al., 2013; Zhang et al., 2015), and modulation of hippocampal theta activity (Ma et al., 2009c). Taken together, anatomical and functional studies strongly suggest relaxin-3/RXFP3 signalling might act synergistically with LC/NA and DR/5-HT systems within shared downstream structures to modulate arousal and stress-related behaviours.

Furthermore, depletion/disruption of LC/NA and DR/5-HT systems has been associated with a range of behavioural symptoms in animals. A reduction in monoamine signalling is strongly associated with depressive- (such as behavioural despair in mice) and anxiety-like behaviours. For example, methamphetamine can be used experimentally in rodent models of monoamine depletion to acutely induce the presynaptic release of monoamines such as NA and 5-HT, and causes their depletion following withdrawal from chronic use (Kita et al., 2003; Bamford et al., 2008; Yamamoto et al., 2010). This monoamine depletion is largely responsible for the symptoms associated with methamphetamine withdrawal syndrome that includes increased anxiety and depressive-like behaviours, as demonstrated in rodent studies (Kokkinidis et al., 1986; Cryan et al., 2003; Kitanaka et al., 2010). Therefore, based on the evidence described above, it is possible that during methamphetamine withdrawal relaxin-3/RXFP3 signalling may 'compensate' for the reduced monoamine signalling and might act to alleviate the negative affective features of methamphetamine withdrawal.

1.6 Hypotheses and Aims

In light of the current literature, including that summarised above, this thesis describes three studies that investigate different aspects of a central hypothesis that:

"Relaxin-3/RXFP3 signalling modulates the function of the hippocampus and related cortical and limbic brain areas, in line with the established roles of other brainstem arousal systems; and the relaxin-3/RXFP3 system may be relevant to the development or treatment of several neurodegenerative and psychiatric disorders that involve excitatory/inhibitory imbalance".

Aim 1 (Chapter 2): *Determine the identity of RXFP3-positive neurons in the hippocampus, and the role played by RXFP3 signalling within the dentate gyrus in learning and memory.*

Firstly, based on the overlap between the restricted topographical distribution of neurons expressing RXFP3 mRNA with the more extensive distribution of GABAergic interneurons, it was hypothesised that RXFP3 is expressed by a subpopulation of GABA neurons in the hippocampus, in particular the SST/GABA neurons that have a similar restricted topographical distribution. In the absence of a validated RXFP3 antibody, these studies determined which hippocampal neurons received a relaxin-3 innervation by immunohistochemical staining with a characterised monoclonal relaxin-3 antisera, and antisera for GABA, SST, PV and CR.

Secondly, based on the important role of DG hilus SST/GABA neurons in modulating learning and memory (Baratta et al., 2002; Andrews-Zwilling et al., 2010; Spiegel et al., 2013), and the likely expression of RXFP3 by SST/GABA populations in this region, it was hypothesised that RXFP3 depletion from the dorsal DG hilus would alter spatial memory. To test this hypothesis, the behaviour of adult 'floxed RXFP3' mice which had undergone bilateral viral-induced, Cre-recombinase-mediated deletion of RXFP3 from the dorsal DG hilus in tests of spatial learning and memory, was examined. The specificity of the observed effects and the effectiveness of the intended restriction of RXFP3 depletion to the dorsal DG hilus was tested by probing for any changes in anxiety-like behaviour in these mice, which are more generally associated with changes in ventral hippocampal activity (Bannerman et al., 2014).

Aim 2 (Chapter 3): *Determine whether the number of relaxin-3-positive and/or negative neurons in the nucleus incertus is altered in a transgenic mouse model of human tauopathy*

Relaxin-3-containing nerve fibres innervate the hippocampus and other brain structures that are dysfunctional in AD and tauopathies, and these disorders strongly affect the brainstem (Braak et al., 2011; Iba et al., 2015; Lee et al., 2015). Therefore, we hypothesised that relaxin-3-positive (and negative) neurons in the NI might be affected in a rodent model of tauopathy. If these neurons were reduced in number by the tauopathy related neuronal degeneration, it would raise the possibility that this loss might contribute to the decline in cognitive performance observed in these mice (Ramsden et al., 2005; Kremer et al., 2011; Hunsberger et al., 2015), with implications for AD and tauopathy patients. In these studies, the brains from 8 month-old transgenic tau-P301L mice and age-matched controls were studied. The numbers of relaxin-3-positive and -negative neurons in the NI were counted in age- and strain-matched controls and tau-P301L mice following immunohistochemical staining. In addition, the number of NI neurons displaying phosphorylated tau (p-tau)-IR was assessed.

Aim 3 (Chapter 4): *Determine whether reduced relaxin-3/RXFP3 signalling is able to alter the anxiety and depressive-like symptoms observed during methamphetamine withdrawal*

Based on the possible synergistic roles of relaxin-3/RXFP3 and monoamine signalling systems (Miyamoto et al., 2008; Lawther et al., 2015), it was hypothesized that endogenous relaxin-3/RXFP3 signalling might compensate for the reduced monoamine signalling and increased anxiety and depressive-like behaviours that are observed during withdrawal from chronic

methamphetamine treatment in mice (Kokkinidis et al., 1986; Cryan et al., 2003; Kitanaka et al., 2010). To test this hypothesis, 'global' relaxin-3 and RXFP3 KO mice and their respective WT littermates, were subjected to multiple daily methamphetamine or vehicle injections for 10 days; and then treatment was halted to induce methamphetamine withdrawal. Behavioural testing for relative levels of innate anxiety and depressive-like symptoms was conducted over the subsequent 3 weeks period.

CHAPTER 2

Role of relaxin-3/RXFP3 signalling in hippocampus

2.1 Introduction

This Chapter contains a body of experimental work, complete with Introduction, Methods, Results, Conclusion, Bibliography and Supplementary Information, which is presented as a manuscript that was accepted for publication in the peer-reviewed scientific journal, *Hippocampus*, on 18 January, 2017.

HIPPOCAMPUS 27:529–546 (2017)

Relaxin-3 Inputs Target Hippocampal Interneurons and Deletion of Hilar Relaxin-3 Receptors in "Floxed-RXFP3" Mice Impairs Spatial Memory

M. Haidar,[1,2] G. Guèvremont,[3] C. Zhang,[1,2] R.A.D. Bathgate,[1,2,4] E. Timofeeva,[3] C.M. Smith,[1,2,5†] and A.L. Gundlach [1,2,6*†]

ABSTRACT: **Hippocampus is innervated by γ-aminobutyric acid (GABA) "projection" neurons of the *nucleus incertus* (NI), including a population expressing the neuropeptide, relaxin-3 (RLN3). In studies aimed at gaining an understanding of the role of RLN3 signaling in hippocampus via its $G_{i/o}$-protein-coupled receptor, RXFP3, we examined the distribution of RLN3-immunoreactive nerve fibres and RXFP3 mRNA-positive neurons in relation to hippocampal GABA neuron populations. RLN3-positive elements were detected in close-apposition with a substantial population of somatostatin (SST)- and GABA-immunoreactive neurons, and a smaller population of parvalbumin- and calretinin-immunoreactive neurons in different hippocampal areas, consistent with the relative distribution patterns of RXFP3 mRNA and these marker transcripts. In light of the functional importance of the dentate gyrus (DG) hilus in learning and memory, and our anatomical data, we examined the possible influence of RLN3/RXFP3 signaling in this region on spatial memory. Using viral-based Cre/*LoxP* recombination methods and adult mice with a floxed Rxfp3 gene, we deleted Rxfp3 from DG hilar neurons and assessed spatial memory performance and affective behaviors. Following infusions of an $AAV^{(1/2)}$-Cre-IRES-eGFP vector, Cre expression was observed in DG hilar neurons, including SST-positive cells, and *in situ* hybridization histochemistry for RXFP3 mRNA confirmed receptor depletion relative to levels in floxed-RXFP3 mice infused with an $AAV^{(1/2)}$-eGFP (control) vector. RXFP3 depletion within the DG hilus impaired spatial reference memory in an appetitive T-maze task reflected by a reduced percentage of correct choices and increased time to meet criteria, relative to control. In a continuous spontaneous alternation Y-maze task, RXFP3-depleted mice made fewer alternations in the first minute, suggesting impairment of spatial working memory. However, RXFP3-depleted and control mice displayed similar locomotor activity, anxiety-like behavior in light/dark box and elevated-plus maze tests, and learning and long-term memory retention in the Morris water maze. These data indicate endogenous RLN3/RXFP3 signaling can modulate hippocampal-dependent spatial reference and working memory via effects on SST interneurons, and further our knowledge of hippocampal cognitive processing. © 2017 Wiley Periodicals, Inc.**

KEY WORDS: **Cre/LoxP; dentate gyrus; GABA/somatostatin interneurons; nucleus incertus; RXFP3**

[1] **The Florey Institute of Neuroscience and Mental Health, Parkville, Victoria, Australia;** [2] **Florey Department of Neuroscience and Mental Health, The University of Melbourne, Victoria, Australia;** [3] **Department of Psychiatry and Neurosciences, Faculty of Medicine, Laval University, Quebec, Canada;** [4] **Department of Biochemistry and Molecular Biology, The University of Melbourne, Victoria, Australia;** [5] **School of Medicine, Deakin University, Victoria, Australia;** [6] **Department of Anatomy and Neuroscience, The University of Melbourne, Victoria, Australia**

Additional Supporting Information may be found in the online version of this article.

Grant sponsor: National Health and Medical Research Council of Australia; Grant numbers: 1024885, 1067522; Grant sponsors: Brain & Behavior Research Foundation (USA) NARSAD Independent Investigator Award; Victorian Government Operational Infrastructure Support Programme; Natural Sciences and Engineering Research Council of Canada; Canadian Institutes of Health Research; Alzheimer's Australia Dementia Research Foundation, Postgraduate Scholarship; Bethlehem Griffiths Research Foundation, Postgraduate Scholarship.

*Correspondence to: Prof Andrew L. Gundlach, The Florey Institute of Neuroscience and Mental Health, 30 Royal Parade, Parkville, Victoria 3052, Australia. E-mail: andrew.gundlach@florey.edu.au

†These authors jointly supervised this research.

Accepted for publication 12 January 2017.

DOI 10.1002/hipo.22709

Published online 18 January 2017 in Wiley Online Library (wileyonlinelibrary.com).

INTRODUCTION

The hippocampus plays an important role in learning and memory, in both rodents and humans (O'Keefe and Nadel, 1978; Burgess et al., 2002). The hilus (or hilar region) of the dentate gyrus (DG) contains a diverse population of interneurons, which are thought to be crucial in mediating these roles (Freund and Buzsaki, 1996). Interneurons within the DG hilus (as well as hippocampal CA1 and CA3 fields) receive GABAergic and cholinergic inputs from the medial septum/diagonal band of Broca (MS/DB) (Freund and Antal, 1988; Dutar et al., 1995; Vertes and Kocsis, 1997), which together with a number of other subcortical structures [e.g., supramammillary nucleus (Kocsis and Vertes, 1997; Ruediger et al., 2011) and median raphe (MR) (Vertes et al., 1999; McKay et al., 2013)] constitute the "septohippocampal system" (Freund and Antal, 1988; Dutar et al., 1995; Vertes and Kocsis, 1997). The majority of GABAergic septal projection neurons terminate on DG hilus interneurons (Freund and Antal, 1988; Amaral et al., 2007) participating in the control of hippocampal theta oscillations (Vertes and Kocsis, 1997; Vertes, 2005; Lubenov and Siapas, 2009), and the processing of cognitive and spatial maps (O'Keefe, 1993; Leutgeb et al., 2005; Schiller et al., 2015).

In addition to these well characterized forebrain subcortical sources of afferent input, brainstem GABA projections to the hippocampus have been characterized (see Brown and McKenna, 2015, for review). GABAergic projections from the nucleus incertus (NI) (Nunez et al., 2006; Olucha-Bordonau et al., 2012; Ma et al., 2013; Sanchez-Perez et al., 2015) and nucleus of Gudden (VTg) (Bassant and Poindessous-Jazat, 2001; Kocsis et al., 2001; Bassant and Poindessous-Jazat, 2002) can regulate hippocampal theta rhythm (4–8 Hz in rodents and 4–12 Hz in humans), which is important for spatial navigation and memory formation. The NI, which sits within the dorsal tegmentum, sends strong GABA-positive projections to the MS/DB, hippocampus, supramammillary nucleus and MR nucleus, amongst other hypothalamic and limbic circuits that influence hippocampal activity (Goto et al., 2001; Olucha-Bordonau et al., 2003). Stimulation of the NI in urethane-anesthetized rats increased theta and decreased delta rhythm activity in the hippocampus, whereas electrolytic lesions of the NI abolished hippocampal theta rhythm (Nunez et al., 2006).

More recently, it was reported that lidocaine infusion into the NI impaired long-term spatial memory of adult rats in a Morris water maze (MWM) (Nategh et al., 2015) and delayed learning and impaired retention in a passive avoidance learning (PAL) task (Nategh et al., 2016), which are both hippocampal-dependent memory tasks. In the latter study, perforant path-DG short-term synaptic plasticity was also examined upon NI inactivation, both before a paired-pulse stimulation, and before or after tetanic stimulation, in freely moving rats; revealing that NI inactivation did not change the perforant path-DG granule cell synaptic input, but decreased the excitability of DG granule cells, consistent with an effect of normal NI activity to inhibit the inhibitory interneurons in the DG and disinhibit granule cells (Nategh et al., 2016).

A large population of NI neurons express abundant levels of the neuropeptide relaxin-3 (RLN3) (Bathgate et al., 2002; Burazin et al., 2002), which acts via its cognate $G_{i/o}$-protein coupled receptor, relaxin family peptide receptor 3 (RXFP3) (Liu et al., 2003; Bathgate et al., 2006). RLN3 neurons in the NI co-express glutamate decarboxylase (GAD), the enzyme involved in converting glutamate to GABA (Ma et al., 2007). RLN3-positive efferents overlap extensively with NI forebrain projections (Ma et al., 2007; Ma et al., 2009c; Smith et al., 2010), and in a GAD2-Cre reporter mouse, injection of a Cre-dependent viral vector expressing enhanced yellow fluorescent protein (eYFP) into the NI produced strong eYFP colocalization with RLN3-IR in NI neurons, and in hippocampus (including DG hilus) extensive eYFP-IR was observed, suggesting RLN3- and GAD-positive neurons in the NI provide projections to the hippocampus (S Ma, personal communication). RLN3-positive fibres make close contacts with MS/DB neurons which project to the hippocampus, including populations that express choline acetyltransferase (ChAT) or GAD67 and/or parvalbumin (PV) cells (Olucha-Bordonau et al., 2012), which are known to act as "pacemaker" cells for hippocampal theta rhythm. Furthermore, the distribution of RLN3 fibres strongly overlaps with that of RXFP3 mRNA in the MS/DB and hippocampus, and other forebrain areas (Tanaka et al., 2005; Ma et al., 2007; Smith et al., 2010). Injection of a RXFP3-selective agonist peptide (R3/I5; Liu et al., 2005) into the MS increased hippocampal theta rhythm in urethane-anesthetized rats, which was significantly attenuated by prior injection of a selective RXFP3 antagonist (R3(BΔ23-27)R/I5, Kuei et al., 2007). In conscious rats, R3/I5 injection into the MS increased hippocampal theta rhythm in a home cage environment, whereas injections of R3(BΔ23-27)R/I5 dose-dependently reduced hippocampal theta rhythm in rats exploring a novel, enriched context, and impaired performance in a spontaneous alternation task (SAT) (Ma et al., 2009a). However, the neurochemical mechanism(s) by which the RLN3/RXFP3 system modulates hippocampal activity are largely unknown and there are no studies of this system in mice.

In the present studies designed to address this gap in knowledge, the first aim was to determine which hippocampal neurons are potentially regulated by RLN3/RXFP3 signaling. We initially examined the regional distribution of RXFP3 mRNA in the mouse hippocampus, but due to the current unavailability of a fully validated RXFP3 antibody, double-label immunohistochemistry studies to neurochemically phenotype RXFP3-positive neurons were not possible. Therefore, we conducted a series of double- and triple-label immunohistochemical experiments using a characterized monoclonal RLN3 antisera and antisera raised against key markers expressed by the hippocampus, including GABA, the neuropeptide somatostatin (SST), and the calcium-binding proteins PV and calretinin (CR). Next we assessed the behavioral role of the RLN3/RXFP3 system within the DG hilus in "floxed-RXFP3" mice, in which the endogenous RXFP3 gene is flanked by two *loxP* sites ("floxed"). In these floxed-RXFP3 mice, RXFP3 can be "conditionally" deleted from neurons within discrete brain regions of adult mice by local viral delivery of the Cre recombinase restriction enzyme, which detects *loxP* sites and deletes the stretch of DNA between them (Ryding et al., 2001). Thus, this approach provides temporal control and spatial specificity of receptor deletion.

These studies have revealed that RLN3-positive fibres terminate on a population of SST- and GABA-positive neurons, and a smaller population of PV- and CR- positive neurons. Appositions were observed most notably with SST-positive neurons in the DG hilus, as well as in CA1 and CA3 fields. Interestingly, conditional hippocampal RXFP3 depletion in the DG hilus impaired spatial reference memory in mice, in an appetitive T-maze reference memory task and spatial working memory in a continuous SAT in a Y-maze. We also assessed anxiety-like behavior, based on the key functional influence of the ventral hippocampus on stress and anxiety (Bannerman et al., 2004; Engelmann et al., 2006), and the substantial number of neuroanatomical and functional studies that suggest a role for RLN3/RXFP3 signaling in responses to stress and anxiety (Banerjee et al., 2010; Smith et al., 2011, 2014; Watanabe et al., 2011; Shabanpoor et al., 2012; Ma et al., 2013; Ryan et al., 2013). Notably however, anxiety-like behavior was unaltered, suggesting a likely regional functional specificity of

RLN3/RXFP3 signaling within the hippocampus, although the viral spread did not extend across the entire dorsoventral extent of the DG hilus in the ventral hippocampus, therefore likely reducing any potential effect on anxiety-like behavior. Taken together, these findings suggest that *endogenous* RLN3/RXFP3 signaling modulates neurons within the DG hilus, particularly a population of GABA/SST-expressing neurons, to promote spatial reference and working memory (Andrews-Zwilling et al., 2012).

MATERIALS AND METHODS

Mice

"Floxed-RXFP3" mice, generated by Gen-O-way (Paris, France), were kindly supplied by Janssen Pharmaceutical Companies of Johnson & Johnson (La Jolla, CA), and bred within The Florey Institute of Neuroscience and Mental Health Animal Facility. These mice possess a 5′-*loxP* site located 1.4 kb upstream of the RXFP3 5′UTR, while a 3′-*loxP* site is located directly after the STOP codon and upstream of the 3′UTR. Floxed-RXFP3 mice were originally generated on a 129SV/B6 mixed background before being subjected to successive rounds of backcrossing onto a C57BL/6 background for 8–10 generations, via a >99% purity speed congenic approach. All studies were conducted with approval from The Florey Institute of Neuroscience and Mental Health Animal Ethics Committee and were in accordance with ethical guidelines issued by the National Health and Medical Research Council of Australia.

Behavioral experiments were performed on male homozygous RXFP3-floxed mice between 11 and 20 weeks of age ($n = 12–13$ per group). Mice were group housed (mixed treatments, ~4 mice per box) for the duration of studies. Mice were acclimatized to behavioral rooms 24 h prior to testing, and were maintained on a 12-h light-dark cycle (lights on 0700–1900) with regular chow and water available *ad libitum*, except during a food restriction regime used during T-maze testing (see below).

Detection of RXFP3 mRNA by *In Situ* Hybridization Histochemistry

Mice were deeply anesthetized with 5% isoflurane inhalation (Delvet, Seven Hills, NSW, Australia) and then administered sodium pentobarbital (100 mg kg^{-1}, 0.1 mL, i.p.) and transcardially perfused with 0.1 M phosphate buffer (PB, 2.7 mM KCI, 11.2 mM Na_2HPO_4, 1.8 mM KH_2PO_4, pH 7.4) followed by 4% paraformaldehyde (PFA) in 0.1 M PB. Mice were decapitated and their brains removed and post-fixed in 4% PFA in 0.1 M PB for 6 days. Brains were then transferred to a solution of 4% PFA and 20% sucrose in 0.1 M PB and kept at 4°C overnight. Brains were frozen on dry ice and 25 µm sections were cut using a sliding microtome (Histoslide 2000, Heidelberg, Germany). Levels of RXFP3 mRNA expression in the hippocampus were analyzed by *in situ* hybridization as described (Martin and Timofeeva, 2010; Lenglos et al., 2014; Lenglos et al., 2015). An RXFP3 riboprobe was generated from the 907-bp fragment of rat RLN3 receptor RXFP3 cDNA (Gene bank NM_001008310; the probe included 274–1180 bp sequence of the complete 1431 bp rat RXFP3 cDNA; forward primer: 5′-AGCGCC-GTTTACTGGGTGGTTTG-3′; reverse primer: 5′-TGGGGTTGAGGCAGCTGTTGGAGT-3′). NCBI BLAST sequencing revealed that the cDNA for rat RXFP3 is 93% homologous to mouse RXFP3.

Double- and Triple-Label Immunohistochemistry for RLN3 and GABA, CR, PV, or SST

For analysis of RLN3 in nerve fibres in relation to key neurochemical markers of hippocampal neurons, a sequential double- and triple-label immunohistochemistry protocol was used. To enhance immunoreactivity in cell bodies, 10-week-old male mice ($n = 3$) were administered colchicine (20 µg in 5 µl) into the lateral ventricle using a stereotaxic procedure (described below), at a rate of 1 µL per min. Sixteen (16) h post-surgery, mice were transcardially perfused (4% PFA in 0.1 M PB) and post-fixed in 4% PFA in 0.1 M PB for 1 h at RT, then transferred to a solution of 20% sucrose in 0.1 M PB and kept at 4°C overnight. Brains were then embedded in O.C.T. (Tissue-Tek; Sakura Finetek, USA) and frozen over dry ice and stored at −80°C. Forty (40) µm coronal sections were cut and collected into 4 series spanning from −1.22 mm to −3.80 mm from Bregma using a cryostat (Cryocut 1800, Leica Microsystems, Heerbrugg, Switzerland) at −18°C and stored in cryoprotectant solution (30% ethylene glycol, 30% glycerol, 0.05M PB) at −20°C.

All sections were washed 3 × 5 min with 0.1% Triton X-100 in 0.1 M PB, and then blocked in 10% normal horse serum (NHS) in 0.1% Triton X-100, 0.1 M PB for 1 h at RT. Sections were incubated with a mouse monoclonal RLN3 antibody (HK4-144-10; Kizawa et al., 2003; Tanaka et al., 2005; Ma et al., 2013) in 2% NHS and 0.1% Triton X-100 in 0.1M PB overnight at RT (for dilutions and information about the primary antisera used, see Supporting Information Table S1). On the following day, sections were washed 3 × 5 min in 0.1 M PB, followed by incubation in donkey anti-mouse Alexa-594 (JIR, 715585151, 1:500) or donkey anti-mouse Alexa-647 (JIR, 715605151, 1:500) in 0.1 M PB for 1 h at RT. Following application of the secondary antibody for visualization of RLN3-IR, sections were washed 3 × 5 min with 0.1 M PB and incubated with either: (1) rabbit anti-GABA (Sigma, A2052, 1:3,000) (2) rabbit anti-PV (Abcam, ab11427, 1:1,000) and rat anti-SST (Millipore, MAB354, 1:200) (3) and rabbit anti-CR (Swant, CR7697, 1:1,000) in 2% NHS, 0.1% Triton X-100, 0.1 M PB overnight at RT. Sections were washed 3 × 5 min in 0.1 M PB before incubation in the following secondary antibodies (1) donkey anti-rabbit Alexa-488 (Life Tech, A21206, 1:500) (2) donkey anti-rat Alexa-488 (Life

Tech, A21208, 1:500) and donkey anti-rabbit Alexa-594 (JIR, 711585152, 1:500) and (3) donkey anti-rabbit Alexa-488 (Life Tech, A21206, 1:500) in 0.1 M PB for 1 h at RT. Following the secondary antisera incubation, sections were washed 3 × 5 min with 0.1 M PB and mounted on glass slides using Fluoromount-G (Southern Biotech, Birmingham, AL).

Resultant staining was observed under a LSM 780 Zeiss Axio Imager 2 confocal laser scanning microscope (Carl Zeiss AG, Jena, Germany). Each fluorescence channel was imaged sequentially using a 20× objective for mosaic z stacks (1 µm intervals) and the total proportions of GABA-, SST-, PV- and CR- positive neurons contacted by RLN3-IR fibres were manually counted from the dorsal hippocampus of a representative unilateral coronal section from three mice (−2.54 mm from Bregma) based on the strong RLN3 fibre innervation observed at this coronal level. Mosaic z-stack images covering the entire hippocampus from each representative coronal section were obtained with 10% overlap between each image on the *X–Y* plane, and a defined region was set up for the z plane to scan from the bottom to the top of each image comprising the mosaic. Z-stack images (63× objective, 0.1 µm intervals) were taken to further evaluate putative contacts between RLN3-IR nerve fibres and hippocampal cellular markers. A putative contact was scored when an RLN3-IR fibre/terminal bouton was observed immediately adjacent to the cell body of a neuron expressing a hippocampal marker.

Adeno-associated Viral (AAV) Vectors

The AAV mosaic serotype 1/2 with capsid from AAV1 and ITR (internal terminal repeats) AAV2 was purified and harvested as described (Ganella et al., 2013). The AAV$^{(1/2)}$-Cre-IRES-eGFP viral vector encodes Cre recombinase and an enhanced green fluorescent protein marker (eGFP) linked by an internal ribosome entry site (IRES) sequence, allowing for the expression of Cre recombinase and eGFP from a single vector. The control AAV$^{(1/2)}$-eGFP construct was also packaged in a 1/2 mosaic capsid, encoding the expression of eGFP marker protein. Transcription of both constructs was driven by the chicken β-actin (sCAG) promoter. The titres were assessed visually in HEK293T cells under a fluorescent microscope and by measuring genomic copies (gc) per ml (g mL^{-1}), using quantitative polymerase chain reaction (qPCR). The resulting titre of AAV$^{(1/2)}$-Cre-IRES-eGFP and the control AAV$^{(1/2)}$-eGFP vector were ∼2 × 10^{11} g mL^{-1}.

Stereotaxic Surgery

Mice were initially anesthetized with 5% isoflurane inhalation (Delvet) mixed with oxygen till loss of righting reflex, then secured in a small animal stereotaxic frame (Kopf Instruments, Tujunga, CA) with 1.5–2% isoflurane delivered through a small animal nose cone. Analgesic (Meloxicam 20 mg kg^{-1}; Troy Laboratories, Smithfield, NSW, Australia) was then administered intraperitoneally (i.p., 0.1 mL), and eyes were moistened with lubricating eye ointment (Lacri-Lube, Allergen, NJ). A small midline incision was made to expose the skull, which was then cleaned/dried with 6% hydrogen peroxide. AAV$^{(1/2)}$-Cre-IRES-eGFP viral vector or control AAV$^{(1/2)}$-eGFP viral vector was loaded into a glass capillary injector which was connected to polyethylene tubing and a 10 µl Hamilton syringe (0.46 mm diameter, Harvard Apparatus, Holliston, MA, USA), and mounted on an infusion pump (PicoPlus, Harvard). Small holes were drilled through the skull above the injection sites, and the glass capillary was lowered to the following coordinates from Bregma based on the mouse brain atlas (Paxinos and Franklin, 2001): anterior–posterior, −2.3 mm; medial-lateral, −1.60 mm; dorsal-ventral, −2.1 mm; adjusted proportionally for skull size, determined by Bregma-interaural distance). Viral vectors were infused at a rate of 0.1 µL min^{-1} to a total volume of 1 µL. After each infusion, the injector was left in place for 7 min, retracted 1.0 mm, and left for another min to minimize deposition of virus in the injection tract, before being slowly removed. After surgery, the skin incision site and holes in the skull were closed/sealed with glue (superglue, Daiso, Hiroshima, Japan) and a single suture. After surgery mice were placed in recovery chambers (30°C, Thermacage, Datesand, Manchester, UK) for ∼1 h, and left to recover for 3 weeks to allow for Cre expression, RXFP3 gene deletion, and subsequent RXFP3 protein depletion.

Validation of Cre Expression (Cre-IR) within SST Neurons

In studies to assess Cre-recombinase expression in the targeted area and the expression of Cre within SST-positive neurons, coronal sections (40 µm) were washed 3 × 5 min with 0.1% Triton X-100 in 0.1 M PB, and then blocked in 10% NHS in 0.1% Triton X-100 and 0.1 M PB for 1 h at RT. Tissue were then incubated with rabbit polyclonal Cre antibody (Novagen, 69050-3, 1:500, $n = 3$) and rat monoclonal anti-SST (Millipore, MAB354, 1:200, $n = 3$) in 2% NHS and 0.1% Triton X-100 overnight at RT. On the following day, sections were washed 3 × 5 min in 0.1 M PB, followed by incubation in anti-rabbit Alexa-594 secondary antibody (Jackson ImmunoResearch Laboratories, Address, USA, 120330, 1:500) and anti-rat Alexa-594 secondary antibody (1:500) in 0.1 M PB. Sections were then washed 3 × 5 min with 0.1 M PB and mounted on glass slides using Fluoromount-G (Southern Biotech, Birmingham, AL). The resulting staining was observed under a Zeiss Axio Imager 2 confocal laser-scanning microscope (Carl Zeiss AG, Jena, Germany).

Validation of RXFP3 mRNA Deletion

RXFP3 mRNA loss following AAV$^{(1/2)}$-Cre-IRES-eGFP injection, was measured in mice injected bilaterally with AAV$^{(1/2)}$-Cre-IRES-eGFP ($n = 5$), or with AAV$^{(1/2)}$-eGFP ($n = 3$). Twenty-one days after stereotaxic surgery, mice were transcardially perfused (4% PFA in 0.1 M PB). For quantitative analyses, slides were examined with dark-field microscopy using an Olympus BX61 microscope (Olympus Canada, Richmond Hill, ON, Canada). Images were acquired with a DVC-

2000C digital camera (Thorslabs Scientific Imaging, Austin, TX) and analyzed with Stereo Investigator software (MBF Bioscience, Williston, VT). Brain sections from Bregma −1.7 mm to −2.7 mm (based on a stereotaxic atlas of mouse brain (Paxinos and Franklin, 2001)) were used for quantitative analyses. The optical density (OD) was obtained by defining the contour of the region of interest (DG and CA3), and three background contours (regions without positive hybridization signal) were collected to correct for the average background signal. This analysis was taken from 3 to 5 sections on each side of the brain for bilaterally injected mice, and from 7 to 12 sections from unilaterally injected mice. The mean OD of $AAV^{(1/2)}$-Cre injected tissue was normalized to the mean value of RXFP3 mRNA in $AAV^{(1/2)}$-GFP injected tissue, to obtain the relative level of RXFP3 mRNA for each section.

Validation of Cre Targeting of Dentate Gyrus Hilus

Following confirmation that local hippocampal injection of $AAV^{(1/2)}$-Cre-IRES-eGFP viral vector resulted in Cre expression and deletion of RXFP3 mRNA in floxed-RXFP3 mice, in subsequent studies, the presence of Cre-IR throughout the DG hilus was taken as sufficient evidence of adequate RXFP3 depletion within this structure. For all histological analyses a 1-in-3 series of brain sections was collected spanning from −1.22 mm to −3.80 mm from Bregma (Paxinos and Franklin, 2001), and only mice which had consistent expression of Cre-IR throughout the DG hilus of dorsal hippocampus were included in behavioral analyses. Of the 16 mice that received bilateral $AAV^{(1/2)}$-Cre-IRES-eGFP injections, four mice were excluded from the analyses due to a lack of transduced neurons present in the DG hilus. No viral spread was observed outside the DG and CA3.

Behavioral Tests

All behavioral experiments were conducted during the light phase, between 0900 and 1700 h, and were conducted from 21 days after surgery in the following order: (1) Automated locomotor cell; (2) Morris water maze (MWM); (3) Light/dark box; (4) Elevated plus maze; (5) Continuous spontaneous alternation test, and; (6) Appetitive spatial reference T-maze test. All mice were sacrificed 3 days after behavioral testing for histological analyses.

Automated Locomotor Cell

Mice were tested in a 27 × 27 cm^2 automated locomotor cell (Med Associates, Fairfax, VT), illuminated by 70 lux light, for a total duration of 1 h. The total distance travelled was tracked by a photobeam array. Data was analyzed using Activity Monitor, v.9.02 software (v.6.02; Med Associates).

Morris Water Maze (MWM)

In a test of hippocampus-dependent spatial reference long-term memory, mice were trained in a circular pool (1.2 m diameter) to locate a hidden platform (10 cm diameter) which was submerged ~0.5–1 cm beneath opaque water, made using non-toxic white paint and maintained at 18–22°C. The pool was surrounded by distal extra-maze cues. The acquisition phase consisted of six consecutive training days with four trials per day, with an inter-trial interval (ITI) of 30 min. For each trial, mice were placed in from a semi-random starting location (N, NW, E, SE) facing the pool wall, and were allowed to swim until they found the hidden platform or for a maximum of 30 s. If a mouse failed to locate the platform within the allocated time, the experimenter guided the mouse to the platform. The mouse then remained on the platform for 30 s, before being returned to its home cage, and allowed to dry under a heat lamp. For the acquisition sessions, a mean latency to locate the target quadrant was calculated for each mouse by averaging the latency to reach the platform across all four trials. Twenty-four (24) h after the last training day, the platform was removed from the target quadrant and the mice were allowed to swim freely for a duration of 120 s. The percent time spent in the target quadrant and the number of platform crossings was calculated.

Anxiety-like Behavior—Light/Dark Box

Mice were placed in the automated cells described above with half of the locomotor cell fitted with a black Perspex box, which was impermeable to visible light. The other half was exposed to a light-emitting diode array, illuminated the light side to ~700 lux in the centre and 650 lux in the corners, creating an aversive environment. For testing, mice were placed in the dark side of the apparatus for 10 min. A small opening in the Perspex box allowed access between both sides of the cell. Time spent in and number of entries into the light side was recorded using Activity Monitor software (v.6.02; Med Associates).

Elevated Plus Maze (EPM)

The apparatus consisted of four 30 cm long and 6 cm wide arms extending from a central square (6 × 9 × 6 cm^3), elevated 39 cm above the ground. High (15 cm) walls enclosed two opposing "closed" arms, while the two opposite arms were "open". Mice were placed in the centre of the apparatus, and were allowed to roam freely for 10 min. Movement was tracked from above using Top Scan Lite 2.0 software, and the time spent in the open arms, and the number of entries into the closed and open arms, were assessed.

Spatial Working Memory: Continuous Spontaneous Alternation Test (SAT)

The SAT was conducted using an enclosed Y-maze, with each arm 10-cm wide and 30-cm long, with 17 cm high walls. The maze was cleaned with water between tests and for testing; mice were placed in the centre of the arena facing the "home" arm. Mice are allowed free access to the three arms of the maze for a total of 10 min during which the sequence of arm

entries was recorded using Ethovision XT software. From these sequences, proportions of arms entered that were different from those previously entered were calculated to arrive at a percentage alternation score (PAS). An "alternation" is determined from successive entries of three arms in which three different arms are entered. PAS was calculated by dividing the number of observed alternations by the number of maximum possible alternations (total number of entries −2) and multiplying the quotient by 100.

Spatial Reference Memory: Appetitive T-Maze Test

Acquisition and reversal learning in a reward-based T-maze (each arm was 7.6 cm wide and each opposing arm was 26.7 cm long, with a 28.9 cm home arm, with 13 cm high walls) was tested as described (Moy et al., 2007). Acquisition of this task demands the use of allocentric spatial cues and is affected by hippocampal lesions (Deacon et al., 2002; Reisel et al., 2002; von Engelhardt et al., 2008). The maze was surrounded by distal 3D spatial cues placed 40 cm above and outside each arm. Before testing, mice were food deprived to 85–90% of their free-feeding body weight 5 days before testing and throughout the duration of the experiment. Mice were habituated (with four trials per day) to the T-maze and trained to obtain a food reward (0.2 g of chocolate-flavored rice puffs) from cups located at the ends of the two choice arms. Only when the mice could readily run from the start arm to a choice arm and consume their reward was acquisition commenced. After 5 days of habituation, 10 successive trials per day were initiated. One choice arm was designated the "reward" arm with a food reward (0.2 g chocolate-flavored rice puffs) placed at the end of the arm. The reward arm was on the left for half the mice, and on the right for the remainder, and this was randomized between treatment groups. At the beginning of each session, the mouse was placed in a start box at the bottom of the home arm. The start box door was opened, and the mouse was given the choice between entering either arm. Following a correct choice the mouse was given time to consume the food reward and then guided back into the start box to begin the next session. If the mouse made an incorrect choice it was left in the maze for 15 s before being guided back to the start box. To meet criterion, mice were required to make 80% correct choices for 3 consecutive days before reversal training commenced, in which the reward arm was switched to the opposite arm and 10 trials per day were initiated. Testing was stopped after criterion for individual mice was met during reversal. Time spent in junction before choice were recorded using Ethovision XT software; and the number of correct choices, and number of days to meet criterion were recorded by an observer.

Statistical Analysis

All graphs and statistical analysis were conducted using Graph Pad Prism (v.6) (GraphPad, La Jolla, CA). All data are expressed as mean ± SEM. Shapiro–Wilks test were employed to assess the shape of data distributions. For data sets which met the assumptions of normality, comparison of data was performed using either one-way ANOVA or two-way RM ANOVA, followed by appropriate post-hoc comparisons, as described or unpaired t test. For data sets which did not meet the assumption of normality, the non-parametric equivalent of a t test, the Mann–Whitney U test was used. Results were considered statistically significant if $P < 0.05$.

RESULTS

Distribution of RXFP3 mRNA and RLN3-Positive Innervation in Hippocampus

In agreement with previous studies in mouse (Smith et al., 2010) and rat (Ma et al., 2009c), the present study identified RXFP3 mRNA expression in mouse hippocampal formation (Fig. 1A) particularly in the DG hilus (Fig. 1B), across the stratum oriens layer of CA1, with less expression in the pyramidal layer of CA1 (Fig. 1C). RXFP3 mRNA was also detected in cells across the pyramidal, stratum oriens and radiatum layers of CA3 (Fig. 1D). Furthermore, the RXFP3 mRNA expression pattern overlapped the distribution of neuronal fibres and terminals containing RLN3-IR in the hippocampus (Fig. 2A), with abundant fibres observed in the DG hilus (Fig. 2B), and similar to RXFP3 mRNA levels, a smaller density of neuronal fibres containing RLN3-IR was observed in the pyramidal layer of CA1 and the stratum oriens of CA1 (Fig. 2C). Dense RLN3-positive fibres were detected across the pyramidal layer and radiatum of CA3 (Fig. 2D).

These results are also in agreement with the distribution of RXFP3 mRNA reported in the Allen Brain Institute atlas of gene expression (Fig. 3A). Notably, the distribution of RXFP3 mRNA and RLN3-positive nerve fibres is similar to that of a proportion or population of γ-aminobutyric acid (GABA) neurons in the hippocampus, as reflected by the pattern of GAD67 mRNA expression (Fig. 3B), as well as other populations of GABA neurons that express the neuropeptide, SST (Fig. 3C) and the calcium-binding proteins, PV (Fig. 3D) and CR (Fig. 3E), which are co-expressed with GABA in the hippocampus (Freund and Buzsaki, 1996; Jinno and Kosaka, 2002b; Baraban and Tallent, 2004).

RLN3 Innervation of Hippocampal Interneurons

For the analysis of RLN3-IR in neuronal fibres in relation to other markers of hippocampal neurons, a sequential double and triple label immunohistochemistry protocol was used with RLN3 *and* GABA, SST and the calcium-binding proteins, PV and CR (Fig. 4). Boutons containing RLN3-IR were observed in apposition to neurons positive for GABA (Fig. 4B), SST, PV (Fig. 4A; Supporting Information Fig. S1) and CR (Fig. 4C); and the number and proportions of the GABA-, SST-, PV-, and CR- positive neurons contacted by fibres containing RLN3-IR were counted in the unilateral dorsal hippocampus of a representative coronal section (−2.54 mm from Bregma), from three mice (see Materials and Methods for details), based

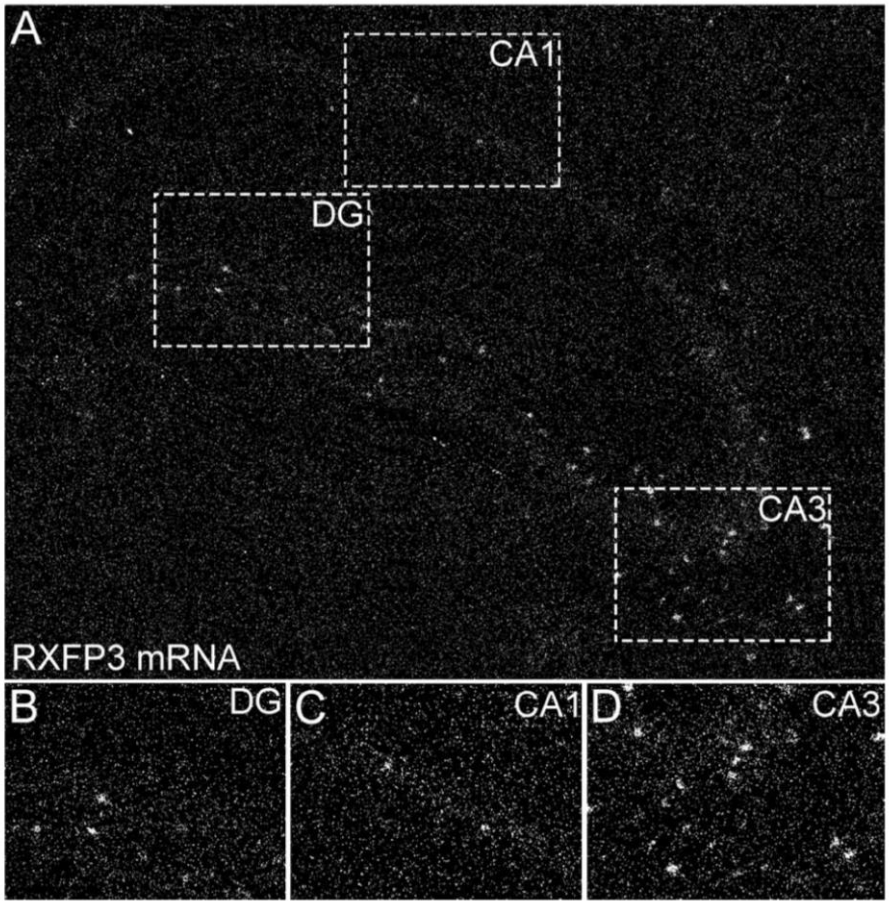

FIGURE 1. RXFP3 mRNA in the mouse dorsal hippocampus. Representative dark-field photomicrographs of emulsion autoradiographic analysis of RXFP3 mRNA expression in the hippocampus. (A) Silver grains for RXFP3 mRNA were detected in the DG hilus (B), the pyramidal layer and stratum oriens of the CA1 (C) and the radiatum, pyramidal layer and stratum oriens of the CA3 (D). Boxed areas in (A) indicate the areas illustrated in magnified images in (B–D).

on the strong RLN3 innervation observed at this level (Supporting Information Table S2).

A high density of SST neurons was detected within the DG hilus and stratum radiatum of CA1 and CA3 with the highest density in the oriens layer of both subfields, and in the material assessed, ~26% of SST-positive neurons (6 ± 1 of 23 ± 3 neurons counted, $n = 3$) in the DG hilus received contacts from fibres containing RLN3-IR. Similarly, ~14% of SST-positive neurons (5 ± 1 of 34 ± 6, $n = 3$) in the stratum oriens layer of CA1 and ~33% of SST-positive neurons (3 ± 2 of 8 ± 3, $n = 3$) in the stratum radiatum of CA3 were contacted by fibres containing RLN3-IR. Furthermore, we observed RLN3-positive bouton contacts on a subpopulation of GABA-positive neurons, representing ~12% of GABA-positive neurons (5 ± 0 of 46 ± 11, $n = 3$) in the DG hilus and ~15% of GABA-positive neurons (6 ± 2 of 38 ± 9, $n = 3$) in the stratum oriens layer of CA1. Notably, the number of neurons innervated by fibres containing RLN3-IR is similar for both SST and GABA populations with a total of 40 SST-positive neurons and 44 GABA-positive neurons (Supporting Information Table S2).

In contrast, neuronal fibres containing RLN3-IR were observed to innervate a smaller population of PV- and CR-positive neurons in the hippocampus, with ~23% of PV-positive neurons (1 ± 0 of 4 ± 1, $n = 3$) in the DG hilus innervated, and ~7% of PV-positive neurons (3 ± 1 of 45 ± 8) in the oriens layer of the CA3, and ~7% of PV-positive neurons (a total of 17 of 268) in all subfields of the hippocampus. Similarly, ~9% of CR-positive neurons (2 ± 1 of 23 ± 4, $n = 3$) in the DG hilus were innervated by fibres containing RLN3-IR, with only ~5% of CR-positive neurons (a total of 18 of 399, $n = 3$) innervated in all subfields of the hippocampus, in the material examined (Supporting Information Table S2).

In Vivo Validation of AAV$^{(1/2)}$-Cre-IRES-eGFP and Cre Expression in SST Neurons

Based on the reported role of SST-positive neurons in the DG hilus in learning and memory (Baratta et al., 2002; Andrews-Zwilling et al., 2010; Spiegel et al., 2013), and the appositions observed between RLN3-positive afferents and

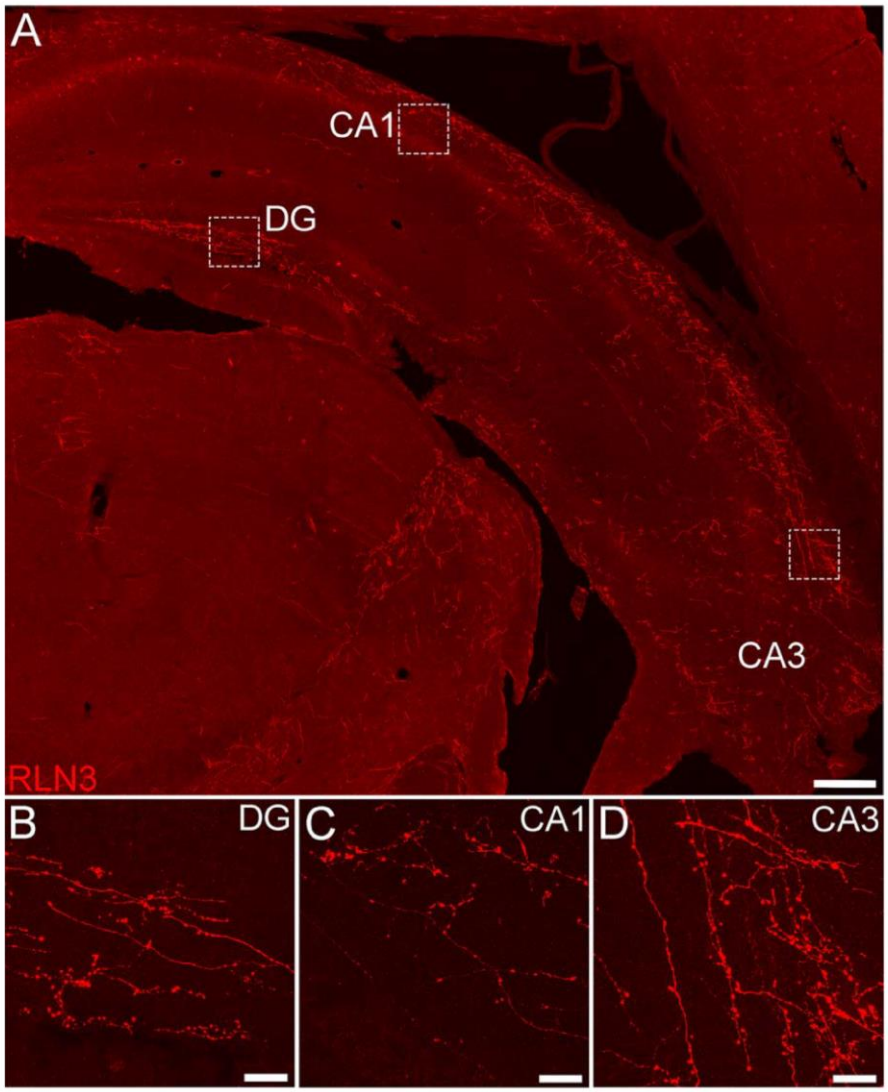

FIGURE 2. RLN3-positive nerve fibres and terminals in the mouse dorsal hippocampus. Mosaic confocal image (×20 magnification represented as z-stack maximum projections, 1 μm intervals) of mouse dorsal hippocampus illustrating RLN3-positive nerve fibres and terminals (A). Nerve fibres and terminals containing RLN3-IR were detected in the DG hilus (B), the pyramidal layer and stratum oriens of the CA1 (C) and the radiatum, pyramidal layer and stratum oriens on the CA3 (D). Boxed areas in (A) indicate the areas illustrated in magnified images (×63 maximum projections z-stacks, 0.1 μm intervals) (B–D). Scale bars, 200 μm (A) and 20 μm (B–D). [Color figure can be viewed at wileyonlinelibrary.com]

SST-positive neurons in the DG hilus, we examined the functional role of RXFP3 in this region by conditionally deleting RXFP3 in the DG hilus in adult floxed-RXFP3 mice using an AAV$^{(1/2)}$-Cre-IRES-eGFP viral vector. To validate that the AAV$^{(1/2)}$-Cre-IRES-eGFP viral vector effectively drove Cre recombinase expression *in vivo* and transduced hippocampal DG hilus SST-positive neurons, sections from adult floxed-RXFP3 mice (injected bilaterally in the DG hilus with AAV$^{(1/2)}$-Cre-IRES-eGFP) were processed for Cre- and SST-IR. Examination of these sections revealed abundant eGFP (Fig. 5A) and Cre-IR (Fig. 5B) in neurons in the DG hilus. Importantly, Cre-IR was observed in the majority of SST-positive neurons present in the DG hilus of injected mice (Fig. 5C,D; Supporting Information Fig. S2).

Confirmation of Conditional RXFP3 Deletion Within the DG Hilus

Six (6) weeks after bilateral injections of AAV$^{(1/2)}$-Cre-IRES-eGFP into the DG hilus, a significant reduction in RXFP3 mRNA was observed in the DG hilus, relative to control AAV$^{(1/2)}$-eGFP bilaterally injected mice ($t_{(14)} = 3.64$, $P < 0.01$, $n = 3$–5 mice per group, Fig. 6A–C). Although Cre-IR was observed in CA3, a significant reduction in RXFP3 mRNA was not observed in this area in AAV$^{(1/2)}$-Cre-IRES-eGFP bilaterally injected mice, relative to control, AAV$^{(1/2)}$-eGFP injected mice ($t_{(14)} = 2.06$, $P = 0.058$, Fig. 6D). Therefore, while Cre was present in some CA3 neurons, it is presumed that an insufficient number of RXFP3 mRNA-positive neurons were transduced to produce a detectible decrease

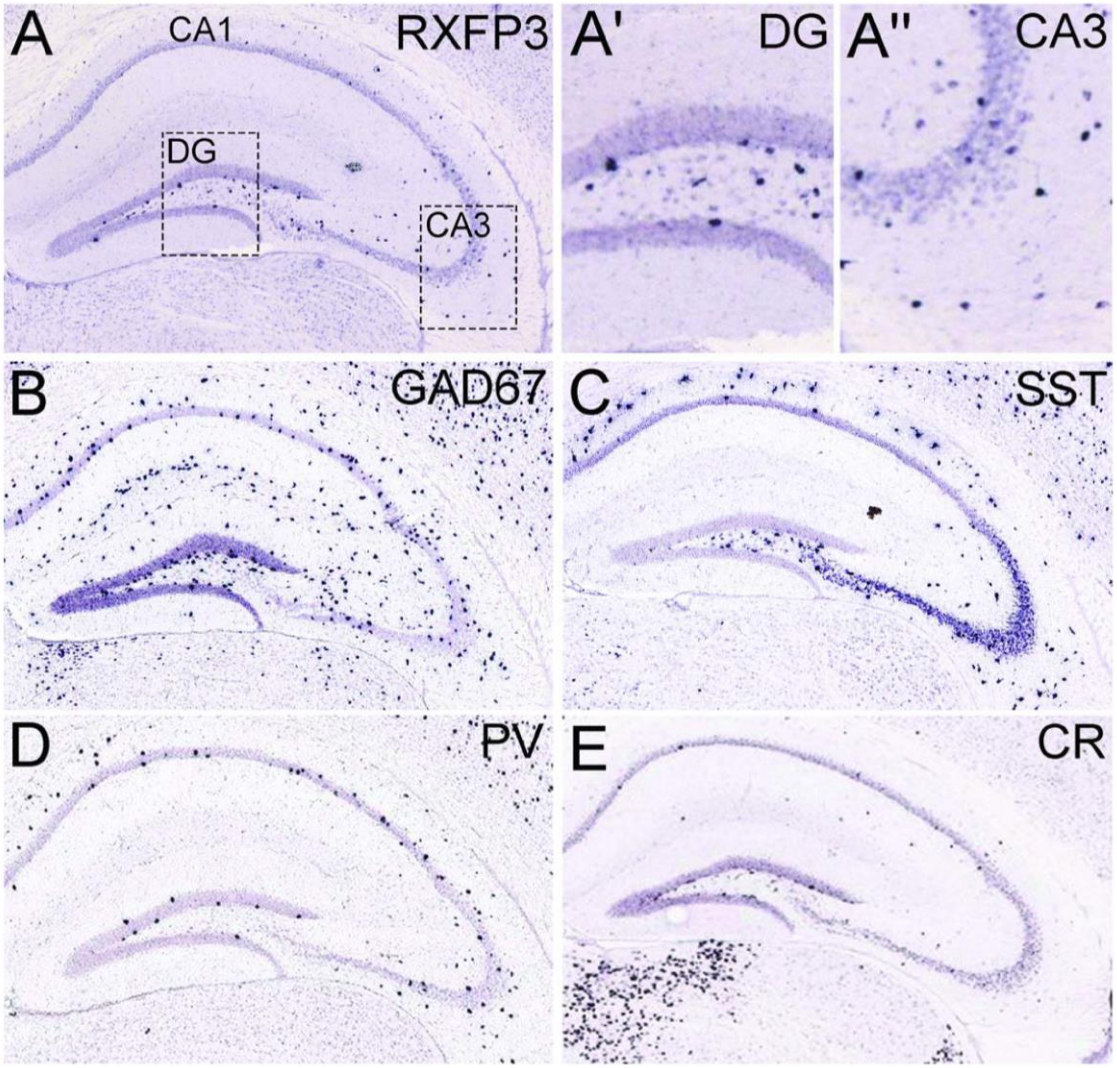

FIGURE 3. Comparative distribution in mouse dorsal hippocampus of RXFP3 mRNA and mRNAs encoding peptide and protein markers of hippocampal interneurons. (A) Distribution of RXFP3 mRNA in adult mouse hippocampus with abundant expression detected in neurons located in CA1 stratum oriens, across the CA3 region and within the DG hilus with higher magnification views of CA3 and DG (boxed areas) provided (A′, A″). The comparative distribution of GAD67 (B), SST (C), PV (D), and CR (E) mRNAs illustrate the strong similarity between the distribution of RXFP3 mRNA positive neurons and some of the GAD67, SST, PV, and CR mRNA positive neurons in the CA1 stratum oriens, CA3 region and hilus, suggesting that RXFP3 is expressed by a population of GABA interneurons (or projection neurons) in these areas. Images adapted from the Allen Brain Institute Gene Expression Atlas <www.brain-map.org>. [Color figure can be viewed at wileyonlinelibrary.com]

in mRNA levels. Viral spread was observed along the rostrocaudal extent of the dorsal DG hilus and CA3 in $AAV^{(1/2)}$-Cre-IRES-eGFP treated mice, but did not reach the ventral DG hilus/CA3 regions (Fig. 6E).

RXFP3 Deletion from DG Hilus Impaired Spatial Reference Memory in an Appetitive T-Maze Task

In an appetitive T-maze task, $AAV^{(1/2)}$-Cre-IRES-eGFP-treated mice made significantly fewer correct choices compared to $AAV^{(1/2)}$-eGFP-treated control mice, but a significant increase in performance over days tested was observed in both groups (RM two-way ANOVA, main effect of treatment, $F_{(1,21)} = 9.18$, $P = 0.0064$; main effect of day, $F_{(4,84)} = 32.6$, $P < 0.0001$; treatment × day interaction, $F_{(4,84)} = 1.89$, $P = 0.120$; Bonferroni post hoc analysis between treatments within days 1–3, $P < 0.05$, Fig. 7A). Although mice from both treatment groups met the criterion of 80% correct choices for 3 consecutive days, $AAV^{(1/2)}$-Cre-IRES-eGFP mice took significantly longer to meet the criterion than $AAV^{(1/2)}$-eGFP mice ($U = 35$, $P = 0.0210$, Fig. 7B).

When the criterion of correct choices was met during acquisition, the reward arm was swapped to the opposite arm, and reversal learning was commenced. This was done to test

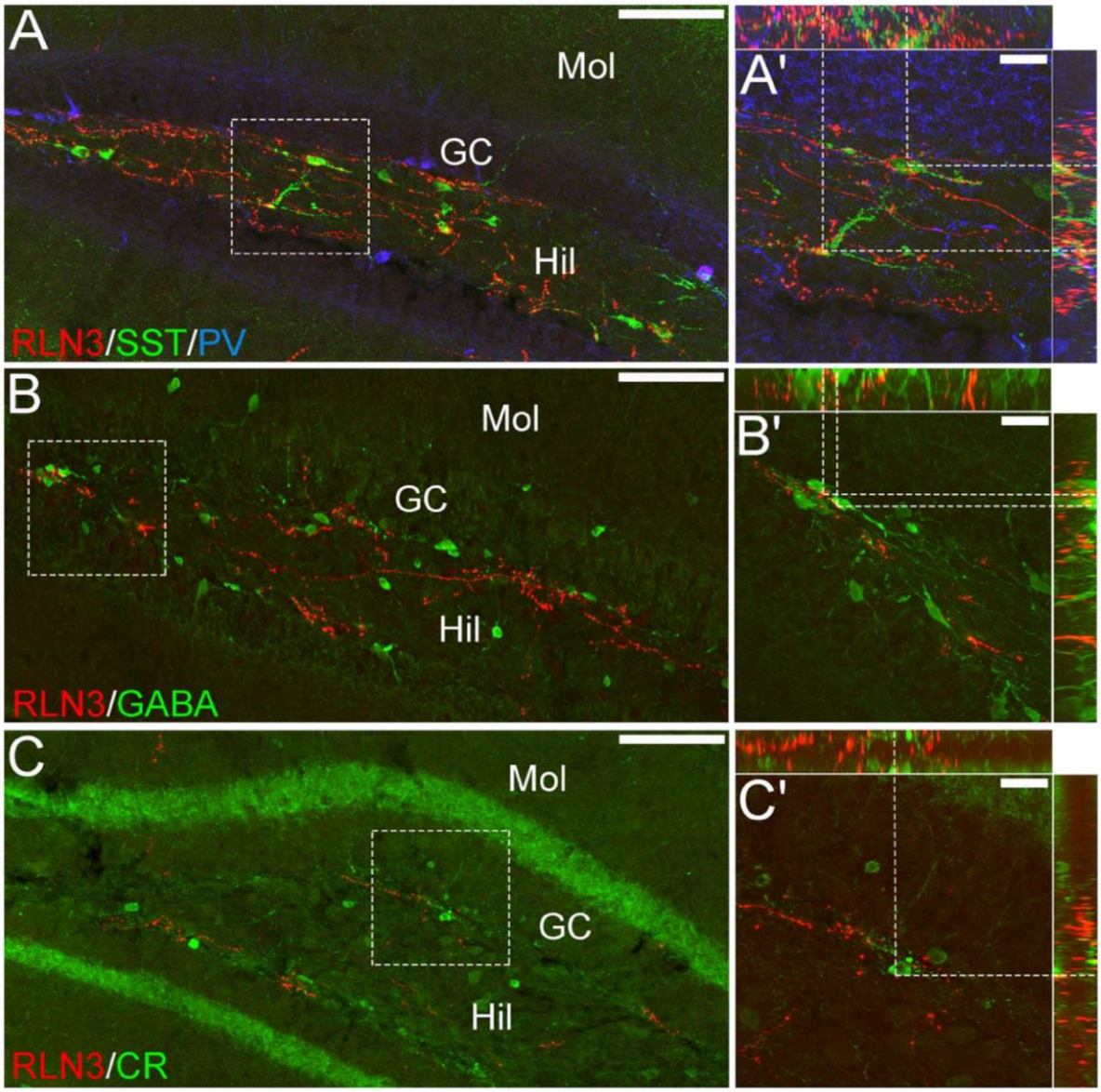

FIGURE 4. Comparative distribution of RLN3-immunoreactive nerve fibres and neurons positive for amino acid, peptide or protein markers of hippocampal interneurons in dorsal hippocampus of adult mouse. Mosaic confocal images (×20 magnification represented as z-stack maximum projections, 1 μm intervals) of mouse DG illustrating (A) RLN3 (red), SST (green) and PV (blue) immunoreactivity, (B) RLN3 (red) and GABA (green) immunoreactivity, and (C) RLN3 (red) and CR (green) immunoreactivity. Boxed areas in A-C are further illustrated (×63 magnification z-stacks, 0.1 μm intervals) and represented as three-dimensional orthogonal maximum projections orientated in 3 planes (*y*/*x*, *x*/*z*, and *y*/*z*) (A′–C′). Dotted lines in these panels indicate appositions of RLN3-positive elements with hippocampal neurons in the *y*/*x*, *x*/*z*, and *y*/*z* planes. Scale bars represent 100 μm (A–C) and 20 μm (A′–C′). [Color figure can be viewed at wileyonlinelibrary.com]

whether AAV$^{(1/2)}$-Cre-IRES-eGFP-treated mice displayed a resistance to alter/change a learned behavior (i.e., altered behavioral flexibility). Two-way repeated measures ANOVA did not reveal a main effect of treatment ($F_{(1,20)} = 1.79$, $P = 0.196$), nor an interaction effect ($F_{(4,80)} = 0.403$, $P = 0.806$) in % correct choice during reversal, however a main effect of day was observed ($F_{(1,\ 24)} = 4.46$, $P = 0.045$, Fig. 7A). Interestingly, during reversal, AAV$^{(1/2)}$-Cre-IRES-eGFP mice spent significantly more time in the T-maze centre junction before making a choice. No differences were observed between groups in time taken to meet the learning response criterion ($U = 66.5$, $P = 0.780$, Fig. 7B).

RXFP3 Deletion from DG Hilus Impaired Spatial Working Memory in a Continuous SAT in a Y-Maze

In studies to measure spatial working memory, mice were assessed in a continuous SAT in a Y-maze. RXFP3 depletion in

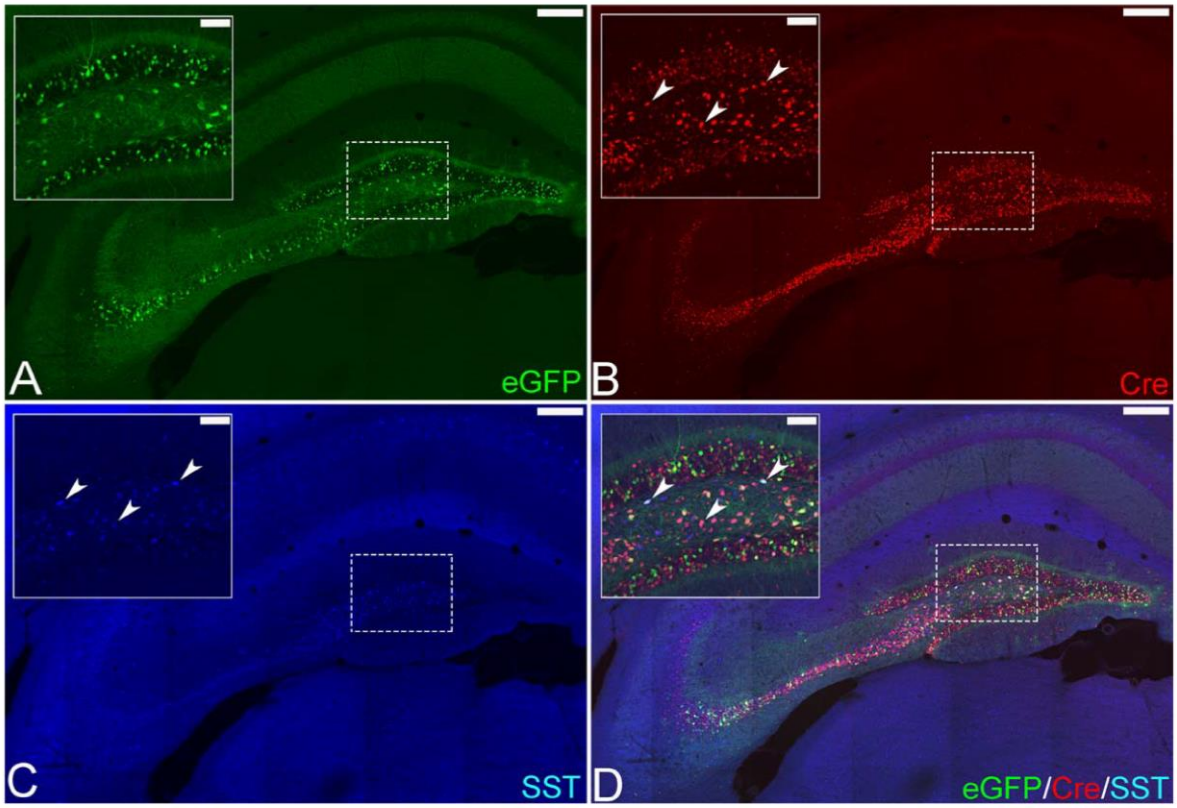

FIGURE 5. Comparative distribution of eGFP, Cre-recombinase and somatostatin (SST) in hilar neurons of dorsal hippocampus in mice injected with the AAV$^{(1/2)}$-Cre-IRES-eGFP viral vector. Bilateral injections of AAV$^{(1/2)}$-Cre-IRES-eGFP into the DG of floxed-RXFP3 mice resulted in expression of eGFP (A) and Cre-immunoreactivity (B) in neurons of the DG hilus. Cre-immunoreactivity and endogenous eGFP immunofluorescence were consistently observed in SST-immunoreactive neurons in the region (C, D), consistent with the likely deletion of any RXFP3 expression from these neurons. In the higher magnification images (inserts), arrowheads indicate some of many neurons in which eGFP, Cre and SST are co-localized. Scale bars, 100 μm (A–D) and 20 μm (insets). [Color figure can be viewed at wileyonlinelibrary.com]

the DG hilus significantly impaired spontaneous alternation in the percent alternation score (PAS) in the first 1-min time bin ($t_{(22)} = 3.92$, $P = 0.0007$, Fig. 8), with a PAS score of 67.6% for AAV$^{(1/2)}$-eGFP-treated controls, and 35.8% for AAV$^{(1/2)}$-Cre-IRES-eGFP-treated mice. A t test revealed AAV$^{(1/2)}$-eGFP mice performed significantly better than chance (PAS 50%) ($t_{(24)} = 3.02$, $P = 0.0059$), relative to AAV$^{(1/2)}$-Cre-IRES-eGFP mice that performed significantly below chance ($t_{(24)} = 2.26$, $P = 0.0329$) in the first min of the SAT test. However, over a total test time of 3 min, a significant difference between treatments was not observed ($t_{(22)} = 1.18$, $P = 0.0822$), with control mice performance only just above chance (PAS, 52.1 ± 3.35; $t_{(24)} = 0.630$, $P = 0.536$), and poorer performance observed for AAV$^{(1/2)}$-Cre-IRES-eGFP mice (PAS, 44.8 ± 3.54; $t_{(25)} = 1.80$, $P = 0.0844$).

RXFP3 Deletion from DG Hilus Did Not Alter Learning and Long-Term Memory Retention in a Morris Water Maze

We next determined whether depletion of RXFP3 from the DG hilus impaired spatial learning and long-term retrieval in a MWM. A two-way repeated measures ANOVA revealed a significant main effect of day ($F_{(5,110)} = 35.4$, $P = < 0.0001$), but no main effect of treatment was observed ($F_{(1,22)} = 0.0240$, $P = 0.878$), nor an interaction ($F_{(5,110)} = 0.272$, $P = 0.928$, Fig. 9A) in the latency (s) to locate the hidden platform during acquisition. Twenty-four (24) h after the last acquisition day, in the probe trial, both treatment groups spent significantly more time in the target quadrant relative to the other quadrants in the first 1 min time bin (one-way ANOVA, $F_{(7,84)} = 11.3$, $P < 0.0001$) and in the total duration of 2 min (one-way ANOVA, $F_{(7,84)} = 29.2$, $P < 0.0001$, Fig. 9B). Bonferroni's planned comparison tests confirmed that both AAV$^{(1/2)}$-Cre-IRES-eGFP-treated mice and AAV$^{(1/2)}$-eGFP-treated control mice spent significantly more percent time in the target quadrant than in the adjacent quadrant to the right (AAV$^{(1/2)}$-eGFP; $p < 0.0001$, AAV$^{(1/2)}$-Cre-IRES-eGFP; $p < 0.05$), the adjacent quadrant to the left ($P < 0.0001$) and to the opposite quadrant ($P < 0.0001$). No significant differences were observed between treatment groups in the percent time spent in the target quadrant in the first min ($t_{(21)} = 0.0605$, $P = 0.952$) and the total 2-min test duration ($t_{(21)} = 1.009$, $P = 0.325$). The time each group spent in the target quadrant on probe day was compared with a "chance" value of 30 s (i.e., the amount of time a mouse would be expected to spend in the target

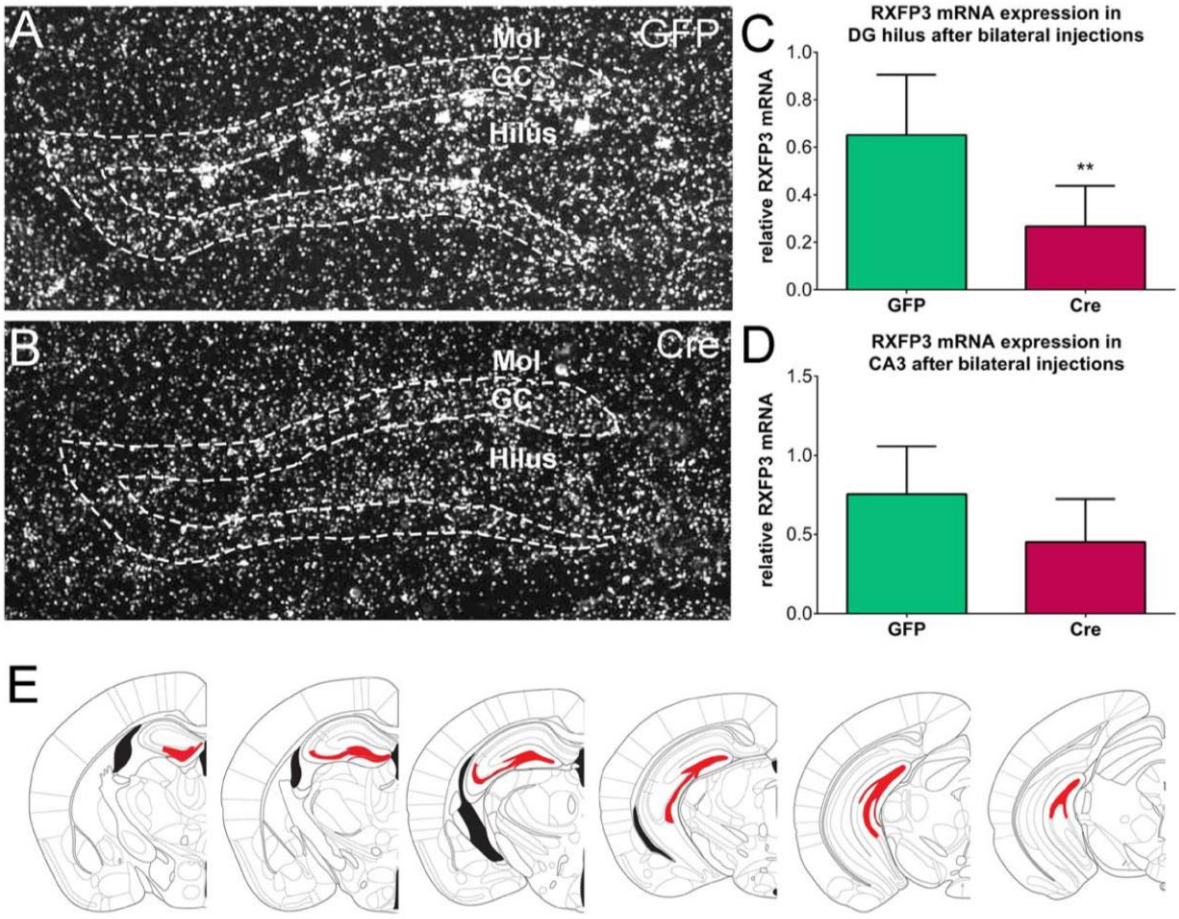

FIGURE 6. Effect of an AAV$^{(1/2)}$-Cre-IRES-eGFP or an AAV$^{(1/2)}$-eGFP viral vector injection into the dorsal DG hilus of floxed-RXFP3 mice on levels of RXFP3 mRNA in the target and CA3 regions, and a schematic illustration of the virus distribution observed. Representative dark-field photomicrographs of nuclear emulsion autoradiographic images of the distribution of RXFP3 mRNA in DG hilus of floxed RXFP3 mice labeled by an [^{35}S]-riboprobe (Lenglos et al., 2014) following bilateral injections of either (A) AAV$^{(1/2)}$-eGFP, or (B) AAV$^{(1/2)}$-Cre-IRES-eGFP. A significant reduction in relative RXFP3 mRNA levels was observed after bilateral AAV$^{(1/2)}$-Cre-IRES-eGFP injections into the DG hilus, relative to bilateral AAV$^{(1/2)}$-eGFP (control) injections in (C) hilus and (D) CA3 (unpaired t-test, ** $P<0.01$, $n=3$–5 mice per group). Data are expressed as mean ± SEM. (E) Schematic representation of viral spread observed within the DG of treated mice. The distribution of virus and Cre recombinase was similar on both sides of the hippocampus in all of the mice included in the final behavioral analysis. [Coronal brain images adapted from a stereotaxic mouse brain atlas (Paxinos and Franklin 2001)]. [Color figure can be viewed at wileyonlinelibrary.com]

quadrant over a total duration of 2 min if no spatial memory had been formed). Both groups spent significantly more than 25% (15 s) of their time in the target quadrant in the first min (AAV$^{(1/2)}$-GFP, $t_{(24)}=3.91$, $P=0.0007$; AAV$^{(1/2)}$-Cre, $t_{(24)}=4.01$, $P=0.0005$ and significantly more than 25% (30 s) of their time in the target quadrant in the total 2 min duration (AAV$^{(1/2)}$-GFP, $t_{(24)}=5.80$, $P<0.0001$; AAV$^{(1/2)}$-Cre, $t_{(24)}=4.00$, $P=0.0005$), suggesting intact spatial long-term memory on probe day.

RXFP3 Deletion from DG Hilus Did Not Alter General Locomotor Activity or Innate Anxiety in an EPM and L/D Box

No differential effects were observed between treatments in the total distance travelled in a locomotor cell 21 days after viral injections ($t_{(23)}=0.551$, $P=0.587$; Supporting Information Table S3). This result was consistent across 5-min bins within a total duration of 1 h, and both groups significantly decreased their distance travelled over time (RM 2-way ANOVA, main effect of treatment ($F_{(1,23)}=0.303$, $P=0.587$); time ($F_{(11,253)}=15.6$, $P<0.0001$); treatment × time interaction ($F_{(11,253)}=0.520$, $P=0.889$).

Twenty-four (24) h after the probe day in the MWM, the different groups of mice were tested in an EPM to measure stress-induced anxiety-like behavior. RXFP3 depletion from DG hilus did not induce any changes relative to AAV$^{(1/2)}$-GFP control mice in the time spent in the open arms ($t_{(23)}=0.886$, $P=0.139$; Supporting Information Table S3), or the number of entries into the open arms ($t_{(23)}=0.498$, $P=0.623$). Similarly, in the *L/D* box, no differences were observed between groups in the total time spent in the light side ($t_{(22)}=0.886$, $P=0.385$; Supporting Information Table S3) or entries into the light side ($t_{(22)}=1.528$, $P=0.141$).

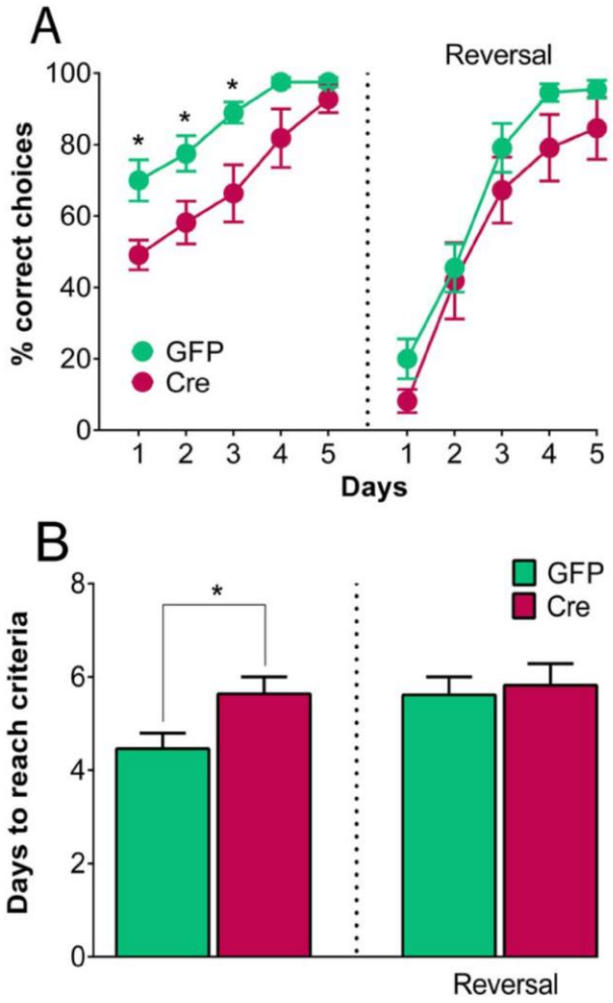

FIGURE 7. Effect of RXFP3 deletion in the DG hilus of adult floxed-RXFP3 mice on subsequent spatial reference memory in an appetitive T-maze. An AAV$^{(1/2)}$-Cre-IRES-eGFP or an AAV$^{(1/2)}$-eGFP (control) viral vector was injected bilaterally into the DG of groups of floxed-RXFP3 mice and their spatial memory was tested after a 3-week recovery period. (A) During acquisition training, mice with RXFP3 deleted from DG hilus made significantly less correct choices than control mice on day 1–3 of testing in a hippocampus-dependent spatial reference memory task—an appetitive T-maze. RXFP3 deleted and control mice performed similarly during reversal training (two-way repeated measures ANOVA, Bonferroni post-hoc analysis, * $P<0.05$). (B) Mice with RXFP3 deleted from DG hilus took significantly more days of training than control mice to meet criteria during acquisition (Mann–Whitney U-test, * $P<0.05$). No treatment differences were observed during reversal training. Data are expressed as mean ± SEM, $n = 12–13$ mice per group. [Color figure can be viewed at wileyonlinelibrary.com]

DISCUSSION

In the present study, in light of the distinct topography of RXFP3 mRNA in the mouse hippocampus, we conducted a histochemical analysis of the possible association of RLN3-positive nerve fibres with some established hippocampal neuron types; and a behavioral analysis of mice after depletion of RXFP3 from the DG hilus. The main findings were firstly, that RXFP3 mRNA was confirmed to be expressed in distinct layers of the hippocampus, with strong expression in neurons within the DG hilus, and non-principal neurons located within the pyramidal and stratum oriens layer of CA1 and across the pyramidal layer, stratum oriens and radiatum of CA3. Interestingly, neuronal fibres and terminals containing RLN3-IR were identified making consistent close contacts with GABA- and SST- positive neurons and, to a lesser degree, contacts with PV- and CR-positive neurons. Secondly, in this first study to manipulate RLN3/RXFP3 signaling within the hippocampus by deletion of RXFP3 from DG hilus neurons, we observed a strong and consistent deficiency in an appetitive reference memory task in a T-maze, and impairment in spatial working memory in a Y-maze SAT test. In contrast, depletion of RXFP3 from the DG hilus did not affect the ability of mice to learn and acquire the location of a hidden platform in a MWM test of long-term memory retention. Furthermore, hilar RXFP3 depletion did not alter anxiety-like behavior in an EPM or L/D box. Overall, this study identified key behavioral consequences of RXFP3 depletion from DG hilus and the neurochemical phenotype of RLN3/RXFP3 targeted neurons in the hippocampus, providing new insights into the complex role of this modulatory neuropeptide system in learning and memory.

Our first goal was to assess the neurochemical anatomy of the RLN3/RXFP3 system within the hippocampus. A detailed mapping of the distribution of RXFP3 mRNA/binding sites and RLN3-IR has been completed in mouse (Smith et al., 2010), rat (Ma et al., 2009c; Olucha-Bordonau et al., 2012) and non-human primate (Ma et al., 2009c) brain and the results are consistent with the present analysis in the mouse hippocampus. Based on the overlap between the restricted topographic distributions of neurons expressing RXFP3 mRNA with the extensive distribution of GABAergic interneurons, we hypothesized that RXFP3 is expressed by a subpopulation of GABA neurons in the hippocampus. This in turn predicted that neuronal fibres expressing RLN3-IR would make close contacts with GABA-positive neurons in the hippocampus, particularly in the DG hilus and the oriens layer of CA1, and this was demonstrated experimentally. Notably, RLN3-positive fibres were also found to make a significant number of contacts with SST-positive neurons in these areas. As the majority of SST neurons (~90%) in the DG hilus co-express GABA (Kosaka et al., 1988), our results indicate there is a subpopulation of RXFP3-positive neurons which co-express both GABA and SST in the hippocampus. Interestingly, RLN3-positive fibres and terminals were also observed to make close contacts with PV- and CR-positive neurons in the hippocampus, but their incidence was approximately half that for contacts with GABA- and SST-positive neurons. PV and CR label distinct, non-overlapping subsets of inhibitory hippocampal interneurons (Xu et al., 2010), therefore, it is likely that a majority of RXFP3-positive neurons in the hippocampus express GABA and SST, while non-overlapping smaller subpopulations of RXFP3-positive neurons co-express PV or CR.

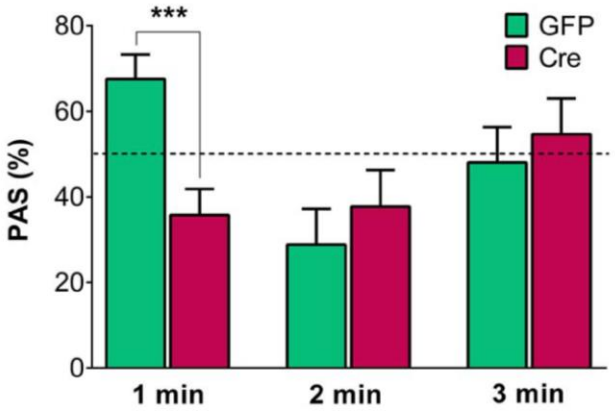

FIGURE 8. Effect of RXFP3 deletion in the DG hilus of adult floxed-RXFP3 mice on subsequent performance in a spontaneous alternation task in a Y-maze. An AAV$^{(1/2)}$-Cre-IRES-eGFP or an AAV$^{(1/2)}$-eGFP (control) viral vector was injected bilaterally into the DG of groups of floxed-RXFP3 mice and their performance in a spontaneous alternation task in a Y-maze was tested after a 3-week recovery period. Mice with RXFP3 deleted from DG hilus displayed a significant reduction in percent alternation score (PAS) in the first min of a spontaneous alternation task (SAT) in the Y-maze, relative to control mice. No treatment differences in PAS were observed during the 2nd or 3rd min bins of the test (Unpaired *t* test, *** $P<0.001$, $n=12–13$ mice per group). Horizontal dotted line indicates 50% chance level. [Color figure can be viewed at wileyonlinelibrary.com]

SST neurons constitute one of the largest groups of GABA neurons within the DG, with all these SST-positive neurons located within the hilus (Scharfman and Myers, 2012). Retrograde tracing studies in mice indicate that a large proportion (44%) of SST-positive neurons in the DG hilus project to the septal region (Zappone and Sloviter, 2001; Jinno and Kosaka, 2002a), and directly innervate GABAergic and cholinergic neurons in that region (Toth et al., 1993; Gulyas et al., 2003). In turn, SST hippocampal-septal neurons are reciprocally innervated by cholinergic and GABAergic septal neurons (Freund and Antal, 1988; Freund and Buzsaki, 1996). The high percentage of SST DG hilus neurons that innervate the septum and the high incidence of RLN3 inputs to SST- and GABA-positive neurons in the DG hilus, suggest RLN3/RXFP3 signaling plays an important role in the hippocampo-septal and septo-hippocampal circuitry, modulating cognition and learning and memory. Therefore, it will be of interest to further investigate the precise anatomical connectivity of those neurons and circuits influenced by the RLN3/RXFP3 system and its resultant functional impact.

However, there is a considerable amount of existing evidence regarding the functional role of SST-containing DG hilus interneurons that might inform the possible effects of RXFP3 signaling on hippocampal activity. Activation of SST DG hilus interneurons reduces long-term potentiation (LTP) in the mouse DG (Baratta et al., 2002), a cellular process involved in learning and memory; and an age-dependent reduction in SST and GAD67 DG hilus neurons in apolipoprotein E4 (apoE4) knock-in mice correlated with learning and memory deficits in the MWM test (Andrews-Zwilling et al., 2010). Notably, a similar result was observed in a study of rat DG hilus neurons (Spiegel et al., 2013). In early studies, global depletion of SST in rats by cysteamine hydrochloride, a somatostatin inhibiting agent, impaired learning and memory in a passive avoidance task (Yamazaki et al., 1996); and similar studies have shown impairment in spatial discrimination in mice (Guillou et al., 1998; Epelbaum et al., 2009; Tuboly and Vecsei, 2013). Interestingly, optogenetic inhibition of GABAergic DG hilus

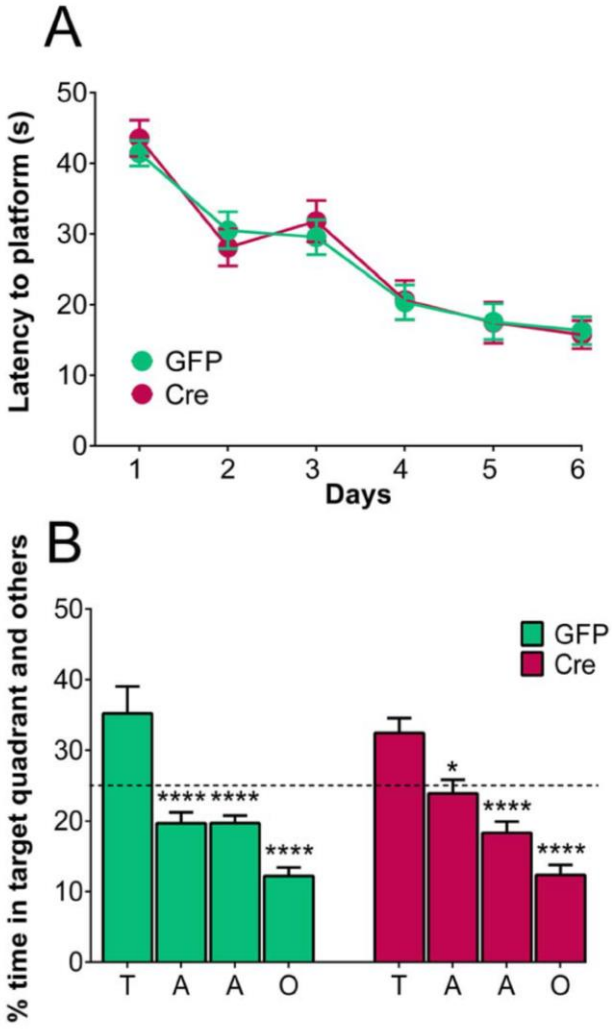

FIGURE 9. Effect of RXFP3 deletion in the DG hilus of adult floxed-RXFP3 mice on spatial learning and long-term reference memory in a Morris water maze (MWM) test. An AAV$^{(1/2)}$-Cre-IRES-eGFP or an AAV$^{(1/2)}$-eGFP (control) viral vector was injected bilaterally into the DG of groups of floxed-RXFP3 mice and their performance in a Morris water maze (MWM) test was tested after a 3-week recovery period. (A) Mice with RXFP3 deleted from DG hilus and matched control mice displayed normal spatial learning in the MWM. (B) On the probe day, both groups spent significantly more time in the target quadrant relative to other quadrants (one-way ANOVA, Bonferroni post-hoc analysis, * $P<0.05$, **** $P<0.0001$, $n=12–13$ mice per group). Data are expressed as mean ± SEM. Horizontal dotted line indicate 25% chance level. Abbreviations: T, target quadrant (SW), A, adjacent quadrants (NW, SE) and O opposite quadrant (NE). [Color figure can be viewed at wileyonlinelibrary.com]

interneuron activity impairs spatial learning and memory retrieval (Andrews-Zwilling et al., 2012), although this effect was via the entire GABA interneuron population with no implicit selectivity for SST/GABA neurons. Multiple studies have reported that SST interneurons inhibit excitatory synaptic transmission excitability, resulting in silencing or hyperpolarization in hippocampus (see Liguz-Lecznar et al., (2016) for review); and increases in inhibition (of hippocampal interneurons) is well-known to be an important cellular mechanism in learning and memory (McEchron and Disterhoft, 1997; Knott et al., 2002; Ruediger et al., 2011). In more recent studies, an enhancement in inhibition onto CA1 pyramidal neurons during learning in a trace eye blink conditioning task, was found to be mediated by an increase in intrinsic excitability of SST interneurons in mice and rats (McKay et al., 2013), and inactivating SST dendrite-targeting interneurons during aversive stimuli increased CA1 pyramidal cell population responses and prevented fear learning in mice (Lovett-Barron et al., 2014).

Therefore, our second goal was to assess the behavioral effects of Cre-recombinase-induced deletion of RXFP3 in the DG hilus of adult floxed-RXFP3 mice. In these studies we observed a strong and consistent deficiency in the performance of $AAV^{(1/2)}$-Cre-IRES-eGFP-treated floxed-RXFP3 mice in an appetitive reference memory task in a T-maze. In a continuous spontaneous alternation Y-maze task, RXFP3-depleted mice made fewer alternations in the first min of the task, suggesting impairment in spatial working memory. In terms of the functional implications of these findings, it is proposed that the RLN3-containing inputs to the GABA/SST-positive neurons and other GABA neuron populations in the DG hilus can regulate hippocampal and cognitive processing. If this is the case, depletion of RXFP3 from GABA and/or GABA/SST neurons in the DG hilus may disrupt disinhibition of target neurons, and weaken synaptic inhibition of excitatory neurons, a key component in compromised cognitive processes. This, in turn, could produce impaired learning and memory, via effects within the directly targeted hippocampus and via remote, relayed effects in the MS/DB. Further studies are required to explore this hypothesis, including an examination of the effect of RXFP3 activation by validated RXFP3-specific agonist peptides (Liu et al., 2005; Shabanpoor et al., 2012; Zhang et al., 2015) on DG hilus SST neuron activity, perhaps in a strain of SST reporter mice (Ma et al., 2006; Peng et al., 2013).

In contrast to these effects, however, a deficiency in spatial learning and long-term memory was not observed based on the performance of $AAV^{(1/2)}$-Cre-IRES-eGFP-treated floxed-RXFP3 mice in the MWM. The differences observed in these tests of memory retention suggest a specific role for hilar RLN3/RXFP3 signaling in learning and memory that may reflect the different neurochemical and psychological processes involved in acquiring memory. Optimal performance in the MWM requires the use of allocentric strategies where distal cues provide a geometric reference to an animal's current location and this form of memory consolidation is primarily hippocampal-dependent (Vorhees and Williams, 2006; Garthe et al., 2009). While effective performance in the appetitive T-maze task also requires the use of hippocampal-dependent allocentric strategies whereby the animal is rewarded for choosing a constant, designated goal arm on the basis of its spatial location (Deacon et al., 2002; Reisel et al., 2002; Sanderson et al., 2008; von Engelhardt et al., 2008), differences in memory consolidation between these two spatial reference memory tests have been highlighted (Hodges, 1996; Deacon et al., 2002; Bannerman et al., 2012). The most prominent refers to the distinct differences in the motivational aspect of both tasks. The MWM is motivated by the desire to escape onto a safe platform, whereas the appetitive T-maze is motivated by food reward. Therefore, differences in reinforcement may affect the strategy adopted and activate different brain circuits involved in motivation and reward. Furthermore, although both tests require the use of allocentric strategies, the appetitive T-maze requires the mouse to use spatial information to guide selection between two alternative responses and to learn to make a constant body turn for a food reward. Taken together, the results from the present study suggest RXFP3 in the DG hilus is not essential for spatial tasks that rely solely on the use of allocentric spatial maps, but may influence tasks which integrate multiple strategies for using spatial information to guide selection between alternative responses that lead to a reinforcing reward. Moreover, in regard to the contradictory effects observed in the spontaneous alternation Y-maze task and MWM in the present study, spontaneous alternation has been shown to be a more reliable measure in detecting hippocampal dysfunction than the commonly used MWM (Rawlins and Olton, 1982; Reisel et al., 2002; Deacon and Rawlins, 2005). Although both tasks detect spatial memory deficits in mice with whole lesions of the hippocampus (Morris et al., 1982; Lalonde, 2002; Deacon and Rawlins, 2005), consistent with the results from the present study, a deficit in spatial memory following deletion of the GluR-A (GluR1) AMPA receptor subunit was only detected in a spontaneous alternation T-maze task, whereas spatial reference memory was not affected in a MWM (Reisel et al., 2002).

In a continuous SAT in a Y-maze, mice with RXFP3 depleted from the DG hilus displayed significantly lower rates of alternation (PAS, 36%) relative to control mice (PAS, 68%) in the first min of the task, demonstrating an impairment in spatial working memory. After 3 min, DG hilus RXFP3 depleted mice still displayed low rates of alternation (PAS 47%), but the control mice had similar rates (PAS, 52%), suggesting poor spatial working memory performance in both treatment groups. However, the weak performance of the control group assessed over a 3-min session is not surprising. The continuous nature of the task means there is considerable inter-trial interference, a likely reason for low rates of performance in both T-maze (Gerlai et al., 1994) and Y-maze (Hsiao et al., 1996; Deacon et al., 2002) tasks (for review, see Deacon and Rawlins, 2006). Therefore, the decline in PAS observed over the subsequent 2 and 3 min time bins in both groups is likely due to methodological issues associated with the task, whereby the first min is the period in which the most reliable measures are observed.

Lastly, RXFP3 depletion from the DG hilus did not alter anxiety-like behavior in an EPM or L/D box, tested 1 and 3 days, respectively, after the MWM test with its associated swim stress (Engelmann et al., 2006). In the mice studied, we observed $AAV^{(1/2)}$ spread along the rostral-caudal length of the DG hilus and CA3, including part of the ventral hippocampus, which is functionally implicated in the control of emotion and affect, and wherein RLN3-positive nerve fibres and RXFP3 mRNA are abundant (Ma et al., 2009b; Smith et al., 2010). However, the viral injections in the present study did not cover the entire dorsoventral extent of the DG hilus in ventral hippocampus, reducing the likelihood of observing an effect on anxiety-like behavior. The RLN3/RXFP3 system in mice and rats has been shown to be involved in stress responses (Tanaka et al., 2005; Banerjee et al., 2010) and modulation of anxiety-like behavior (Ryan et al., 2013; Zhang et al., 2015), with pronounced changes in RLN3 mRNA expression and RLN3-IR levels in response to stressors (Tanaka et al., 2005; Lenglos et al., 2013; Ma et al., 2013; Walker et al., 2015; Calvez et al., 2016). Therefore, further studies with more extensive and/or focused depletion of RXFP3 in ventral hippocampus are warranted.

CONCLUSIONS

The anatomical distribution of the RLN3/RXFP3 system in the major nodes of the septohippocampal system (Ma et al., 2009c; Smith et al., 2010; Olucha-Bordonau et al., 2012) suggests it contributes to important neuronal circuits that control learning and memory. This first study to investigate the specific role of RLN3/RXFP3 signaling in the mouse hippocampus has demonstrated neuronal contacts with distinct populations of GABAergic neurons in the hippocampus, and that depletion of RXFP3 within the DG hilus can produce impairments in spatial reference and working memory in an appetitive T-maze and spontaneous alternation task in a Y-maze, respectively. These data suggest that the RLN3-containing pathway from the NI to the hippocampus can mediate inhibitory control of local and septal target neurons via RXFP3, and modulate memory processes.

ACKNOWLEDGMENTS

The authors thank Timothy Lovenberg and Steve Sutton (Janssen Companies of Johnson & Johnson, La Jolla, CA) for commissioning and providing the floxed-RXFP3 mice; Sharon Layfield for the production of viral vectors; Verena Wimmer for technical assistance with immunohistochemistry and confocal imaging; and the Core Animal Services at The Florey Institute of Neuroscience and Mental Health for the maintenance of the floxed-RXFP3 mouse colony. The authors declare that there is no conflict of interest.

REFERENCES

Amaral DG, Scharfman HE, Lavenex P. 2007. The dentate gyrus: Fundamental neuroanatomical organization (dentate gyrus for dummies). Prog Brain Res 163:3–22.

Andrews-Zwilling Y, Bien-Ly N, Xu Q, Li G, Bernardo A, Yoon SY, Zwilling D, Yan TX, Chen L, Huang Y. 2010. Apolipoprotein E4 causes age- and Tau-dependent impairment of GABAergic interneurons, leading to learning and memory deficits in mice. J Neurosci 30:13707–13717.

Andrews-Zwilling Y, Gillespie AK, Kravitz AV, Nelson AB, Devidze N, Lo I, Yoon SY, Bien-Ly N, Ring K, Zwilling D, Potter GB, Rubenstein JL, Kreitzer AC, Huang Y. 2012. Hilar GABAergic interneuron activity controls spatial learning and memory retrieval. PLoS One 7:e40555.

Banerjee A, Shen PJ, Ma S, Bathgate RA, Gundlach AL. 2010. Swim stress excitation of nucleus incertus and rapid induction of relaxin-3 expression via CRF1 activation. Neuropharmacology 58:145–155.

Bannerman DM, Rawlins JN, McHugh SB, Deacon RM, Yee BK, Bast T, Zhang WN, Pothuizen HH, Feldon J. 2004. Regional dissociations within the hippocampus—Memory and anxiety. Neurosci Biobehav Rev 28:273–283.

Bannerman DM, Bus T, Taylor A, Sanderson DJ, Schwarz I, Jensen V, Hvalby O, Rawlins JN, Seeburg PH, Sprengel R. 2012. Dissecting spatial knowledge from spatial choice by hippocampal NMDA receptor deletion. Nat Neurosci 15:1153–1159.

Baraban SC, Tallent MK. 2004. Interneuron diversity series: Interneuronal neuropeptides—Endogenous regulators of neuronal excitability. Trends Neurosci 27:135–142.

Baratta MV, Lamp T, Tallent MK. 2002. Somatostatin depresses long-term potentiation and Ca^{2+} signaling in mouse dentate gyrus. J Neurophysiol 88:3078–3086.

Bassant MH, Poindessous-Jazat F. 2001. Ventral tegmental nucleus of Gudden: A pontine hippocampal theta generator? Hippocampus 11:809–813.

Bassant MH, Poindessous-Jazat F. 2002. Sleep-related increase in activity of mesopontine neurons in old rats. Neurobiol Aging 23:615–624.

Bathgate RAD, Samuel CS, Burazin TCD, Layfield S, Claasz AA, Reytomas IG, Dawson NF, Zhao C, Bond C, Summers RJ, Parry LJ, Wade JD, Tregear GW. 2002. Human relaxin gene 3 (H3) and the equivalent mouse relaxin (M3) gene. Novel members of the relaxin peptide family. J Biol Chem 277:1148–1157.

Bathgate RAD, Lin F, Hanson NF, Otvos L Jr., Guidolin A, Giannakis C, Bastiras S, Layfield SL, Ferraro T, Ma S, Zhao C, Gundlach AL, Samuel CS, Tregear GW, Wade JD. 2006. Relaxin-3: Improved synthesis strategy and demonstration of its high-affinity interaction with the relaxin receptor LGR7 both in vitro and in vivo. Biochemistry 45:1043–1053.

Brown RE, McKenna JT. 2015. Turning a negative into a positive: Ascending GABAergic control of cortical activation and arousal. Front Neurol 6:135.

Burazin TCD, Bathgate RAD, Macris M, Layfield S, Gundlach AL, Tregear GW. 2002. Restricted, but abundant, expression of the novel rat gene-3 (R3) relaxin in the dorsal tegmental region of brain. J Neurochem 82:1553–1557.

Burgess N, Maguire EA, O'Keefe J. 2002. The human hippocampus and spatial and episodic memory. Neuron 35:625–641.

Calvez J, de Avila C, Matte LO, Guevremont G, Gundlach AL, Timofeeva E. 2016. Role of relaxin-3/RXFP3 system in stress-induced binge-like eating in female rats. Neuropharmacology 102: 207–215.

Deacon RM, Bannerman DM, Kirby BP, Croucher A, Rawlins JN. 2002. Effects of cytotoxic hippocampal lesions in mice on a cognitive test battery. Behav Brain Res 133:57–68.

Deacon RM, Rawlins JN. 2005. Hippocampal lesions, species-typical behaviours and anxiety in mice. Behav Brain Res 156:241–249.

Deacon RM, Rawlins JN. 2006. T-maze alternation in the rodent. Nat Protoc 1:7–12.

Dutar P, Bassant MH, Senut MC, Lamour Y. 1995. The septohippocampal pathway: Structure and function of a central cholinergic system. Physiol Rev 75:393–427.

Engelmann M, Ebner K, Landgraf R, Wotjak CT. 2006. Effects of Morris water maze testing on the neuroendocrine stress response and intrahypothalamic release of vasopressin and oxytocin in the rat. Horm Behav 50:496–501.

Epelbaum J, Guillou JL, Gastambide F, Hoyer D, Duron E, Viollet C. 2009. Somatostatin, Alzheimer's disease and cognition: An old story coming of age? Prog Neurobiol 89:153–161.

Freund TF, Antal M. 1988. GABA-containing neurons in the septum control inhibitory interneurons in the hippocampus. Nature 336: 170–173.

Freund TF, Buzsaki G. 1996. Interneurons of the hippocampus. Hippocampus 6:347–470.

Ganella DE, Callander GE, Ma S, Bye CR, Gundlach AL, Bathgate RAD. 2013. Modulation of feeding by chronic rAAV expression of a relaxin-3 peptide agonist in rat hypothalamus. Gene Ther 20:703–716.

Garthe A, Behr J, Kempermann G. 2009. Adult-generated hippocampal neurons allow the flexible use of spatially precise learning strategies. PLoS One 4:e5464.

Gerlai R, Marks A, Roder J. 1994. T-maze spontaneous alternation rate is decreased in S100 beta transgenic mice. Behav Neurosci 108:100–106.

Goto M, Swanson LW, Canteras NS. 2001. Connections of the nucleus incertus. J Comp Neurol 438:86–122.

Guillou JL, Micheau J, Jaffard R. 1998. The opposite effects of cysteamine on the acquisition of two different tasks in mice are associated with bidirectional testing-induced changes in hippocampal adenylyl cyclase activity. Behav Neurosci 112:900–908.

Gulyas AI, Hajos N, Katona I, Freund TF. 2003. Interneurons are the local targets of hippocampal inhibitory cells which project to the medial septum. Eur J Neurosci 17:1861–1872.

Hodges H. 1996. Maze procedures: The radial-arm and water maze compared. Brain Res Cogn Brain Res 3:167–181.

Hsiao K, Chapman P, Nilsen S, Eckman C, Harigaya Y, Younkin S, Yang F, Cole G. 1996. Correlative memory deficits, Abeta elevation, and amyloid plaques in transgenic mice. Science 274:99–102.

Jinno S, Kosaka T. 2002a. Immunocytochemical characterization of hippocamposeptal projecting GABAergic nonprincipal neurons in the mouse brain: A retrograde labeling study. Brain Res 945:219–231.

Jinno S, Kosaka T. 2002b. Patterns of expression of calcium binding proteins and neuronal nitric oxide synthase in different populations of hippocampal GABAergic neurons in mice. J Comp Neurol 449: 1–25.

Kizawa H, Nishi K, Ishibashi Y, Harada M, Asano T, Ito Y, Suzuki N, Hinuma S, Fujisawa Y, Onda H, Nishimura O, Fujino M. 2003. Production of recombinant human relaxin 3 in AtT20 cells. Regul Pept 113:79–84.

Knott GW, Quairiaux C, Genoud C, Welker E. 2002. Formation of dendritic spines with GABAergic synapses induced by whisker stimulation in adult mice. Neuron 34:265–273.

Kocsis B, Vertes RP. 1997. Phase relations of rhythmic neuronal firing in the supramammillary nucleus and mammillary body to the hippocampal theta activity in urethane anesthetized rats. Hippocampus 7:204–214.

Kocsis B, Di Prisco GV, Vertes RP. 2001. Theta synchronization in the limbic system: The role of Gudden's tegmental nuclei. Eur J Neurosci 13:381–388.

Kosaka T, Wu JY, Benoit R. 1988. GABAergic neurons containing somatostatin-like immunoreactivity in the rat hippocampus and dentate gyrus. Exp Brain Res 71:388–398.

Kuei C, Sutton S, Bonaventure P, Pudiak C, Shelton J, Zhu J, Nepomuceno D, Wu J, Chen J, Kamme F, Seierstad M, Hack MD, Bathgate RAD, Hossain MA, Wade JD, Atack J, Lovenberg TW, Liu C. 2007. R3(BΔ23-27)R/I5 chimeric peptide, a selective antagonist for GPCR135 and GPCR142 over relaxin receptor LGR7: In vitro and in vivo characterization. J Biol Chem 282:25425–25435.

Lalonde R. 2002. The neurobiological basis of spontaneous alternation. Neurosci Biobehav Rev 26:91–104.

Lenglos C, Mitra A, Guevremont G, Timofeeva E. 2013. Sex differences in the effects of chronic stress and food restriction on body weight gain and brain expression of CRF and relaxin-3 in rats. Genes Brain Behav 12:370–387.

Lenglos C, Mitra A, Guevremont G, Timofeeva E. 2014. Regulation of expression of relaxin-3 and its receptor RXFP3 in the brain of diet-induced obese rats. Neuropeptides 48:119–132.

Lenglos C, Calvez J, Timofeeva E. 2015. Sex-specific effects of relaxin-3 on food intake and brain expression of corticotropin-releasing factor in rats. Endocrinology 156:523–533.

Leutgeb S, Leutgeb JK, Moser MB, Moser EI. 2005. Place cells, spatial maps and the population code for memory. Curr Opin Neurobiol 15:738–746.

Liguz-Lecznar M, Urban-Ciecko J, Kossut M. 2016. Somatostatin and somatostatin-containing neurons in shaping neuronal activity and plasticity. Front Neural Circuits 10:48.

Liu C, Eriste E, Sutton S, Chen J, Roland B, Kuei C, Farmer N, Jornvall H, Sillard R, Lovenberg TW. 2003. Identification of relaxin-3/INSL7 as an endogenous ligand for the orphan G-protein-coupled receptor GPCR135. J Biol Chem 278:50754–50764.

Liu C, Chen J, Kuei C, Sutton S, Nepomuceno D, Bonaventure P, Lovenberg TW. 2005. Relaxin-3/insulin-like peptide 5 chimeric peptide, a selective ligand for G-protein-coupled receptor (GPCR)135 and GPCR142 over leucine-rich repeat-containing G protein-coupled receptor 7. Mol Pharmacol 67:231–240.

Lovett-Barron M, Kaifosh P, Kheirbek MA, Danielson N, Zaremba JD, Reardon TR, Turi GF, Hen R, Zemelman BV, Losonczy A. 2014. Dendritic inhibition in the hippocampus supports fear learning. Science 343:857–863.

Lubenov EV, Siapas AG. 2009. Hippocampal theta oscillations are travelling waves. Nature 459:534–539.

Ma Y, Hu H, Berrebi AS, Mathers PH, Agmon A. 2006. Distinct subtypes of somatostatin-containing neocortical interneurons revealed in transgenic mice. J Neurosci 26:5069–5082.

Ma S, Bonaventure P, Ferraro T, Shen PJ, Burazin TC, Bathgate RA, Liu C, Tregear GW, Sutton SW, Gundlach AL. 2007. Relaxin-3 in GABA projection neurons of nucleus incertus suggests widespread influence on forebrain circuits via G-protein-coupled receptor-135 in the rat. Neuroscience 144:165–190.

Ma S, Olucha-Bordonau FE, Hossain MA, Lin F, Kuei C, Liu C, Wade JD, Sutton SW, Nunez A, Gundlach AL. 2009a. Modulation of hippocampal theta oscillations and spatial memory by relaxin-3 neurons of the nucleus incertus. Learn Mem 16:730–742.

Ma S, Sang Q, Lanciego JL, Gundlach AL. 2009b. Localization of relaxin-3 in brain of *Macaca fascicularis*: Identification of a nucleus incertus in primate. J Comp Neurol 517:856–872.

Ma S, Shen PJ, Sang Q, Lanciego JL, Gundlach AL. 2009c. Distribution of relaxin-3 mRNA and immunoreactivity and RXFP3-binding sites in the brain of the macaque, *Macaca fascicularis*. Ann N Y Acad Sci 1160:256–258.

Ma S, Blasiak A, Olucha-Bordonau FE, Verberne AJ, Gundlach AL. 2013. Heterogeneous responses of nucleus incertus neurons to corticotrophin-releasing factor and coherent activity with hippocampal theta rhythm in the rat. J Physiol (Lond) 591:3981–4001.

Martin J, Timofeeva E. 2010. Intermittent access to sucrose increases sucrose-licking activity and attenuates restraint stress-induced

activation of the lateral septum. Am J Physiol Regul Integr Comp Physiol 298:R1383–1398.

McEchron MD, Disterhoft JF. 1997. Sequence of single neuron changes in CA1 hippocampus of rabbits during acquisition of trace eyeblink conditioned responses. J Neurophysiol 78:1030–1044.

McKay BM, Oh MM, Disterhoft JF. 2013. Learning increases intrinsic excitability of hippocampal interneurons. J Neurosci 33:5499–5506.

Morris RG, Garrud P, Rawlins JN, O'Keefe J. 1982. Place navigation impaired in rats with hippocampal lesions. Nature 297:681–683.

Moy SS, Nadler JJ, Young NB, Perez A, Holloway LP, Barbaro RP, Barbaro JR, Wilson LM, Threadgill DW, Lauder JM, Magnuson TR, Crawley JN. 2007. Mouse behavioral tasks relevant to autism: Phenotypes of 10 inbred strains. Behav Brain Res 176:4–20.

Nategh M, Nikseresht S, Khodagholi F, Motamedi F. 2015. Nucleus incertus inactivation impairs spatial learning and memory in rats. Physiol Behav 139:112–120.

Nategh M, Nikseresht S, Khodagholi F, Motamedi F. 2016. Inactivation of nucleus incertus impairs passive avoidance learning and long term potentiation of the population spike in the perforant path-dentate gyrus evoked field potentials in rats. Neurobiol Learn Mem 130:185–193.

Nunez A, Cervera-Ferri A, Olucha-Bordonau F, Ruiz-Torner A, Teruel V. 2006. Nucleus incertus contribution to hippocampal theta rhythm generation. Eur J Neurosci 23:2731–2738.

O'Keefe J. 1993. Hippocampus, theta, and spatial memory. Curr Opin Neurobiol 3:917–924.

O'Keefe J, Nadel L. 1978. The Hippocampus as a Cognitive Map. Oxford: Clarendon Press.

Olucha-Bordonau FE, Teruel V, Barcia-Gonzalez J, Ruiz-Torner A, Valverde-Navarro AA, Martinez-Soriano F. 2003. Cytoarchitecture and efferent projections of the nucleus incertus of the rat. J Comp Neurol 464:62–97.

Olucha-Bordonau FE, Otero-Garcia M, Sanchez-Perez AM, Nunez A, Ma S, Gundlach AL. 2012. Distribution and targets of the relaxin-3 innervation of the septal area in the rat. J Comp Neurol 520:1903–1939.

Paxinos G, Franklin KBJ. 2001. The Mouse Brain in Stereotaxic Coordinates. Sydney: Academic Press.

Peng Z, Zhang N, Wei W, Huang CS, Cetina Y, Otis TS, Houser CR. 2013. A reorganized GABAergic circuit in a model of epilepsy: Evidence from optogenetic labeling and stimulation of somatostatin interneurons. J Neurosci 33:14392–14405.

Rawlins JN, Olton DS. 1982. The septo-hippocampal system and cognitive mapping. Behav Brain Res 5:331–358.

Reisel D, Bannerman DM, Schmitt WB, Deacon RM, Flint J, Borchardt T, Seeburg PH, Rawlins JN. 2002. Spatial memory dissociations in mice lacking GluR1. Nat Neurosci 5:868–873.

Ruediger S, Vittori C, Bednarek E, Genoud C, Strata P, Sacchetti B, Caroni P. 2011. Learning-related feedforward inhibitory connectivity growth required for memory precision. Nature 473:514–518.

Ryan PJ, Buchler E, Shabanpoor F, Hossain MA, Wade JD, Lawrence AJ, Gundlach AL. 2013. Central relaxin-3 receptor (RXFP3) activation decreases anxiety- and depressive-like behaviours in the rat. Behav Brain Res 244:142–151.

Ryding AD, Sharp MG, Mullins JJ. 2001. Conditional transgenic technologies. J Endocrinol 171:1–14.

Sanchez-Perez AM, Arnal-Vicente I, Santos FN, Pereira CW, ElMlili N, Sanjuan J, Ma S, Gundlach AL, Olucha-Bordonau FE. 2015. Septal projections to nucleus incertus in the rat: Bidirectional pathways for modulation of hippocampal function. J Comp Neurol 523:565–588.

Sanderson DJ, Good MA, Seeburg PH, Sprengel R, Rawlins JN, Bannerman DM. 2008. The role of the GluR-A (GluR1) AMPA receptor subunit in learning and memory. Prog Brain Res 169: 159–178.

Scharfman HE, Myers CE. 2012. Hilar mossy cells of the dentate gyrus: A historical perspective. Front Neural Circuits 6:106.

Schiller D, Eichenbaum H, Buffalo EA, Davachi L, Foster DJ, Leutgeb S, Ranganath C. 2015. Memory and space: Towards an understanding of the cognitive map. J Neurosci 35:13904–13911.

Shabanpoor F, Hossain MA, Ryan PJ, Belgi A, Layfield S, Kocan M, Zhang S, Samuel CS, Gundlach AL, Bathgate RAD, Separovic F, Wade JD. 2012. Minimization of relaxin-3 leading to high affinity analogues with increased selectivity for relaxin-family peptide 3 receptor (RXFP3) over RXFP1. J Med Chem 55:1671–1681.

Smith CM, Shen PJ, Banerjee A, Bonaventure P, Ma S, Bathgate RA, Sutton SW, Gundlach AL. 2010. Distribution of relaxin-3 and RXFP3 within arousal, stress, affective, and cognitive circuits of mouse brain. J Comp Neurol 518:4016–4045.

Smith CM, Ryan PJ, Hosken IT, Ma S, Gundlach AL. 2011. Relaxin-3 systems in the brain—The first 10 years. J Chem Neuroanat 42:262–275.

Smith CM, Walker AW, Hosken IT, Chua BE, Zhang C, Haidar M, Gundlach AL. 2014. Relaxin-3/RXFP3 networks: An emerging target for the treatment of depression and other neuropsychiatric diseases? Front Pharmacol 5:46.

Spiegel AM, Koh MT, Vogt NM, Rapp PR, Gallagher M. 2013. Hilar interneuron vulnerability distinguishes aged rats with memory impairment. J Comp Neurol 521:3508–3523.

Tanaka M, Iijima N, Miyamoto Y, Fukusumi S, Itoh Y, Ozawa H, Ibata Y. 2005. Neurons expressing relaxin 3/INSL 7 in the nucleus incertus respond to stress. Eur J Neurosci 21:1659–1670.

Toth K, Borhegyi Z, Freund TF. 1993. Postsynaptic targets of GABAergic hippocampal neurons in the medial septum-diagonal band of broca complex. J Neurosci 13:3712–3724.

Tuboly G, Vecsei L. 2013. Somatostatin and cognitive function in neurodegenerative disorders. Mini Rev Med Chem 13:34–46.

Vertes RP. 2005. Hippocampal theta rhythm: A tag for short-term memory. Hippocampus 15:923–935.

Vertes RP, Kocsis B. 1997. Brainstem-diencephalo-septohippocampal systems controlling the theta rhythm of the hippocampus. Neuroscience 81:893–926.

Vertes RP, Fortin WJ, Crane AM. 1999. Projections of the median raphe nucleus in the rat. J Comp Neurol 407:555–582.

von Engelhardt J, Doganci B, Jensen V, Hvalby O, Gongrich C, Taylor A, Barkus C, Sanderson DJ, Rawlins JN, Seeburg PH, Bannerman DM, Monyer H. 2008. Contribution of hippocampal and extra-hippocampal NR2B-containing NMDA receptors to performance on spatial learning tasks. Neuron 60:846–860.

Vorhees CV, Williams MT. 2006. Morris water maze: Procedures for assessing spatial and related forms of learning and memory. Nat Protoc 1:848–858.

Walker AW, Smith CM, Chua BE, Krstew EV, Zhang C, Gundlach AL, Lawrence AJ. 2015. Relaxin-3 receptor (RXFP3) signalling mediates stress-related alcohol preference in mice. PLoS One 10:e0122504.

Watanabe Y, Tsujimura A, Takao K, Nishi K, Ito Y, Yasuhara Y, Nakatomi Y, Yokoyama C, Fukui K, Miyakawa T, Tanaka M. 2011. Relaxin-3-deficient mice showed slight alteration in anxiety-related behavior. Front Behav Neurosci 5:50.

Xu X, Roby KD, Callaway EM. 2010. Immunochemical characterization of inhibitory mouse cortical neurons: Three chemically distinct classes of inhibitory cells. J Comp Neurol 518:389–404.

Yamazaki M, Matsuoka N, Maeda N, Ohkubo Y, Yamaguchi I. 1996. FK960 *N*-(4-acetyl-1-piperazinyl)-*p*-fluorobenzamide monohydrate ameliorates the memory deficits in rats through a novel mechanism of action. J Pharmacol Exp Ther 279:1157–1173.

Zappone CA, Sloviter RS. 2001. Commissurally projecting inhibitory interneurons of the rat hippocampal dentate gyrus: A colocalization study of neuronal markers and the retrograde tracer Fluoro-gold. J Comp Neurol 441:324–344.

Zhang C, Chua BE, Yang A, Shabanpoor F, Hossain MA, Wade JD, Rosengren KJ, Smith CM, Gundlach AL. 2015. Central relaxin-3 receptor (RXFP3) activation reduces elevated, but not basal, anxiety-like behaviour in C57BL/6J mice. Behav Brain Res 292:125–132.

Supplementary Information – Tables 1-3 and Figures 1-2

Table S1. List of primary antibodies used in immunofluorescence studies

Antigen	Immunogene	Host, Antibody	Source/Cat No.	Dilution
RLN3	N-terminal region of mature RLN3 peptide	Mouse, monoclonal	Florey Institute of Neuroscience and Mental Health, Melbourne, Australia	1:5
GABA	γ-Aminobutyric acid (GABA) conjugated to BSA	Rabbit, polyclonal	Sigma-Aldrich, St. Louis, MO, USA, A2052	1:3,000
SST	Amino acids 1-14 of cyclic somatostatin conjugated to bovine thyroglobulin using carbodimide	Rat, monoclonal	Millipore, Darmstadt, Germany, MAB354	1:200
PV	Full-length native protein (purified) corresponding to rat parvalbumin.	Rabbit, polyclonal	Abcam, Cambridge, UK, ab11427	1:1,000
CR	Recombinant human calretinin containing a 6-his tag at the N-terminal.	Rabbit, polyclonal	Swant, Bellinzona, Switzerland, CR7697	1:1,000

For further details see Chapter 2 Materials and Methods.

Table S2. Hippocampal neuron populations and proportion innervated by RLN3 fibres

Immunological Marker	Field	Layer	No. of positive neurons	No. and (%) of neurons contacted by relaxin-3 fibres
GABA		Hilus	46.3 ± 11	5.3 ± 0.3 (12)
	DG	GC	7.67 ± 2.2	ND
		Mol	25.3 ± 2.0	ND
		Average	*79.3 ± 14*	*5.3 ± 0.3 (7)*
		LMol	67.3 ± 7.22	1.0 ± 0.6 (2)
		Rad	27.0 ± 2.3	0.7 ± 0.3 (3)
	CA1	Pyr	33.0 ± 5.0	1.5 ± 1.2 (5)
		Or	38.0 ± 9.1	5.7 ± 2.3 (15)
		Average	*165 ± 7.9*	*8.3 ± 2.7 (5)*
		Rad	26.0 ± 4.5	1.7 ± 1.2 (6)
	CA3	Pyr	23.0 ± 8.1	2.0 ± 1.0 (9)
		Or	76.3 ± 17	4.0 ± 1.0 (5)
		Average	*125 ± 26*	*7.7 ± 0.9 (6)*
	Total Average		**123 ± 15**	**7.0 ± 1.0 (6%)**
SST		Hilus	23.3 ± 2.9	6.0 ± 1.0 (26)
	DG	GC	0.67 ± 0.7	ND
		Mol	ND	ND
		Average	*24.0 ± 3.5*	*6.0 ± 1.0 (25)*
		LMol	0.67 ± 0.7	ND
		Rad	2.33 ± 1.2	0.3 ± 0.3 (14)
	CA1	Pyr	4.00 ± 2.3	ND
		Or	34.0 ± 6.1	4.7 ± 0.7 (14)
		Average	*41.0 ± 8.7*	*5.0 ± 0.6 (12)*
		Rad	8.33 ± 2.8	2.7 ± 2.9 (33)
	CA3	Pyr	7.67 ± 0.9	0.3 ± 0.3(4)
		Or	64.3 ± 4.1	6.0 ± 2.5 (9)
		Average	*80.3 ± 2.4*	*9.0 ± 1.5 (11)*
	Total Average		**48.4 ± 9.0**	**6.7 ± 1.0 (14%)**
PV		Hilus	4.33 ± 0.88	1.0 ± 0.0 (23)
	DG	GC	9.67 ± 2.4	1.0 ± 0.8 (10)
		Mol	0.67 ± 0.67	ND
		Average	*14.7 ± 1.9*	*2.0 ± 0.6 (14)*
		LMol	ND	ND
		Rad	1.67 ± 0.3	ND
	CA1	Pyr	26.0 ± 3.0	0.7 ± 0.3 (3)
		Or	11.7 ± 3.0	0.7 ± 0.3 (6)
		Average	*39.3 ± 5.8*	*1.3 ± 0.7 (3)*
		Rad	7.33 ± 1.8	0.7 ± 0.3 (9)
	CA3	Pyr	27.0 ± 3.6	1.0 ± 0.6 (4)
		Or	45.3 ± 7.8	3.3 ± 1.2 (7)
		Average	*79.7 ± 8.4*	*5.0 ± 1.5 (6)*
	Total Average		**44.6 ± 10**	**3.0 ± 0.8 (7%)**
CR		Hilus	23.3 ± 3.5	2.0 ± 0.6 (9)
	DG	GC	1.00 ± 1.0	ND
		Mol	25.7 ± 4.6	0.3 ± 0.3 (1)
		Average	*50.0 ± 7.1*	*2.3 ± 0.7 (5)*
		LMol	17.3 ± 1.2	ND
		Rad	31.0 ± 8.6	ND
	CA1	Pyr	18.0 ± 4.7	ND
		Or	34.0 ± 3.1	3.3 ± 1.9 (10)
		Average	*100 ± 7.4*	*3.3 ± 1.9 (3)*
	CA3	Rad	22.3 ± 7.4	2.3 ± 0.9 (10)

Pyr	7.00 ± 3.6	0.7 ± 0.7 (10)
Or	20.3 ± 7.9	1.3 ± 0/9 (7)
Average	*49.7 ± 17*	4.3 ± 2.3 (9)
Total Average	**66.7 ± 10**	**3.3 ± 1.0 (5%)**

Quantification of the total number of GABA-, SST-, PV-, and CR- positive neurons in all layers of the DG, and CA1 and CA3 fields, and the total number and proportion of GABA-, SST-, PV- and CR- positive cells observed to be in close apposition with relaxin-3-positive nerve fibres. Data are expressed as mean ± SEM, *n* = 3 mice. Abbreviations in alphabetical order: CR, calretinin; DG, dentate gyrus; GC, granule cell layer; LMol, lacunosum moleculare layer; Mol, molecular layer; ND, not detected; Or, stratum oriens; PV; parvalbumin; Pyr, pyramidal cell layer; Rad, stratum radiatum; SST, somatostatin. For further details see Chapter 2 Materials and Methods.

Table S3. General locomotor activity and anxiety-like behaviour of AAV$^{(1/2)}$-eGFP and AAV$^{(1/2)}$-Cre-IRES-eGFP treated mice

Behavioural Test	Behavioural Measure	GFP mice	Cre mice
Locomotor Activity	Total distance travelled (m)	114 ± 6.3	109 ± 5.7
Elevated Plus Maze	Time in open arms (s) No. of entries in open arms	53.7 ± 7.8 6.92 ± 0.96	55.4 ± 9.6 7.67 ± 1.2
Light/Dark Box	Time in light side (s) No. of entries into light side	195 ± 17 28.5 ± 3.4	215 ± 14 35.5 ± 2.9

Data are expressed as mean ± SEM, n = 12 – 13 mice per group. No treatment differences were observed in the total distance travelled (m) in a 60 min locomotor test ($t_{(23)}$ = 0.551, p = 0.587; n = 12 – 13 per group), or the time spent in the open arms (s) ($t_{(23)}$ = 0.886, p = 0.139) or entries into open arms ($t_{(23)}$ = 0.498, p = 0.623) in a 10 min EPM test, or in the time spent in the light side (s) ($t_{(22)}$ = 0.886, p = 0.385) and entries into the light side ($t_{(22)}$ = 1.528, p = 0.141) in a 10 min L/D box. For further details see Materials and Methods.

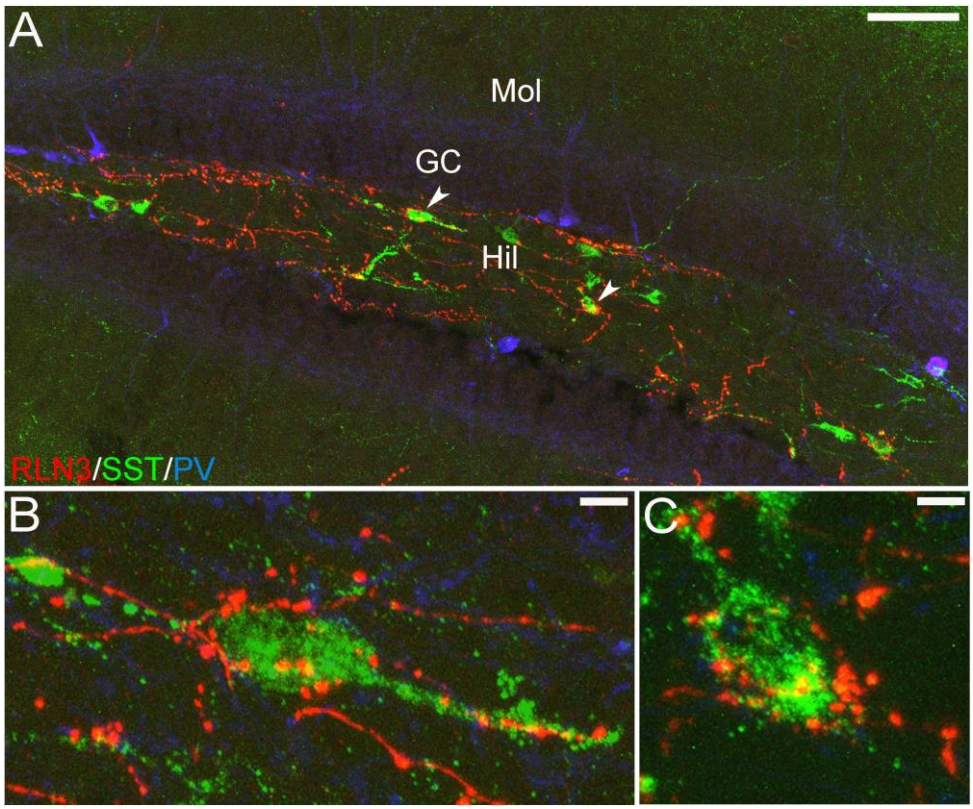

Figure S1. Comparative distribution of RLN3-immunoreactive nerve fibres and hippocampal neurons immunoreactive for somatostatin (SST) and parvalbumin (PV) in the dorsal DG hilus of adult mouse hippocampus.

Mosaic confocal images (20× magnification represented as z-stack maximum projections, 1 µm intervals) of mouse DG (reproduced from Figure 4), illustrating **(A)** RLN3 (red), SST (green) and PV (blue) immunoreactivity. Further details of the putative interactions between RLN3 inputs and SST neurons were recorded in this section. The DG hilar SST-positive neurons indicated by arrowheads in **A**, are illustrated at higher resolution in **(B)** and **(C)**. There are several points of close apposition between the RLN3 fibres/boutons and the soma and proximal/distal processes of the SST neurons (yellow). Scale bars, 100 µm **(A)** and 20 µm **(B**, **C)**.

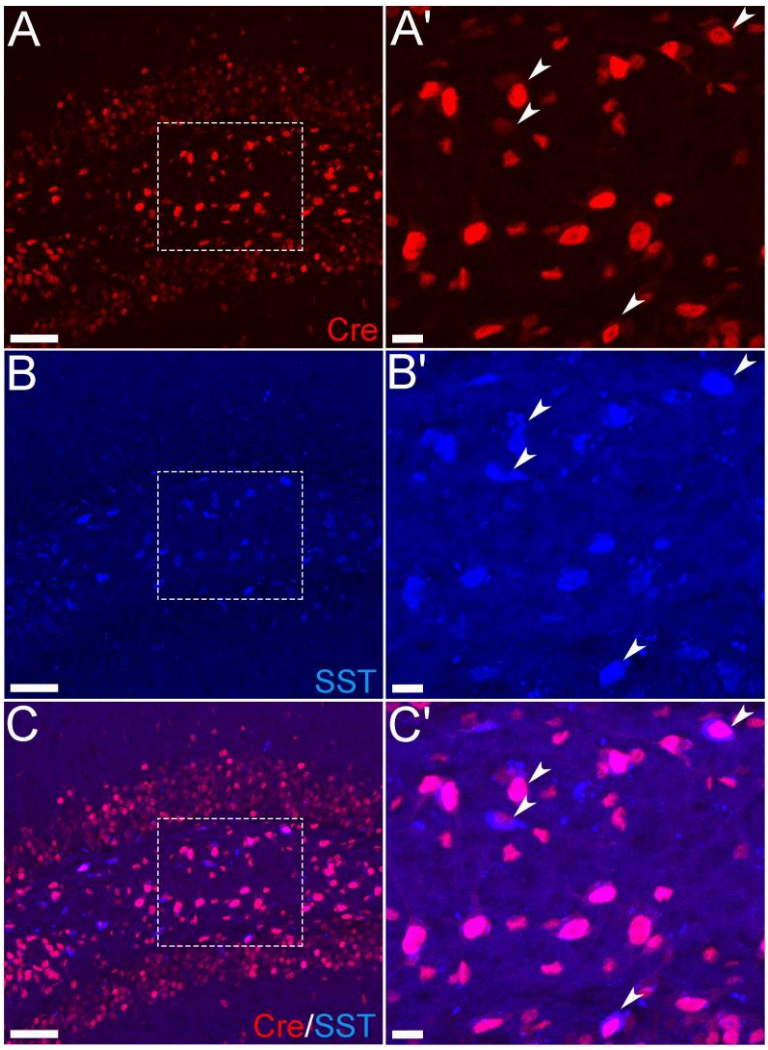

Figure S2. Comparative distribution of Cre-recombinase and somatostatin (SST) in DG hilar neurons of dorsal hippocampus in mice injected with the AAV$^{(1/2)}$-Cre-IRES-eGFP viral vector.

Bilateral injections of AAV$^{(1/2)}$-Cre-IRES-eGFP into the DG of floxed-RXFP3 mice resulted in expression of Cre-immunoreactivity (red) **(A, A)** in SST neurons (blue) **(B, B)** of the DG hilus. Cre-immunoreactivity (pink) was consistently observed in nuclei of SST-immunoreactive neurons in the region **(C, C)**, consistent with the deletion of RXFP3 expression from these neurons. In the higher magnification images of the boxed areas (**A, B, C**), arrowheads indicate examples of neurons in which Cre and SST are co-localized. Scale bars, 100 µm **(A-C)** and 20 µm **(A-C)**

CHAPTER 3

Neurochemical characterisation of the nucleus incertus in a mouse model of tauopathy

3.1 Introduction

Tau is a microtubule-associated protein first described in 1975 (Weingarten et al., 1975), which plays an important role in maintaining cell structure and cytoarchitectural stability. Under pathological conditions tau becomes hyperphosphorylated (Goedert and Spillantini, 2006; Wang and Mandelkow, 2016) resulting in dissociation from microtubules. The unbound tau assembles into intracellular neurofibrillary tangles (NFTs) in neuronal cell bodies, leading to disruption of intracellular neuronal function and neuronal death, as well as altered axonal transport. The accumulation of NFTs is characteristic of many neurodegenerative diseases, including Alzheimer's disease (AD) (Alzheimer, 1907), progressive supranuclear palsy, Pick's disease, Huntington's disease, frontotemporal dementia with parkinsonism-17 (FTDP-17) (Hutton et al., 1998) and other tauopathies (Irwin, 2016). In AD, NFTs were initially thought to first accumulate in the entorhinal cortex and progressively spread to limbic areas (i.e. hippocampal formation and cingulate cortex) followed by neocortical areas (Braak and Braak, 1991). More recently, in post-mortem brains from patients with AD and related tauopathies, Braak and colleagues (2011) found NFTs to initially form in noradrenergic (NA) projection neurons of the locus coeruleus (LC), and thereafter in neurons of other brainstem nuclei with diffuse cortical projections, including the dorsal raphe (DR) nuclei.

Interestingly, following brainstem formation of NFTs, the first cortical regions to display NFT pathology are the anatomically connected trans-entorhinal and neocortical regions (Braak et al., 2011). This observation suggests that upstream brainstem regions might trigger cortical NFT pathology. For example, in post-mortem AD brains, NFTs have been detected in regions that receive LC and DR projections, including the hippocampus and cingulate cortex (Arnold et al., 1991; Tekin et al., 2001) and diminished levels of NA and 5-HT have been detected in these regions (Aral et al., 1984; Reinikainen et al., 1988; Storga et al., 1996). Furthermore, in an early study the loss of LC NA neurons was found to correlate significantly with NFT accumulation in the cingulate cortex (Bondareff et al., 1987). In line with this, inoculation of synthetic tau fibrils in the LC of transgenic mutant tau mice (tau-P301S, which express hyperphosphorylated tau) induces a time-dependent spread of NFTs from the injection site to anatomically connected forebrain regions including the hippocampus and cingulate cortex (Iba et al., 2015), suggesting that cell-to-cell transmission of NFTs can occur along efferent brain projections (Clavaguera et al., 2009; de Calignon et al., 2012; Liu et al.,

2012; Ahmed et al., 2014). Two potential mechanisms are likely to contribute to this effect. Firstly, a release of tau aggregates into the extracellular space near axonal terminals may be taken up by downstream synaptically connected neurons. Secondly, this release of tau aggregates is likely promoted by their own formation within presynaptic neurons, as NFTs can cause leakage of the presynaptic membrane. Therefore, these two mechanisms likely facilitate release of tau 'seeds' from presynaptic sites (e.g. from brainstem neuron terminals), which can then diffuse along the synaptic cleft and be taken up by postsynaptic neurons, which subsequently initiates tau aggregation in these downstream cells (e.g. within the cerebral cortex) (Wang and Mandelkow, 2016; Wu et al., 2016).

In addition to potentially 'triggering' cerebral cortical/hippocampal NFT formation, tau pathology within the brainstem is important for another reason. The release of brainstem neurotransmitters such as the monoamines, 5-HT and NA, plays a critical role in cortical and hippocampal function. In AD and other tauopathies, the function of these regions is impaired not only due to disruption of cortical/hippocampal neurons themselves, but also due to disruption of brainstem neurons that normally modulate these areas via monoamine and other neurotransmitter actions. Notably, total RNA levels in 5-HT and NA neurons within the brainstem of AD patients are significantly reduced (Mann et al., 1982; Mann et al., 1984), and pre-clinical rodent studies suggest that targeting these neuronal populations represents a promising research avenue for the treatment of neurodegenerative disorders (Himeno et al., 2011; Jurgensen et al., 2011; Kalinin et al., 2012; for review see Trillo et al., 2013).

GABA projections from the adjacent pontine brainstem region, the nucleus NI (Nunez et al., 2006; Ma et al., 2007; Olucha-Bordonau et al., 2012; Ma et al., 2013; Sanchez-Perez et al., 2015), is likely to perform synergistic and complementary roles to monoamine signalling within shared efferent target brain regions (for review Smith et al., 2014a). For example, NI GABA-positive projections regulate hippocampal theta rhythm (4-8 Hz in rodents and 4-12 Hz in humans), which is important for spatial navigation and memory formation (Vertes et al., 1994), and is similarly modulated by parallel 5-HT/DR and NA/LC ascending systems (Kocsis et al., 2007; Sorman et al., 2011).

As mentioned (see General Introduction), the NI is the primary source of the neuropeptide relaxin-3 (Bathgate et al., 2002; Burazin et al., 2002), which acts via its cognate $G_{i/o}$-protein-

coupled receptor, RXFP3 (Liu et al., 2003; Bathgate et al., 2006). The distribution of relaxin-3-positive nerve fibres and RXFP3 mRNA strongly overlap with NI forebrain projections, with dense relaxin-3-positive nerve fibres and RXFP3 mRNA present in regions heavily affected in AD, including the cingulate cortex, hippocampus and septum (Ma et al., 2007; Ma et al., 2009b; Smith et al., 2010); and anatomical studies have identified relaxin-3 neuronal contacts with distinct neuronal populations in septum (Olucha-Bordonau et al., 2012) and hippocampus (see Chapter 2). In addition to anatomical studies, the functional role of the NI (Nunez et al., 2006; Ma et al., 2013; Pereira et al., 2013; Nategh et al., 2015) and medial septum (Ma et al., 2009c) in hippocampal activity and cognition is well established.

Therefore, the NI GABA/relaxin-3 system represent an ascending brainstem network, which may act in a similar fashion to the 5-HT/DR and NA/LC systems and the main aim of the studies described in this Chapter was to examine the state of NI relaxin-3 neurons in a mouse model of tauopathy, the tau-P301L transgenic mice (Terwel et al., 2005; Terwel et al., 2008). This study is an important first step to determining whether damage to the NI relaxin-3 system occurs and may contribute to the 'seeding' of hippocampal/cortical tauopathy, and/or the cognitive decline that results from disrupted brainstem innervation of, and neurotransmission in, the hippocampus and cortex.

Triple-fluorescence immunohistochemistry was performed to characterise the expression of NeuN (neuronal nuclei, a neuronal specific nuclear protein, Mullen et al., 1992), relaxin-3, and NFTs in NI neurons of 7 - 8 month old tau-P301L transgenic mice (Terwel et al., 2005; Terwel et al., 2008), and age matched FVB/N controls. In P301L mice, NFTs progressively develop in neurons of the brainstem and midbrain (Dutschmann et al., 2010), and forebrain regions, such as the cortex (Hampton et al., 2010), hippocampus (Gotz and Nitsch, 2001; Harris et al., 2012) and septal nuclei (Kohler et al., 2010), and neurological symptoms are present at 6-7 months of age (Terwel et al., 2005).

3.2 Materials and Methods

All studies were conducted with approval from The Florey Institute of Neuroscience and Mental Health Animal Ethics Committee and were in accordance with ethical guidelines issued by the National Health and Medical Research Council of Australia.

3.2.1 Mice

Experiments were conducted using 7 - 8 month old male tau-P301L transgenic mice (*n* = 6), and age- and sex-matched FVB/N controls (*n* = 3). The tau-P301L mice line used were generated and characterised previously (Dutschmann et al., 2010; Trillo et al., 2013) and bred within the Howard Florey Laboratories, Parkville. These mice express the longest human tau isoform with the P301L mutation (tau-4R/2N-P301L) under the control of the mouse *thy1* gene promoter to provide neuron-specific expression commencing in the third postnatal week (Terwel et al., 2005). Transgenic mice were generated on a FVB/N genetic background, and mice homozygous for the tau-P301L transgene were genotyped by polymerase chain reaction (PCR) with a forward primer specific for the thy1-tau-P301L mouse gene promoter (5'-CTG-GGGCGGTCAATAAT-3') and a reverse primer specific for human tau cDNA (5'-CAA-GGTCCCCGTTTCTCC-3') (Terwel et al., 2005).

3.2.2 Brain fixation and sectioning

Mice were deeply anaesthetised with 5% isoflurane inhalation (Delvet, Seven Hills, NSW, Australia) and then administered sodium pentobarbital (11 mg/kg 0.1 ml, i.p.) and transcardially perfused with 0.1 M phosphate buffer (PB, 2.7 nM KCl, 11.2 mM Na_2HPO_4, pH 7.4) followed by 4% paraformaldehyde (PFA) in 0.1 M PB. Mice were decapitated and their brains dissected and post-fixed in 4% PFA in 0.1 M PB for 1 h on ice. Brains were transferred to 20% sucrose in 0.1 M PB and kept at 4°C overnight. Brains were then embedded in O.C.T. (Tissue-Tek, Sakura Finetek, USA) and frozen on dry ice. Forty (40) µm coronal sections were cut using a cryostat (Cryocut 1800, Leica Microsystems, Heerbrugg, Switzerland) at -18°C and stored in cryoprotectant solution (30% ethylene glycol, 30% glycerol, 0.05M PB) at -20°C. For quantitative analysis, four coronal sections of the NI spanning -5.25 mm to -5.45 mm from Bregma were collected from each brain.

3.2.3 Immunohistochemistry for NeuN, relaxin-3 and p-tau

All sections were washed 3 × 5 min in 0.1% Triton X-100 in 0.1 M PB, and then blocked in 10% normal horse serum (NHS) in 0.1% Triton X-100, 0.1 M PB for 1h at RT. Sections were incubated with (1) a mouse monoclonal relaxin-3 antibody (HK-4-144-10; 1:5; Kizawa et al., 2003; Tanaka et al., 2005; Ma et al., 2013) in 2% NHS and 0.1% Triton X-100 in 0.1 M PB overnight at RT. On the following day, sections were washed 3 × 5 min in 0.1 M PB, followed by secondary incubation in (1) donkey anti-mouse Alexa-594 (JIR, 715585151, 1:500) for 1h at RT. Following the incubation in the secondary antibody for visualisation of relaxin-3-immunoreactivity, sections were then washed 3 × 5 min in 0.1 M PB, followed by primary incubation in (2) a mouse monoclonal NeuN antibody (Millipore, MAB377, 1:1000) and (3) rabbit polyclonal phospho tau (p-tau) serine 199/202 antibody (tauPS199/202) (Chemicon, AB9674, 1:500) in 2% NHS and 0.1% Triton X-100 in 0.1 M PB overnight at RT. This antibody recognises pre-, i-NFTs and e-NFTs phosphorylated at serine 199 and 202 (Kimura et al., 1996; Augustinack et al., 2002).

Sections were washed 3 × 5 min in 0.1 M PB, followed by secondary incubation in (2) donkey anti-mouse 647 (Jackson ImmunoResearch, 711546152, 1:500) and (3) donkey anti-rabbit 488 (Jackson ImmunoResearch, 715605151, 1:500) in 0.1 M PB for 1h at RT. Following the secondary antisera incubation, sections were washed 3 × 5 min with 0.1 M PB and mounted on glass slides using Fluoromount-G (Southern Biotech, Birmingham, AL, USA). Notably, the relaxin-3 and NeuN primary antibodies were from the same host species, therefore, cross-reactivity with the secondary antibody binding to two targets occurred. However, a sequential protocol was used to immunostain for relaxin-3 first, followed by NeuN on the subsequent day, which ensured accurate immunostaining of relaxin-3-positive neurons (i.e. not all NeuN-positive neurons were detected as relaxin-3 positive, and the expression of relaxin-3 in the present study is consistent with previous reports). However, although using this approach will detect all relaxin-3-positive neurons to co-express NeuN, it is reasonable to assume all relaxin-3 containing neurons will express NeuN as only neurons express relaxin-3. As such, this protocol allowed the differentiation between relaxin-3-positive and negative neurons in the NI, and was sufficient for quantitative purposes.

Anti-tauPS199/202 antibody is specific for extra-neuronal NFTs (eNFTs) phosphorylated at serine 199 and 202 and characterised by atrophic neuronal staining with no basal dendrites,

as well as pre- and intra-neuronal- NFTs (iNFTs) characterised by punctate neuronal staining and a homogeneously stained soma with slightly damaged basal dendrites, respectively (Augustinack et al., 2002). The specificity of anti-tauPS199/202 for NFTs has been confirmed with no neuronal or extra-neuronal expression in brain sections from non-transgenic mice (Terwel et al., 2005; Boekhoorn et al., 2006; Terwel et al., 2008; Dutschmann et al., 2010).

3.2.4 Imaging

Immunostaining was observed under a LSM 780 Zeiss Axio Imager 2 confocal laser scanning microscope (Carl Zeiss AG, Jena, Germany). Mosaic z-stack images were obtained with a 63× objective and 1 µm z-intervals covering the entire NI from 4 coronal sections for each mouse (from -5.25 mm to -5.45 mm from Bregma) and obtained with 10% overlap with each image on the X-Y plane.

3.2.5 3D Data analysis

Z-stacks were loaded into Amira (v.6.0.1, FEI) to create an isosurface (3D surface representation). Cells were counted by manually placing landmarks in the cell bodies of the labelled 3D representation of the neurons.

3.2.6 Statistical analysis

Statistical analysis and graphical representations of the data were conducted using Graph Pad Prism (v.6) (GraphPad, La Jolla, CA, USA). All data are expressed as mean ± SEM. For comparison of data, a one-way ANOVA was performed followed by a Bonferroni's multiple comparisons test. Results were considered statistically significant if $p < 0.05$.

3.3 Results

3.3.1 Relaxin-3 and NeuN immunostaining in the NI of 7 - 8 month old FVB/N control mice

In agreement with studies in 8 week old C57BL/6J wildtype mice (Smith et al., 2010), the present study identified relaxin-3-positive neurons within the NI of 7 - 8 month old FVB/N control mice located medioventral to the LC and along the medial and ventral border of the ventral tegmental nucleus (see **Figure. 3.1**). Relaxin-3-positive nerve fibres were also observed within the NI region in addition to the nearby pontine central gray (CG) and an area adjacent to the fourth ventricle.

3.3.2 Relaxin-3, NeuN and p-tau immunostaining in the NI of 7 - 8 month old tau-P301L mice

The topographical distribution of relaxin-3-positive neurons and nerve fibres, and NeuN-positive neurons, in 7 - 8 month old tau-P301L mice was similar to that in FVB/N age-matched control mice (see **Figure. 3.2**), although quantitative assessment of the number of positive neurons revealed significant differences between the two groups of mice (see below). P-tau-positive neurons were observed predominantly in the lateral regions of the NI, and in surrounding areas such as LC. As previously observed (Dutschmann et al., 2010), p-tau positive nerve fibres was detected in the NI.

3.3.3 Quantitative analysis of relaxin-3-, NeuN- and p-tau-positive neurons in the NI of 7 - 8 month old tau-P301L and FVB/N control mice

There was a non-significant difference in the total number of neurons in the NI of 7 - 8 month old tau-P301L mice compared to age-matched control mice, i.e. the number of NeuN-*positive* neurons was 25% lower in the tau-P301L mice (**Figure 3.3A**; unpaired t-test, t (4) = 2.34, p = 0.0792). Similarly, the number of relaxin-3-*negative* neurons was not significantly different in tau-P301L mice relative to FVB/N controls, although there was a 21% numerical reduction (**Figure 3.3A**; unpaired t-test, t (4) = 1.14, p = 0.316). In contrast, the number of relaxin-3-

positive neurons was 35% lower in tau-P301L mice than in the FVB/N age-matched controls (**Figure 3.3A**; unpaired t-test, t (7) = 3.03, p = 0.0193). When the % differences in the number of stained NI neurons observed in tau-P301L mice and controls were calculated, it equated to a ~20% reduction in relaxin-3-*negative* neurons and an ~35% reduction in relaxin-3-*positive* neurons. However, these differences were not statistically significance (**Figure 3B**; unpaired t-test, t (7) = 1.61, p = 0.152), perhaps due to the small sample size. Thus, these initial findings suggest that alterations in the number and/or immunostaining characteristics of neurons within the NI *may* occur in this mouse model of tauopathy and indicate that further studies are warranted. There may also be differential effects on populations of relaxin-3-positive and -negative NI neurons; but further studies are also required to address this issue.

Notably, a significantly larger proportion of relaxin-3-negative NI neurons (~30%) were found to contain p-tau, (a marker of NFTs), than relaxin-3-positive NI neurons, which rarely displayed p-tau (~5%) (**Figure 3C**; unpaired t-test, t (7) = 3.96, p = 0.0054). These findings suggest that at this time-point (7 - 8 months), some or many of those relaxin-3-expressing neurons affected by the tauopathy have either died or no longer express detectable levels of relaxin-3 peptide (see Discussion).

3.4 Discussion

This Chapter describes the first study to neurochemically phenotype the NI and relaxin-3 system in a transgenic mouse model of tauopathy, and provides important preliminary insights into the potential involvement of the NI and relaxin-3 system in tauopathies and related neurodegenerative disorders, including the impact on NFTs on these neurons and their response to the insult. The NI is a small, heterogeneous brainstem nucleus that sends strong GABAergic projections to hippocampus and forebrain regions that influence hippocampal activity (Goto et al., 2001; Olucha-Bordonau et al., 2003; Brown and McKenna, 2015), and the NI is important for normal cognitive behaviours, including memory (Nunez et al., 2006; Nategh et al., 2015). Similarly, the relaxin-3/RXFP3 system is also an important modulator of hippocampal activity as well as cognitive-related behaviour via actions within the septum (Ma et al., 2009c) and hippocampus (see Chapter 2). As such, if NI and/or relaxin-3-positive neurons are damaged or lost in tauopathies, this might contribute to septohippocampal dysfunction and related cognitive symptoms. Consistent with this possibility, this study observed a 35% reduction in the number of relaxin-3-immunopositive NI neurons in 7 - 8 month old tau-P301L mice, relative to the number in appropriate age-matched control mice. A trend for a reduction (~20%) in the number of relaxin-3-negative NI neurons was also observed.

The present studies did not examine whether the density and characteristics of relaxin-3-positive axonal projections and terminals within the hippocampus and other target regions were altered to a similar or greater extent. Based on recent studies describing impairments of SHS GABAergic (Levenga et al., 2013; Soler et al., 2017) and cholinergic neurons (Belarbi et al., 2009; Belarbi et al., 2011; Hara et al., 2017) in mouse models of tauopathy, some alterations would be predicted. For example, in a recent study, early onset deterioration of GABAergic SHS connections particularly on PV-positive hippocampal interneurons in a mouse model expressing human mutated tau (mutations G272V, P301L, and R406W, VLW transgenic strain) in 2-month old VLW mice was observed, and more severe effects were observed in 8-month old VLW mice, mainly by p-tau expressing PV-positive hippocampal interneurons (Soler et al., 2017). In THY-Tau22 transgenic mice, the retrograde transport of FG through the SHS is impaired, which was found to be associated with a significant reduction in the number of ChAT-positive neurons in the MS (Belarbi et al., 2011). Taken together, analysis of the relaxin-

3/RXFP3 system within the hippocampus (and other target regions including the septal nuclei) represents an important future direction, which could also be extended by examining the state of relaxin-3 cell bodies and axons/terminals at different stages of tauopathy progression. These studies might also indicate whether the relaxin-3-positive neurons that are 'compromised' in 7 - 8 month old tau-P301L mice represent a sub-population with distinct projection targets, or whether more 'broad' changes are evident.

A further interesting finding in the present studies was the rare detection of relaxin-3-*and* p-tau staining in NI neurons in the 7 - 8 month tau-P301L mice. In this experiment, the presence of NFTs was assessed with a tau phospho-serine 199/202 antibody, tauPS199/202, and staining was predominantly observed in the lateral NI, with cells in this area accounting for ~30% of the relaxin-3-negative neurons that displayed p-tau staining (NFTs). Based on the significant reduction in relaxin-3-positive neurons detected and the retained expression of NeuN staining within p-tau positive neurons, it is possible that the expression/production of relaxin-3 in normally 'relaxin-3 capable' neurons has 'ceased' during earlier stages of NFT production, but before neuronal death, producing a hypo-functionality of relaxin-3 signalling. For example, it may be possible for NI neurons to no longer express 'detectable' levels of relaxin-3 peptide immunoreactivity, due to a tauopathy related down-regulation of relaxin-3 mRNA expression and subsequent reductions in peptide translation and processing (i.e. the neurons contained no relaxin-3 peptide or only very low undetectable levels, due to cellular compromise and reprogramming perhaps preceding neuronal death. Notably, three morphological stages of NFT production/toxicity have been identified: (1) pre-NFTs, defined by punctate NFT staining within the cytoplasm with well-preserved dendrites and a centred nucleus; (2) iNFTs, characterised by punctate NFT staining within the cytoplasm as well as slightly damaged dendrites, and; (3) eNFTs identified by the absence of basal dendrites and the presence of atrophic neuronal staining resulting from the death of the tangle-bearing neurons (Kimura et al., 1996; Augustinack et al., 2002; Serrano-Pozo et al., 2011). Morphological stages of NFTs progress sequentially throughout development of tauopathies (Kimura et al., 1996; Augustinack et al., 2002), whereby a healthy neuron develops punctate phospho-tau inclusions and becomes a pre-NFT cell, thereafter giving rise to an iNFT, and after neuronal death occurs eNFTs remain. Although some reports suggest the tauPS199/202 antibody is specific for eNFTs, pre- and i-NFTs have also been shown to be phosphorylated at

serine 199 and 202 and this antibody has been shown to recognise pre- and i-NFTs (Kimura et al., 1996; Augustinack et al., 2002). As 30% of relaxin-3-negative, NeuN-positive neurons display p-tau staining with the tauPS199/202 antibody, a large proportion of the NFTs detected in the present study are likely to be pre- or i-NFTs. However, future studies should confirm this by more closely examining the morphological characteristics of NFTs in the mice studied here. If pre- or i-NFTs predominate, expression/production of relaxin-3 in neurons may be susceptible to the effects of NFTs at early stages of the disease (i.e. before the expression of eNFTs). This is consistent with reports on other GABA/neuropeptide systems including SST and NPY neurons in hippocampus (Ramos et al., 2006), and the expression/detection of SST receptor 2 (SSTR2) in LC neurons (Ádori et al., 2015). There are early decreases and selective losses of these peptides and receptor preceding the onset of advanced AD pathology. As such, it is crucial for future studies to determine the time course of changes in relaxin-3 immunoreactive peptide by neurochemically phenotyping the NI at earlier and later stages of disease progression (within subject design), along with measures of relaxin-3 mRNA to better detect relaxin-3-capable neurons under these conditions.

Additionally, as mentioned, RXFP3 mRNA and binding sites are highly expressed in the MS/DB and hippocampus, and strongly overlap with NI projections and relaxin-3-positive nerve fibres and terminals (Ma et al., 2007; Ma et al., 2009b; Smith et al., 2010). As such, expression of NFTs within NI relaxin-3 neurons may facilitate the release of tau ‘seeds’ from presynaptic projection sites within the hippocampus and other downstream target regions, which might be taken up by postsynaptic neurons in these forebrain regions, triggering NFT accumulation in downstream neurons. Therefore, a potentially important future study could determine whether lesion/ablation of the NI in young tau-P301L mice alters the progression of tauopathy within the hippocampus and other regions that normally receive NI/relaxin-3 innervation.

Having established that relaxin-3 peptide levels in NI neurons are reduced in this mouse model of tauopathy, a major future challenge will be to determine whether a reduction in relaxin-3/RXFP3 signalling within key downstream regions (i.e. MS/DB and hippocampus) contributes to their dysfunction and cognitive decline. One potential approach could involve the generation of double mutant relaxin-3 KO/tau-P301L transgenic mice, and assessing whether the rate of cognitive decline is greater in the absence of relaxin-3 signalling. Acute

or perhaps preferably chronic pharmacological RXFP3 antagonism in tau-P301L mice might achieve this same goal. Conversely, increasing relaxin-3/RXFP3 signalling might provide some indication of the pre-clinical therapeutic potential of this system for treating neurodegenerative disorders. Chronic pharmacological treatment with RXFP3 agonists, or a viral approach whereby excitatory Designer Receptors Exclusively Activated by Designer Drugs (DREADDs) are driven by a relaxin-3 specific promoter within the NI could be tested. In the case of an excitatory hM3Dq DREADD study, subsequent semi-chronic administration of CNO ligand would result in activation of remaining/resilient NI relaxin-3 neurons in tau-P301L mice (or other models), which may alter (slow) the progression of cognitive decline. Conversely, CNO-mediated activation of the inhibitory hM4Di DREADD in separate tau-P301L mice might accelerate (or slow) the progression of cognitive decline.

The tau-P301L mouse used has been validated as a model of human tauopathy (Terwel et al., 2005; Terwel et al., 2008; Dutschmann et al., 2010), and the pathology in tau-P301L mice is similar to that in other mutant tau mice (Hasegawa et al., 1997; Lewis et al., 2000; Gotz et al., 2001; Allen et al., 2002; Belarbi et al., 2011; Levenga et al., 2013; Soler et al., 2017). Notably, the P301L tau mutation is associated with FTDP-17 (Goedert and Spillantini, 2000; Lewis et al., 2000), and therefore, tau-P301L mice phenotypically recapitulate features of human FTDP-17 rather than classic features of AD. It will be valuable for future studies to confirm/confound and extend the observed results in mouse models that better recapitulate the hallmark pathology of AD by, for example, crossing tau-P301L mice with transgenic mice with Aβ amyloidosis, and to eventually match these studies with studies of the NI and its targets in post-mortem human AD brains.

3.5 Conclusions

The brainstem contains discrete neuronal populations, including 5-HT and NA neurons within the DR and LC, respectively, that project to and modulate brain regions important for cognitive functions, including MS/DB and hippocampus. Damage to these brainstem regions and their axonal projections is thought to contribute to cognitive dysfunction observed in tauopathies and related neurodegenerative diseases, and may also ‘seed’ the development of tauopathy within downstream brain structures. Characterising other brainstem systems that are important for the normal function of key forebrain targets and that are damaged by

or resilient to tauopathies is also key to increasing our understanding of neurodegenerative disease aetiology. To this end, this study provides an important foundation for further research to investigate the role and therapeutic potential of relaxin-3/RXFP3 signalling in tauopathies and other neurodegenerative diseases.

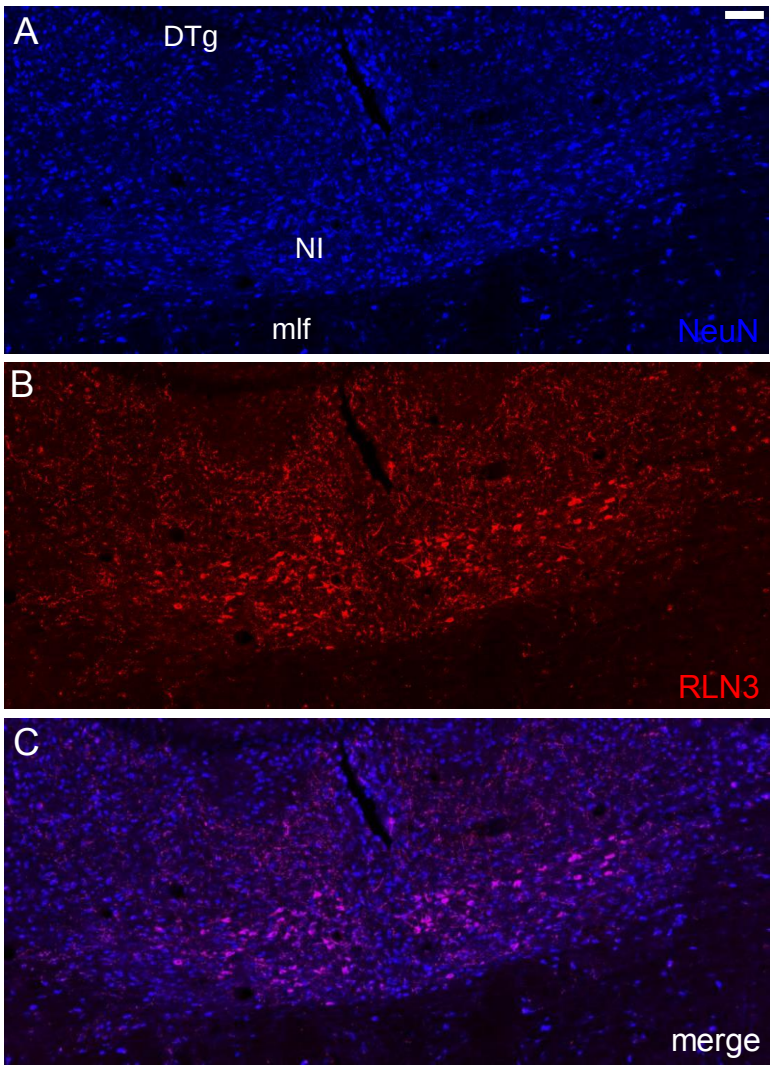

Figure 3.1. Relaxin-3- and NeuN- positive neurons in the NI of 7 - 8 month old FVB/N control mice.

Maximum intensity projection of mosaic z-stack confocal images (63× magnification, 1 µm z-intervals) illustrating **(A)** NeuN (blue) and **(B)** relaxin-3 (RLN3) (red) and **(C)** both RLN3/NeuN in the nucleus incertus (NI) and surrounding regions of 7 - 8 month old FVB/N control mice. DTg, dorsal tegmental nucleus; mlf, medial longitudinal fasciculus. Scale bar represents 100 µm.

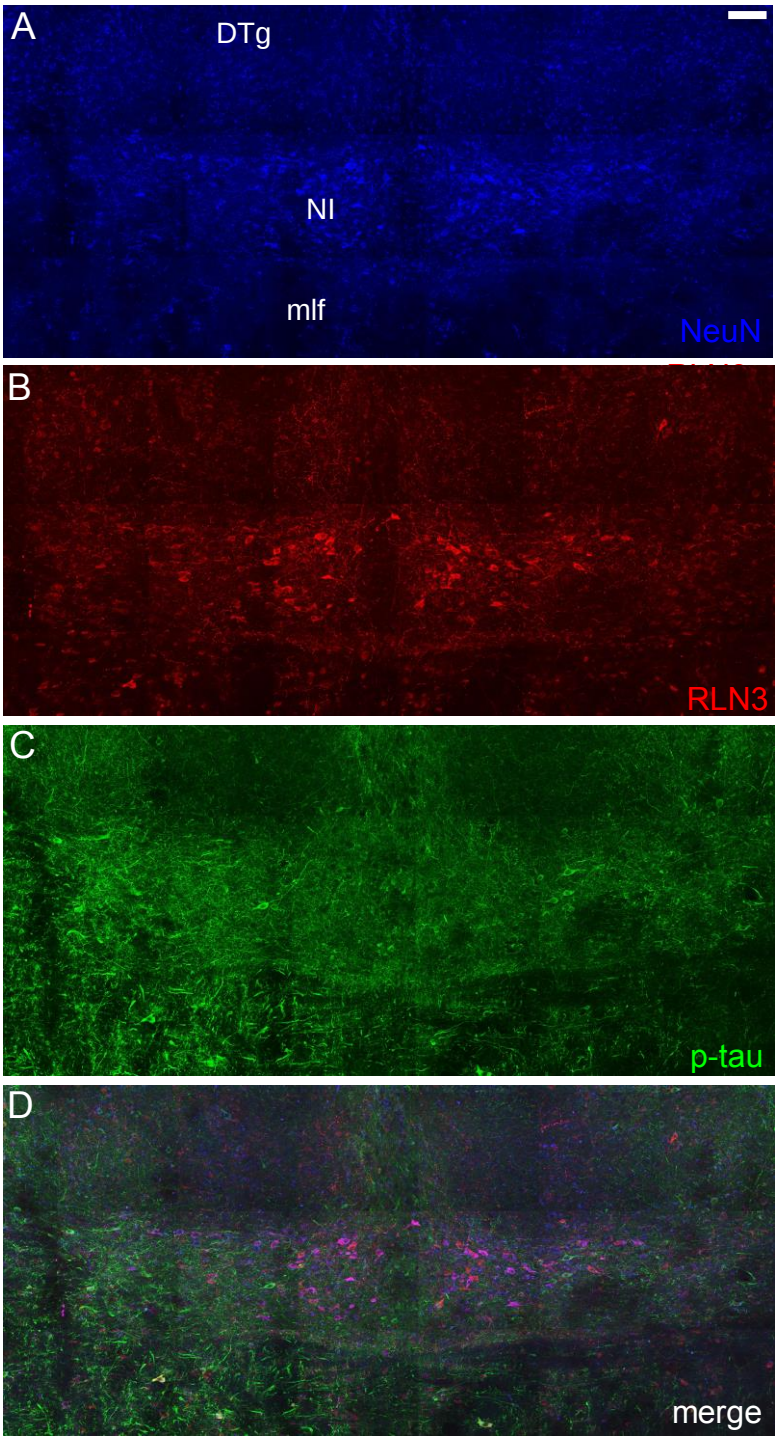

Figure 3.2. Relaxin-3-, NeuN- and phospho-tau- positive neurons in the NI of 7 - 8 month old tau-P301L transgenic mice.

Maximum intensity projection of mosaic z-stack confocal images (63× magnification, 1 µm z-intervals) illustrating (**A**) NeuN (blue), (**B**) relaxin-3 (RLN3) (red), (**C**) p-tau (green) and (**D**) an overlay of NeuN/RLN3/p-tau in the nucleus incertus (NI) and surrounding regions of 7 - 8 month old tau-P301L mice. DTg, dorsal tegmental nucleus; mlf, medial longitudinal fasciculus. Scale bar, represents 100 µm.

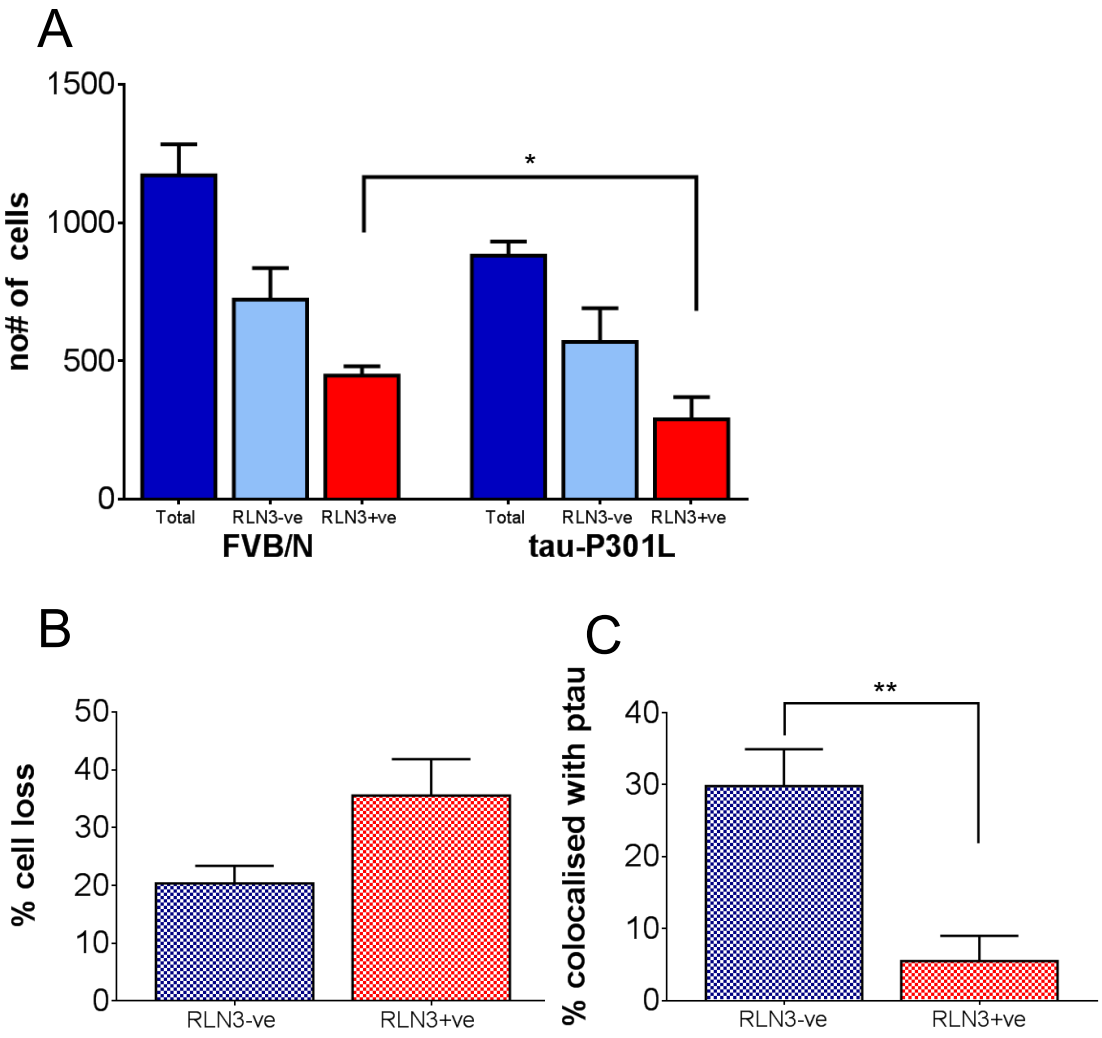

Figure 3.3. Quantification of relaxin-3-negative and positive neurons in the NI of tau-P301L transgenic mice and FVB/N age matched control mice.

(A) Quantification of the total number of neurons, and the number of relaxin-3 (RLN3)- negative and -positive neurons from 4 coronal sections (from -5.25 mm to -5.45 mm from Bregma) of the nucleus incertus (NI) of 7 - 8 month old FVB/N control and tau-P301L mice. **(B)** The total proportion (%) of RLN3-negative and -positive neurons detected in P301L-tau mice relative to FVB/N control mice. **(C)** The proportion (%) of RLN3-negative and -positive neurons that contain p-tau in the NI of tau-P301L mice. Unpaired samples t-test, *, $p < 0.05$, ** $p < 0.01$. Data are expressed as mean ± SEM, $n = 3 – 6$ mice per group.

CHAPTER 4

Relaxin-3/RXFP3 system and possible interactions with monoamine signalling

4.1 Introduction

This Chapter contains a body of experimental research, complete with Introduction, Methods, Results, Conclusion and Bibliography, which is presented as a manuscript that was accepted for publication in the peer-reviewed scientific journal, *Neurochemical Research*, on 18 May 2015.

Neurochem Res (2016) 41:481–491
DOI 10.1007/s11064-015-1621-2

ORIGINAL PAPER

Sensitivity to Chronic Methamphetamine Administration and Withdrawal in Mice with Relaxin-3/RXFP3 Deficiency

Mouna Haidar[1,2] · Monica Lam[1,3,4] · Berenice E. Chua[1,5] · Craig M. Smith[1,2] · Andrew L. Gundlach[1,2,3]

Received: 10 April 2015 / Revised: 14 May 2015 / Accepted: 18 May 2015 / Published online: 29 May 2015

Abstract Methamphetamine (METH) is a highly addictive psychostimulant, and cessation of use is associated with reduced monoamine signalling, and increased anxiety/depressive states. Neurons expressing the neuropeptide, relaxin-3 (RLN3), and its cognate receptor, RXFP3, constitute a putative 'ascending arousal system', which shares neuroanatomical and functional similarities with serotonin (5-HT)/dorsal raphe and noradrenaline (NA)/locus coeruleus monoamine systems. In light of possible synergistic roles of RLN3 and 5-HT/NA, endogenous RLN3/RXFP3 signalling may compensate for the temporary reduction in monoamine signalling associated with chronic METH withdrawal, which could alter the profile of 'behavioural despair', bodyweight reductions, and increases in anhedonia and anxiety-like behaviours observed following chronic METH administration. In studies to test this theory, Rln3 and Rxfp3 knockout (KO) mice and their wildtype (WT) littermates were injected once daily with saline or escalating doses of METH (2 mg/kg, i.p. on day 1, 4 mg/kg, i.p. on day 2 and 6 mg/kg, i.p. on day 3–10). WT and Rln3 and Rxfp3 KO mice displayed an equivalent sensitivity to behavioural despair (Porsolt swim) during the 2-day METH withdrawal and similar bodyweight reductions on day 3 of METH treatment. Furthermore, during a 3-week period after the cessation of chronic METH exposure, Rln3 KO, Rxfp3 KO and corresponding WT mice displayed similar behavioural responses in paradigms that measured anxiety (light/dark box, elevated plus maze), anhedonia (saccharin preference), and social interaction. These findings indicate that a whole-of-life deficiency in endogenous RLN3/RXFP3 signalling does not markedly alter behavioural sensitivity to chronic METH treatment or withdrawal, but leave open the possibility of a more significant interaction with global or localised manipulations of this peptide system in the adult brain.

Keywords Relaxin-3 · Rxfp3 · Knockout mice · Methamphetamine · Monoamines · Arousal

Special Issue: In Honor of Dr. Philip Beart.

Craig M. Smith and Andrew L. Gundlach jointly supervised this research.

✉ Andrew L. Gundlach
andrew.gundlach@florey.edu.au

[1] The Florey Institute of Neuroscience and Mental Health, 30 Royal Parade, Parkville, Victoria 3052, Australia

[2] Florey Department of Neuroscience and Mental Health, The University of Melbourne, Parkville, Victoria, Australia

[3] Department of Anatomy and Neuroscience, The University of Melbourne, Parkville, Victoria, Australia

[4] Present Address: Faculty of Health Sciences, La Trobe University, Bundoora, Victoria, Australia

[5] Present Address: INC Research, Oakleigh, Victoria, Australia

Introduction

Methamphetamine (METH) is a highly addictive psychostimulant, and cessation of its use is associated with withdrawal symptoms including increased anxiety and depressive states [1, 2], classified under the 'amphetamine-type stimulant withdrawal syndrome' by the American Psychiatric Association (DSM-IV). Acute METH administration increases central monoamine neurotransmission by stimulating the release of presynaptic stores of serotonin (5-HT), noradrenaline (NA) and dopamine [3–6]. Following relatively low to moderate chronic METH doses,

monoamines can be depleted from presynaptic terminals and this effect is compounded by down-regulation of postsynaptic receptors, resulting in markedly reduced monoamine signalling within limbic and/or hypothalamic brain regions such as the amygdala, hippocampus, septum and paraventricular nucleus [7–9]. These decreases have been associated with a range of related behavioural symptoms in animals, including depressive-like behaviours (such as 'behavioural despair' in mice) that are detected within 2 days of withdrawal [10, 11], and anxiety-like behaviours, observed after 5 days of drug abstinence [12].

Considerable anatomical evidence suggests neurons expressing the neuropeptide relaxin-3 (RLN3) contribute to a brainstem ascending arousal network [13–15], similar to parallel ascending monoaminergic 5-HT and NA systems [16, 17]. The main source of RLN3 neurons is the *nucleus incertus* [18–21], which lies in a region of the midline pons adjacent to serotonergic and noradrenergic neurons within the dorsal raphe nuclei and locus coeruleus, respectively. Furthermore, these three neural systems display highly overlapping efferent projection patterns, and RLN3 signalling has been implicated in behaviours and neurophysiological processes that are well characterised roles of 5-HT and NA [for review see, 22], such as anxiety [23], control of the HPA axis [24], and responses to stress [25, 26]. These shared roles are presumably mediated by similar synergistic or apposing modulation of shared downstream limbic and hypothalamic target regions. Therefore, it is possible that by signalling through its $G_{i/o}$-protein-coupled receptor, RXFP3 (relaxin family peptide 3 receptor) [27–29], RLN3 could compliment 5-HT- and NA-associated functions, analogously to the role of the excitatory neuropeptide, orexin, in complimenting monoaminergic control of arousal and sleep/wake states [30, 31]. In addition to likely actions on shared downstream target regions, RLN3/RXFP3 signalling may also directly modulate other arousal systems. For example, RLN3-positive axonal projections and Rxfp3 mRNA expression are concentrated within parts of the dorsal raphe. In contrast, locus coeruleus and the ventral tegmental area appear to lack any clear RLN3/RXFP3 inputs [15], suggesting little or no direct modulation of these structures and their monoaminergic neurons. However, the concentration of RLN3/RXFP3 elements within major nodes of the limbic system including areas such as the interpeduncular nucleus, adjacent to the ventral tegmental area, suggests RLN3 signalling may modulate mesocorticolimbic dopaminergic pathways indirectly [23].

In light of possible synergistic roles of RLN3 and monoamines, endogenous RLN3/RXFP3 signalling may compensate for the temporary reduction in monoamine signalling that occurs during chronic METH withdrawal, and alter the profile of 'behavioural despair' observed. This study therefore utilised backcrossed C57Bl/6J Rln3 knockout (KO) [32] and Rxfp3 KO mice [33] to explore this possibility. Furthermore, initial exposure to METH can result in reduced bodyweight due to its actions in supressing appetite and increasing metabolic activity [34]. As endogenous RLN3/RXFP3 signalling promotes food consumption in mice [35], we also assessed whether Rln3/Rxfp3 KO mice are more susceptible to METH-related reductions in bodyweight. An escalating daily dosage regime of 2 mg/kg on day 1, 4 mg/kg on day 2 and 6 mg/kg on days 3–10 was used, as it likely represents the minimum dose schedule sufficient to induce reduced bodyweight after 3 exposures [36] and increased behavioural despair (forced swim and tail suspension immobility) during the 48 h withdrawal period [10]. However, this dose regime is below that at which damage and loss of synapses and even death of monoaminergic neurons is reported [3]. Furthermore, as we hypothesised that RLN3/RXFP3 deficiency might render mice more sensitive than wildtype (WT) controls to the consequences of METH, using a low, 'minimum' dose schedule offers the best opportunity to avoid 'ceiling' effects and observe potentially increased anxiety- and depressive-like behaviours in Rln3 and Rxfp3 KO mice.

Experimental 5-HT depletion in rats significantly increased Rln3 mRNA expression in the nucleus incertus [37], a finding suggesting endogenous RLN3 tone may be high in WT mice during METH withdrawal, relative to a complete lack of tone in the KO mice, increasing the potential for observable phenotypic differences. In addition, repeated intermittent METH treatment and subsequent withdrawal is a stressor associated with increased central corticotropin-releasing factor (CRF) expression [1, 38, 39]; and nucleus incertus RLN3 neurons are activated in response to CRF and stress in rats via CRF_1 receptors [25, 26, 40]. In line with this data, Rxfp3 KO mice displayed significantly reduced alcohol preference for several weeks after a chronic stress regimen [41]. Therefore, we also tested whether Rln3 and Rxfp3 KO mice displayed emergent phenotypes following monoamine withdrawal, such as increased anhedonia and anxiety, or decreased social interaction and novelty-induced locomotor response, during the weeks following chronic METH administration.

Materials and Methods

Generation of Rln3 and Rxfp3 KO Mice

Rln3 KO mice (Lexicon Genetics Inc., The Woodlands, TX, USA) and Rxfp3 KO mice (Deltagen Inc., San Carlos, CA, USA) were kindly supplied by Janssen Pharmaceutical Companies of Johnson & Johnson (San Diego, CA, USA), and were originally generated on a 129SV:B6 mixed

background before being subjected to successive rounds of backcrossing onto a C57BL/6J background for more than 10 generations. All studies were conducted with approval from The Florey Institute of Neuroscience and Mental Health Animal Ethics Committee and were in accordance with ethical guidelines issued by the National Health and Medical Research Council of Australia.

Two separate cohorts of mice (designated Rln3 and Rxfp3 cohorts) were generated from heterozygous parents, and genotypes were identified by polymerase chain reaction (PCR) from DNA extracted from tail samples, as described [33, 42]. Experiments were performed on female Rln3 and Rxfp3 KO mice and their WT littermates, at 8–10 weeks of age ($n = 8$–14 per group). Mice from each cohort were separately group-housed (mixed genotypes; 4–6 per box) for the duration of the studies, weighed twice weekly, and were maintained on a 12-h light–dark cycle (lights on from 700 to 1900) with regular chow and two bottles of water available ad libitum. However, mice were single housed over a 24 h period during the saccharin preference studies (once weekly: (i) pre-treatment, (ii) METH treatment, and (iii) post-treatment; see below for details).

Methamphetamine (METH) Administration and Dosage Regime

Methamphetamine hydrochloride C-II was purchased from Sigma–Aldrich (Missouri, USA), dissolved in 0.9 % w/v saline (SAL) and administered to mice intraperitoneally (i.p., 0.2 ml/10 g) once daily for ten consecutive days, according to an escalating dose regime of 2 mg/kg (day 1), 4 mg/kg (day 2), and 6 mg/kg (days 3–10). METH concentrations of 0.1, 0.2 and 0.3 mg/ml were used for the 2, 4 and 6 mg/kg doses, respectively, so that 0.2 ml was injected per 10 g bodyweight for all dosages. Control mice were injected with the identical volume of 0.9 % w/v SAL. METH doses were gradually increased to allow habituation and reduce possible adverse reactions that can occur when injecting naïve mice with high doses. Additionally, it has been postulated that an escalating dose regime represents a more accurate representation of the gradual dose progression seen in human abusers [43]. Importantly, the chosen dosage regime has been shown to be sufficient to induce transient alterations in striatal gene transcription and behaviour following administration and during withdrawal phases [44].

Behavioural Tests

All behavioural experiments were conducted during the light phase from 900 to 1700. Although Rln3 KO and WT mice were tested separately from Rxfp3 KO and WT mice, behavioural tests were conducted at the same age and time relative to METH/SAL treatment/withdrawal in both cohorts.

Automated Locomotor Cell

Mice were individually placed in a 27 × 27 cm locomotor cell (Med Associates, Vermont, USA), illuminated by 70 lux light. The total distance travelled during 1 h was tracked by a photobeam array and analysed via Activity Monitor, v.6.02 software (Med Associates). Each mouse was tested four times: (i) immediately after i.p. SAL or 2 mg/kg METH on injection day 1; (ii) immediately after i.p. SAL or 6 mg/kg METH on injection day 10; (iii) on withdrawal day 9, and; (iv) on withdrawal day 16.

Two-Bottle Choice Saccharin Preference Test

To measure anhedonia, this test assessed the interest of mice to seek a sweet reward (saccharin), relative to drinking water. Mice were habituated to the presence of two drink bottles containing water in their home-cage, throughout the duration of the experiment. Mice were individually housed and provided two pre-weighed drinking bottles—one containing 10 % saccharin sodium hydrate solution and the other drinking water, at three time points: (i) pre METH/SAL (three days before treatment); (ii) day 5 METH/SAL treatment (mice isolated immediately after day 4 METH/SAL injection, and bottles weighed 24 h later, immediately before day 5 METH/SAL injection) and; (iii) on treatment withdrawal day 11. To avoid side preference, saccharin was randomly placed on the left- or right-hand side. After 24 h, the bottles were weighed and mice were returned to group-housing. Saccharin preference was calculated as the percentage volume of saccharin solution consumed over total fluid intake over the 24 h period.

Forced Swim Test

Mice were subjected to two consecutive forced swim tests, 24 and 48 h following the last METH/SAL treatment to measure behavioural despair. Each mouse was individually placed into a beaker (18.5 cm diameter × 19.0 cm height) filled with water to a depth of 5 cm from the top of the beaker (25 ± 2 °C), for a total duration of 5 min. Mice were videoed from the side, and the latency to adopt the Porsolt posture and the time spent in the Porsolt posture during the last 3 min were manually measured by a blinded investigator. The Porsolt posture was defined as immobility of all four limbs, with only minimal movements necessary to stay afloat [45].

Elevated Plus Maze

Animals were tested in an elevated plus maze on withdrawal day 5, as a previous study detected a significant increase in anxiety-like behaviour in mice using this paradigm after 5 days of drug abstinence [12]. The apparatus consisted of four arms (each 30 cm long × 6 cm wide) extending from a central square (6 × 6 cm), elevated 39 cm off the ground. 15 cm high walls enclosed two opposing 'closed' arms, while the other two opposite arms were 'open'. Mice were placed in the centre of the apparatus, and were allowed to roam freely for 10 min. Movement was tracked from above using Top Scan Lite 2.0 software, and the time spent in the open arms, and the number of entries into the closed and open arms, were assessed.

Social Avoidance

Mice were placed in a 33 × 30 × 29 cm high box under dim lighting (20–25 lux), which contained a mesh cylindrical cage (8 cm diameter) located in the centre of the apparatus, for 15 min on the day before testing to habituate. On the day of experimentation (7 days following METH/SAL treatment), mice were habituated to the apparatus again for 10 min. Immediately afterwards, the test mouse was briefly removed and a 'novel' 5 week-old female mouse (C57Bl/6J) was placed under the mesh cage. The test mouse was then placed back into the apparatus and allowed to roam freely for 10 min.

Mice were videoed from above, and the location of the test mouse nose point and centre point was tracked and later analysed using Top Scan Lite 2.0 software. The test mouse was deemed to engage in social interaction when its nose point was within 2 cm of the cage (the interaction zone), and was defined as avoiding the novel mouse when its centre point was >8 cm from the centred mesh cage/cup (outer zone).

Light/Dark Box

On day 14 of withdrawal, mice were placed in the automated locomotor cells described above. Half of the locomotor cell was fitted with a black Perspex box which was impermeable to visible light (but permeable to the detection photobeams), creating the 'dark side'. The other half was exposed to a light-emitting diode array, illuminating this 'light side' to 700 lux in the centre and 650 lux in the corners, creating an aversive stimulus. Mice were placed into the dark side of the arena, and were allowed to roam freely for 10 min, with a small opening in the Perspex box allowing passage between both sides. Using Activity Monitor software (v.6.02; Med Associates), the time spent in and number of entries into the light side were recorded.

Statistical Analysis

All graphs were constructed using Graph Pad Prism (v.6), and statistical analysis was conducted using the Statistical Package for Social Sciences (v.19.0). Data from Rln3 and Rxfp3 cohorts were analysed together using three-way ANOVA, followed by appropriate post hoc comparisons as described. Data from the saccharin preference test were analysed using four-way ANOVA with repeated measures with time as repeated measures factor; and cohort, genotype and treatment as independent variables.

Results

These studies demonstrated that Rln3 and Rxfp3 KO mice display an equivalent sensitivity as WT mice to increased behavioural despair during the 2 day METH withdrawal period and to the reductions in bodyweight observed on day 3 of METH treatment; but that depressive-like behavioural phenotypes did not emerge in Rln3 KO, Rxfp3 KO or WT mice during a 3 week period following cessation of 10 days METH exposure.

Reductions in Bodyweight in Rln3 and Rxfp3 KO and WT Mice Following METH Treatment

On day 4 of METH/SAL treatment (just prior to 4th injection), all four METH-treated groups demonstrated reduced mean bodyweights compared to their pre-METH weights, while in contrast, all four SAL-treated groups gained bodyweight during the equivalent time (Fig. 1). This was reflected by an overall significant difference between treatments, that was more profound in the Rxfp3 cohort than the Rln3 cohort (three-way ANOVA, treatment × cohort interaction, $F_{(1,119)} = 97.1$, $p = 0.007$; within Rxfp3 cohort, main effect of treatment, $F_{(1,67)} = 32.5$, $p < 0.001$; within Rln3 cohort, main effect of treatment, $F_{(1,52)} = 6.57$, $p = 0.013$). Furthermore, when inspected individually 3 of the 4 METH groups weighed significantly less than their SAL-treated controls: Rln3 KO METH (three-way ANOVA, post-test within Rln3 cohort, within KO, between treatments, $F_{(1,28)} = 6.61$, $p = 0.016$), Rxfp3 WT METH (within Rxfp3 cohort, within WT, between treatments, $F_{(1,32)} = 16.1$, $p < 0.001$) and Rxfp3 KO METH groups (within Rxfp3 cohort, within KO, between treatments, $F_{(1,35)} = 16.4$, $p < 0.001$). However, when weighed at subsequent time-points, the bodyweight of mice in all groups recovered and continued to increase in line with normal growth curves (data not shown).

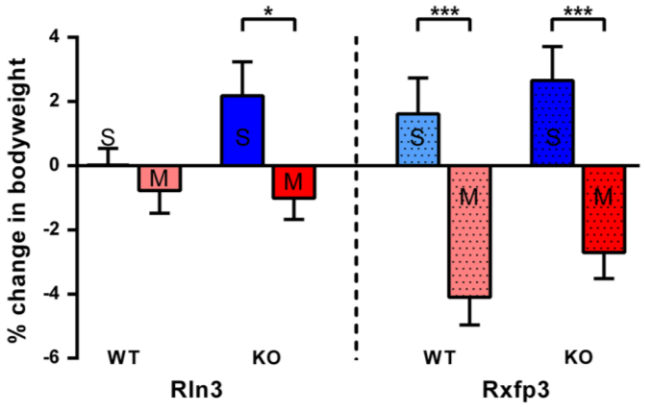

Fig. 1 Changes in bodyweight of Rln3 and Rxfp3 KO mice and their WT littermates following 3 days of METH or SAL treatment. Rln3 and Rxfp3 KO mice and their WT littermates administered with escalating doses of METH for 3 days (2, 4 and 6 mg/kg, i.p., on day 1, 2 and 3, respectively) displayed a significant reduction in body weight, relative to equivalent SAL-treated mice. Data are expressed as mean ± SEM, $n = 8$–14 per group. Three-way ANOVA, post-tests between treatments, $^{*}p < 0.05$; $^{***}p < 0.001$

Increased Behavioural Despair in Rln3 KO, Rxfp3 KO and WT Mice During METH Withdrawal Period

Importantly, the chronic METH dose schedule used in the present studies induced subtle increases in behavioural despair during the 48 h withdrawal period, resulting in several significant effects of treatment. Overall, however, Rln3 and Rxfp3 KO mice did not display significant differences in behaviour, relative to their respective WT controls.

For example, on day 1 of withdrawal Rln3 WT mice treated with METH entered the Porsolt posture sooner than those treated with SAL (three-way ANOVA, within Rln3 cohort, within WT, between treatments, $F_{(1,18)} = 1.09$, $p = 0.037$; Fig. 2a). Although this effect did not reach significance in Rxfp3 WT mice (three-way ANOVA, within Rxfp3 cohort, within WT, between treatments, $F_{(1,14)} = 1.09$, $p = 0.314$), across both cohorts a main effect of treatment nonetheless was present within WT mice (three-way ANOVA, within WT, main effect of treatment, $F_{(1,32)} = 4.52$, $p = 0.041$). Importantly, METH-treated KO mice from both cohorts recorded latencies that were roughly equivalent to their METH-treated WT controls (three-way ANOVA, within METH, between genotypes, $F_{(1,36)} = 0.074$, $p = 0.787$), suggesting that Rln3/Rxfp3 deficiency does not alter sensitivity to METH withdrawal in this measure and at this time. Notably however, SAL-treated KO mice recorded latencies that were shorter than their SAL-treated WT counterparts (three-way ANOVA, within SAL, between genotypes $F_{(1,36)} = 8.94$, $p = 0.005$), which likely contributed to the lack of observable effects of METH treatment within this genotype (three-way ANOVA, within KO, between treatments, $F_{(1,40)} = 1.49$, $p = 0.229$; genotype × treatment interaction, $F_{(1,72)} = 5.83$, $p = 0.018$). Latency to adopt the Porsolt posture appeared to be more sensitive to METH treatment and less variable than measures of the time spent immobile during the last 3 min of the trial, as no significant effects were observed in relation to treatment (main effect of treatment, $F_{(1,72)} = 1.11$, $p = 0.196$; treatment × genotype interaction $F_{(1,73)} = 0.233$, $p = 0.631$; treatment × cohort interaction, $F_{(1,72)} = 0.045$, $p = 0.833$; Fig. 2b), or genotype (main effect of genotype, $F_{(1,72)} = 0.826$, $p = 0.367$; genotype × cohort interaction, $F_{(1,72)} = 0.957$, $p = 0.331$).

On day 2 of withdrawal, large variation was present between the Rln3 and Rxfp3 cohorts in measures of both latency to enter the Porsolt posture (3 way ANOVA, main effect of cohort, $F_{(1,73)} = 18.6$, $p < 0.001$; cohort × treatment interaction, $F_{(1,73)} = 0.548$, $p = 0.461$; cohort × genotype interaction, $F_{(1,73)} = 0.120$, $p = 0.730$; Fig. 2c), and the time spent in the Porsolt posture (main effect of cohort, $F_{(1,73)} = 20.8$, $p < 0.001$; cohort × treatment interaction, $F_{(1,73)} = 13.0$, $p = 0.136$, cohort × genotype interaction, $F_{(1,73)} = 0.003$, $p = 0.956$; Fig. 2d). Despite this, METH-treated mice entered the Porsolt posture faster than SAL controls (main effect of treatment, $F_{(1,73)} = 4.38$, $p = 0.04$), although there was no difference between genotypes in this measure (main effect of genotype, $F_{(1,73)} = 0.031$, $p = 0.860$). Notably, METH treatment also markedly increased the time mice spent in the Porsolt posture during the last 3 min of the trial relative to SAL controls within the Rln3 cohort (within Rln3 cohort, main effect of treatment, $F_{(1,40)} = 4.21$, $p = 0.047$). No treatment effects were observed within the Rxfp3 cohort however (within Rxfp3 cohort, main effect of treatment, $F_{(1,33)} = 0.026$, $p = 0.873$), and no differences between genotypes were observed (main effect of genotype $F_{(1,73)} = 0.01$, $p = 0.920$).

Evaluation of Depressive-Like Phenotypes in Rln3 and Rxfp3 KO Mice Following Chronic METH Exposure

During the 3 week withdrawal period Rln3 and Rxfp3 KO mice did not display consistent changes in behaviour relative to WT controls (which would have predicted emergent phenotypes), in measures of anhedonia, anxiety, social interaction and novelty-induced locomotor activity (Table 1). Furthermore, no marked, reproducible changes in behaviour were induced by prior METH treatment, in agreement with several reports that depressive-like behaviours are generally only observable 24–48 h after withdrawal from similar chronic METH doses [10, 11] (but see also [12]).

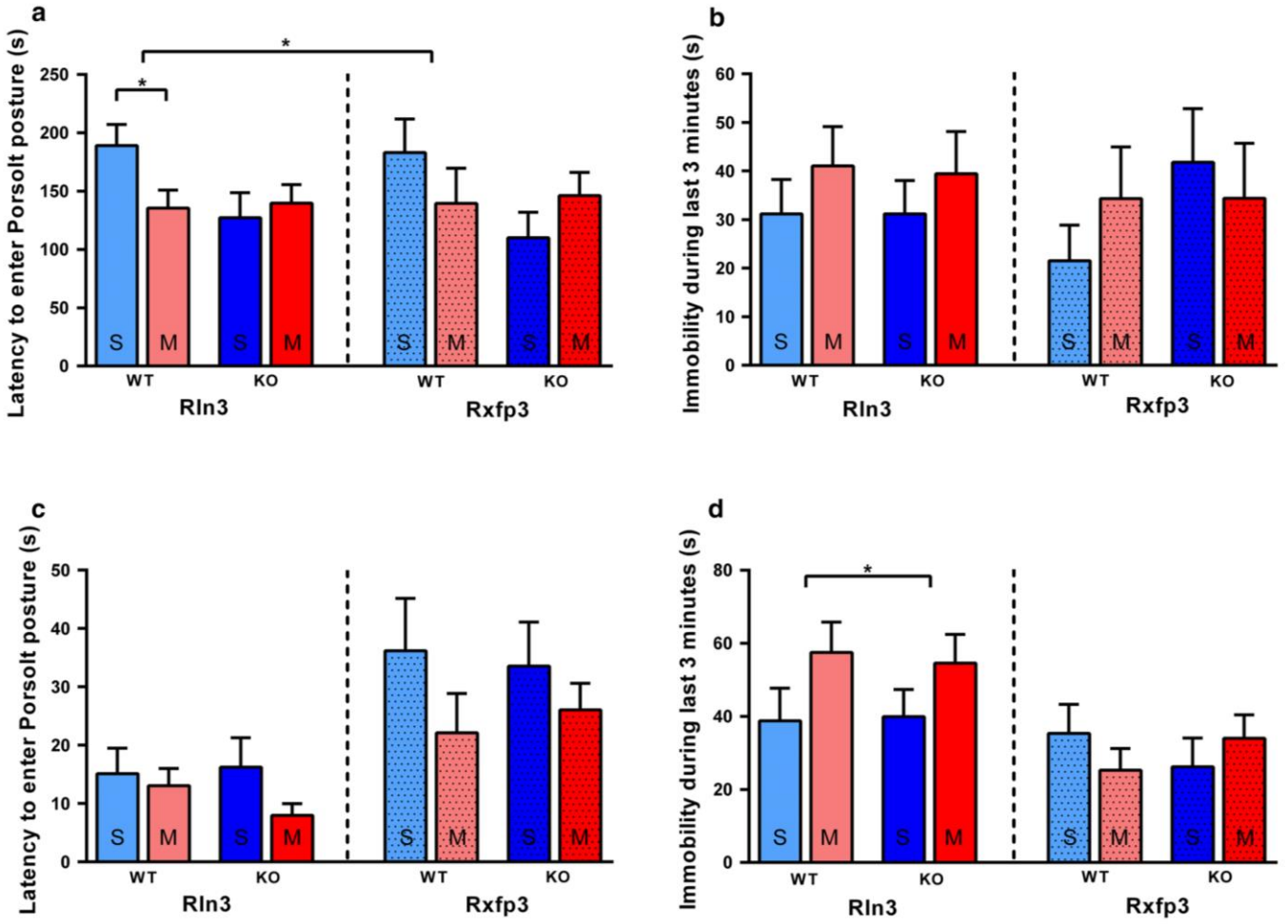

Fig. 2 METH treatment (2, 4 and 6 mg/kg, i.p., on day 1, 2 and 3-10, respectively) induced some signs of behavioural despair in the Porsolt swim test relative to SAL treated mice, however no genotype differences were observed. **a**, **c** Latency to enter Porsolt posture. **a** 1 day following treatment, Rln3 WT mice treated with METH entered the Porsolt posture sooner than SAL-treated Rln3 WT mice, **c** 2 days following treatment, METH-treated mice within both cohorts entered the Porsolt posture more rapidly than SAL-treated mice (**b**, **d**). Time spent in Porsolt posture. **b** 1 day following treatment, time spent in Porsolt posture in the last 3 min time bin, was similar within both METH and SAL-treated cohorts. **d** 2 days following treatment, METH treated mice spent significantly more time in the Porsolt posture in the last 3 min time bin, relative to SAL-treated mice within the Rln3 WT/KO cohort. Data are expressed as mean ± SEM, $n = 8$–14 per group. Three-way ANOVA, main effect of treatment $^*p < 0.05$

Specifically, there were no significant overall differences in saccharin preference between treatment groups and genotypes at each of the three time points studied (3 way ANOVAs for each time point, main effects of treatment, all $p > 0.05$; main effects of genotype, all $p > 0.05$; treatment × genotype, treatment × cohort, and genotype × cohort interactions, all $p > 0.05$). Furthermore, when each of the four METH treated groups were studied in isolation, there were no significant differences in saccharin preference between the pre-treatment time point versus day 7 treatment or day 14 withdrawal (paired *t*-tests, all $p > 0.05$), suggesting that METH treatment did not strongly modulate this behaviour.

In measures of general anxiety, METH treatment did not induce any changes relative to SAL in the time spent in the open arms (3 way ANOVA, main effect of treatment, $F_{(1,73)} = 0.174$, $p = 0.677$, cohort × treatment interaction, $F_{(1,73)} = 0.005$, $p = 0.947$) or the number of entries into open arms of the elevated plus maze (main effect of treatment $F_{(1,72)} = 3.12$, $p = 0.081$; cohort × treatment interaction, $F_{(1,72)} = 0.143$, $p = 0.707$). Despite significant variation between cohorts (main effect of cohort, $F_{(1,73)} = 6.23$, $p = 0.015$), notably, KO mice spent more time in the open arms than WT littermates (main effect of genotype, $F_{(1,73)} = 4.61$, $p = 0.035$). However, this genotype effect was not replicated in the number of entries into open arms (main effect of genotype, $F_{(1,72)} = 0.813$, $p = 0.370$, genotype × treatment interaction, $F_{(1,72)} = 1.34$, $p = 0.250$), and again this parameter revealed no differences between METH versus SAL treatment (main effect of treatment, $F_{(1,72)} = 3.12$, $p = 0.081$). Within the Rln3 cohort, while METH treatment reduced the latency

Table 1 Performance of Rln3 and Rxfp3 KO mice and their WT littermates in a battery of behavioural tests measuring depressive- and anxiety-like behaviours during a 3 week METH/SAL withdrawal period

Behavioural Test	Rln3 Cohort				Rxfp3 Cohort			
	WT Sal	WT Meth	KO Sal	KO Meth	WT Sal	WT Meth	KO Sal	KO Meth
Saccharin preference								
Pre-treatment (%)	88.3 ± 1.1	86.1 ± 3.1	82.0 ± 6.4	86.6 ± 1.6	81.3 ± 4.5	68.8 ± 9.6	79.9 ± 2.1	83.1 ± 1.6
Day 7 of treatment (%)	86.6 ± 3.0	84.0 ± 2.0	84.5 ± 1.6	78.9 ± 3.5	72.3 ± 7.8	71.5 ± 6.6	80.3 ± 1.9	77.7 ± 6.6
Day 14 of withdrawal (%)	91.5 ± 2.6	84.2 ± 3.5	83.9 ± 3.7	81.3 ± 4.3	72.9 ± 12.4	69.5 ± 8.9	72.8 ± 7.6	76.9 ± 6.4
Elevated plus maze								
Time in open arms (s)	70.4 ± 9.5	72.8 ± 8.8	95.1 ± 15.3#	99.1 ± 15.9#	54.8 ± 8.8	54.6 ± 8.2	63.9 ± 13.5#	72.9 ± 11.8#
Entries into open arms (#)	11.2 ± 1.4	11.4 ± 1.8	10.2 ± 1.2	13.0 ± 2.1	6.4 ± 0.8	7.6 ± 1.2	6.9 ± 1.3	10.5 ± 1.4
Latency to enter open arms (s)	36.7 ± 16.9	19.6 ± 5.86	57.8 ± 21.1	11.0 ± 3.90*	11.2 ± 2.96	11.7 ± 2.65	87.3 ± 41.3	25.0 ± 10.6
Light dark box								
Latency to enter light side (s)	32.3 ± 9.5	34.0 ± 7.9	25.0 ± 5.4#	20.2 ± 2.7#	42.5 ± 11.1	15.4 ± 2.1*	21.4 ± 3.4#	19.0 ± 4.0#
Time in light side (s)	136 ± 29.4	159 ± 26.5	184 ± 23	175 ± 19.9	153 ± 28.6	215 ± 49	171 ± 21.9	220 ± 21.5
Entries into light side (#)	31.3 ± 4.5	28.2 ± 2.9	32.2 ± 3.5	28.3 ± 1.5	33.0 ± 4.2	33.1 ± 2.9	30.7 ± 2.8	33.1 ± 3.7
Social avoidance								
Latency to interact (s)	1.0 ± 0.4	1.1 ± 0.8	4.9 ± 3.3	2.9 ± 1.1	0.5 ± 0.4	2.1 ± 1.1	2.6 ± 0.9	3.2 ± 1.1
Time spent interacting (s)	308 ± 31.9	285 ± 17.4	291 ± 17.1	285 ± 11.3	315 ± 22.1	302 ± 21.6	335 ± 19.8	262 ± 31.0
Number of interactions(#)	56.0 ± 5.7	65.5 ± 3.3	60.6 ± 5.9	58.2 ± 1.9	58.0 ± 6.0	54.3 ± 1.6	53.0 ± 2.2	51.5 ± 5.0
Locomotor activity								
Total distance travelled (m)								
Day 1 of treatment	98.0 ± 16.14	214 ± 16.1***	75.0 ± 5.2	196 ± 10.9***	65.5 ± 7.4	213 ± 22.9***	67.6 ± 4.9	236 ± 9.4***
Day 10 of treatment	68.3 ± 5.7	228 ± 32.4***	57.1 ± 3.9	275 ± 26.1***	58.9 ± 5.7	244 ± 33.8***	62.5 ± 6.0	299 ± 20.4***
Day 9 of withdrawal	58.0 ± 8.9	86.9 ± 6.19*	66.1 ± 5.6	82.9 ± 5.8	121 ± 52.7	95.3 ± 19.3	80.4 ± 8.0	85.0 ± 7.0
Day 16 of withdrawal	79.5 ± 10.2	80.9 ± 7.2	74.2 ± 6.5	79.9 ± 7.4	62.5 ± 5.6	72.4 ± 5.3	76.5 ± 9.0	90.5 ± 19.2

Data are expressed as mean ± SEM, $n = 8$–14 per group. No genotype differences in performance were detected, except for the following observations: (i) Rln3 KO mice displayed a significant reduction in saccharin preference, relative to WT littermates, (ii) At 5 days post-METH/SAL treatment, both Rln3 and Rxfp3 KO mice administered METH or SAL, spent significantly more time in the open arms of an EPM, relative to WT littermates, (iii) At 7 days post-METH/SAL treatment, both Rln3 and Rxfp3 KO mice administered METH or SAL, had a significantly reduced latency to enter the light side of a light/dark box, relative to WT littermates

Locomotor Activity. A significant increase in locomotor activity was observed on day 1 and day 10 of METH treatment relative to SAL-treated mice, within both Rln3 and Rxfp3 cohorts; however, on day 9 and day 16 post-METH treatment, the distance travelled in locomotor cells was not significantly different between treatment groups. Three-way ANOVA, main effect of genotype #$p < 0.05$, and main effect of treatment *$p < 0.05$ and ***$p < 0.001$

for KO mice to enter the open arms relative to SAL treated mice (post-test within Rln3 cohort, within KO, main effect of treatment, $F_{(1,22)} = 4.75$, $p = 0.04$), this effect was not observed in the Rxfp3 cohort (post-test within Rxfp3 cohort, within KO, main effect of treatment, $F_{(1,19)} = 2.33$, $p = 0.143$).

In the light/dark box, there were no genotype or treatment differences in the total time spent in, and the number of entries into, the light side (3 way ANOVAs for each data set, main effects of treatment and genotype, all $p > 0.05$; genotype × treatment and cohort × treatment interactions, all $p > 0.05$). KO mice displayed slightly reduced latencies to enter the light side compared to WT controls (main effect of genotype, $F_{(1,74)} = 4.79$, $p = 0.032$, genotype × treatment interaction, $F_{(1,74)} = 1.03$, $p = 0.314$), but due to the absence of similar genotype effects in the other parameters measured, the physiological significance of these findings is not clear. Within the Rxfp3 cohort, METH treatment reduced the latency for WT mice to enter the light side, relative to SAL (within RXFP3 cohort, within WT, main effect of treatment, $F_{(1,14)} = 5.72$, $p = 0.031$), but this effect was not observed in Rln3 WT mice (within Rln3 cohort, within WT, main effect of treatment $F_{(1,18)} = 0.020$, $p = 0.888$).

In the social avoidance test, interactions with a novel mouse were defined as occurring when the nose point of the test mouse was within 2 cm of the cage housing the novel mouse. No significant genotype or treatment differences were observed in the latency to interact, total time spent interacting, or the number of interaction bouts (3 way ANOVA for each data set, main effects of treatment and genotype, all $p > 0.05$; genotype × treatment and cohort × treatment interactions, all $p > 0.05$).

Finally, as expected the distance travelled in locomotor cells was markedly increased during the hour after injection of 2 mg/kg METH (3 way ANOVA, main effect of treatment, $F_{(1,83)} = 243$, $p < 0.001$; post-tests within each cohort and genotype, between treatments, all $p < 0.001$) and 6 mg/kg METH (main effect of treatment $F_{(1,82)} = 196$, $p < 0.001$, post-tests within each cohort and genotype, between treatments, all $p < 0.001$). However, no differences between genotypes were observed (2 mg/kg, main effect of genotype, $F_{(1,83)} = 0.199$, $p = 0.657$; post-tests within each cohort and treatment, all $p > 0.05$; 6 mg/kg, main effect of genotype, $F_{(1,82)} = 2.719$, $p = 0.103$, post-tests within each cohort and treatment, all $p > 0.05$). On days 9 and 16 of withdrawal, the distance travelled in locomotor cells was not significantly different between treatment groups (day 9, main effect of treatment, $F_{(1,73)} = 0.266$, $p = 0.608$; day 16; main effect of treatment, $F_{(1,73)} = 1.12$, $p = 0.294$) or genotypes (day 9, main effect of genotype, $F_{(1,73)} = 0.944$, $p = 0.334$; day 16, main effect of genotype, $F_{(1,73)} = 0.777$, $p = 0.381$). On day 9 of withdrawal, WT METH treated mice from the Rln3 cohort travelled further than WT SAL controls (post-test within Rln3 cohort, within WT, between treatment, $F_{(1,18)} = 7.11$, $p = 0.016$), but this effect was not observed in other groups (day 9 and 16 within each cohort and genotype, between treatments, all others $p > 0.05$).

Discussion

The aim of this study was to investigate whether a deficiency in RLN3/RXFP3 signalling altered the behavioural response of mice to chronic escalating METH treatment (1-6 mg/kg over 10 days) and its withdrawal, including the nature and severity of any depressive- and anxiety-like phenotypes, in light of earlier reports in C57Bl/6J mice. The main findings were that firstly, Rln3 and Rxfp3 KO mice display an equivalent sensitivity to their WT littermates to METH-induced changes in bodyweight, and exhibit a similar degree of increased behavioural despair as WT mice during the initial 2 days of METH withdrawal. Secondly, depressive-like phenotypes do not emerge in Rln3 or Rxfp3 KO mice in the 3 weeks following the cessation of chronic METH exposure. While the data generated in germline knockout strains does not support a strong interaction of RLN3/RXFP3 and major monoamine systems in mice, our results extend previous studies [10, 11], by further illustrating that the METH schedule used can induce 'depressive-like' behaviour within the 2 days post-METH, highlighting the link between central changes during the withdrawal period in the generation of depressive-like behaviour.

Treatment of mice with an escalating METH dose schedule significantly decreased bodyweight relative to pre-METH values on day 3, and significantly increased 'behavioural-despair' measured by a decreased latency to adopt the Porsolt posture and an increase in time spent in the Porsolt posture in the forced swim test, during the initial 2 days of withdrawal from 10 days METH-treatment. These observable differences were not so extreme to preclude Rln3 and/or Rxfp3 KO mice from exhibiting more severe weight loss and immobility if endogenous RLN3/RXFP3 normally counteracts imbalances in monoamine and CRF signalling. However, due to the relatively inconsistent and subtle effects of METH treatment/withdrawal observed, it is perhaps not possible to infer whether or not a genetic deficiency in RLN3/RXFP3 signalling increases resiliency to depressive-like behaviour in response to chronic METH treatment. Behavioural despair was examined during the critical 48 h withdrawal period as previous reports suggest this measure is perhaps the most sensitive for measuring behavioural changes at this time [10]. However, it would be of interest to test whether Rln3/

Rxfp3 deletion renders mice more or less sensitive to other types of behavioural change (such as anxiety-like behaviour in the elevated plus maze or light/dark box) during this 48 h period [10–12].

The present findings, in which RLN3/RXFP3 deficiency did not alter behaviour during monoamine depletion, seem to contradict revious evidence (see Introduction) which predicts endogenous RLN3/RXFP3 signalling acts synergistically with monoamines to modulate shared downstream target regions. However, it should be noted that developmental compensation is common in whole-of-life KO mice, and such effects may have concealed observable phenotypes. Hence, further pharmacological studies using RXFP3 agonists/antagonists [23, 35], or studies using conditional Rln3 and/or Rxfp3 KO mice would be of interest. Additionally, although evidence is accumulating that RLN3/RXFP3 signalling is able to modulate the same downstream brain areas as monoamine systems, such as the septum [46, 47] and extended amygdala [23], it is not known whether RLN3/RXFP3 signalling targets the same or different/neighbouring neurons and circuits to those directly innervated by 5-HT, NA and DA networks. In this regard, the direct effects of RXFP3 activation on individual and populations of brain neurons is largely unknown (but see Blasiak et al. [48]). Hence, determining the neurochemical phenotype of RXFP3-positive neurons will be an important advance, but a fully characterised, specific RXFP3 antibody is currently unavailable, preventing traditional double-label immunohistochemical approaches to neurochemically 'phenotype' RXFP3-positive neurons. An alternative approach is to histologically identify RXFP3-positive neurons with the use of a reporter gene mouse strain, which would allow the immunohistochemical identification of RXFP3-positive neurons and key monoamine receptors at potential sites of direct and/or indirect interactions. Such studies could determine if relaxin-3/RXFP3 signalling acts synergistically with 5-HT and/or other monoamines or in a negative regulatory manner in different brain areas/circuits. Apart from initial studies of 5-HT and relaxin-3 systems in the rat [37], there have been no systematic investigations of this nature. Furthermore, although there is some complimentary data on the nature of inputs to relaxin-3 neurons [e.g. CRF [40]), more research is required to explore the impact of the various monoamine transmitter systems in rats and mice [21].

In the present studies, the chronic METH treatment schedule did not induce long-term changes in anhedonia, anxiety, or social interaction in Rln3 or Rxfp3 KO mice. This is in contrast to recent studies in our laboratory, in which Rxfp3 KO mice and WT littermates were subjected to repeated exposure to acute stress, including 30 min of restraint stress once daily for seven consecutive days, followed by two consecutive days of forced swim stress. This paradigm resulted in a significant reduction in alcohol preference in Rxfp3 KO mice over a period of six weeks, relative to WT littermates, suggesting RLN3/RXFP3 deficiency ameliorates long-term stress responsiveness following a chronic stressor [41]. Furthermore, RLN3 neurons within the rat NI express high levels of CRF_1 receptor [26, 40], and the majority of these neurons display increased Fos immunoreactivity and increased relaxin-3 mRNA following restraint stress or icv injection of CRF [26, 40]. RLN3 expression in the NI is increased following a repeated swim stress, and this effect is blocked via pre-administration of a CRF_1 antagonist [25]. Therefore, as restraint and swim stress are well documented to induce elevated CRF signalling and there are putative links between RLN3 and stress/CRF systems [25, 26, 40], it is possible that a chronic METH paradigm that only 'mildly' activated CRF tone and signalling (among other systems) was not sufficient to cause long-term changes in depressive- and anxiety-like behaviours in germline, 'whole-of-life' Rln3 and Rxfp3 KO mice.

Conclusion

The anatomical distribution of the RLN3/RXFP3 system in mouse and rat brain [14, 15, 26] suggests it contributes to an 'ascending arousal system', which shares neuroanatomical and functional similarities with the 5-HT/dorsal raphe and NA/locus coeruleus monoamine systems (see [22] for review). However, in the current study, Rln3 and Rxfp3 KO mice displayed sensitivity equivalent to WT littermate mice to chronic METH treatment and withdrawal. Nonetheless, to our knowledge, this is the first study to characterise the response of female C57BL/6 mice to a chronic METH treatment regime and we have demonstrated that the METH schedule used effectively reduced bodyweight after 3 days, increased behavioural despair during the first 48 h of withdrawal, and strongly increased acute locomotor activity on day 1 and 10 of METH treatment. Furthermore, we have demonstrated that longer-lasting changes in anhedonia, anxiety and social interaction are not evident after the METH dose regime used, raising the possibility that different METH regimes or more specific depletion of serotonin and/or elevations in CRF signalling may be required to reveal the nature of interactions between the monoamine systems and RLN3/RXFP3 networks.

Acknowledgments This research was supported by National Health and Medical Research Council of Australia Project Grants 1005988 and 1024885 (ALG), grants from the Pratt and Besen Family Foundation (ALG), a Brain & Behavior Research Foundation (USA) NARSAD Independent Investigator Award (ALG), and the Victorian Government Operational Infrastructure Support Programme. MH is

the recipient of a postgraduate scholarship from the Alzheimer's Australia Dementia Research Foundation. The authors thank Timothy Lovenberg and Steve Sutton (Janssen Companies of Johnson & Johnson, San Diego, CA, USA) for commissioning and providing the original Rln3 and Rxfp3 knockout mice.

Conflict of interest The authors declare that they have no conflict of interest.

References

1. Barr AM, Markou A, Phillips AG (2002) A 'crash' course on psychostimulant withdrawal as a model of depression. Trends Pharmacol Sci 23:475–482
2. Cruickshank CC, Dyer KR (2009) A review of the clinical pharmacology of methamphetamine. Addiction 104:1085–1099
3. Bamford NS, Zhang H, Joyce JA, Scarlis CA, Hanan W, Wu NP, Andre VM, Cohen R, Cepeda C, Levine MS, Harleton E, Sulzer D (2008) Repeated exposure to methamphetamine causes long-lasting presynaptic corticostriatal depression that is renormalized with drug readministration. Neuron 58:89–103
4. Barr AM, Panenka WJ, MacEwan GW, Thornton AE, Lang DJ, Honer WG, Lecomte T (2006) The need for speed: an update on methamphetamine addiction. J Psychiatry Neurosci 31:301–313
5. Yamamoto BK, Moszczynska A, Gudelsky GA (2010) Amphetamine toxicities: classical and emerging mechanisms. Ann New York Acad Sci 1187:101–121
6. Kita T, Wagner GC, Nakashima T (2003) Current research on methamphetamine-induced neurotoxicity: animal models of monoamine disruption. J Pharmacol Sci 92:178–195
7. Panenka WJ, Procyshyn RM, Lecomte T, MacEwan GW, Flynn SW, Honer WG, Barr AM (2013) Methamphetamine use: a comprehensive review of molecular, preclinical and clinical findings. Drug Alcohol Depend 129:167–179
8. Reichel CM, Ramsey LA, Schwendt M, McGinty JF, See RE (2012) Methamphetamine-induced changes in the object recognition memory circuit. Neuropharmacology 62:1119–1126
9. Armstrong BD, Noguchi KK (2004) The neurotoxic effects of 3,4-methylenedioxymethamphetamine (MDMA) and methamphetamine on serotonin, dopamine, and GABA-ergic terminals: an in vitro autoradiographic study in rats. Neurotoxicology 25:905–914
10. Cryan JF, Hoyer D, Markou A (2003) Withdrawal from chronic amphetamine induces depressive-like behavioral effects in rodents. Biol Psychiatry 54:49–58
11. Kokkinidis L, Zacharko RM, Anisman H (1986) Amphetamine withdrawal: a behavioral evaluation. Life Sci 38:1617–1623
12. Kitanaka N, Kitanaka J, Tatsuta T, Tanaka K, Watabe K, Nishiyama N, Morita Y, Takemura M (2010) Withdrawal from fixed-dose injection of methamphetamine decreases cerebral levels of 3-methoxy-4-hydroxyphenylglycol and induces the expression of anxiety-related behavior in mice. Neurochem Res 35:749–760
13. Tanaka M, Yoshida M, Emoto H, Ishii H (2000) Noradrenaline systems in the hypothalamus, amygdala and locus coeruleus are involved in the provocation of anxiety: basic studies. Eur J Pharmacol 405:397–406
14. Ma S, Bonaventure P, Ferraro T, Shen PJ, Burazin TCD, Bathgate RAD, Liu C, Tregear GW, Sutton SW, Gundlach AL (2007) Relaxin-3 in GABA projection neurons of nucleus incertus suggests widespread influence on forebrain circuits via G-protein–coupled receptor-135 in the rat. Neuroscience 144:165–190
15. Smith CM, Shen PJ, Banerjee A, Bonaventure P, Ma S, Bathgate RAD, Sutton SW, Gundlach AL (2010) Distribution of relaxin-3 and RXFP3 within arousal, stress, affective and cognitive circuits of mouse brain. J Comp Neurol 518:4016–4045
16. Lesch KP, Waider J (2012) Serotonin in the modulation of neural plasticity and networks: implications for neurodevelopmental disorders. Neuron 76:175–191
17. Saper CB, Scammell TE, Lu J (2005) Hypothalamic regulation of sleep and circadian rhythms. Nature 437:1257–1263
18. Goto M, Swanson LW, Canteras NS (2001) Connections of the nucleus incertus. J Comp Neurol 438:86–122
19. Olucha-Bordonau FE, Teruel V, Barcia-Gonzalez J, Ruiz-Torner A, Valverde-Navarro AA, Martinez-Soriano F (2003) Cytoarchitecture and efferent projections of the nucleus incertus of the rat. J Comp Neurol 464:62–97
20. Ryan PJ, Ma S, Olucha-Bordonau FE, Gundlach AL (2011) Nucleus incertus—an emerging modulatory role in arousal, stress and memory. Neurosci Biobehav Rev 35:1326–1341
21. Ma S, Gundlach AL (2015) Ascending control of arousal and motivation: role of nucleus incertus and its peptide neuromodulators in behavioural responses to stress. J Neuroendocrinol. doi:10.1111/jne.12259
22. Smith CM, Walker AW, Hosken IT, Chua BE, Zhang C, Haidar M, Gundlach AL (2014) Relaxin-3/RXFP3 networks: an emerging target for the treatment of depression and other neuropsychiatric diseases? Front Pharmacol 5:46
23. Ryan PJ, Buchler E, Shabanpoor F, Hossain MA, Wade JD, Lawrence AJ, Gundlach AL (2013) Central relaxin-3 receptor (RXFP3) activation decreases anxiety—and depressive-like behaviours in the rat. Behav Brain Res 244:142–151
24. Watanabe Y, Miyamoto Y, Matsuda T, Tanaka M (2011) Relaxin-3/INSL7 regulates the stress-response system in the rat hypothalamus. J Mol Neurosci 43:169–174
25. Banerjee A, Shen PJ, Ma S, Bathgate RAD, Gundlach AL (2010) Swim stress excitation of nucleus incertus and rapid induction of relaxin-3 expression via CRF1 activation. Neuropharmacology 58:145–155
26. Tanaka M, Iijima N, Miyamoto Y, Fukusumi S, Itoh Y, Ozawa H, Ibata Y (2005) Neurons expressing relaxin 3/INSL 7 in the nucleus incertus respond to stress. Eur J Neurosci 21:1659–1670
27. Bathgate RAD, Lin F, Hanson NF, Otvos L Jr, Guidolin A, Giannakis C, Bastiras S, Layfield SL, Ferraro T, Ma S, Zhao C, Gundlach AL, Samuel CS, Tregear GW, Wade JD (2006) Relaxin-3: improved synthesis strategy and demonstration of its high-affinity interaction with the relaxin receptor LGR7 both in vitro and in vivo. Biochemistry 45:1043–1053
28. Liu C, Eriste E, Sutton S, Chen J, Roland B, Kuei C, Farmer N, Jornvall H, Sillard R, Lovenberg TW (2003) Identification of relaxin-3/INSL7 as an endogenous ligand for the orphan G-protein–coupled receptor GPCR135. J Biol Chem 278:50754–50764
29. Chen J, Kuei C, Sutton SW, Bonaventure P, Nepomuceno D, Eriste E, Sillard R, Lovenberg TW, Liu C (2005) Pharmacological characterization of relaxin-3/INSL7 receptors GPCR135 and GPCR142 from different mammalian species. J Pharmacol Exp Ther 312:83–95
30. Yamanaka A, Beuckmann CT, Willie JT, Hara J, Tsujino N, Mieda M, Tominaga M, Yagami K, Sugiyama F, Goto K, Yanagisawa M, Sakurai T (2003) Hypothalamic orexin neurons regulate arousal according to energy balance in mice. Neuron 38:701–713
31. Tsujino N, Sakurai T (2013) Role of orexin in modulating arousal, feeding and motivation. Front Behav Neurosci 7:28
32. Smith CM, Lawrence AJ, Sutton SW, Gundlach AL (2009) Behavioral phenotyping of mixed background (129S5:B6) relaxin-3 knockout mice. Ann NY Acad Sci 1160:236–241
33. Hosken IT, Sutton SW, Smith CM, Gundlach AL (2014) Relaxin-3 receptor (Rxfp3) gene knockout mice display reduced running

wheel activity: implications for role of relaxin-3/RXFP3 signalling in sustained arousal. Behav Brain Res 278:167–175
34. Kobeissy FH, Jeung JA, Warren MW, Geier JE, Gold MS (2008) Changes in leptin, ghrelin, growth hormone and neuropeptide-Y after an acute model of MDMA and methamphetamine exposure in rats. Addict Biol 13:15–25
35. Smith CM, Chua BE, Zhang C, Walker AW, Haidar M, Hawkes D, Shabanpoor F, Hossain MA, Wade JD, Rosengren KJ, Gundlach AL (2014) Central injection of relaxin-3 receptor (RXFP3) antagonist peptides reduces motivated food seeking and consumption in C57BL/6 J mice. Behav Brain Res 268:117–126
36. Fantegrossi WE, Ciullo JR, Wakabayashi KT, De La Garza II R, Traynor JR, Woods JH (2008) A comparison of the physiological, behavioral, neurochemical and microglial effects of methamphetamine and 3,4-methylenedioxymethamphetamine in the mouse. Neuroscience 151:533–543
37. Miyamoto Y, Watanabe Y, Tanaka M (2008) Developmental expression and serotonergic regulation of relaxin 3/INSL7 in the nucleus incertus of rat brain. Regul Pept 145:54–59
38. Vuong SM, Oliver HA, Scholl JL, Oliver KM, Forster GL (2010) Increased anxiety-like behavior of rats during amphetamine withdrawal is reversed by CRF2 receptor antagonism. Behav Brain Res 208:278–281
39. Reinbold ED, Scholl JL, Oliver KM, Watt MJ, Forster GL (2014) Central CRF receptor antagonism reduces anxiety states during amphetamine withdrawal. Neurosci Res 89:37–43
40. Ma S, Blasiak A, Olucha-Bordonau FE, Verberne AJ, Gundlach AL (2013) Heterogeneous responses of nucleus incertus neurons to corticotrophin-releasing factor and coherent activity with hippocampal theta rhythm in the rat. J Physiol (Lond) 591:3981–4001
41. Walker AW, Smith CM, Chua BE, Krstew EV, Zhang C, Gundlach AL, Lawrence AJ (2015) Relaxin-3 receptor (RXFP3) signalling mediates stress-related alcohol preference in mice. PLoS ONE 10:e0122504
42. Smith CM, Hosken IT, Sutton SW, Lawrence AJ, Gundlach AL (2012) Relaxin-3 null mutation mice display a circadian hypoactivity phenotype. Genes Brain Behav 11:94–104
43. Segal DS, Kuczenski R (1997) An escalating dose "binge" model of amphetamine psychosis: behavioral and neurochemical characteristics. J Neurosci 17:2551–2566
44. Piechota M, Korostynski M, Sikora M, Golda S, Dzbek J, Przewlocki R (2012) Common transcriptional effects in the mouse striatum following chronic treatment with heroin and methamphetamine. Genes Brain Behav 11:404–414
45. Porsolt RD, Anton G, Blavet N, Jalfre M (1978) Behavioural despair in rats: a new model sensitive to antidepressant treatments. Eur J Pharmacol 47:379–391
46. Ma S, Shen PJ, Sang Q, Lanciego JL, Gundlach AL (2009) Distribution of relaxin-3 mRNA and immunoreactivity and RXFP3-binding sites in the brain of the macaque, *Macaca fascicularis*. Ann NY Acad Sci 1160:256–258
47. Olucha-Bordonau FE, Otero-Garcia M, Sanchez-Perez AM, Nunez A, Ma S, Gundlach AL (2012) Distribution and targets of the relaxin-3 innervation of the septal area in the rat. J Comp Neurol 520:1903–1939
48. Blasiak A, Blasiak T, Lewandowski MH, Hossain MA, Wade JD, Gundlach AL (2013) Relaxin-3 innervation of the intergeniculate leaflet of the rat thalamus—neuronal tract-tracing and in vitro electrophysiological studies. Eur J Neurosci 37:1284–1294

CHAPTER 5

General Discussion

5.1 Introduction

Since the discovery of relaxin-3 in 2001, our understanding of the roles played by this highly conserved neuropeptide within the brain has grown rapidly. As a major neurotransmitter in an ascending neural network that innervates a broad range of brain regions, relaxin-3 signalling has been implicated in a diverse range of functional modalities. This diversity of action is further reflected by the studies described in this thesis, which expand our knowledge of relaxin-3/RXFP3 neurobiology within three distinct domains, by exploring the role of relaxin-3/RXFP3 signalling in: (*i*) controlling hippocampal function and memory; (*ii*) the possible progression of neurodegenerative diseases; and (*iii*) affective states and stress responses. These aspects are briefly reviewed below.

(i) Hippocampal function and memory. In Chapter 2 the published manuscript included describes the neurochemical characterisation of neurons in the mouse dorsal hippocampus targeted by relaxin-3 inputs, and the behavioural consequences of specific RXFP3 depletion in mouse DG hilus. These studies revealed that relaxin-3-positive nerve fibres are in close apposition with GABAergic neurons in the hippocampus, particularly SST-positive GABA neurons, which in turn, strongly suggests RXFP3 is expressed by these neurons. These studies also revealed that conditional Cre-dependent deletion of RXFP3 from neurons in the DG hilus resulted in impairment in spatial reference and working memory, in an appetitive T-maze task and spontaneous alternation task in a Y-maze, respectively. These effects were potentially mediated by a weakening of the synaptic inhibition of pyramidal neuron dendrites in the DG granule cell layer, *or* via inhibition of GABAergic and/or cholinergic neurons in the MS innervated by SST-positive GABA projection neurons from the DG hilus (**Figure 5.1**, Bassant et al., 2005; Amaral et al., 2007; Mendez and Bacci, 2011; Lovett-Barron et al., 2014; Schmid et al., 2016); and potential experiments to explore this putative mechanism are described in detail below (Section 5.2). In hippocampus, inhibitory interneurons regulate excitatory principal cell activity, shaping information processing and orchestrating network activity that underlies learning and memory. Those targeting distinct pyramidal neuron that are recruited at defined phases of behaviour and learning, include SST and PV-basket neurons (Caroni, 2015). SST/GABA neurons in CA1/3 and DG hilus are critical to hippocampal function and contribute to disease aetiology in human AD and rodent AD models (Huh et al., 2016; Katona et al., 2016; Schmid et al., 2016; Stefanelli et al., 2016). Taken together, our novel

experimental data, in combination with other studies in rat (Olucha-Bordonau et al., 2012) and mouse (Haidar M, Tin K, Gundlach AL, unpublished data) reveal that the relaxin-3/RXFP3 system contributes to learning and memory via modulation of GABAergic neurons in the hippocampus as well as modulation of the septum (**Figure 5.1**). These studies suggest that the relaxin-3/RXFP3 system is similar to other characterised neuropeptide modulatory neuronal circuits that influence cognitive processing (Hokfelt et al., 2003; Ogren et al., 2010).

Additionally, these studies describe the characterisation, validation and use of a new 'floxed RXFP3' strain of mouse, paving the way for future studies of regional and temporal control of RXFP3 gene deletion and RXFP3 protein depletion. Together, these studies build upon earlier data, which demonstrate that the NI (Nunez et al., 2006; Pereira et al., 2013; Nategh et al., 2015) and relaxin-3/RXFP3 signalling (Ma et al., 2009c) are able to modulate hippocampal function and associated behaviours such as spatial memory.

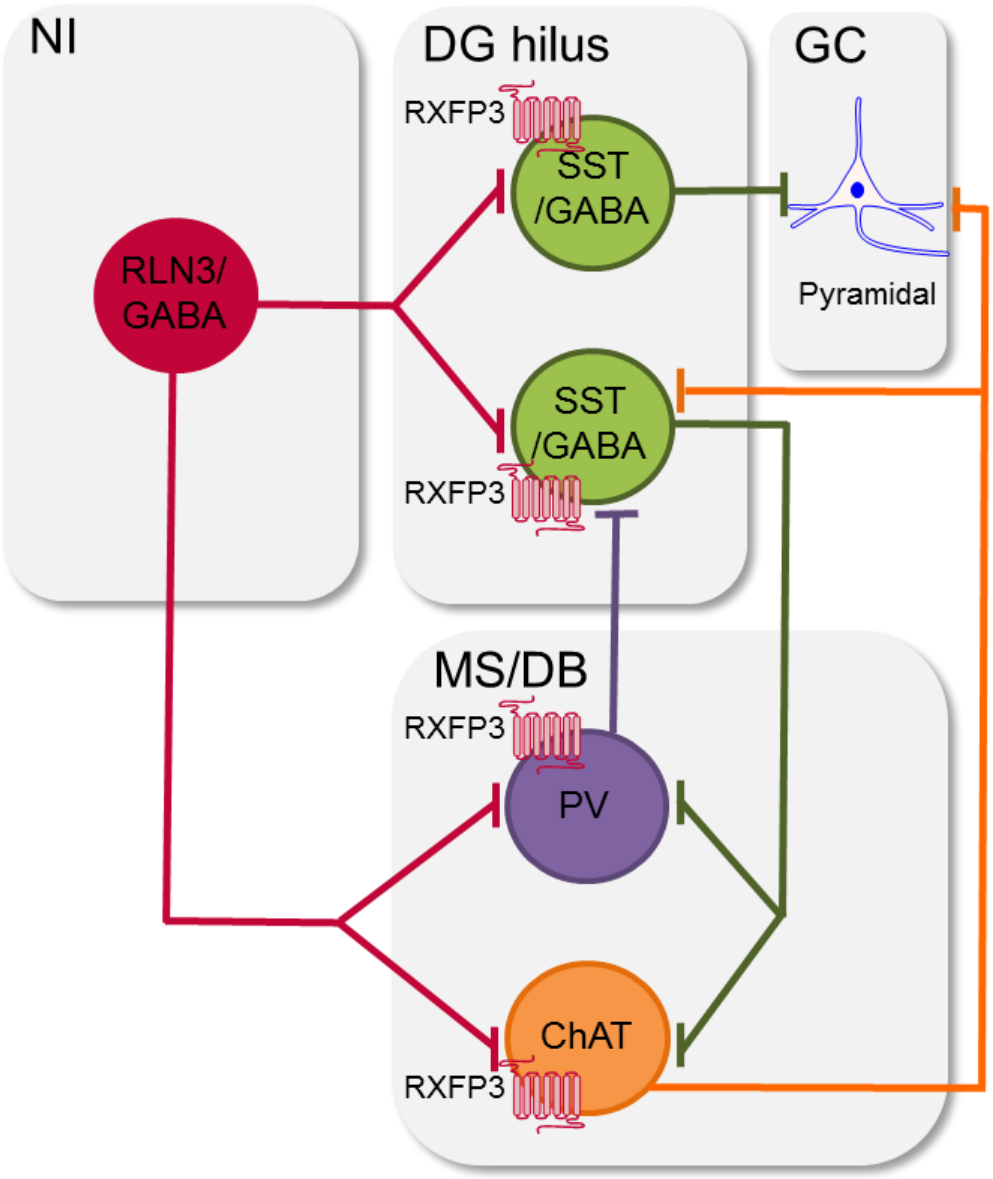

Figure 5.1 Putative circuit mechanisms by which the relaxin-3/RXFP3 system modulates activity in the hippocampus and medial septum/diagonal band of Broca.

The relaxin-3/RXFP3 system is anatomically positioned to modulate the activity of the SHS and HSS, which are pathways important for cognitive functions and related behaviours. The ascending relaxin-3 projections from the NI innervate local and/or projection SST/GABA neurons in the DG hilus, and PV and ChAT neurons in the MS/DB, and these neurons likely express RXFP3. Abbreviations: ChAT, choline acetyltransferase; DG hilus, dentate gyrus hilus; GC, granule cell; HSS, hippocamposeptal system; MS/DB, medial septum/diagonal band of Broca; NI, nucleus incertus; PV, parvalbumin; RXFP3, relaxin family peptide receptor 3, SHS, septohippocampal system; SST, somatostatin.

(ii) The progression of neurodegenerative diseases. In Chapter 3, studies were described that aimed to determine the state of relaxin-3-positive and negative neurons in the NI in a mouse model of tauopathy (tau-P301L), particularly their level of p-tau staining as a reflection of the presence of NFTs. In these quantitative immunohistochemical studies the number of NI relaxin-3-positive neurons was found to be reduced by ~35% in 7 - 8 month old tau-P301L mice, relative to the number in age- and strain-matched controls. Relaxin-3-negative NI neurons were also reduced by ~20%; but this change did not reach statistical significance in the cohorts used. Interestingly, very few if any relaxin-3-positive neurons displayed signs of NFTs (p-tau staining), highlighting the importance of expanding these studies to examine the state of these neuron populations at earlier time-points, and to assess the levels of relaxin-3-positive axons within the hippocampus and other downstream targets of the NI. These findings are consistent with the hypothesis that compromised function of NI relaxin-3 neurons might contribute to the dysfunction of the hippocampus and other brain structures that gives rise to cognitive impairment during AD and other neurodegenerative disorders. Although only an initial insight, this hypothesis and data are consistent with evidence that the brainstem is a major site of tauopathy (Braak et al., 2011; Trillo et al., 2013), and that NI relaxin-3 neurons can modulate the hippocampus and associated behaviours such as memory (see above).

(iii) Affective states and stress responses. In Chapter 4, the studies described were an investigation of whether relaxin-3 or RXFP3 deficiency exacerbated methamphetamine withdrawal symptoms. As mentioned, the NI and relaxin-3/RXFP3 system has been proposed to perform synergistic and/or complementary roles to monoamine signalling within shared or functional-linked target brain regions and neural circuits (for review see, Smith et al., 2014a). Depletion/disruption of ascending monoamine systems (i.e. NA/LC and 5-HT/DR systems) have been described in models of disease, including AD and related neurodegenerative disease, as well as in affective disorders, such as depression and anxiety, which can also be associated with neurodegenerative disease. The studies conducted assessed whether an absence of relaxin-3/RXFP3 signalling might alter the reported depressive- and anxiety- like behavioural profile observed in response to the reduction in monoamine signalling association with methamphetamine withdrawal. Whole-of-life relaxin-3 and RXFP3 KO mice and their WT littermates were injected once daily with saline or escalating doses of methamphetamine and during the subsequent withdrawal phase, relaxin-3 and RXFP3 KO

mice displayed similar measures of despair, body weight change and anxiety-like behaviours. These data indicate that a whole-of-life deficiency in endogenous relaxin-3/RXFP3 signalling does not markedly alter behavioural sensitivity to chronic methamphetamine treatment or withdrawal, under the experimental conditions used. Nonetheless, this study was the first to characterise the response of female C57BL/6J mice to a chronic methamphetamine treatment regime and demonstrated that the methamphetamine schedule used strongly increased acute locomotor activity and effectively reduced body weight and increased behavioural despair in a Porsolt forced swim test.

Although the broad common theme present in these three experimental studies (Chapters) is an effort to examine the ability of relaxin-3/RXFP3 signalling to control brain activity and behaviour, the implications that each experimental study has for the others is somewhat limited, and this is largely due to logistical issues such as differential availability of the different transgenic mouse strains used during the course of this research program. Therefore, as a comprehensive interpretation and discussion of the separate studies has been provided in each experimental Chapter, further discussion here will focus on important emerging experimental tools and techniques that can be used to further progress relaxin-3/RXFP3 research, and how each of these might be applied to the three broad research domains described above.

5.2 Emerging 'tools' and techniques to progress relaxin-3/RXFP3 research

5.2.1 RXFP3-Cre transgenic mice

To date, despite comprehensive mapping studies of the distribution of RXFP3 mRNA in rat and mouse brain (Ma et al., 2007; Smith et al., 2010), which allow speculation about the likely target cells, the precise neurochemical phenotype of RXFP3-positive neurons throughout the rat and mouse brain remains largely unknown. This is due to several factors including an absence of routine double-label *in situ* hybridisation studies using probes for RXFP3 and other mRNA species; and a lack of antibodies that specifically and reliably detect RXFP3 (Lee et al 2016, Meadows et al 2014), which unfortunately for the field, is not uncommon for peptide and other GPCRs.

One common approach to address such limitations is to use a reporter line of mouse or rat in which the receptor of interest is coupled to the expression of a fluorescent or other protein that allows its detection by conventional immunohistochemistry and microscopy. In this regard, our laboratory first obtained a RXFP3-Cre recombinase mouse line from the Genstat program and developed a putative RXFP3 reporter line by crossing these mice that express Cre recombinase under the control of the RXFP3 promoter with mice that ubiquitously express enhanced YFP (eYFP) under the control of a strong Rosa26 promoter, upstream of a floxed stop codon. Thus, in the progeny, Cre excises the stop codon exclusively within the Cre recombinase (RXFP3) positive neurons, and eYFP is expressed only in these neurons. If the Cre recombinase remains constrained to only those neurons that express RXFP3, these mice can be used to assess the distribution of RXFP3 neurons in adult brain and during development. The successful use of these mice could therefore accelerate anatomical and functional studies of the relaxin-3/RXFP3 system and their potential usefulness for the research areas investigated in this thesis is highlighted below.

Hippocampal function and memory. The work described in Chapter 2 and a comprehensive study of the rat MS (Olucha-Bordonau et al., 2012) assessed relaxin-3-positive neural terminations on specific populations of hippocampal and MS neurons, respectively. The observation of relaxin-3-positive fibres/boutons in close apposition with GABA neuron populations in the hippocampus strongly suggests RXFP3 is expressed by these GABA neurons. Therefore, RXFP3-Cre-YFP mice are potentially useful for determining the neurochemical characteristics of RXFP3-positive neurons in the hippocampus (and septum) by immunostaining for GABAergic neuron markers and visualising the co-expression (or absence of) with eYFP, either endogenous or immuno-amplified fluorescent staining.

An alternative/complementary approach to neurochemically phenotype RXFP3-target neurons is to apply RNAscope® protocols. RNAscope® *in situ* hybridization is a powerful new technique which allows the detection of multiple mRNA species in individual neurons and which can identify the chemical phenotype of RXFP3-expressing neurons in specific loci. Indeed, using this technique, very recent studies in our laboratory have identified that a major RXFP3-positive hippocampal neuron population in the *rat* ventral hippocampus is SST-positive, while a smaller population is SST-negative (Rytova V, Ma S, Gundlach AL, unpublished data). Current studies are further examining the chemical phenotype of this

latter population. In addition to the use of RXFP3-Cre mice, RNAscope® suggests an exciting future for the further neurochemical phenotyping of RXFP3 neurons in both mice and rats, particularly while a fully validated and effective (sensitive) RXFP3 antisera is not available.

Furthermore, in addition to facilitating the neurochemical phenotyping of RXFP3-positive neurons, the RXFP3-Cre reporter mouse strain has additional functional/behavioural applicability. Selective targeting/modulation of RXFP3 targeted neurons in hippocampus offers the potential of further identifying the importance of RXFP3 targeted neurons in the modulation of spatial memory and other hippocampal-dependent functions. For example, to inhibit the activity of the RXFP3-positive neuron population, a viral vector encoding the Cre-dependent inhibitory hM4Di DREADD (e.g. AAV-DIO-hM4Di) could be injected into the hippocampus of RXFP3-Cre mice, followed by subsequent repeated/semi-chronic administration of the CNO ligand, which would result in inhibition only of neurons that express Cre and RXFP3. These studies could assess the effect of this inhibition in relevant spatial learning and memory tasks. hM4Di activation by CNO results in hyperpolarization and transient neuronal silencing (Armbruster et al., 2007; Ferguson et al., 2011; Rogan and Roth, 2011), and in addition to examining behavioural outputs, whether neighbouring cells are activated (i.e. disinhibited) could be assessed via c-*fos* immunohistochemistry or other similar approaches. Conversely, to assess effect of activating RXFP3-positive neurons on spatial learning and memory tasks, the same approach could be adopted using a viral vector encoding a Cre-dependent excitatory hM3Dq DREADD (e.g. AAV-DIO-hM3Dq). In related studies, neuronal activity of RXFP3-positive neurons could be determined following exposure to spatial memory tasks, by immunostaining for c-*fos* in RXFP3/eYFP reporter mice following a spatial memory task.

Importantly, to further explore potential neuronal mechanism(s) associated with RXFP3 modulation in the hippocampus, this reporter mouse or an alternate RXFP3-Cre/tdTomato strain with stronger endogenous fluorescence could be used to visualise RXFP3-positive neurons in brain slices for *in vitro* studies to examine the response of RXFP3 neurons following RXFP3 activation by specific agonists (e.g. R3/I5 or RXFP3-A2; Liu et al., 2003; Shabanpoor et al., 2012) or their modulation by other transmitters and peptides. The former studies are of particular interest as recent studies have shown that RXFP3-expressing neurons in different

brain areas and/or within a single brain region can be activated *or* inhibited by RXFP3 agonists (Blasiak et al., 2013; Kania et al., 2017).

Additionally, following validation of the expression of RXFP3 by specific hippocampal GABA neuron populations, future studies should examine the neurophysiological response of RXFP3-positive SST/GABA neurons and other subtypes (e.g. PV/GABA neurons) following activation or inhibition of RXFP3. These experiments are essential to determine the potential direct and/or indirect neuronal modulation of GABA transmission in the hippocampus.

Progression of neurodegenerative diseases. Studies described in Chapter 3 demonstrated that the number of relaxin-3-positive neurons in the NI is reduced in tau-P301L tauopathy mice. However, future studies could determine whether this manifests as a loss of relaxin-3/RXFP3 signalling within key downstream regions such as MS/DB, hippocampus and cingulate cortex, and secondly whether this contributes to dysfunction in these areas and associated cognitive decline. In addition to studies to examine relaxin-3-positive nerve fibres (see Chapter 3), an alternative approach could be the generation of double mutant RXFP3-eYFP reporter mice/tau-P301L transgenic mice to examine the relative level of expression of p-tau within RXFP3-positive neurons relative to other populations. The expression of p-tau within downstream RXFP3-positive neurons would further suggest impairment of RXFP3 signalling in anatomically connected brain regions. Furthermore, such an observation would be in line with NFT/relaxin-3-positive neurons in the NI potentially facilitating the release of tau 'seeds' from presynaptic projections within the hippocampus and other downstream target regions, which could be taken up by postsynaptic neurons in these forebrain regions, triggering NFT accumulation in downstream (anatomically connected) RXFP3-positive neurons. If RXFP3-positive neurons which co-express p-tau at earlier stages of disease progression are preserved, important subsequent studies in double mutant RXFP3-eYFP/tau-P301L mice could assess the therapeutic potential of activating the remaining RXFP3 neurons and measuring whether any cognitive enhancement is observed.

Affective states and stress responses. The studies described in Chapter 4 did not reveal an effect of the presence or absence of endogenous relaxin-3/RXFP3 signalling in whole-of-life KO mice, on the assessed responses to chronic methamphetamine treatment and withdrawal. Nonetheless, other evidence suggests the relaxin-3/RXFP3 system plays a role in affective

states and stress responses (Tanaka et al., 2005; Banerjee et al., 2010; Ma et al., 2010; Watanabe et al., 2011; Ryan et al., 2013), potentially via parallel mechanisms to those of the brainstem ascending monoamine systems (**Figure 5.2**, Smith et al., 2014a). Therefore, further studies are required to examine the anatomical and functional basis for interactions between relaxin-3 and monoamine systems (i.e. NA/LC and 5-HT/DR).

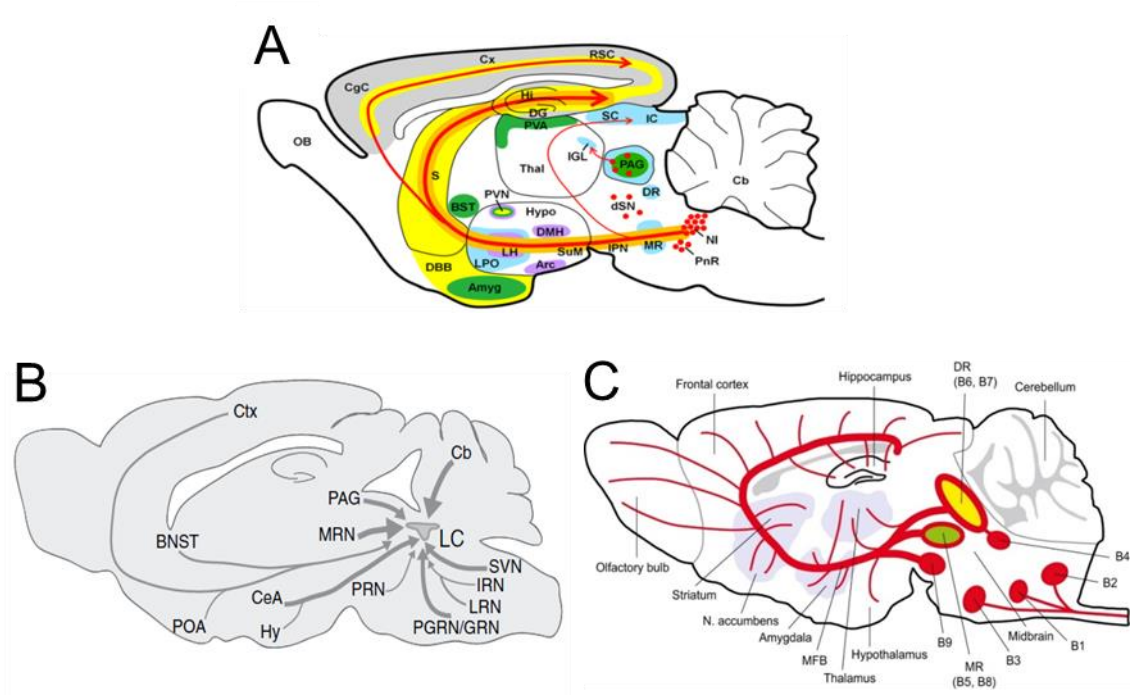

Figure 5.2 Distribution and projection patterns of the relaxin-3/RXFP3 system and noradrenaline/locus coeruleus serotonin/raphe nuclei monoamine brainstem systems.

Anatomical data suggests the **(A)** relaxin-3/RXFP3 system contributes to a brainstem ascending arousal system, similar to parallel ascending monoaminergic **(B)** noradrenaline/locus coeruleus (Schwarz and Luo, 2015) and **(C)** serotonin/raphe nuclei (Lesch and Waider, 2012) systems. These three neural systems display highly overlapping regional efferent projection patterns.

For example, it will be important to examine which specific subpopulations of neurons express RXFP3 in key stress and affective regions in brainstem (e.g. DR) as well as downstream anatomically connected brain regions (e.g. PVN, amygdala, ventral hippocampus), to determine the precise neural substrates through which relaxin-3/RXFP3 modulates stress and affective related brain regions. This can be achieved with the use of RXFP3-eYFP reporter mice. For example, high densities of relaxin-3-positive nerve fibres and RXFP3 mRNA are present within the DR. Therefore, it is possible that GABA and/or 5-HT neurons within this

area express RXFP3, which would support the proposal that relaxin-3 might confer at least some of its functional effects by directly or indirectly influencing 5-HT neurons. In particular, it might be possible that relaxin-3 may increase (disinhibit) the activity of these neurons, if RXFP3 is expressed by GABAergic interneurons within the DR, which normally act to inhibit local 5-HT neurons. Furthermore, the likelihood that the relaxin-3 and monoamine systems have shared downstream targets has only been shown at a regional level, and the RXFP3-eYFP reporter mouse could facilitate experiments to determine at the cellular level which monoamine receptors are expressed by RXFP3-eYFP-positive neurons. For example, the broad regional distribution of relaxin-3-positive nerve fibres in areas such as the hippocampus, septum, midline thalamus, and parts of the hypothalamus and amygdala are similar to that of 5-HT- and NA-positive nerve fibres (Lambert et al., 2000; Samuels and Szabadi, 2008; Hale et al., 2012; Lesch and Waider, 2012) and these regions express receptors for 5-HT and NA (e.g. 5HT1A/2A and alpha 1(α1) adrenoceptors; Marazziti et al., 1994; Pieribone et al., 1994; Burnet et al., 1995). Therefore, it is possible that RXFP3 is co-expressed with subtypes of monoamine receptors within shared downstream target neurons.

Subsequent studies could then determine the electrophysiological responses of RXFP3-eYFP-positive neurons to activation or inhibition of 5-HT and NA receptors, and examine the physiological effects observed following RXFP3 activation or inhibition by RXFP3 agonists (e.g. R3/I5 or RXFP3-A2, Liu et al., 2003; Shabanpoor et al., 2012) or antagonists (e.g. R3(BΔ23-27)R/I5, Kuei et al., 2007), respectively. A synergistic effect may occur, because for example, activation of postsynaptic 5-HT_{1A} evokes hyperpolarization and/or inhibitory effects of target neurons in various brain regions, including the hippocampus (Hirose et al 1990), lateral septum (Van den Hooff and Galvan, 1992), and IGL (Ying et al., 1993). Similarly, activation of RXFP3 in the rat IGL with an RXFP3-agonist (R3/I5) was shown to evoke inhibitory effects (decrease in firing rate and hyperpolarization) in the majority of IGL neurons (Blasiak et al., 2013), an effect probably associated with the inhibition of cAMP production caused by RXFP3 activation (Liu et al., 2005).

Furthermore, studies to examine the responsiveness of RXFP3-eYFP-positive neurons to stress related behaviours in regions such as the amygdala and hypothalamus will provide insights into the role of relaxin-3/RXFP3 signalling in affective states and stress responses. For example, this could be accomplished by examining changes in c-Fos levels in RXFP3-eYFP-

positive neurons during withdrawal of chronic methamphetamine treatment, as well as other well-known stressors, including chronic restraint and swim stress. An increase in the number of c-*fos*-positive neurons was observed following treatment with methamphetamine within the PVN and central amygdala (Giardino et al., 2011; Tomita et al., 2013; Zuloaga et al., 2014), two regions central to the regulation of the hypothalamic-pituitary-adrenal (HPA) axis. Based on the expression of RXFP3 mRNA within these two brain regions (amongst other stress responsive regions, Ma et al., 2007; Smith et al., 2010) and the proposed role of the relaxin-3/RXFP3 system in affective states and stress responses based on studies in the rat (Tanaka et al., 2005; Banerjee et al., 2010; Ma et al., 2010; Watanabe et al., 2011; Ryan et al., 2013), it will be of interest to observe the profile of RXFP3-positive neurons during methamphetamine withdrawal and other stress regimes.

5.2.2 Relaxin-3-Cre mice

As described in Chapter 1, the ability of the NI to regulate hippocampal theta rhythm and spatial learning and memory has been examined in rats (Nunez et al., 2006; Ma et al., 2013; Nategh et al., 2015). However, the contribution of the relaxin-3-positive population of NI neurons is less clear. Studies in our laboratory are attempting to address this issue, by trying to develop a promoter sequence suitable for use in viral vectors that can drive relaxin-3 cell specific expression. If such a promoter can be produced and fully optimised, it will allow for studies to better determine the specific role of relaxin-3-positive GABA neurons in the NI in hippocampal activity and related cognitive behaviours. For studies with a cell-specific promoter, one key restriction is the allowable size of foreign DNA (5 kb) that can be inserted into an AAV-vector (Dong et al., 1996; Wu et al., 2010), if this virus is preferred, highlighting a possible disadvantage in the development of a reliable and specific relaxin-3 cell specific viral vector.

An alternative method particularly for further studies in mice, would be the development of a relaxin-3-Cre mouse strain in which Cre recombinase expression is driven by the relaxin-3 promoter. Importantly, such a mouse line has recently been produced by a US laboratory in collaboration with our laboratory and validation studies are currently underway. Therefore, possible use of these mice in studies to learn more about the role of NI and relaxin-3 signalling in the research areas investigated in the thesis studies are described below.

Hippocampal function and memory. Relaxin-3-Cre mice will facilitate studies to inhibit or activate NI relaxin-3 (GABA) neuronal activity and examine the effect on hippocampal theta rhythm and spatial learning and memory. This could be achieved by injections of Cre-dependent inhibitory hM4Di or excitatory hM3Dq DREADDs, respectively, followed by administration of the CNO ligand, which would result in modulation (inhibition or excitation) of relaxin-3-positive GABA neurons in the NI. As described, these experiments are crucial to investigate the hypothesis that relaxin-3 neurons in the NI are important for healthy cognition. Another application of relaxin-3-Cre mice would be to use Cre-dependent neural tract-tracing to determine whether the NI is the sole source of the relaxin-3 innervation to the hippocampus (and other interconnected components of the SHS), or whether the more diffuse populations of relaxin-3 in the pontine raphe nucleus, the anterior and ventrolateral periaqueductal grey, and in the area dorsal to the substantia nigra also innervate these regions.

Progression of neurodegenerative diseases. Having established that relaxin-3-positive neurons in the NI are affected by tauopathy in tau-P301L mice, a future challenge is to examine the therapeutic potential of the relaxin-3/RXFP3 system in neurodegenerative disease. In similar experiments to those described above, this could be achieved by generating double mutant relaxin-3-Cre/tau-P301L transgenic mice and inhibiting or activating the remaining relaxin-3-positive neurons in the NI with the use of Cre-dependent inhibitory hM4Di or excitatory hM3Dq DREADDs. If modulation of the relaxin-3/RXFP3 system is therapeutic, an increased rate in cognitive decline in behavioural measures of spatial learning and memory might be predicted following CNO activation of Cre-dependent inhibitory hM4Di within NI relaxin-3-positive neurons of relaxin-3-Cre/tau-P301L mice. Conversely, acute CNO activation of Cre-dependent excitatory hM3Dq within the remaining relaxin-3 NI neurons might enhance cognitive performance and chronic activation might slow the rate of cognitive decline.

Furthermore, to observe the anatomical characteristics of NI relaxin-3 neuron efferent projections in relaxin-3-Cre/tau-P301L mice, injections of a Cre-dependent AAV vector could drive expression of fluorescent protein only in relaxin-3-positive cells expressing Cre recombinase. These experiments are crucial to addressing the following important questions: (1) Are relaxin-3-positive nerve fibres (originating from relaxin-3 NI neurons)

impaired/reduced in forebrain regions (e.g. hippocampus and cingulate cortex) of relaxin-3-Cre/tau-P301L mice, and (2) does the degree of impairment of relaxin-3-positive inputs correlate with NFT expression in these forebrain regions. Importantly, these experiments will also allow studies to distinguish between relaxin-3-positive nerve fibres originating from the NI versus relaxin-3 fibres originating from the pontine raphe nucleus, the periaqueductal grey, and/or dorsal to the substantia nigra. Together, these experiments will provide insights into the therapeutic potential of the relaxin-3/RXFP3 system in neurodegenerative disease.

Affective states and stress responses. As described, relaxin-3-positive neurons in the rat NI are reported to express 5-HT_{1A} receptors (Miyamoto et al., 2008), and 5-HT depletion induced by local infusion of PCPA within the DR significantly increased relaxin-3 mRNA expression in the NI, suggesting 5-HT neurons from the DR or other raphe nuclei directly innervate NI relaxin-3 neurons and act to inhibit relaxin-3 expression. Further experiments are required to assess this interaction. This can be achieved by recording the electrophysiological activity of relaxin-3 neurons in the NI following administration with 5-HT, in which hyperpolarization of NI relaxin-3 neurons is expected following 5-HT activation. Furthermore, the NI is a highly stress-reactive nucleus (Tanaka et al., 2005; Ryan et al., 2011), and all relaxin-3 neurons in the rat NI co express CRF-R1 (Ma et al., 2013). The majority of relaxin-3 neurons in the rat NI exhibit depolarization (excitation) in response to CRF infusion (Ma et al., 2013), but similar studies have not been conducted in mice. Therefore, future studies should address this by recording the electrophysiological effects of CRF on identified relaxin-3 NI neurons in relaxin-3-Cre/reporter protein mice.

5.2.3 Studies of relaxin-3/RXFP3 in humans

A major long-term goal of research on the relaxin-3/RXFP3 system is to apply the knowledge gained in animals to the equivalent human physiology and pathology, and to identify therapeutic applications of RXFP3-targeted drugs. Such studies would provide a valuable basis for further translational research. The relatively high degree of amino acid conservation across species indicates that the structure (and function) of the relaxin-3 peptide has been highly constrained during evolution. Accordingly, identification of mutations and/or polymorphisms within the relaxin-3 and/or RXFP3 genes that might be present in patients suffering from affective and neurodegenerative disease are important.

In the first study of this type related to the relaxin-3/RXFP3 system, patients diagnosed with a familial form of schizophrenia were found to have a mutation within a chromosomal locus that contains the RXFP3 gene (Bespalova et al., 2005), suggesting a potential relationship between RXFP3 and schizophrenia. In another gene association study, a polymorphism in the relaxin-3 gene and two in the RXFP3 gene were observed in schizophrenia patients undergoing treatment with antipsychotic medications and who displayed co-morbid metabolic syndromes (Munro et al., 2012). However, these studies are limited and have not been confirmed in larger genome-wide association studies (GWAS). Due to improvements in and reduced costs of gene sequencing, more information about the profile of RXFP3 expression in neurodegenerative and neuropsychiatric disorders should become available in the near future. Such experiments have been successful in linking other neuropeptide receptor systems to neurodegenerative (Bertram and Tanzi, 2009; Huang and Mucke, 2012) and affective disorders, including major depressive disorder (MDD) (Wray et al 2012). For example, a single nucleotide polymorphism in the SST gene increases the risk for AD in carriers of the apoE4 gene (Vepsalainen et al., 2007), and polymorphisms in the neuropeptide galanin gene have been observed in patients with MDD (Wray et al., 2012), in line with the proposed role of galanin in MDD and related stress states (Weiss et al., 1998).

In a more recent study, putative RXFP3 immunoreactivity was reported to be increased in post-mortem neocortex of depressed AD patients relative to controls, and unaffected in non-depressed AD patients (Lee et al., 2016). Interestingly, levels of putative RXFP1 protein in the parietal cortex were reported to be correlated with the severity of depression symptoms. In contrast, cortical levels of RXFP1 and RXFP3 immunoreactivity did not correlate with dementia severity and β-amyloid accumulation (Lee et al., 2016). However, several technical limitations need to be considered as part of an evaluation of this data, particularly the full validation of the specificity of RXFP1 and RXFP3 antibodies used. Additionally, further comprehensive studies of RXFP3 levels (and gene transcript and binding properties) in post-mortem brain samples from AD patients (and MDD patients) from brain regions important in cognition and emotional regulation (i.e. hippocampus, septum, amygdala and hypothalamus) are crucial, as well as levels of relaxin-3 immunoreactivity and the state of the NI in post-mortem brains from relevant patient groups.

Assays for detecting cerebrospinal fluid (CSF) levels of neuropeptides and transmitters in patients diagnosed with AD and neuropsychiatric diseases, are commonplace. For example, SST levels detected in CSF are significantly reduced in patients diagnosed with AD and elderly patients with MDD, relative to healthy age-matched controls, and the reductions in CSF levels of SST correlates with CSF CRF levels in both AD and MD patients (Molchan et al., 1993). In a similar study, a significant correlation between reduced levels of the monoamine metabolite, 5-hydroxyindoleacetic (5HIAA), in CSF with CSF SST levels was reported in AD and MDD patients (Molchan et al., 1991), suggesting SST may interact with 5-HT in AD and affective disorders. Similarly, reduced CSF levels of NA in AD patients relative to age-matched healthy controls have also been reported (Martignoni et al., 1992). Similar studies of CSF relaxin-3 levels in patients with neurodegenerative and/or neuropsychiatric disease may indicate the potential involvement of the relaxin-3/RXFP3 system in these disease states.

5.3 Concluding remarks

Since the discovery of the highly conserved, neuropeptide, relaxin-3 and the subsequent identification of RXFP3 as its cognate receptor more than a decade ago, experimental studies have yielded exciting insights into the role of the relaxin-3/RXFP3 signalling system in modulating arousal and several motivated behaviours, along with related cognitive processes. The neuroanatomical distribution of relaxin-3 and RXFP3 indicate relaxin-3 containing GABAergic neurons are an integral part of the SHS (Ma et al., 2009c; Smith et al., 2010; Olucha-Bordonau et al., 2012), contributing to neuronal circuits that play key roles in cognition.

The studies described in this thesis extend this knowledge, and demonstrate, firstly, that relaxin-3 nerve fibres terminate on specific types of GABAergic neurons in the hippocampus, and secondly, that selective depletion of RXFP3 from the dorsal DG hilus in adult mice impairs spatial reference and working memory. In line with a role for relaxin-3/RXFP3 signalling in healthy cognition, separate studies demonstrated a reduction in relaxin-3-positive neurons in the NI of tau-P301L transgenic mice that display a human form of tauopathy, relative to the number of these neurons in healthy age-matched controls. These studies suggest that effects on the relaxin-3/RXFP3 system may contribute to the cognitive decline observed in tauopathies and related conditions. These findings invite further investigations of the

involvement of the relaxin-3/RXFP3 system in tauopathies and related neurodegenerative diseases and studies to examine the therapeutic potential of RXFP3-related drugs in the treatment of these conditions.

Furthermore, based on the possible complementary roles of the relaxin-3/RXFP3 system and ascending monoaminergic systems in modulating stress and affective states, the effect of altered endogenous relaxin-3/RXFP3 signalling in whole-of-life relaxin-3 and RXFP3 KO mice on affective- and depressive-like behaviours following chronic methamphetamine treatment (monoamine depletion) was investigated. While these studies did not reveal genotype effects on behavioural sensitivity to chronic methamphetamine treatment in whole-of-life relaxin-3 and RXFP3 KO mice, these studies suggest that further research to examine whether more specific depletion of monoamines and/or localised manipulations of endogenous relaxin-3/RXFP3 signalling in the adult brain might reveal significant interactions between monoamine and relaxin-3 signalling networks.

There is an urgent global need for basic and translational research to provide a better understanding of the brain circuits that are dysfunctional in neurodegenerative and affective disorders, and to identify novel structural and molecular targets that might provide better symptomatic treatments and a meaningful slowing of disease progression. Importantly, the current studies form part of a broader, worldwide scientific endeavour to better understand neuropeptides and their neuromodulatory role within important neuronal circuits during 'healthy' and normal cognitive processing as well as under pathological conditions in neurodegenerative and neuropsychiatric disorders, which are often comorbid.

Overall, the research described in this thesis has laid the foundation for ongoing preclinical studies to investigate the effects of relaxin-3/RXFP3 signalling in normal brain and in models of neurodegenerative disease and psychiatric illness. In the long term, it is hoped the knowledge gained from such research on the relaxin-3/RXFP3 system can be applied to clinical testing, to assess the therapeutic potential of RXFP3-targeted drugs.

Bibliography

Acsady L, Arabadzisz D, Freund TF (1996). Correlated morphological and neurochemical features identify different subsets of vasoactive intestinal polypeptide-immunoreactive interneurons in rat hippocampus. *Neuroscience* **73**, 299-315.

Acsady L, Kamondi A, Sik A, Freund T, Buzsaki G (1998). GABAergic cells are the major postsynaptic targets of mossy fibers in the rat hippocampus. *J Neurosci* **18**, 3386-3403.

Acsady L, Katona I, Martinez-Guijarro FJ, Buzsaki G, Freund TF (2000). Unusual target selectivity of perisomatic inhibitory cells in the hilar region of the rat hippocampus. *J Neurosci* **20**, 6907-6919.

Ádori C, Glück L, Barde S, Yoshitake T, Kovacs GG, Mulder J, Maglóczky Z, Havas L, Bölcskei K, Mitsios N (2015). Critical role of somatostatin receptor 2 in the vulnerability of the central noradrenergic system: new aspects on Alzheimer's disease. *Acta Neuropathol* **129**, 541-563.

Ahmed Z, Cooper J, Murray TK, Garn K, McNaughton E, Clarke H et al. (2014). A novel in vivo model of tau propagation with rapid and progressive neurofibrillary tangle pathology: the pattern of spread is determined by connectivity, not proximity. *Acta Neuropathol* **127**, 667-683.

Albert-Gasco H, Garcia-Aviles A, Moustafa S, Sanchez-Sarasua S, Gundlach AL, Olucha-Bordonau FE, Sanchez-Perez AM (2017). Central relaxin-3 receptor (RXFP3) activation increases ERK phosphorylation in septal cholinergic neurons and impairs spatial working memory. *Brain Struct Funct* **222**, 449-463.

Allen B, Ingram E, Takao M, Smith MJ, Jakes R, Virdee K et al. (2002). Abundant tau filaments and nonapoptotic neurodegeneration in transgenic mice expressing human P301S tau protein. *The Neurosci* **22**, 9340-9351.

Alzheimer A (1907). Uber eine eigenartige Erkrankung der Hirnrinde. *Allgemeine Zeitschrife Psychiatrie* **64**, 146-148.

Amaral DG, Kurz J (1985). An analysis of the origins of the cholinergic and noncholinergic septal projections to the hippocampal formation of the rat. *J Comp Neurol* **240**, 37-59.

Amaral DG, Scharfman HE, Lavenex P (2007). The dentate gyrus: fundamental neuroanatomical organization (dentate gyrus for dummies). *Prog Brain Res* **163**, 3-22.

Andrews-Zwilling Y, Bien-Ly N, Xu Q, Li G, Bernardo A, Yoon SY, Zwilling D, Yan TX, Chen L, Huang Y (2010). Apolipoprotein E4 causes age- and Tau-dependent impairment of GABAergic interneurons, leading to learning and memory deficits in mice. *J Neurosci* **30**, 13707-13717.

Antonucci F, Alpar A, Kacza J, Caleo M, Verderio C, Giani A et al. (2012). Cracking down on inhibition: selective removal of GABAergic interneurons from hippocampal networks. *J Neurosci* **32**, 1989-2001.

Aral H, Kosaka K, Iizuka R (1984). Changes of biogenic amines and their metabolites in postmortem brains from patients with alzheimer-type dementia. *J Neurochem* **43**, 388-393.

Armbruster BN, Li X, Pausch MH, Herlitze S, Roth BL (2007). Evolving the lock to fit the key to create a family of G protein-coupled receptors potently activated by an inert ligand. *Proc Natl Acad Sci USA* **104**, 5163-5168.

Arnold SE, Hyman BT, Flory J, Damasio AR, Van Hoesen GW (1991). The topographical and neuroanatomical distribution of neurofibrillary tangles and neuritic plaques in the cerebral cortex of patients with Alzheimer's disease. *Cereb Cortex* **1**, 103-116.

Augustinack JC, Schneider A, Mandelkow EM, Hyman BT (2002). Specific tau phosphorylation sites correlate with severity of neuronal cytopathology in Alzheimer's disease. *Acta Neuropathol* **103**, 26-35.

Bamford NS, Zhang H, Joyce JA, Scarlis CA, Hanan W, Wu NP et al. (2008). Repeated exposure to methamphetamine causes long-lasting presynaptic corticostriatal depression that is renormalized with drug readministration. *Neuron* **58**, 89-103.

Banerjee A, Shen PJ, Ma S, Bathgate RA, Gundlach AL (2010). Swim stress excitation of nucleus incertus and rapid induction of relaxin-3 expression via CRF1 activation. *Neuropharmacology* **58**, 145-155.

Bannerman D, Grubb M, Deacon R, Yee B, Feldon J, Rawlins J (2003). Ventral hippocampal lesions affect anxiety but not spatial learning. *Behav Brain Res* **139**, 197-213.

Bannerman DM, Sprengel R, Sanderson DJ, McHugh SB, Rawlins JN, Monyer H, Seeburg PH (2014). Hippocampal synaptic plasticity, spatial memory and anxiety. *Nat Rev Neurosci* **15**, 181-192.

Baraban SC, Tallent MK (2004). Interneuron diversity series: Interneuronal neuropeptides--endogenous regulators of neuronal excitability. *Trends Neurosci* **27**, 135-142.

Baratta MV, Lamp T, Tallent MK (2002). Somatostatin depresses long-term potentiation and Ca2+ signaling in mouse dentate gyrus. *J Neurophysiol* **88**, 3078-3086.

Bassant MH, Simon A, Poindessous-Jazat F, Csaba Z, Epelbaum J, Dournaud P (2005). Medial septal GABAergic neurons express the somatostatin sst2A receptor: functional consequences on unit firing and hippocampal theta. *J Neurosci* **25**, 2032-2041.

Bathgate RA, Halls ML, van der Westhuizen ET, Callander GE, Kocan M, Summers RJ (2013). Relaxin family peptides and their receptors. *Physiol Rev* **93**, 405-480.

Bathgate RA, Samuel CS, Burazin TC, Layfield S, Claasz AA, Reytomas IG et al. (2002). Human relaxin gene 3 (H3) and the equivalent mouse relaxin (M3) gene. Novel members of the relaxin peptide family. *J Biol Chem* **277**, 1148-1157.

Bathgate RA, Lin F, Hanson NF, Otvos L, Jr., Guidolin A, Giannakis C et al. (2006). Relaxin-3: improved synthesis strategy and demonstration of its high-affinity interaction with the relaxin receptor LGR7 both in vitro and in vivo. *Biochemistry* **45**, 1043-1053.

Belarbi K, Schindowski K, Burnouf S, Caillierez R, Grosjean ME, Demeyer D, Hamdane M, Sergeant N, Blum D, Buee L (2009). Early Tau pathology involving the septo-hippocampal pathway in a Tau transgenic model: relevance to Alzheimer's disease. *Curr Alzheimer Res* **6**, 152-157.

Belarbi K, Burnouf S, Fernandez-Gomez FJ, Desmercieres J, Troquier L, Brouillette J et al. (2011). Loss of medial septum cholinergic neurons in THY-Tau22 mouse model: what links with tau pathology? *Curr Alzheimer Res* **8**, 633-638.

Bergado JA, Frey S, López J, Almaguer-Melian W, Frey JU (2007). Cholinergic afferents to the locus coeruleus and noradrenergic afferents to the medial septum mediate LTP-reinforcement in the dentate gyrus by stimulation of the amygdala. *Neurobiol Learn Mem* **88**, 331-341.

Bering R, Draguhn A, Diemer NH, Johansen FF (1997). Ischemia changes the coexpression of somatostatin and neuropeptide Y in hippocampal interneurons. *Exp Brain Res* **115**, 423-429.

Berridge CW, Schmeichel BE, España RA (2012). Noradrenergic modulation of wakefulness/arousal. *Sleep Med Rev* **16**, 187-197.

Bertram L, Tanzi RE (2009). Genome-wide association studies in Alzheimer's disease. *Hum Mol Gen* **18**, R137-R145.

Bespalova IN, Angelo GW, Durner M, Smith CJ, Siever LJ, Buxbaum JD, Silverman JM (2005). Fine mapping of the 5p13 locus linked to schizophrenia and schizotypal personality disorder in a Puerto Rican family. *Psychiatr Genet* **15**, 205-210.

Billova S, Galanopoulou AS, Seidah NG, Qiu X, Kumar U (2007). Immunohistochemical expression and colocalization of somatostatin, carboxypeptidase-E and prohormone convertases 1 and 2 in rat brain. *Neuroscience* **147**, 403-418.

Blasiak A, Blasiak T, Lewandowski MH, Hossain MA, Wade JD, Gundlach AL (2013). Relaxin-3 innervation of the intergeniculate leaflet of the rat thalamus - neuronal tract-tracing and in vitro electrophysiological studies. *Eur J Neurosci* **37**, 1284-1294.

Blasiak A, Siwiec M, Grabowiecka A, Blasiak T, Czerw A, Blasiak E, Kania A, Rajfur Z, Lewandowski MH, Gundlach AL (2015). Excitatory orexinergic innervation of rat nucleus incertus--Implications for ascending arousal, motivation and feeding control. *Neuropharmacology* **99**, 432-447.

Boekhoorn K, Terwel D, Biemans B, Borghgraef P, Wiegert O, Ramakers GJ et al. (2006). Improved long-term potentiation and memory in young tau-P301L transgenic mice before onset of hyperphosphorylation and tauopathy. *J Neurosci* **26**, 3514-3523.

Bondareff W, Mountjoy C, Roth M, Rossor M, Iversen L, Reynolds G, Hauser D (1987). Neuronal degeneration in locus ceruleus and cortical correlates of Alzheimer disease. *Alzheimer Dis Assoc Disord* **1**, 256-262.

Borbely E, Scheich B, Helyes Z (2013). Neuropeptides in learning and memory. *Neuropeptides* **47**, 439-450.

Braak H, Braak E (1991). Neuropathological stageing of Alzheimer-related changes. *Acta Neuropathol* **82**, 239-259.

Braak H, Thal DR, Ghebremedhin E, Del Tredici K (2011). Stages of the pathologic process in Alzheimer disease: age categories from 1 to 100 years. *J Neuropathol Exp Neurol* **70**, 960-969.

Branchek TA, Smith KE, Gerald C, Walker MW (2000). Galanin receptor subtypes. *Trends Pharmacol Sci* **21**, 109-117.

Brown RE, McKenna JT (2015). Turning a negative into a positive: Ascending GABAergic control of cortical activation and arousal. *Front Neurol* **6**, 135.

Burazin TC, Bathgate RA, Macris M, Layfield S, Gundlach AL, Tregear GW (2002). Restricted, but abundant, expression of the novel rat gene-3 (R3) relaxin in the dorsal tegmental region of brain. *J Neurochem* **82**, 1553-1557.

Burazin TC, Johnson KJ, Ma S, Bathgate RA, Tregear GW, Gundlach AL (2005). Localization of LGR7 (relaxin receptor) mRNA and protein in rat forebrain: correlation with relaxin binding site distribution. *Ann N Y Acad Sci* **1041**, 205-210.

Burnet P, Eastwood S, Lacey K, Harrison P (1995). The distribution of 5-HT 1A and 5-HT 2A receptor mRNA in human brain. *Brain Res* **676**, 157-168.

Cai Z, Ratka A (2012). Opioid system and Alzheimer's disease. *Neuromol Med* **14**, 91-111.

Caroni P (2015). Inhibitory microcircuit modules in hippocampal learning. *Curr Opin Neurobiol* **35**, 66-73.

Cervera-Ferri A, Rahmani Y, Martínez-Bellver S, Teruel-Martí V, Martínez-Ricós J (2012). Glutamatergic projection from the nucleus incertus to the septohippocampal system. *Neurosci Lett* **517**, 71-76.

Chen J, Kuei C, Sutton SW, Bonaventure P, Nepomuceno D, Eriste E, Sillard R, Lovenberg TW, Liu C (2005). Pharmacological characterization of relaxin-3/INSL7 receptors GPCR135 and GPCR142 from different mammalian species. *J Pharmacol Exp Ther* **312**, 83-95.

Chronwall B, Skirboll L, O'Donohue T (1985). Demonstration of a pontine-hippocampal projection containing a ranatensin-like peptide. *Neurosci Lett* **53**, 109-114.

Clavaguera F, Bolmont T, Crowther RA, Abramowski D, Frank S, Probst A et al. (2009). Transmission and spreading of tauopathy in transgenic mouse brain. *Nat Cell Biol* **11**, 909-913.

Cobb SR, Davies CH (2005). Cholinergic modulation of hippocampal cells and circuits. *J Physiol* **562**, 81-88.

Cowan W, Guillery R, Powell T (1964). The origin of the mamillary peduncle and other hypothalamic connexions from the midbrain. *J Anat* **98**, 345.

Cryan JF, Hoyer D, Markou A (2003). Withdrawal from chronic amphetamine induces depressive-like behavioral effects in rodents. *Biol Psychiatry* **54**, 49-58.

Danik M, Puma C, Quirion R, Williams S (2003). Widely expressed transcripts for chemokine receptor CXCR1 in identified glutamatergic, gamma-aminobutyric acidergic, and cholinergic neurons and astrocytes of the rat brain: a single-cell reverse transcription-multiplex polymerase chain reaction study. *J Neurosci Res* **74**, 286-295.

Danik M, Cassoly E, Manseau F, Sotty F, Mouginot D, Williams S (2005). Frequent coexpression of the vesicular glutamate transporter 1 and 2 genes, as well as coexpression with genes for choline acetyltransferase or glutamic acid decarboxylase in neurons of rat brain. *J Neurosci Res* **81**, 506-521.

de Calignon A, Polydoro M, Suarez-Calvet M, William C, Adamowicz DH, Kopeikina KJ et al. (2012). Propagation of tau pathology in a model of early Alzheimer's disease. *Neuron* **73**, 685-697.

Dong J-Y, Fan P-D, Frizzell RA (1996). Quantitative analysis of the packaging capacity of recombinant adeno-associated virus. *Hum Gene Ther* **7**, 2101-2112.

Donizetti A, Grossi M, Pariante P, D'Aniello E, Izzo G, Minucci S, Aniello F (2008). Two neuron clusters in the stem of postembryonic zebrafish brain specifically express relaxin-3 gene: first evidence of nucleus incertus in fish. *Dev Dyn* **237**, 3864-3869.

Dun NJ, Dun SL, Wong RK, Forstermann U (1994). Colocalization of nitric oxide synthase and somatostatin immunoreactivity in rat dentate hilar neurons. *Proc Natl Acad Sci U S A* **91**, 2955-2959.

Dutschmann M, Menuet C, Stettner GM, Gestreau C, Borghgraef P, Devijver H, Gielis L, Hilaire G, Van Leuven F (2010). Upper airway dysfunction of Tau-P301L mice correlates with tauopathy in midbrain and ponto-medullary brainstem nuclei. *J Neurosci* **30**, 1810-1821.

Fanselow MS, Dong H-W (2010). Are the dorsal and ventral hippocampus functionally distinct structures? *Neuron* **65**, 7-19.

Ferguson SM, Eskenazi D, Ishikawa M, Wanat MJ, Phillips PE, Dong Y, Roth BL, Neumaier JF (2011). Transient neuronal inhibition reveals opposing roles of indirect and direct pathways in sensitization. *Nat Neurosci* **14**, 22-24.

Ford B, Holmes CJ, Mainville L, Jones BE (1995). GABAergic neurons in the rat pontomesencephalic tegmentum: codistribution with cholinergic and other tegmental neurons projecting to the posterior lateral hypothalamus. *J Comp Neurol* **363**, 177-196.

Forro T, Valenti O, Lasztoczi B, Klausberger T (2015). Temporal organization of GABAergic interneurons in the intermediate CA1 hippocampus during network oscillations. *Cereb Cortex* **25**, 1228-1240.

Franklin KB, Paxinos G (1997). Mouse brain in stereotaxic coordinates. Academic press.

Freund T, Gulyas A, Acsady L, Görcs T, Toth K (1990). Serotonergic control of the hippocampus via local inhibitory interneurons. *Proc Natl Acad Sci USA* **87**, 8501-8505.

Freund TF, Antal M (1988). GABA-containing neurons in the septum control inhibitory interneurons in the hippocampus. *Nature* **336**, 170-173.

Freund TF, Buzsaki G (1996). Interneurons of the hippocampus. *Hippocampus* **6**, 347-470.

Frotscher M, Léránth C (1985). Cholinergic innervation of the rat hippocampus as revealed by choline acetyltransferase immunocytochemistry: a combined light and electron microscopic study. *J Comp Neurol* **239**, 237-246.

Fujisawa S, Buzsáki G (2011). A 4 Hz oscillation adaptively synchronizes prefrontal, VTA, and hippocampal activities. *Neuron* **72**, 153-165.

Gainer H (1981). The biology of neurosecretory neurons. *Adv Biochem Psychopharmacol* **28**, 5-20.

Ganella D, Callander G, Ma S, Bye C, Gundlach A, Bathgate R (2013). Modulation of feeding by chronic rAAV expression of a relaxin-3 peptide agonist in rat hypothalamus. *Gene Ther* **20**, 703-716.

Giardino WJ, Pastor R, Anacker AM, Spangler E, Cote DM, Li J, Stenzel-Poore M, Phillips TJ, Ryabinin AE (2011). Dissection of corticotropin-releasing factor system involvement in locomotor sensitivity to methamphetamine. *Genes, Brain Behav* **10**, 78-89.

Goedert M, Spillantini MG (2000). Tau mutations in frontotemporal dementia FTDP-17 and their relevance for Alzheimer's disease. *Biochimica et Biophysica Acta (BBA)-Mol Basis Dis* **1502**, 110-121.

Goedert M, Spillantini MG (2006). A century of Alzheimer's disease. *Science* **314**, 777-781.

Goto M, Swanson LW, Canteras NS (2001). Connections of the nucleus incertus. *J Comp Neurol* **438**, 86-122.

Gotz J, Nitsch RM (2001). Compartmentalized tau hyperphosphorylation and increased levels of kinases in transgenic mice. *Neuroreport* **12**, 2007-2016.

Gotz J, Chen F, Barmettler R, Nitsch RM (2001). Tau filament formation in transgenic mice expressing P301L tau. *J Biol Chem* **276**, 529-534.

Gotzsche CR, Woldbye DP (2016). The role of NPY in learning and memory. *Neuropeptides* **55**, 79-89.

Gulyas AI, Gorcs TJ, Freund TF (1990). Innervation of different peptide-containing neurons in the hippocampus by GABAergic septal afferents. *Neuroscience* **37**, 31-44.

Hale MW, Shekhar A, Lowry CA (2012). Stress-related serotonergic systems: implications for symptomatology of anxiety and affective disorders. *Cell Mol Neurobiol* **32**, 695-708.

Hampton DW, Webber DJ, Bilican B, Goedert M, Spillantini MG, Chandran S (2010). Cell-mediated neuroprotection in a mouse model of human tauopathy. *J Neurosci* **30**, 9973-9983.

Hara Y, Motoi Y, Hikishima K, Mizuma H, Onoe H, Matsumoto SE, Elahi M, Okano H, Aoki S, Hattori N (2017). Involvement of the septo-hippocampal cholinergic pathway in association with septal acetylcholinesterase upregulation in a mouse model of tauopathy. *Curr Alzheimer Res* **14**, 94-103.

Harris JA, Koyama A, Maeda S, Ho K, Devidze N, Dubal DB, Yu GQ, Masliah E, Mucke L (2012). Human P301L-mutant tau expression in mouse entorhinal-hippocampal network causes tau aggregation and presynaptic pathology but no cognitive deficits. *PLoS One* **7**, e45881.

Hasegawa M, Crowther RA, Jakes R, Goedert M (1997). Alzheimer-like changes in microtubule-associated protein Tau induced by sulfated glycosaminoglycans. Inhibition of microtubule binding, stimulation of phosphorylation, and filament assembly depend on the degree of sulfation. *J Biol Chem* **272**, 33118-33124.

Heilig M, Koob GF, Ekman R, Britton KT (1994). Corticotropin-releasing factor and neuropeptide Y: role in emotional integration. *Trends Neurosci* **17**, 80-85.

Himeno E, Ohyagi Y, Ma L, Nakamura N, Miyoshi K, Sakae N et al. (2011). Apomorphine treatment in Alzheimer mice promoting amyloid-beta degradation. *Ann Neurol* **69**, 248-256.

Hisaw FL (1926). Experimental relaxation of the pubic ligament of the guinea pig. *Proc Soc Exp Biol Med* **23**, 661-663.

Hokfelt T, Bartfai T, Bloom F (2003). Neuropeptides: opportunities for drug discovery. *Lancet Neurol* **2**, 463-472.

Hokfelt T, Broberger C, Xu ZQ, Sergeyev V, Ubink R, Diez M (2000). Neuropeptides--an overview. *Neuropharmacology* **39**, 1337-1356.

Holmes A, Yang RJ, Crawley JN (2002). Evaluation of an anxiety-related phenotype in galanin overexpressing transgenic mice. *J Mol Neurosci* **18**, 151-165.

Holmes A, Heilig M, Rupniak NM, Steckler T, Griebel G (2003). Neuropeptide systems as novel therapeutic targets for depression and anxiety disorders. *Trends Pharmacol Sci* **24**, 580-588.

Holmgren S, Jensen J (2001). Evolution of vertebrate neuropeptides. *Brain Res Bull* **55**, 723-735.

Hosken IT, Sutton SW, Smith CM, Gundlach AL (2015). Relaxin-3 receptor (Rxfp3) gene knockout mice display reduced running wheel activity: implications for role of relaxin-3/RXFP3 signalling in sustained arousal. *Behav Brain Res* **278**, 167-175.

Huang Y, Mucke L (2012). Alzheimer mechanisms and therapeutic strategies. *Cell* **148**, 1204-1222.

Huge V, Rammes G, Beyer A, Zieglgansberger W, Azad SC (2009). Activation of kappa opioid receptors decreases synaptic transmission and inhibits long-term potentiation in the basolateral amygdala of the mouse. *Eur J Pain* **13**, 124-129.

Huh S, Baek SJ, Lee KH, Whitcomb DJ, Jo J, Choi SM, Kim DH, Park MS, Lee KH, Kim BC (2016). The reemergence of long-term potentiation in aged Alzheimer's disease mouse model. *Sci Rep* **6**, 29152.

Hunsberger HC, Rudy CC, Batten SR, Gerhardt GA, Reed MN (2015). P301L tau expression affects glutamate release and clearance in the hippocampal trisynaptic pathway. *J Neurochem* **132**, 169-182.

Hutton M, Lendon CL, Rizzu P, Baker M, Froelich S, Houlden H et al. (1998). Association of missense and 5'-splice-site mutations in tau with the inherited dementia FTDP-17. *Nature* **393**, 702-705.

Iba M, McBride JD, Guo JL, Zhang B, Trojanowski JQ, Lee VM (2015). Tau pathology spread in PS19 tau transgenic mice following locus coeruleus (LC) injections of synthetic tau fibrils is determined by the LC's afferent and efferent connections. *Acta Neuropathol* **130**, 349-362.

Irwin DJ (2016). Tauopathies as clinicopathological entities. *Parkinsonism Relat Disord* **22 Suppl 1**, S29-33.

Iwahara S, Oishi H, Yamazaki S, Sakai K (1972). Effects of chlordiazepoxide upon spontaneous alternation and the hippocampal electrical activity in white rats. *Psychopharmacology (Berl)* **24**, 496-507.

Jennes L, Stumpf WE, Kalivas PW (1982). Neurotensin: topographical distribution in rat brain by immunohistochemistry. *J Comp Neurol* **210**, 211-224.

Jinno S, Kosaka T (2002). Patterns of expression of calcium binding proteins and neuronal nitric oxide synthase in different populations of hippocampal GABAergic neurons in mice. *J Comp Neurol* **449**, 1-25.

Jurgensen S, Antonio LL, Mussi GE, Brito-Moreira J, Bomfim TR, De Felice FG, Garrido-Sanabria ER, Cavalheiro EA, Ferreira ST (2011). Activation of D1/D5 dopamine receptors protects neurons from synapse dysfunction induced by amyloid-beta oligomers. *J Biol Chem* **286**, 3270-3276.

Kalinin S, Polak PE, Lin SX, Sakharkar AJ, Pandey SC, Feinstein DL (2012). The noradrenaline precursor L-DOPS reduces pathology in a mouse model of Alzheimer's disease. *Neurobiol Aging* **33**, 1651-1663.

Kania A, Czerw A, Grabowiecka A, Ávila C, Blasiak T, Rajfur Z, Lewandowski MH, Hess G, Timofeeva E, Gundlach AL (2017). Inhibition of oxytocin and vasopressin neuron activity in rat hypothalamic paraventricular nucleus by relaxin-3/RXFP3 signalling. *J Physiol* **595**, 3425-3447.

Katona L, Micklem B, Borhegyi Z, Swiejkowski DA, Valenti O, Viney TJ, Kotzadimitriou D, Klausberger T, Somogyi P (2016). Behavior-dependent activity patterns of GABAergic long-range projecting neurons in the rat hippocampus. *Hippocampus*, **27**, 359-377.

Kimura T, Ono T, Takamatsu J, Yamamoto H, Ikegami K, Kondo A, Hasegawa M, Ihara Y, Miyamoto E, Miyakawa T (1996). Sequential changes of tau-site-specific phosphorylation during development of paired helical filaments. *Dementia* **7**, 177-181.

Kita T, Wagner GC, Nakashima T (2003). Current research on methamphetamine-induced neurotoxicity: animal models of monoamine disruption. *J Pharmacol Sci* **92**, 178-195.

Kitanaka N, Kitanaka J, Tatsuta T, Tanaka K, Watabe K, Nishiyama N, Morita Y, Takemura M (2010). Withdrawal from fixed-dose injection of methamphetamine decreases cerebral levels of 3-methoxy-4-hydroxyphenylglycol and induces the expression of anxiety-related behavior in mice. *Neurochem Res* **35**, 749-760.

Kizawa H, Nishi K, Ishibashi Y, Harada M, Asano T, Ito Y et al. (2003). Production of recombinant human relaxin 3 in AtT20 cells. *Regul Pept* **113**, 79-84.

Kocsis B, Li S, Hajos M (2007). Behavior-dependent modulation of hippocampal EEG activity by the selective norepinephrine reuptake inhibitor reboxetine in rats. *Hippocampus* **17**, 627-633.

Kohler C, Bista P, Gotz J, Schroder H (2010). Analysis of the cholinergic pathology in the P301L tau transgenic pR5 model of tauopathy. *Brain Res* **1347**, 111-124.

Kokkinidis L, Zacharko RM, Anisman H (1986). Amphetamine withdrawal: a behavioral evaluation. *Life Sci* **38**, 1617-1623.

Kremer A, Maurin H, Demedts D, Devijver H, Borghgraef P, Van Leuven F (2011). Early improved and late defective cognition is reflected by dendritic spines in Tau.P301L mice. *J Neurosci* **31**, 18036-18047.

Kubota K, Sugaya K, Sunagane N, Matsuda I, Uruno T (1985). Cholecystokinin antagonism by benzodiazepines in the contractile response of the isolated guinea-pig gallbladder. *Eur J Pharmacol* **110**, 225-231.

Kuei C, Sutton S, Bonaventure P, Pudiak C, Shelton J, Zhu J et al. (2007). R3(BDelta23 27)R/I5 chimeric peptide, a selective antagonist for GPCR135 and GPCR142 over relaxin receptor LGR7: in vitro and in vivo characterization. *J Biol Chem* **282**, 25425-25435.

Lambert G, Johansson M, Agren H, Friberg P (2000). Reduced brain norepinephrine and dopamine release in treatment-refractory depressive illness: evidence in support of the catecholamine hypothesis of mood disorders. *Arch Gen Psychiatry* **57**, 787-793.

Lawther AJ, Clissold ML, Ma S, Kent S, Lowry CA, Gundlach AL, Hale MW (2015). Anxiogenic drug administration and elevated plus-maze exposure in rats activate populations of relaxin-3 neurons in the nucleus incertus and serotonergic neurons in the dorsal raphe nucleus. *Neuroscience* **303**, 270-284.

Leao RN, Mikulovic S, Leao KE, Munguba H, Gezelius H, Enjin A, Patra K, Eriksson A, Loew LM, Tort AB, Kullander K (2012). OLM interneurons differentially modulate CA3 and entorhinal inputs to hippocampal CA1 neurons. *Nat Neurosci* **15**, 1524-1530.

Lee JH, Ryan J, Andreescu C, Aizenstein H, Lim HK (2015). Brainstem morphological changes in Alzheimer's disease. *Neuroreport* **26**, 411-415.

Lee JH, Koh SQ, Guadagna S, Francis PT, Esiri MM, Chen CP, Wong PT, Dawe GS, Lai MK (2016). Altered relaxin family receptors RXFP1 and RXFP3 in the neocortex of depressed Alzheimer's disease patients. *Psychopharmacology (Berl)* **233**, 591-598.

Lesch KP, Waider J (2012). Serotonin in the modulation of neural plasticity and networks: implications for neurodevelopmental disorders. *Neuron* **76**, 175-191.

Levenga J, Krishnamurthy P, Rajamohamedsait H, Wong H, Franke TF, Cain P, Sigurdsson EM, Hoeffer CA (2013). Tau pathology induces loss of GABAergic interneurons leading to altered synaptic plasticity and behavioral impairments. *Acta Neuropathol Commun* **1**, 34.

Lewis J, McGowan E, Rockwood J, Melrose H, Nacharaju P, Van Slegtenhorst M, Gwinn-Hardy K, Murphy MP, Baker M, Yu X (2000). Neurofibrillary tangles, amyotrophy and progressive motor disturbance in mice expressing mutant (P301L) tau protein. *Nature genet* **25**, 402-405.

Li Q, Bartley AF, Dobrunz LE (2017). Endogenously released neuropeptide Y suppresses hippocampal short-term facilitation and is impaired by stress-induced anxiety. *J Neurosci* **37**, 23-37.

Liu C, Chen J, Kuei C, Sutton S, Nepomuceno D, Bonaventure P, Lovenberg TW (2005). Relaxin-3/insulin-like peptide 5 chimeric peptide, a selective ligand for G protein-coupled receptor (GPCR)135 and GPCR142 over leucine-rich repeat-containing G protein-coupled receptor 7. *Mol Pharmacol* **67**, 231-240.

Liu C, Eriste E, Sutton S, Chen J, Roland B, Kuei C, Farmer N, Jornvall H, Sillard R, Lovenberg TW (2003). Identification of relaxin-3/INSL7 as an endogenous ligand for the orphan G-protein-coupled receptor GPCR135. *J Biol Chem* **278**, 50754-50764.

Liu L, Drouet V, Wu JW, Witter MP, Small SA, Clelland C, Duff K (2012). Trans-synaptic spread of tau pathology in vivo. *PLoS One* **7**, e31302.

Liu MY, Wang S, Yao WF, Zhang ZJ, Zhong X, Sha L, He M, Zheng ZH, Wei MJ (2014). Memantine improves spatial learning and memory impairments by regulating NGF signaling in APP/PS1 transgenic mice. *Neuroscience* **273**, 141-151.

Lovett-Barron M, Kaifosh P, Kheirbek MA, Danielson N, Zaremba JD, Reardon TR, Turi GF, Hen R, Zemelman BV, Losonczy A (2014). Dendritic inhibition in the hippocampus supports fear learning. *Science* **343**, 857-863.

Lübke J, Deller T, Frotscher M (1997). Septal innervation of mossy cells in the hilus of the rat dentate gyrus: an anterograde tracing and intracellular labeling study. *Exp Brain Res* **114**, 423-432.

Ma S, Gundlach AL (2015). Ascending control of arousal and motivation: Role of nucleus incertus and its peptide neuromodulators in behavioural responses to stress. *J Neuroendocrinol* **27***,* 457-467.

Ma S, Sang Q, Lanciego JL, Gundlach AL (2009a). Localization of relaxin-3 in brain of Macaca fascicularis: identification of a nucleus incertus in primate. *J Comp Neurol* **517**, 856-872.

Ma S, Shen PJ, Sang Q, Lanciego JL, Gundlach AL (2009b). Distribution of relaxin-3 mRNA and immunoreactivity and RXFP3-binding sites in the brain of the macaque, Macaca fascicularis. *Ann N Y Acad Sci* **1160**, 256-258.

Ma S, Blasiak A, Olucha-Bordonau FE, Verberne AJ, Gundlach AL (2013). Heterogeneous responses of nucleus incertus neurons to corticotrophin-releasing factor and coherent activity with hippocampal theta rhythm in the rat. *J Physiol* **591**, 3981-4001.

Ma S, Kastman H, Olucha-Bordonau FE, Capogna M, Hossain A, Wade JD, Verberne AJM, Gundlach AL (2010). Relaxin-3 receptor activation in the central amygdala enhances fear extinction in the rat: implications for relaxin-3 control of emotion. *Society for Neuroscience Annual Meeting, poster presentation* **P809.24**.

Ma S, Bonaventure P, Ferraro T, Shen PJ, Burazin TC, Bathgate RA, Liu C, Tregear GW, Sutton SW, Gundlach AL (2007). Relaxin-3 in GABA projection neurons of nucleus incertus suggests widespread influence on forebrain circuits via G-protein-coupled receptor-135 in the rat. *Neuroscience* **144**, 165-190.

Ma S, Olucha-Bordonau FE, Hossain MA, Lin F, Kuei C, Liu C, Wade JD, Sutton SW, Nunez A, Gundlach AL (2009c). Modulation of hippocampal theta oscillations and spatial memory by relaxin-3 neurons of the nucleus incertus. *Learn Mem* **16**, 730-742.

Maccaferri G, Lacaille JC (2003). Interneuron Diversity series: Hippocampal interneuron classifications--making things as simple as possible, not simpler. *Trends Neurosci* **26**, 564-571.

Mann DM, Yates PO, Hawkes J (1982). The noradrenergic system in Alzheimer and multi-infarct dementias. *J Neurol Neurosurg Psychiatry* **45**, 113-119.

Mann DM, Yates PO, Marcyniuk B (1984). Alzheimer's presenile dementia, senile dementia of Alzheimer type and Down's syndrome in middle age form an age related continuum of pathological changes. *Neuropathol Appl Neurobiol* **10**, 185-207.

Manns ID, Mainville L, Jones BE (2001). Evidence for glutamate, in addition to acetylcholine and GABA, neurotransmitter synthesis in basal forebrain neurons projecting to the entorhinal cortex. *Neuroscience* **107**, 249-263.

Manns JR, Eichenbaum H (2006). Evolution of declarative memory. *Hippocampus* **16**, 795-808.

Marazziti D, Marracci S, Palego L, Rotondo A, Mazzanti C, Nardi I, Ladinsky H, Giraldo E, Borsini F, Cassano G (1994). Localization and gene expression of serotonin1A (5HT 1A) receptors in human brain postmortem. *Brain Res* **658**, 55-59.

Martignoni E, Blandini F, Petraglia F, Pacchetti C, Bono G, Nappi G (1992). Cerebrospinal fluid norepinephrine, 3-methoxy-4-hydroxyphenylglycol and neuropeptide Y levels in Parkinson's disease, multiple system atrophy and dementia of the Alzheimer type. *J Neural Transm Park Dis Dement Sect* **4,** 191-205.

Matsumoto M, Kamohara M, Sugimoto T, Hidaka K, Takasaki J, Saito T, Okada M, Yamaguchi T, Furuichi K (2000). The novel G-protein coupled receptor SALPR shares sequence similarity with somatostatin and angiotensin receptors. *Gene* **248**, 183-189.

McGowan BM, Stanley SA, Smith KL, Minnion JS, Donovan J, Thompson EL et al. (2006). Effects of acute and chronic relaxin-3 on food intake and energy expenditure in rats. *Regul Pept* **136**, 72-77.

McNaughton N, Gray JA (2000). Anxiolytic action on the behavioural inhibition system implies multiple types of arousal contribute to anxiety. *J Affect Disord* **61**, 161-176.

Meessen H, Olszewski J (1949). A Cytoarchitectonic Atlas of the Rhombencephalon of the Rabbit. *Cytoarchitektonischer Atlas des Rautenhirns des Kaninchens*.

Melander T, Hokfelt T, Rokaeus A, Cuello AC, Oertel WH, Verhofstad A, Goldstein M (1986). Coexistence of galanin-like immunoreactivity with catecholamines, 5-hydroxytryptamine, GABA and neuropeptides in the rat CNS. *J Neurosci* **6**, 3640-3654.

Mendez P, Bacci A (2011). Assortment of GABAergic plasticity in the cortical interneuron melting pot. *Neural Plast* **2011**, 976856.

Mikulovic S, Restrepo CE, Hilscher MM, Kullander K, Leao RN (2015). Novel markers for OLM interneurons in the hippocampus. *Front Cell Neurosci* **9**, 201.

Milner TA, Kurucz OS, Veznedaroglu E, Pierce JP (1995). Septohippocampal neurons in the rat septal complex have substantial glial coverage and receive direct contacts from noradrenaline terminals. *Brain Res* **670**, 121-136.

Mishkin M (1978). Memory in monkeys severely impaired by combined but not by separate removal of amygdala and hippocampus. *Nature* **273**, 297-298.

Miyamoto Y, Watanabe Y, Tanaka M (2008). Developmental expression and serotonergic regulation of relaxin 3/INSL7 in the nucleus incertus of rat brain. *Regul Pept* **145**, 54-59.

Molchan SE, Lawlor BA, Hill JL, Martinez RA, Davis CL, Mellow AM, Rubinow DR, Sunderland T (1991). CSF monoamine metabolites and somatostatin in Alzheimer's disease and major depression. *Biol Psychiatry* **29**, 1110-1118.

Molchan SE, Hill JL, Martinez RA, Lawlor BA, Mellow AM, Rubinow DR, Bissette G, Nemeroff CB, Sunderland T (1993). CSF somatostatin in Alzheimer's disease and major depression:

relationship to hypothalamic-pituitary-adrenal axis and clinical measures. *Psychoneuroendocrinology* **18**, 509-519.

Molgaard S, Ulrichsen M, Boggild S, Holm M-L, Vaegter C, Nyengaard J, Glerup S (2014). Immunofluorescent visualization of mouse interneuron subtypes. *F1000Research* **3**.

Morest DK (1961). Connexions of the dorsal tegmental nucleus in rat and rabbit.*J Anat* **95**, 229.

Morris RG, Inglis J, Ainge JA, Olverman HJ, Tulloch J, Dudai Y, Kelly PA (2006). Memory reconsolidation: sensitivity of spatial memory to inhibition of protein synthesis in dorsal hippocampus during encoding and retrieval. *Neuron* **50**, 479-489.

Moser MB, Rowland DC, Moser EI (2015). Place cells, grid cells, and memory. *Cold Spring Harb Perspect Biol* **7**, a021808.

Mullen RJ, Buck CR, Smith AM (1992). NeuN, a neuronal specific nuclear protein in vertebrates. *Development* **116**, 201-211.

Muller C, Remy S (2014). Dendritic inhibition mediated by O-LM and bistratified interneurons in the hippocampus. *Front Synaptic Neurosci* **6**, 23.

Munro J, Skrobot O, Sanyoura M, Kay V, Susce MT, Glaser PE, de Leon J, Blakemore AI, Arranz MJ (2012). Relaxin polymorphisms associated with metabolic disturbance in patients treated with antipsychotics. *J Psychopharmacol* **26**, 374-379.

Murray EA (1992). Medial temporal lobe structures contributing to recognition memory: The amygdaloid complex versus the rhinal cortex. *The amygdala. Neurobiological aspects of emotion, memory and mental dysfunction.* London, Wiley-Liss, 453-470.

Nategh M, Nikseresht S, Khodagholi F, Motamedi F (2015). Nucleus incertus inactivation impairs spatial learning and memory in rats. *Physiol Behav* **139**, 112-120.

Nestler EJ (1998). Antidepressant treatments in the 21st century. *Biol Psychiatry* **44**, 526-533.

Nunez A, Cervera-Ferri A, Olucha-Bordonau F, Ruiz-Torner A, Teruel V (2006). Nucleus incertus contribution to hippocampal theta rhythm generation. *Eur J Neurosci* **23**, 2731-2738.

Ogren SO, Kuteeva E, Elvander-Tottie E, Hokfelt T (2010). Neuropeptides in learning and memory processes with focus on galanin. *Eur J Pharmacol* **626**, 9-17.

Olucha-Bordonau FE, Teruel V, Barcia-Gonzalez J, Ruiz-Torner A, Valverde-Navarro AA, Martinez-Soriano F (2003). Cytoarchitecture and efferent projections of the nucleus incertus of the rat. *J Comp Neurol* **464**, 62-97.

Olucha-Bordonau FE, Otero-Garcia M, Sanchez-Perez AM, Nunez A, Ma S, Gundlach AL (2012). Distribution and targets of the relaxin-3 innervation of the septal area in the rat. *J Comp Neurol* **520**, 1903-1939.

Osheroff PL, Ho WH (1993). Expression of relaxin mRNA and relaxin receptors in postnatal and adult rat brains and hearts. Localization and developmental patterns. *J Biol Chem* **268**, 15193-15199.

Paxinos G, Butcher L (1985). Organizational principles of the brain as revealed by choline acetyltransferase and acetylcholinesterase distribution and projections. *The rat nervous system.* New York, Academic, 487-521.

Pereira CW, Santos FN, Sanchez-Perez AM, Otero-Garcia M, Marchioro M, Ma S, Gundlach AL, Olucha-Bordonau FE (2013). Electrolytic lesion of the nucleus incertus retards extinction of auditory conditioned fear. *Behav Brain Res* **247**, 201-210.

Pieribone VA, Nicholas AP, Dagerlind A, Hokfelt T (1994). Distribution of alpha 1 adrenoceptors in rat brain revealed by in situ hybridization experiments utilizing subtype-specific probes. *J Neurosci* **14**, 4252-4268.

Ramos B, Baglietto-Vargas D, del Rio JC, Moreno-Gonzalez I, Santa-Maria C, Jimenez S, Caballero C, Lopez-Tellez JF, Khan ZU, Ruano D (2006). Early neuropathology of somatostatin/NPY GABAergic cells in the hippocampus of a PS1× APP transgenic model of Alzheimer's disease. *Neurobiol Aging* **27**, 1658-1672.

Ramsden M, Kotilinek L, Forster C, Paulson J, McGowan E, SantaCruz K et al. (2005). Age-dependent neurofibrillary tangle formation, neuron loss, and memory impairment in a mouse model of human tauopathy (P301L). *J Neurosci* **25**, 10637-10647.

Reinikainen KJ, Paljärvi L, Huuskonen M, Soininen H, Laakso M, Riekkinen PJ (1988). A post-mortem study of noradrenergic, serotonergic and GABAergic neurons in Alzheimer's disease. *J Neurol Sci* **84**, 101-116.

Riley JN, Moore RY (1981). Diencephalic and brainstem afferents to the hippocampal formation of the rat. *Brain Res Bull* **6**, 437-444.

Rispoli V, Marra R, Costa N, Rotiroti D, Tirassa P, Scipione L, De Vita D, Liberatore F, Carelli V (2008). Choline pivaloyl ester enhances brain expression of both nerve growth factor and high-affinity receptor TrkA, and reverses memory and cognitive deficits, in rats with excitotoxic lesion of nucleus basalis magnocellularis. *Behav Brain Res* **190**, 22-32.

Rogan SC, Roth BL (2011). Remote control of neuronal signaling. *Pharmacol Rev* **63**, 291-315.

Ryan PJ, Ma S, Olucha-Bordonau FE, Gundlach AL (2011). Nucleus incertus--an emerging modulatory role in arousal, stress and memory. *Neurosci Biobehav Rev* **35**, 1326-1341.

Ryan PJ, Buchler E, Shabanpoor F, Hossain MA, Wade JD, Lawrence AJ, Gundlach AL (2013). Central relaxin-3 receptor (RXFP3) activation decreases anxiety- and depressive-like behaviours in the rat. *Behav Brain Res* **244**, 142-151.

Samuels ER, Szabadi E (2008). Functional neuroanatomy of the noradrenergic locus coeruleus: its roles in the regulation of arousal and autonomic function part I: principles of functional organisation. *Curr Neuropharmacol* **6**, 235-253.

Sanchez-Perez AM, Arnal-Vicente I, Santos FN, Pereira CW, ElMlili N, Sanjuan J, Ma S, Gundlach AL, Olucha-Bordonau FE (2015). Septal projections to nucleus incertus in the rat: bidirectional pathways for modulation of hippocampal function. *J Comp Neurol* **523**, 565-588.

Sandoval K, Farr S, Banks W, Crider A, Morley J, Witt K (2013). Somatostatin receptor subtype-4 agonist NNC 26-9100 mitigates the effect of soluble Aβ42 oligomers via a metalloproteinase-dependent mechanism. *Brain Res* **1520**, 145-156.

Saper CB, Scammell TE, Lu J (2005). Hypothalamic regulation of sleep and circadian rhythms. *Nature* **437**, 1257-1263.

Schmid LC, Mittag M, Poll S, Steffen J, Wagner J, Geis H-R, Schwarz I, Schmidt B, Schwarz MK, Remy S, Fuhrmann M (2016). Dysfunction of somatostatin-positive interneurons associated with memory deficits in an Alzheimer's disease model. *Neuron* **92**, 114-125.

Schwarz LA, Luo L (2015). Organization of the locus coeruleus-norepinephrine system. *Curr Biol* **25**, R1051-1056.

Scoville WB, Milner B (1957). Loss of recent memory after bilateral hippocampal lesions. *J Neurol Neurosurg Psychiatry* **20**, 11-21.

Serrano-Pozo A, Frosch MP, Masliah E, Hyman BT (2011). Neuropathological alterations in Alzheimer disease. *Cold Spring Harb Perspect Med* **1**, a006189.

Shabanpoor F, Akhter Hossain M, Ryan PJ, Belgi A, Layfield S, Kocan M et al. (2012). Minimization of human relaxin-3 leading to high-affinity analogues with increased selectivity for relaxin-family peptide 3 receptor (RXFP3) over RXFP1. *J Med Chem* **55**, 1671-1681.

Sherwood OD (2004). Relaxin's physiological roles and other diverse actions. *Endocr Rev* **25**, 205-234.

Simmons ML, Chavkin C (1996). Endogenous opioid regulation of hippocampal function. *Int Rev Neurobiol* **39**, 145-196.

Smith CM, Hosken IT, Sutton SW, Lawrence AJ, Gundlach AL (2012). Relaxin-3 null mutation mice display a circadian hypoactivity phenotype. *Genes Brain Behav* **11**, 94-104.

Smith CM, Walker AW, Hosken IT, Chua BE, Zhang C, Haidar M, Gundlach AL (2014a). Relaxin-3/RXFP3 networks: an emerging target for the treatment of depression and other neuropsychiatric diseases? *Front Pharmacol* **5**, 46.

Smith CM, Shen PJ, Banerjee A, Bonaventure P, Ma S, Bathgate RA, Sutton SW, Gundlach AL (2010). Distribution of relaxin-3 and RXFP3 within arousal, stress, affective, and cognitive circuits of mouse brain. *J Comp Neurol* **518**, 4016-4045.

Smith CM, Chua BE, Zhang C, Walker AW, Haidar M, Hawkes D, Shabanpoor F, Hossain MA, Wade JD, Rosengren KJ (2014b). Central injection of relaxin-3 receptor (RXFP3) antagonist peptides reduces motivated food seeking and consumption in C57BL/6J mice. *Behav Brain Res* **268**, 117-126.

Sobreviela T, Clary DO, Reichardt LF, Brandabur MM, Kordower JH, Mufson EJ (1994). TrkA-immunoreactive profiles in the central nervous system: colocalization with neurons containing p75 nerve growth factor receptor, choline acetyltransferase, and serotonin. *J Comp Neurol* **350**, 587-611.

Soler H, Dorca-Arevalo J, Gonzalez M, Rubio SE, Avila J, Soriano E, Pascual M (2017). The GABAergic septohippocampal connection is impaired in a mouse model of tauopathy. *Neurobiol Aging* **49**, 40-51.

Somogyi P, Klausberger T (2005). Defined types of cortical interneurone structure space and spike timing in the hippocampus. *J Physiol* **562**, 9-26.

Sorman E, Wang D, Hajos M, Kocsis B (2011). Control of hippocampal theta rhythm by serotonin: role of 5-HT2c receptors. *Neuropharmacology* **61**, 489-494.

Sotty F, Danik M, Manseau F, Laplante F, Quirion R, Williams S (2003). Distinct electrophysiological properties of glutamatergic, cholinergic and GABAergic rat septohippocampal neurons: novel implications for hippocampal rhythmicity. *J Physiol* **551**, 927-943.

Spiegel AM, Koh MT, Vogt NM, Rapp PR, Gallagher M (2013). Hilar interneuron vulnerability distinguishes aged rats with memory impairment. *J Comp Neurol* **521**, 3508-3523.

Squire LR (2009). The legacy of patient H.M. for neuroscience. *Neuron* **61**, 6-9.

Squire LR, Zola-Morgan S (1991). The medial temporal lobe memory system. *Science* **253**, 1380-1386.

Stefanelli T, Bertollini C, Luscher C, Muller D, Mendez P (2016). Hippocampal somatostatin interneurons control the size of neuronal memory ensembles. *Neuron* **89**, 1074-1085.

Storga D, Vrecko K, Birkmayer J, Reibnegger G (1996). Monoaminergic neurotransmitters, their precursors and metabolites in brains of Alzheimer patients. *Neurosci Lett* **203**, 29-32.

Strange BA, Witter MP, Lein ES, Moser EI (2014). Functional organization of the hippocampal longitudinal axis. *Nat Rev Neurosci* **15**, 655-669.

Streeter GL (1903). Anatomy of the floor of the fourth ventricle.The relations between the surface markings and the underlying structures. *Am J Ant* **2**, 299-313.

Sutin EL, Jacobowitz DM (1988). Immunocytochemical localization of peptides and other neurochemicals in the rat laterodorsal tegmental nucleus and adjacent area. *J Comp Neurol* **270**, 243-270.

Sutton SW, Bonaventure P, Kuei C, Roland B, Chen J, Nepomuceno D, Lovenberg TW, Liu C (2004). Distribution of G-protein-coupled receptor (GPCR)135 binding sites and receptor mRNA in the rat brain suggests a role for relaxin-3 in neuroendocrine and sensory processing. *Neuroendocrinology* **80**, 298-307.

Tanaka M, Iijima N, Miyamoto Y, Fukusumi S, Itoh Y, Ozawa H, Ibata Y (2005). Neurons expressing relaxin 3/INSL 7 in the nucleus incertus respond to stress. *Eur J Neurosci* **21**, 1659-1670.

Tekin S, Mega MS, Masterman DM, Chow T, Garakian J, Vinters HV, Cummings JL (2001). Orbitofrontal and anterior cingulate cortex neurofibrillary tangle burden is associated with agitation in Alzheimer disease. *Ann Neurol* **49**, 355-361.

Teruel-Martí V, Cervera-Ferri A, Nuñez A, Valverde-Navarro AA, Olucha-Bordonau FE, Ruiz-Torner A (2008). Anatomical evidence for a ponto-septal pathway via the nucleus incertus in the rat. *Brain Res* **1218**, 87-96.

Terwel D, Lasrado R, Snauwaert J, Vandeweert E, Van Haesendonck C, Borghgraef P, Van Leuven F (2005). Changed conformation of mutant Tau-P301L underlies the moribund tauopathy, absent in progressive, nonlethal axonopathy of Tau-4R/2N transgenic mice. *J Biol Chem* **280**, 3963-3973.

Terwel D, Muyllaert D, Dewachter I, Borghgraef P, Croes S, Devijver H, Van Leuven F (2008). Amyloid activates GSK-3beta to aggravate neuronal tauopathy in bigenic mice. *Am J Pathol* **172**, 786-798.

Tomita M, Katsuyama H, Watanabe Y, Shibaike Y, Yoshinari H, Tee JW, Iwachidou N, Miyamoto O (2013). c-Fos immunoreactivity of neural cells in intoxication due to high-dose methamphetamine. *J Toxicol Sci* **38**, 671-678.

Tóth K, Freund T, Miles R (1997). Disinhibition of rat hippocampal pyramidal cells by GABAergic afferents from the septum. *J Physiol* **500**, 463-474.

Trillo L, Das D, Hsieh W, Medina B, Moghadam S, Lin B, Dang V, Sanchez MM, De Miguel Z, Ashford JW, Salehi A (2013). Ascending monoaminergic systems alterations in Alzheimer's disease. translating basic science into clinical care. *Neurosci Biobehav Rev* **37**, 1363-1379.

Van den Hooff P, Galvan M (1992). Actions of 5-hydroxytryptamine and 5-HT1A receptor ligands on rat dorso-lateral septal neurones in vitro. *Br J Pharmacol* **106**, 893-899.

van den Pol AN (2012). Neuropeptide transmission in brain circuits. *Neuron* **76**, 98-115.

van der Westhuizen ET, Werry TD, Sexton PM, Summers RJ (2007). The relaxin family peptide receptor 3 activates extracellular signal-regulated kinase 1/2 through a protein kinase C-dependent mechanism. *Mol Pharmacol* **71**, 1618-1629.

van Strien NM, Cappaert NL, Witter MP (2009). The anatomy of memory: an interactive overview of the parahippocampal-hippocampal network. *Nat Rev Neurosci* **10**, 272-282.

Vepsalainen S, Helisalmi S, Koivisto AM, Tapaninen T, Hiltunen M, Soininen H (2007). Somatostatin genetic variants modify the risk for Alzheimer's disease among Finnish patients. *J Neurol* **254**, 1504-1508.

Vertes RP (2005). Hippocampal theta rhythm: a tag for short-term memory. *Hippocampus* **15**, 923-935.

Vertes RP, Martin GF (1988). Autoradiographic analysis of ascending projections from the pontine and mesencephalic reticular formation and the median raphe nucleus in the rat. *J Comp Neurol* **275**, 511-541.

Vertes RP, Kocsis B (1997). Brainstem-diencephalo-septohippocampal systems controlling the theta rhythm of the hippocampus. *Neuroscience* **81**, 893-926.

Vertes RP, Kinney GG, Kocsis B, Fortin WJ (1994). Pharmacological suppression of the median raphe nucleus with serotonin1A agonists, 8-OH-DPAT and buspirone, produces hippocampal theta rhythm in the rat. *Neuroscience* **60**, 441-451.

Wainer BH, Levey AI, Mufson EJ, Mesulam MM (1984). Cholinergic systems in mammalian brain identified with antibodies against choline acetyltransferase. *Neurochem Int* **6**, 163-182.

Wainer BH, Levey AI, Rye DB, Mesulam MM, Mufson EJ (1985). Cholinergic and non-cholinergic septohippocampal pathways. *Neurosci Lett* **54**, 45-52.

Walker AW, Smith CM, Chua BE, Krstew EV, Zhang C, Gundlach AL, Lawrence AJ (2015). Relaxin-3 receptor (RXFP3) signalling mediates stress-related alcohol preference in mice. *PLoS One* **10**, e0122504.

Walker LC, Kastman HE, Koeleman JA, Smith CM, Perry CJ, Krstew EV, Gundlach AL, Lawrence AJ (2016). Nucleus incertus corticotrophin-releasing factor 1 receptor signalling regulates alcohol seeking in rats. *Addict Biol*.

Wang X-J (2002). Pacemaker neurons for the theta rhythm and their synchronization in the septohippocampal reciprocal loop. *J Neurophysiol* **87**, 889-900.

Wang Y, Mandelkow E (2016). Tau in physiology and pathology. *Nat Rev Neurosci* **17**, 5-21.

Watanabe Y, Miyamoto Y, Matsuda T, Tanaka M (2011). Relaxin-3/INSL7 regulates the stress-response system in the rat hypothalamus. *J Mol Neurosci* **43**, 169-174.

Weingarten MD, Lockwood AH, Hwo SY, Kirschner MW (1975). A protein factor essential for microtubule assembly. *Proc Natl Acad Sci USA* **72**, 1858-1862.

Weiss JM, Bonsall RW, Demetrikopoulos MK, Emery MS, West CH (1998). Galanin: a significant role in depression? *Ann N Y Acad Sci* **863**, 364-382.

White C, Ji S, Cai H, Maudsley S, Martin B (2010). Therapeutic potential of vasoactive intestinal peptide and its receptors in neurological disorders. *CNS Neurol Disord Drug Targets* **9**, 661-666.

Wilkinson TN, Speed TP, Tregear GW, Bathgate RA (2005). Evolution of the relaxin-like peptide family. *BMC Evol Biol* **5**, 1.

Woolf NJ, Milov AM, Schweitzer ES, Roghani A (2001). Elevation of nerve growth factor and antisense knockdown of TrkA receptor during contextual memory consolidation. *J Neurosci* **21**, 1047-1055.

Wray N, Pergadia M, Blackwood D, Penninx B, Gordon S, Nyholt D, Ripke S, MacIntyre D, McGhee K, Maclean A (2012). Genome-wide association study of major depressive disorder: new results, meta-analysis, and lessons learned. *Mol Psychiatry* **17**, 36-48.

Wu JW, Hussaini SA, Bastille IM, Rodriguez GA, Mrejeru A, Rilett K et al. (2016). Neuronal activity enhances tau propagation and tau pathology in vivo. *Nat Neurosci* **19**, 1085-1092.

Wu Z, Yang H, Colosi P (2010). Effect of genome size on AAV vector packaging. *Mol Ther* **18**, 80-86.

y Cajal SR (1893). Estructura del asta de ammon y fascia dentata. tip. de Fortanet.

Yamamoto BK, Moszczynska A, Gudelsky GA (2010). Amphetamine toxicities: classical and emerging mechanisms. *Ann N Y Acad Sci* **1187**, 101-121.

Yamano M, Luiten PG (1989). Direct synaptic contacts of medial septal efferents with somatostatin immunoreactive neurons in the rat hippocampus. *Brain Res Bull* **22**, 993-1001.

Ying S-W, Zhang D-X, Rusak B (1993). Effects of serotonin agonists and melatonin on photic responses of hamster intergeniculate leaflet neurons. *Brain Res* **628**, 8-16.

Zhang C, Chua BE, Yang A, Shabanpoor F, Hossain MA, Wade JD, Rosengren KJ, Smith CM, Gundlach AL (2015). Central relaxin-3 receptor (RXFP3) activation reduces elevated, but not basal, anxiety-like behaviour in C57BL/6J mice. *Behav Brain Res* **292**, 125-132.

Zuloaga DG, Johnson LA, Agam M, Raber J (2014). Sex differences in activation of the hypothalamic-pituitary-adrenal axis by methamphetamine. *J Neurochem* **129**, 495-508.